UNIVERSIDADE DE LISBOA
FACULDADE DE CIÊNCIAS
Departamento de Química e Bioquímica

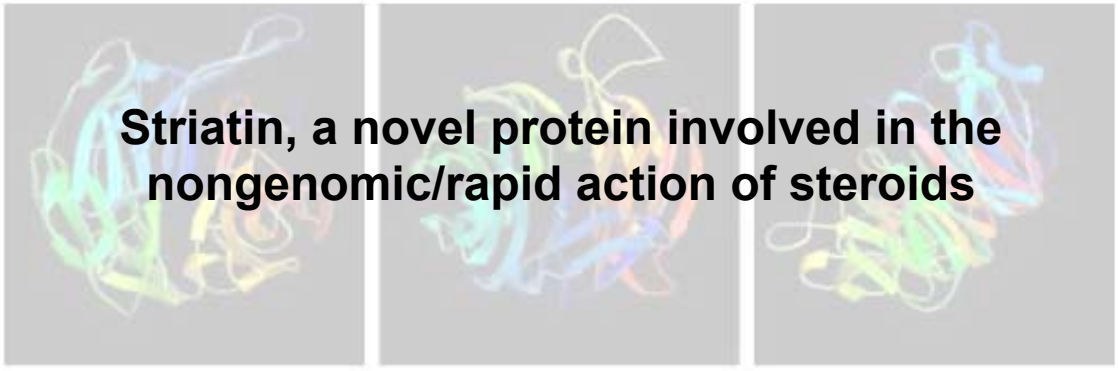

Striatin, a novel protein involved in the nongenomic/rapid action of steroids

Patrícia Pezo Coutinho

Doutoramento em Bioquímica Clínica

2012

UNIVERSIDADE DE LISBOA
FACULDADE DE CIÊNCIAS
Departamento de Química e Bioquímica

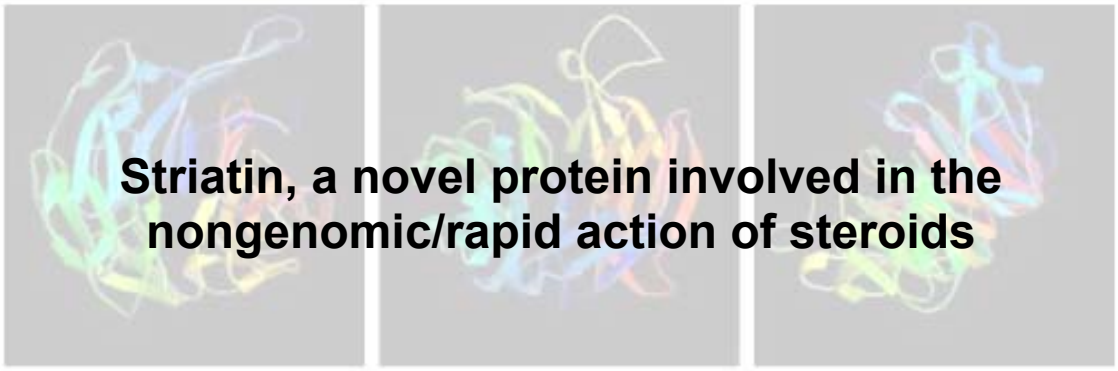

Striatin, a novel protein involved in the nongenomic/rapid action of steroids

Patrícia Pezo Coutinho

Tese orientada pelos Doutores José Romero e Margarida Meireles, especialmente elaborada para a obtenção do grau de doutor em Bioquímica Clínica

2012

FONTES DE FINANCIAMENTO

Esta tese foi financiada pela Bolsa de Investigação com a referência SFRH / BD / 28601 / 2006, financiada pelo POPH - QREN - Formação Avançada, compartici pado pelo Fundo Social Europeu e por fundos nacionais do MCTES, com a participação, em parte dos subsidios oriundos do NHLBI/NIH USA: R01HL090632, R01HL094452, and R01HL096518.

O trabalho realizado deu origem a diversos artigos publicados que podem ser consultados na secção dos suplementos.

Índex

Abbreviations

ACE- Angiotensin-Converting Enzyme

ACTR- hRARβ-stimulatory protein

AF1- Activation Function 1

AF2- Activation Function 2

AIPs- Aldosterone-Induced Proteins

AKT- Protein Kinase B

AME- Apparent Mineralocorticoid Excess

AngII- Angiotensin II

ANOVA- analysis of variance

AR- Androgen Receptor

AT_1- G-protein-coupled receptor, type 1

AT_2- G-protein-coupled receptor, type 2

ATCC- American Type Culture Collection

BSA- Bovine Serum Albumin

CaM- Ca^{2+}-calmodulin

CaMK- Calcium/calmodulin-Dependent Protein Kinase

CAV_1- caveolin 1

CAV2- caveolin 2

CAV3- caveolin 3

CBP- cAMP Response Element Binding Protein

cDNA- complementary Deoxyribonucleic acid

CHIF- Channel-Inducing Factor

Co-IP- co-immunoprecipitation

COX2- Cyclo-Oxygenase 2

CRE- cyclic AMP Response Element

CREB- cyclic AMP response element binding protein

CSD- caveolin scaffolding domain

C_t – Cycle Threshold

D- Flexible hinge region

DAG- Diacylglycerol

DBD- DNA Binding Domain

DMEM- Dulbecco's Modified Eagle's Medium

DNA- Deoxyribonucleic acid

DTT- Dithiothreitol

E2- 17β-Estradiol

eNOS- endothelial nitric oxide synthase

ER- Estrogen Receptor

EGFR- Epidermal Growth Factor Receptor

ENaC- Epithelial Na^+ Channel

ER- Estrogen Receptor

ERK 1/2- Extracellular signal-regulated kinase 1/2

FBS- Foetal Bovine Serum

G6PDH- Glucose-6-phosphate dehydrogenase

GPCR- G-protein coupled receptor

GR- Glucocorticoid Receptor

GRIP1- Glucocorticoid Receptor-Interacting Protein 1

H1- Histone 1

H12- Helix 12

12- HETE- 12-lipoxygenase to generate 12-hydroxyeicosatetraenoic acid

HAT- Histone acetyltransferase

HSD3B2- Type 2 3β-Hydroxysteroid Dehydrogenase

HSP90- Heat Shock Protein 90

HRE- Hormone Response Element

11βHSD- 11β-hydroxysteroid dehydrogenase

11βHSD2- 11β-hydroxysteroid dehydrogenase type II isoform

IgG- Immunoglobulin G

IGF-1R- Insulin-like growth factor 1 receptor

IMM- Immunophilin

IL-6- Interleukin 6

IP_3 - Inositol 1,4,5-triphosphate

kDa- kilo Dalton

LBD- Ligand Binding Domain

MAEC- Mouse Aortic Endothelial cells

MAPK- Mitogen Activated Protein Kinase

β-ME- β-mercaptoethanol

MCP-1 - Monocyte Chemoattractant Protein-1

M-MuLV - Moloney Murine Leukaemia Virus

mTOR- Rapamycin

MR- Mineralocorticoid Receptor

mRNA- Messenger Ribonucleic acid

NCoA2- Nuclear receptor Co-Activator 2

N-CoR- Nuclear Receptor Corepressor

NF-κB- Nuclear Factor kappa-light-chain-enhancer of activated B cells

NLS- Nuclear Localization Signal

NO- Nitric Oxide

NOS- Nitric Oxide Synthase

NR- Nuclear Receptors

NTD- N-terminal domain

OD- Optical Density

PAGE- polyacrylamide gel electrophoresis

PAI-1- Plasminogen Activator Inhibitor-1

PBS- Phosphate Buffered Saline

p/CIP- mouse homolog CBP-interacting protein

PELP1- proline, glutamic acid and leucine-rich protein

peNOS- phosho endothelial nitric oxide synthase

PKA- Protein Kinase A

PKC- Protein Kinase C

PMSF- phenylmethanesulfonylfluoride

PPIase- Peptidylprolyl Isomerase

PI3-k- Phophatidylinositol 3-kinase

PIP_2 -Phosphatylinositol 4,5-biphosphate

PLC- Phopholipase C

PR- Progestrone Receptor

PTEN- Phosphatase with tensin homology

PTGS- post-transcriptional gene silencing

PVDF- polyvinyl difluoride

qPCR- quantitative real time polymerase chain reaction

RAC3- Retinoic Acid Receptor Interacting protein 3

RAR- Retinoic acid Receptor

RNA- Ribonucleic acid

RNAi- Ribonucleic acid interference

rRNA- ribosomal Ribonucleic acid

SDS- sodium dodecyl sulfate

SERMs- Selective Estrogen Receptor Modulators

SGK- Serum and Glucocorticoid-induced Kinase

siRNA- Small interfering Ribonucleic acid

α-SMA- alpha smooth muscle actin

SMRT- Silencing Mediator for RAR and TR

SHR-Steroid Horomone Receptors

StAR- Steroidogenic Acute Regulatory protein

SRC-1- Steroid Receptor Coactivators-1

SRE- Steroid Response Element

SUMO- Small Ubiquitin-related Modifier

TBS- Tris-Buffered Saline

TPR- Tetratricopeptide Repeats

TFIIB- Transcription Factor IIB

TIF2- Transcriptional Intermediary Factor 2

TLR- Toll-like receptor

TNF-α- Tumour Necrosis Factor alpha

TR- Thyroid hormone Receptor

TRAM1- TR-interacting protein 1

tRNA- transfer Ribonucleic acid

VWF- Von Willebrand Factor

Abstract

The cellular responses to steroids are mediated by two general mechanisms: genomic and rapid/nongenomic effects. Identification of the mechanisms underlying aldosterone's rapid versus their genomic actions have been difficult to study and are not clearly understood. I explored the hypothesis that striatin is a critical intermediary of the rapid/nongenomic effects of aldosterone and that striatin serves as a novel link between the actions of the mineralocorticoid and estrogen receptors. In human and mouse endothelial cells, aldosterone promoted an increase in pERK that peaked at 15 minutes. Striatin is a critical mediator in this process as reducing striatin levels with siRNA technology prevented the rise in pERK levels. In contrast, reducing striatin did not significantly affect two well-characterized genomic responses to aldosterone. Down regulation of striatin with siRNA produced similar effects on estrogen's actions – reducing nongenomic, but not the genomic actions investigated. Aldosterone, but not estrogen, increased striatin levels. When endothelial cells were pre-treated with aldosterone, the rapid/nongenomic response to estrogen on peNOS/eNOS ratio was enhanced and accelerated significantly. Importantly, pre-treatment with estrogen did not enhance aldosterone's nongenomic response on pERK. In conclusion, these results indicate that striatin is a novel mediator for both aldosterone's and estrogen's rapid and nongenomic mechanisms of action on pERK and peNOS, respectively, thereby providing evidence for a synergistic effect between the mineralocorticoid receptor and the estrogen receptor. Furthermore, these results suggest a unique level of interactions between steroids on the cardiovascular system that may have broad application for the treatment of cardiovascular diseases.

Introduction

The Merriam-Webster dictionary states that the definition for steroid hormone is: “any of numerous hormones (as estrogen, testosterone, cortisone, and aldosterone) having the characteristic ring structure of steroids and formed in the body from cholesterol”. The etymology of the term itself comes from a mixture of Greek and Latin words like: *stereos,* solid; *oleum,* oil; *eidos,* form and *hormaein,* to set in motion.

Steroids are a class of organic compounds with a chemical structure that contains a gonane core i.e., a specific arrangement of four cycloalkane rings that are joined to each other (Figure 1) or a derived skeleton. Usually, methyl groups are present at the carbons C-10 and C-13. It is also possible for an alkyl side chain to be present at carbon C-17.

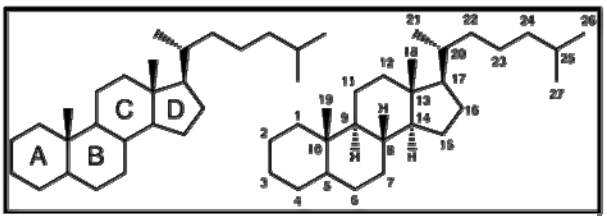

Figure 1- IUPAC recommended ring lettering (left) and atom numbering (right) of cholestane, a prototypical steroid skeleton (2). The four rings A-D form the gonane nucleus of the steroid.

In physiology steroid hormones are involved in various aspects of growth, development, differentiation, reproduction and homeostasis. They exert their effects by means of specific receptors, the steroid hormone receptors, such as estrogen (ER), progesterone (PR), androgen (AR), glucocorticoid (GR) and the mineralocorticoid receptor (MR). Steroid hormone receptors (SHR) belong to the steroid/thyroid hormone receptor superfamily, which includes thyroid hormone (TR), retinoic acid (RAR), and vitamin D_3 receptors, as well as “orphan” receptors, for which no ligands have yet been found.

All members of the steroid and thyroid hormone receptor superfamily (more commonly called nuclear receptors (NR)) share a similar structure consisting of modular domains A though F (from NH_2 to COOH terminus) (4): a variable N-terminal domain (NTD, A/B); a highly conserved DNA Binding Domain (DBD, C); a flexible hinge region (D); and a C-terminal Ligand Binding Domain (LBD, E). The estrogen receptor α is unique in that it contains an additional C-terminal (F) domain with unknown function (5).

A/B REGION (N-TERMINAL DOMAIN)

The A/B region in the different SHR is highly variable, revealing a weak evolutionary conservation, in fact, this is the least conserved region both in size and sequence (6). All the receptors have a unique N- terminal region (100-500 amino acids) whose 3D structure has not been clarified. This poorly defined region contains a transcriptional activation function, referred to as activation function 1 (AF-1) that can operate autonomously (independent of the presence of ligand). The A/B region is potentially involved in multiple protein-protein interactions and the length of this domain has a positive correlation with the activity of AF-1 for different members of the SHR superfamily (7).

C REGION (DNA BINDING DOMAIN)

The DNA binding domain lies toward the centre of the molecule and is a highly conserved residue core. The amino acid sequence of this domain is similar among different steroid receptors (56–79% identity). The 3D structure of the DBD has been resolved for a number of nuclear receptors.

D REGION (HINGE REGION)

The D region, which is a poorly conserved domain, serves as a hinge between the DBD and the LBD, allowing rotation of the DBD. The hinge region allows the DBD and LBD to adopt different conformations without creating a steric hindrance. This domain also harbours a nuclear localization signal (NLS) or at least some elements of a functional nuclear localization signal.

E REGION (LIGAND BINDING DOMAIN)

The largest domain and the hallmark of a nuclear receptor is its moderately conserved ligand-binding domain (LBD). This domain is highly structured, and encodes a wealth of distinct functions most of which operate in a ligand-dependent manner. The highly conserved region of the nuclear receptor proteins lies near the carboxyl terminus.

The LBD is a region where chaperone proteins, such as Hsp90, bind NR when they are present in the cytoplasm. Upon ligand binding, exposure of a nuclear

localization signal in the LBD induces the nuclear translocation of the NR (6). After dissociation of the chaperones, the liganded NR–complexes can bind to particular DNA sites within gene promoters termed hormone response elements (HRE). The HRE-recruited hormone-receptor-complexes are then able to initiate chromatin remodelling and to relay activating or repressing signals to the target genes transcription machinery.

Nuclear receptor pharmacology has made us understand that ligands may exert very diverse effects, this is dependent on individual chemical structure and the allosteric changes induced in the receptor/accessory protein complex (8). Binding of agonistic or antagonistic ligands leads to different allosteric changes of NR making them able to exert positive or negative effects on the expression of target genes by different mechanisms.

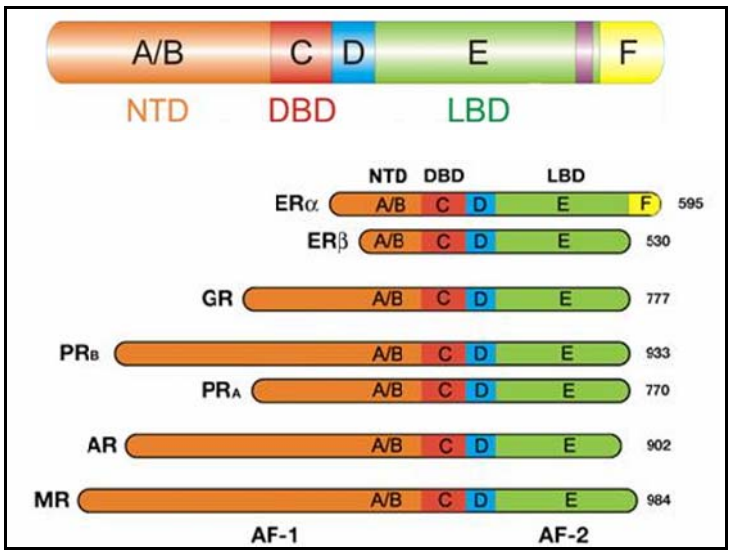

Figure 2- Steroid hormone receptors consist of six domains (A-F) based on regions of conserved sequence and function (5). The domains starting from the N-terminus (left) to C-terminus (right) are: NTD- N-terminal domain; DBD- DNA binding domain; LBD- ligand-binding domain; AF- activation function. The numbers to the right represent the lengths in amino acid residues (6).

Although a lot is known in the field of steroid hormone action, this is a relatively new area and no more than five decades old. Pivotal experiments in the late 1950's and 1960's showed that hormone-binding components exist within the nuclei of target tissues and that steroid hormones act by regulating gene expression,

rather than directly influencing enzymatic processes. The understanding that steroid hormone receptors interact with the general transcription machinery and alter chromatin structure came in the 1970's and 1980's, and details of these mechanisms continue to be elucidated in contemporary bio-medical research.

In addition, the discovery of rapid cellular responses to steroid hormones has led to the identification of membrane-bound receptors that act without affecting gene transcription which is the main focus of this thesis.

The birth of the field of steroid hormone action

Pivotal experiments performed in the late 1950's and early 1960's primarily in the laboratories of Gerald Mueller and Elwood Jensen, set the stage for the development of the field of steroid hormone action. Jensen's laboratory showed that tritiated (H^3) estradiol was specifically taken up and retained in the immature rat uterus, indicating the presence of an "estrogen-binding component" or "estrophilin" later termed "estrogen receptor" by Jensen (9, 10). This was the first time that target tissue specificity was observed for a hormone. During the same period Dr. Mueller's laboratory reported that estrogen treatment induced RNA and protein synthesis. Later the same laboratory showed that uterine responses to estrogen were blocked when both RNA or protein synthesis was inhibited, showing that gene transcription and protein translation were required for its effects (9).

Figure 3- On the right Professor Gerald C. Mueller, M.D., Ph.D. 1920-2010 and on the left Professor Elwood V. Jensen. Ph.D.

Still in the 1960's Jensen in collaboration with Jack Gorski and others demonstrated that after treatment estrogen, or estradiol, travelled from the cell cytosol to the nucleus (9, 10). This led to the belief that the ER bound estrogen in the cytoplasm and then translocated to the nucleus. However, it is currently known that the ER is in fact a nuclear factor that initiates its interaction with estrogen in the nucleus (11). Scientists at this time also concluded that steroid hormones, through their receptors, regulate gene expression rather than influencing enzymatic metabolism directly. It was in 1966 that a collaboration between Gorski and Angelo Notides showed that estrogen treatment resulted in the production of a specific

uterine protein (12). Subsequently, Bert O'Malley's laboratory demonstrated steroid-mediated mRNA induction of ovalbumin in response to estrogen and of avidin in response to progesterone (10). The 60's culminated with the first Gordon Conference on Hormone Action, establishing steroid hormone action as a legitimate and growing field of research.

The early 1970's came with an explosion of research on steroid hormone receptors. In 1972 the first steroid hormone receptor was purified, O'Malley's laboratory purified PR from chicken (13). Soon after the purification of PR, ER and AR were purified, (14, 15) and finally many years later in 1990 MR was purified (16).

The molecular biology revolution

With the advent of recombinant DNA and DNA sequencing technologies in the mid 1970's came the ability to characterize the steroid hormone receptors and their target genes in more detail. Again, O'Malley's laboratory was the first to clone (1977) and sequence (1978) a target gene for steroid hormones, ovalbumin from chicken. Cloning of the first steroid hormone receptor (GR) occurred in 1985 through collaboration between Ronald Evans', Michael Rosenfeld's, and Brad Thompson's laboratories. Shortly after this breakthrough, the receptors for estrogen (1986), progesterone (1987), aldosterone (1987) and androgen (1988) were cloned (17).

Through the work of a number of laboratories in the 1980's and early 1990's, a model for steroid receptor action at gene level began to emerge. In 1983, Keith Yamamoto's and Jan-Åke Gustaffson's laboratories demonstrated for the first time that a steroid hormone receptor (GR) binds DNA in a sequence-specific manner. The receptor binding site, now termed the steroid response element (SRE), is located within the steroid hormone-regulated promoters. In general, SREs are 15-base pair consensus sequences consisting of two half sites, arranged as 6-base pair inverted repeats separated by a few random base pairs. The SREs for various receptors exhibit significant sequence similarity, with SREs for GR, PR and AR oftentimes being identical (18).

In 1988, O'Malley's laboratory was again instrumental in showing that receptors bind the SREs cooperatively as dimmers, with one receptor molecule at

each half site (18). In vitro experiments performed in the mid 1990s demonstrated that receptor binding to DNA is not hormone dependent (19).

Still in the 1980 decade, the laboratories of Etienne-Emile Baulieu, David Toft, and William Pratt discovered that inactive steroid hormone receptors interact with a non-hormone protein, later identified as heat shock protein 90 (hsp90) (20, 21). Heat shock proteins likely stabilize unliganded steroid hormone receptors by preventing folding, aggregation and DNA binding (22). Steroid hormone receptors are the only members of the steroid/thyroid superfamily know to bind to these proteins (23). Experiments performed by the Pratt and Toft laboratories in the late 1980s demonstrated that the dissociation of heat shock proteins from receptors is hormone-dependent (24). During this decade it was also shown that hormone receptors are phosphorylated in a hormone-dependent manner. Edwin Milgrom's laboratory showed that PR is phosphorylated, and with hormone administration, becomes hyperphosphorylated (25) leading investigators to believe that steroid hormone receptor action is dependent on phosphorylation state.

After the discovery that receptors bind the SREs as dimmers, O'Malley's laboratory showed that steroid hormone receptors interact with transcription factor IIB (TFIIB), leading to the hypothesis that steroid hormone receptors facilitate transactivation via protein-protein interactions with general transcription factors. This hypothesis was soon validated when they successfully reconstructed the entire pathway of steroid hormone action in a ligand dependent, receptor-mediated, cell-free transcription system (10). It was shown that ligand-bound receptor binds the SRE and stabilizes the association of general transcription factors. This interaction between receptor and general transcription factors allows for the successful recruitment of polymerases to the promoter and subsequent transcription of the target gene.

These discoveries represented the culmination of three decades of research and led to a well supported model for steroid hormone receptor action: ligand binding induces a conformational change in the receptor, releasing heat shock proteins. The receptor undergoes hormone- and DNA-dependent hyperphosphorylation, dimerizes, and binds its target DNA. The binding of the receptors to the SRE allows for

recruitment of general transcription factors and, subsequently, RNA polymerase to begin efficient transcription (22, 25).

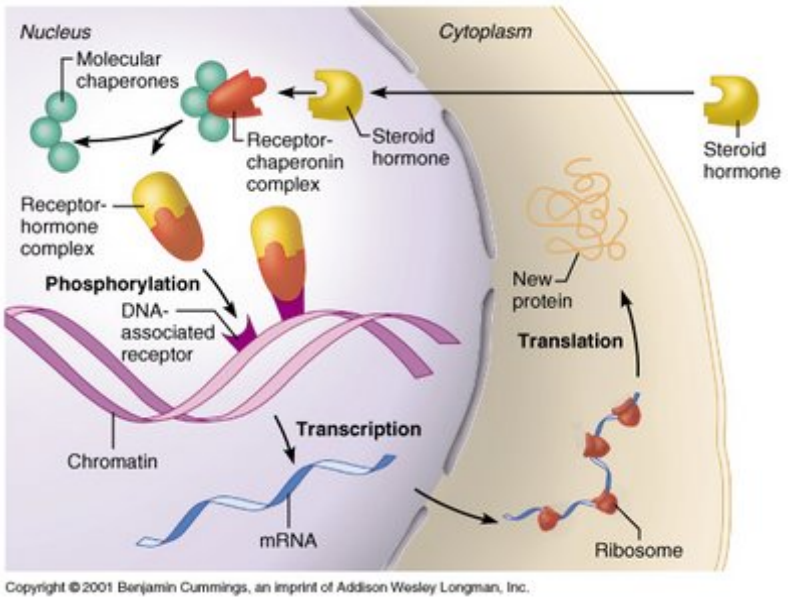

Figure 4- General model of steroid hormone receptor action.

Refining the model

Coactivators. In 1989, experiments performed in the laboratories of both O'Malley and Hinrich Gronemeyer showed that overexpression of one SHR results in the inhibition of itself or other SHRs. These results suggested that there might be other limiting factors, termed "coactivators" that modulate transactivation by steroid hormones. These coactivators are thought to function as bridging factors that, directly or indirectly, facilitate the crucial protein-protein interactions between the steroid hormone receptor and the general transcription machinery to ensure efficient transcription of target genes.

Coactivators can be receptor-specific or general. Two general coactivators, steroid receptor coactivators-1 (SRC-1) and cAMP response element binding protein (CBP), enhance the transcriptional activities of several steroid/thyroid hormone receptors (4). SRC-1 was identified in 1995 by O'Malley's laboratory and has shown to enhance the transcriptional activity of all the steroid receptors tested, without altering basal promoter activity. In 1996, Williams Chin's laboratory showed that

SRC-1 interacts with a variety of steroid and thyroid hormone receptors in a ligand-dependent manner, as well as with TATA-binding protein and TFIIB. Receptor-specific coactivators include the androgen receptor-associated protein 70, first described by Chawnshang Chang's laboratory in 1996.

Corepressors. Besides activating transcription, steroid/thyroid hormone receptors can also silence basal promoter activity of target genes in the absence of hormone or in the presence of an antagonist. This phenomenon was first observed with TR and RAR, which have shown to bind cognate DNA response elements in the absence of hormone and repress basal transcription (4). Competition experiments suggested that this silencing activity requires binding of a "corepressor". The corepressors silencing mediator for RAR and TR (SMRT) and nuclear receptor corepressor (N-CoR) were cloned in 1995 (4). These proteins are thought to act by recruiting additional proteins with histone deacetylase activity, thus inhibiting transcription complex formation through a chromatin dependent mechanism (26). Agonists, but not antagonists, are able to dislodge corepressors bound to unliganded receptors, thus relieving the silencing function. In the case of a mixed agonist and antagonist, such as tamoxifen (for ER), relief of the silencing functions may depend on the relative ratio of coactivators to corepressors (27).

Evidence for corepressor interaction with the classic steroid hormones is also emerging. Recently, ER has been shown to interact with N-CoR (26). In addition, the surprising observation that human PR-A acts as a transdominant transcriptional inhibitor appears to be due to its interaction with the corepressor SMRT and its inability to interact with coactivators (27). As receptor specific coactivators and repressors continue to be discovered, researchers can better understand how steroid hormone receptors alternate between gene silencing and transactivation functions.

The interesting fact about the biology of steroid hormone receptor action on gene expression is that it's dependent on a number of factors, including the nature of the ligand (agonist or antagonist), the isoform or subtype of the receptor, the nature of the steroid response element, and the character and balance of coactivators and corepressors. These factors confer tissue and gene specificity and begin to explain the complexity and diverse cellular roles of steroid hormone receptors.

It has been more than 50 years since two key discoveries were made in the United Kingdom, the isolation of both the steroid hormone aldosterone (28) and the structure of DNA (29) both happened in 1953. Although these discoveries were not connected, the last one allowed for the technologies of molecular biology to elucidate the mechanism by which aldosterone regulates epithelial sodium transport.

The mineralocorticoid receptor

Aldosterone, like other steroid hormones, has an intracellular receptor, which acts through a genomic mechanism to enhance the transcription of specific genes that encode putative aldosterone-induced proteins (AIPs). AIPs mediate the main physiological response to aldosterone, epithelial Na^+ transport. Various studies, now over three decades old (30), clearly demonstrated the presence of an intracellular receptor that specifically bound tritiated aldosterone in mice, these studies were later confirmed in the human kidney (31). In 1987, Arriza *et al.* cloned the human MR by low stringency hybridization with the glucocorticoid receptor cDNA from a human placental library (17). The cloned MR was found to be highly homologous to the GR and curiously, although the affinity of aldosterone for the human MR was similar to what had been reported (31), the receptor had a much higher affinity for cortisol (17).

The human MR is a 107 kDa protein with 984 amino acids and, as with other steroid receptors, contains three main domains, the central DNA-binding domain of 68 amino acids (DBD), the C-terminal ligand-binding domain (LDB), which shares 57% homology with the GR, and the N-terminal domain, which differs both in length and sequence between the two receptors (17). The DBD of the MR corresponds to a highly conserved region among members of the nuclear receptor superfamily showing 94% homology with the GR and $\approx$90% homology with other nuclear receptors. Two groups of four cysteines form α-helixes called “zinc fingers”, one of which lies in the major groove of the DBD facilitating specific contacts during transcription (see Figure 5) (17). The zinc fingers contain a P box, the interacting surface with the half site of the inverse repeat of the hormone (glucocorticoid) response element, and a D box responsible for weak dimerization with the DNA (32, 33). A specific MR response element has not been identified. An additional nuclear export signal is located between the two zinc fingers near the LBD.

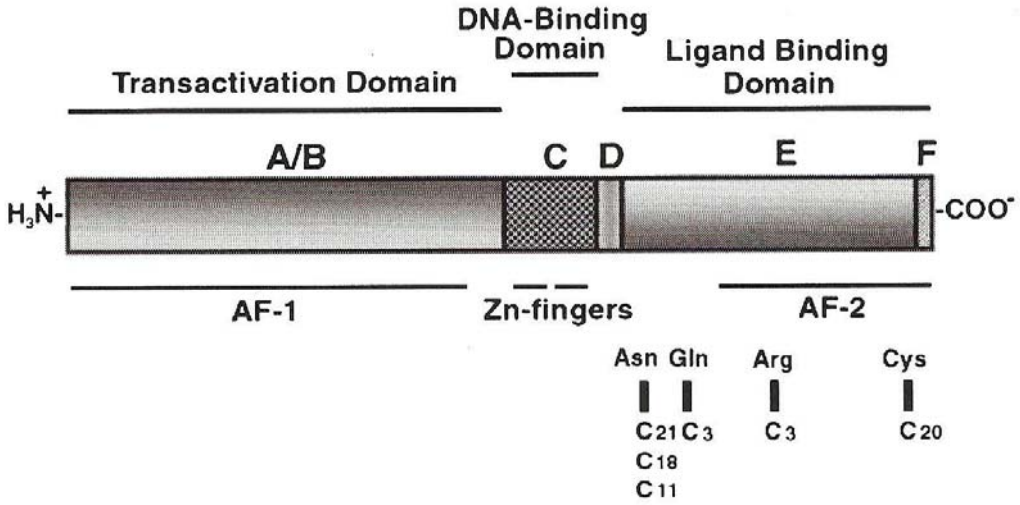

Figure 5- Consensus structure of the MR (1).

The hinge region is located between residues 671 and 732 and contains a proline stretch, which permits a twist of the DBD relative to the LBD, positioning the receptor in contact with the general transcritption machinery (34). This region also possesses weak ligand-independent nuclear localization signal (NLS1) responsible for receptor subcellular translocation.

The MR has an activating function, AF-2, within the LBD that becomes activated in a ligand-dependent manner after agonist binding in the hydrophobic pocket of the LBD. The AF-2 sequence is highly conserved and is located in helix 12 (H12) of MR.

The N-terminal domain of the MR, with 602 amino acids, is the longest and most highly variable among the steroid receptors. While it has only 15% homology with the GR, it has been conserved in evolution and is highly homologous among species. This domain contains multiple functional sites responsible for ligand-independent transactivation or transrepression.

Although the MR LDB binds both to aldosterone and cortisol with high affinity *in vitro*, the GR does not bind to aldosterone and the MR itself binds to cortisol with a lower affinity (17). However, similar binding specificities for aldosterone and cortisol were seen when the MR was isolated from the rat hippocampus (35). This work

suggested that some factor was precluding cortisol access to the MR in the kidney, but not the hippocampus. Subsequently, the groups of John Funder in Melbourne and Chris Edwards in Edinburgh showed that the carbenoxolone-sensitive enzyme, 11β-hydroxysteroid dehydrogenase (11βHSD), was responsible for this phenomenon (36). In epithelial target tissues for aldosterone and in some other tissues, aldosterone specificity is maintained by the type II isoform of 11βHSD (11βHSD2), which converts cortisol to cortisone, thereby rendering it inactive as cortisone does not bind to the MR. Inactivation of 11βHSD by ingestion of large quantities of liquorice or the administration of carbenoxolene (36) results in mineralocorticoid excess in the presence of low aldosterone levels. These features are also seen in the condition of apparent mineralocorticoid excess (AME), an autossomal recessive condition characterized by an early onset of severe low rennin hypertension with hypokalemia, yet low aldosterone levels. AME results from mutations in 11βHSD2 (36).

Ligand-binding specificity

To determine the structural basis of the specificity of the MR for aldosterone binding, Rogerson *et. al.* exploited (37) the differences and the similarities between the LBDs of the MR and GR. The MR binds and is transcriptionally active in response to both aldosterone and cortisol, whereas the GR responds primarily to cortisol (17, 37). To understand the basis of this difference, a series of chimeras was created between the LBD of the GR and the MR (37). The 14 chimeras retained their basic structural integrity in that they all bound tritiated dexamethasone, albeit with variable affinities (38). In those chimeras in which aldosterone binding was seen, trans-activation also occurred. MR sequences in the second region (amino acids 804-874 of the MR sequence) were essential for activation by aldosterone. A second round of chimeras focusing on this region between amino acids 804 and 874 of the MR LBD identified the 820-844 region as the crucial region for aldosterone binding (38).

The crystal structures of the LBD of many of the nuclear hormone receptors have been published, PR (39), AR (40), GR (41, 42). Besides containing all of the determinants for binding the hormone, the LBD also contains the C-terminal activation function-2 helix (AF-2). Crystal structures of several NR LDBs have shown

that correct positioning of the AF-2 is required for recruitment of co-activators of transcription (41-43). Understanding the ligand requirements that lead to the proper positioning of the AF-2 and activation of MR is fundamental to designing drugs that can modulate receptor activation. Overall , the MR LDB shows the three-layered α-helical fold observed in other nuclear receptor LDBs, with aldosterone bound in a fully enclosed pocket containing residues in helixes 3, 4, 5, 6, 7 and 11, and the β-turn (Figure 4*A*). As seen in other steroid receptor LDBs, the C-terminal extension of MR interacts with helix 10 via hydrogen bonds between Asp^{929} and the amide nitrogens of Phe^{981} and His^{982}. The most unusual feature of the structure is that the residues N-terminal to helix 1 (727-737) form a short helix that associates near the coactivator groove of a chrystallographically related molecule. This N-terminal feature is present in all MR complexes.

In general, MR makes interactions with aldosterone in a manner consistent with how other steroid receptors bind their natural ligands (Figure 6, *B* and *C*). There is an extensive hydrogen bond network involving the A-ring ketone of aldosterone, Gln^{776} and Arg^{817} of MR, and several water molecules that firmly lock the A-ring of the steroid in place. Specific to the MR there is a water-mediated hydrogen bond between Gln^{776} and Ser^{810}. AR, GR, and PR have a methionine at this position so this interaction is not possible. Adjacent to the D-ring, the C-18 hydroxyl makes a hydrogen bond to the side chain carbonyl of Asn^{770} on helix 3. Asn^{770} is in position to coordinate a triplet of hydrogen bonds: one between the side chain carbonyl and the C-18 OH of the ligand, and two from the side chain nitrogen to the C-21 OH of the ligand and the backbone carbonyl of Glu^{955}, a residue that lies on a loop preceding the AF-2 helix. The ligand is stabilized further by a pair of hydrogen bonds between the aldosterone C-21 hydroxyl, C-20 ketone, and Thr^{945} located on helix 10. This threonine is conserved in GR and PR but is replaced by leucine in AR.

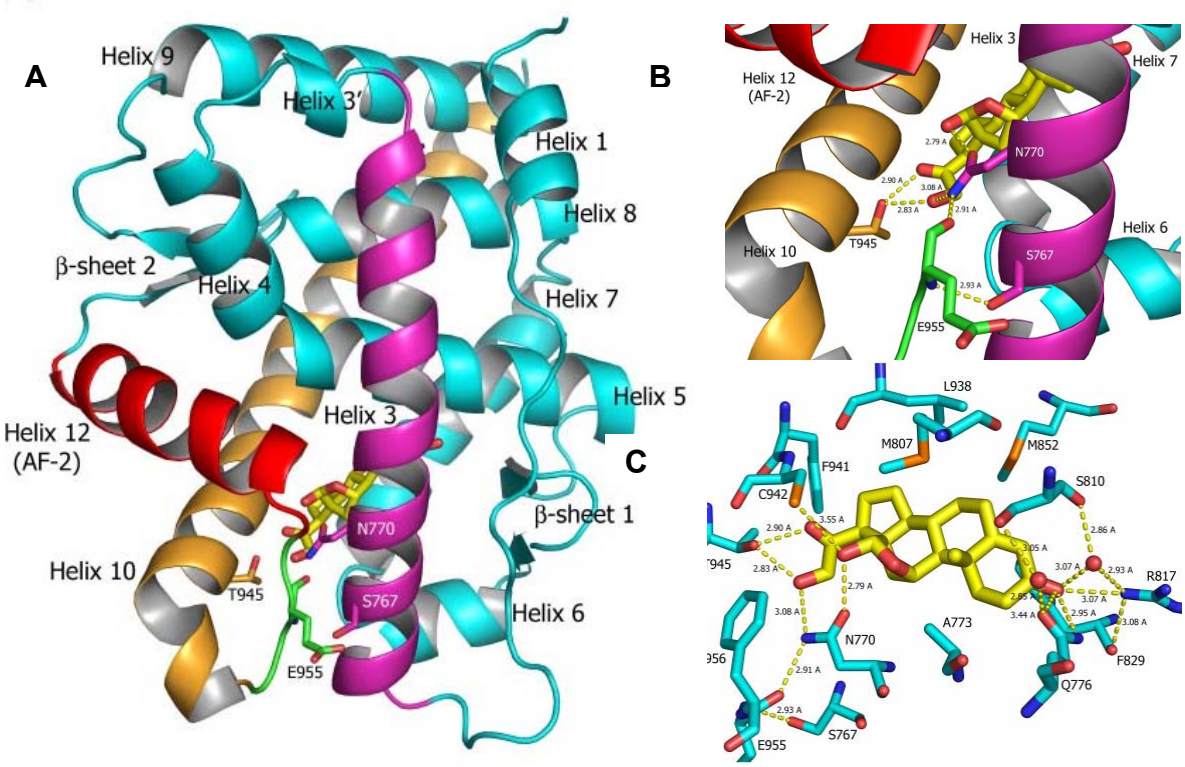

Figure 6- Crystal structure of MR LDB bound to aldosterone. *A*- the overall fold of the MR is very similar to the other steroid receptors. *B,* helix 3 (magenta) residues Asn^{770} and Ser^{767} form hydrogen bonds (yellow dashed lines) with the loop (green) residue Glu^{955} preceding the AF-2 (red). Thr^{945} present on helix 10 (orange) plays a key role in receptor activation by hydrogen bonding to the C-20 carbonyl and C-21 hydroxyl of aldosterone (yellow). *C,* close-up view of MR-aldosterone hydrogen bond network. The 18-OH is positioned for hydrogen bonding with the Asn^{770} carbonyl, whereas the Asn^{770} amide remains in position for hydrogen bonding to the C-21 OH of aldosterone and Glu^{955}, which lies in the loop preceding the AF-2. Thr^{945}, present on helix 10, forms a pair of hydrogen bonds with the C-20 and C-21 substituents of aldosterone. Cysteine 942 is in position to interact with the 18-OH group to give aldosterone three potential hydrogen bonds to helix 10 (41).

It is clear from the crystal structure that the orientation of Thr^{945} is ideal for hydrogen bonding with steroids containing C-20 carbonyls and C-21 hydroxyl groups (Figure 6, *B* and *C*) (41).

In addition to Asn^{770}, Ser^{767} is in position to make a hydrogen bond to the backbone amide of Glu^{955} in the loop preceding the AF-2. This observation suggests that both of the helix 3 residues (Asn^{770} and Ser^{767}) play a role in stabilization and activation of MR. Notably, interference with the interaction between helix 3 and the loop preceding the AF-2 reduces MR activation (44). Amino acid alignments of the

receptors show that an asparagine is conserved in a similar position in all of the oxosteroid receptors, suggesting that the interaction between helix 3 and the loop preceding the AF-2 may be a conserved mechanism of steroid receptor action. Two properties of steroid ligands dictate that an asparagine is required at position 770 in MR to stabilize the helix 3/loop interaction. First is the length of the steroid itself, and second are substituents at the C-11 position of the steroid.

In summary, maximum MR activation occurs only when there is simultaneous stabilization of the loop preceding the AF-2 helix and a strong interaction of the ligand with helix 10. Stabilization of the loop preceding the AF-2 requires hydrogen bonds between Asn^{770} and Ser^{767} on helix 3 and Glu^{955} present on this loop. Ligands that promote this hydrogen bond network and interact with helix 10 via hydrogen bonds or hydrophobic interaction with Thr^{945} induce a stabilization of helix 3 and a movement of the AF-2, enabling coactivator recruitment and ultimately gene transcritption. This series of ligand-mediated activation steps ensures that ligands such as progesterone and cortisone fail to activate MR even though these ligands will be in excess over aldosterone in many tissues. Likewise, spironolactone also fails to activate MR because of an inability to create the hydrogen bonding network and thus behave as a passive MR antagonist.

Genomic Structure and Organization

The human MR gene (NR3C2) is located in chromosome 4 in the q31.1 region (43), spans ≈450 kb and is composed of ten exons (45). The two first exons are referred as exon 1α and 1β and correspond to the 5' untranslated region in the human. They are followed by eight exons that code for the protein with exon 2 encoding the N-terminal domain (NTD or A/B region). Exons 3 and 4 code for the 2 zinc fingers of the DNA binding domain (C region) and the last five exons code for the LDB (45). Alternative transcription for these 5'-untranslated exons generate different mRNA isoforms that are differentially expressed in aldosterone target tissues (46, 47). Mineralocorticoid receptor translation starts 2 bp downstream from the beginning of exon 2 and the translated protein is the same for the two 5'-untranslated isoforms.

There are functional splice variants of the MR. A 12 bp insertion between the two zinc fingers results from the use of a cryptic splice site at the exon3/intron C splice junction creating a splice variant that is expressed in most tissues (44), but its transactivation activities are not significantly different from the wild-type (48-50). A 10 bp deletion in the rat and human MR leads to a truncation in the LBD and unresponsiveness to aldosterone. It is expressed at low levels in the rat and human tissues and does not interfere with the wild-type mRNA activity (51). An additional alternative splice variant skips exons 5 and/or 6, leading to the co-repression of the Δ5 or the Δ5,6 human mineralocorticoid receptor mRNA isoforms (52). This isoform retains de DNA-binding domain and can act in a ligand-independent manner (52).

Post-Translational Modifications of the MR

The MR is a phosphoprotein (53-55) with multiple consensus sites for phosphorylation (Figure 5). Rapid phosphorylation of serine and threonine residues occurs within minutes of exposure to aldosterone. These are mediated in part by protein kinase C alpha (PKCα) activation and might be involved in the rapid, nongenomic effects of aldosterone (56). There is some evidence that phosphorylation by PKCα enhances MR function, but this could be due to phosphorylation of an associated co-regulator rather than a direct effect (57). Inhibition of serine/threonine phosphatases inhibits MR transformation and inhibits DNA binding (55). Except for the nongenomic effects, the role of phosphorylation remains unclear (56, 58).

Sumoylation, modification by SUMO (small ubiquitin-related modifier), is a post-translational modification common to most steroid receptors (59-61). The MR has four sumoylation consensus motifs in the N-terminal end at positions K89, K399, K428 and one in the LBD at K593 of the human sequence (Figure 7). The consensus motifs for sumoylation are named synergy control motifs and are defined by the sequence consensus ΨKXE, where X is any residue and the Ψ is an aliphatic residue. These sites are highly conserved through evolution. Studies have shown that the transcriptional activity of the MR can be modulated by its sumoylation potential, as well as the sumoylation of MR-interacting proteins, and requires the continuous function of the proteosome (62). Acetylation of the receptor is also

theoretically possible as it has a consensus sequence for acetylation, but it remains to be demonstrated (63).

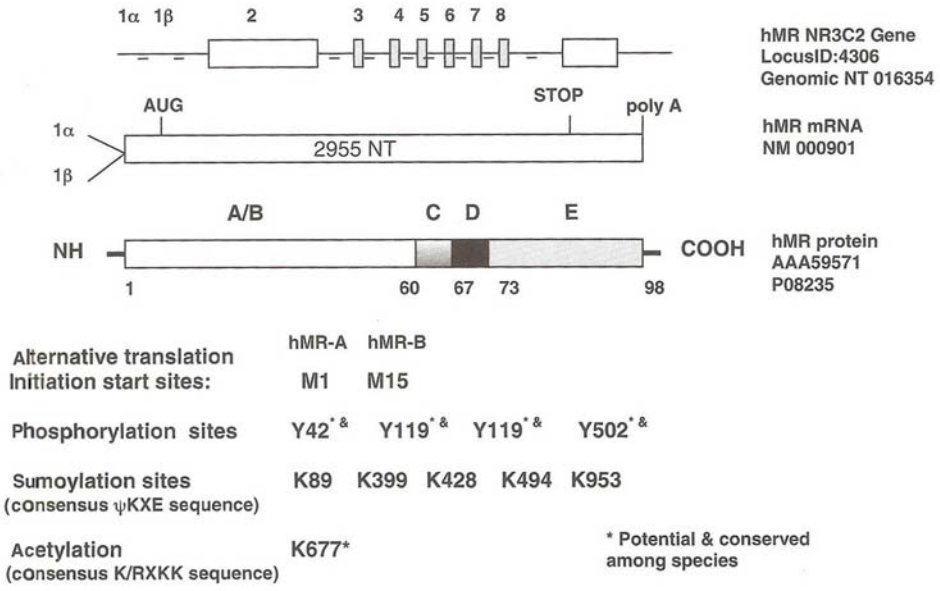

Figure 7- The human mineralocorticoid receptor gene, mRNA, protein functional domains and post-translational modifications. The intron, exon structure of the gene and the two different promoters are shown in the upper part of the figure. The middle part represents the mRNA and in the lower part the MR protein and its different domains are shown (1).

MR Trafficking

In their mature form, steroid receptors are associated to 90-kDa and 70-kDa heat shock proteins, the small acidic protein p23 and proteins that posses tetratricopeptide repeats (TPR), i.e. sequences of 34 amino acids repeated in tandem that are critical for protein-protein interactions. In the steroid receptor heterocomplex, the TPR-acceptor site of hsp90 is normally occupied by either high molecular weight immunophilin (IMM) FKBP52, FKBP51, CyP40 or PP5 (64). IMMs are a family of intracellular receptors for immunosuppressant drugs also characterized for having peptidylprolyl isomerase (PPIase) enzymatic activity, which directs *cis-trans* isomerization of peptidylprolyl bonds (65). The oligomeric structure of untransformed SRs is also found in primarily nuclear receptors such as progesterone and estrogen receptors.

Upon aldosterone binding, the MR moves rapidly, within minutes, towards the nucleus, whereas it cycles back to the cytoplasm upon ligand withdrawal much more slowly, more than 18 hours. A classical model accepted for more than two decades posits that the ligand binding-dependent dissociation of the hsp90-based heterocomplex (a process frequently referred to as “transformation”) is a must for the nuclear translocation of SRs (66, 67). This model was based on the assumption that the chaperone complex anchors the SR to the cytoplasm, impairing its nuclear translocation. The transformation model, although unproven, prevailed until recent years.

A key discovery was that a cytoplasmic dynein co-immunoprecipitates with FKBP52 (68). Dyneins are molecular motors that generate force towards the minus end of microtubules and are related to the retrograde movement of vesicles. Cargo attachment occurs via the dynein intermediate chain, whereas the ATP-hydrolitic domain responsible for the motor function is located in the heavy chains. The actual microtubule-binding site is a small globular unit that protrudes from heavy chains. It then became clear that the dynein-IMM interaction involves the PPIase domain of the IMMs (68, 69), a property that appears to be a common feature for most high molecular weight IMMs associated with SRs (70). Importantly, at least two of the most abundant IMMs found in SR•hsp90 complexes, FKBP52 and PP5, co-localize with microtubules. These observations implied that an active transport system requiring hsp90, IMMs, dynein motor proteins and cytoskeletal tracts moves SRs within the cell towards the nucleus.

If correct, this would mean that the hsp90•IMM complex associated with the untransformed receptor should not dissociate upon ligand biding because it would be required for the retrograde movement of the ligand-receptor complex. Results from an experiment using tritiated aldosterone and a continuous sucrose movement clearly contradict the unproven classical model: transformation is not an early event (69). Also in agreement with the new model, the cytoplasmic-nuclear movement of hsp90•IMM-chaperoned factors is impaired or blocked by hsp90 inhibitors (geldanamycin or radical), overexpression of the PPIase domain of FKBP52 (preventing dynein binding), saturation of the hsp90•IMM binding site with TPR and by overexpression of the dynein complex subunit, p50/dynamitin, which disrupts the

dynein-dynactin complex and dissociates cargo from dynein (Figure 6). Thus, there is ample evidence that validates a model in which the retrograde movement of certain soluble factors occurs in an active manner via cytoskeletal tracts with the hsp90•IMM complex forming the bridge between the cargo and the motor protein responsible for the retrograde movement of SR and that this system can be uncoupled by some inhibitory agents.

Figure 8- The molecular machinery for movement of the MR and the agent for selectively uncoupling the system. Arrows show the sites of uncoupling by hsp90-disrupting agents such as geldanamycin (GA), the TPR domain fragment of PP5, the PPIase domain fragment of FKBP52 and the p50/dynamitin (*Dyt*). Immunophilin TPR domain (*black crescent*). Dynein heavy chains (*HC*), intermediate chains (*IC*) (1).

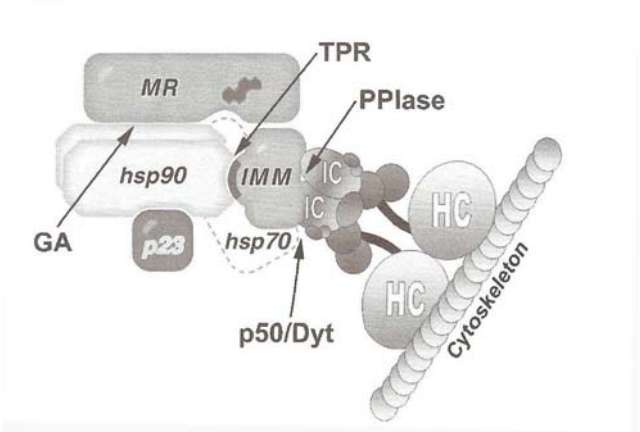

Aldosterone-induced proteins

Although it has been recognized many years ago that aldosterone acted to increase (or decrease) the expression of specific genes (30), the identification of these target genes has only occurred in the past decade or so (71). Six genes are known to be acutely regulated by a rapid and transcriptional response to aldosterone, namely genes encoding the three epithelial Na^+ channel subunits α, β and γ (*SCNNIA,-Band -G*), channel-inducing factor (*FXYD4*), serum and glucocorticoid-induced kinase (*SGK*) and K-ras2 (*KRAS2*) (Figure 9). In addition, there is evidence to support the regulation of three other genes, those encoding glucocorticoid-induced leucine zipper protein (49), N-myc downstream-regulated gene (50), and the kidney specific WNK1 isoform (72).

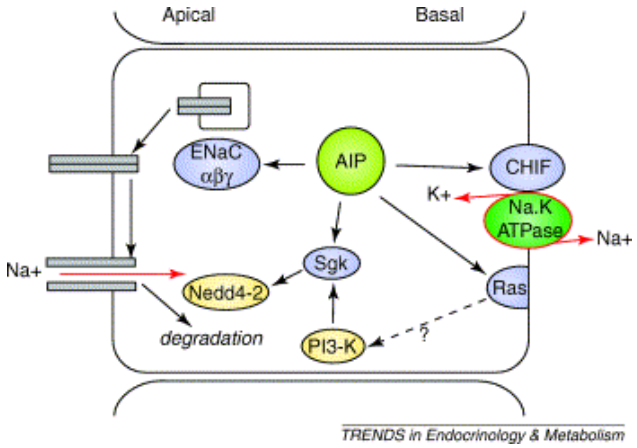

Figure 9- Schematic representation of an aldosterone-responsive epithelial cell. The putative interactions of the AIPs in relation to the epithelial Na^+ channel (ENaC) and the basolateral Na^+ pump (Na.K-ATPase) are shown (65). A possible role for phophatidylinositol 3-kinase (PI3-k) in integrating different signalling pathways (66) is indicated. Abbreviations: CHIF, channel-inducing factor; sgk, serum- and glucocorticoid-induced kinase.

The amiloride-sensitive epithelial Na^+ channel (ENaC) is the key rate-limiting step at the apical membrane for the Na^+ flux across transporting epithelial cells (51, 71). The other key mediator of epithelial Na^+ transport is the energy-dependent pump, Na.K-ATPase, which is located in the basolateral membrane, where it mediates the efflux of Na^+ (71). The activity of Na.K-ATPase increases in response to aldosterone. The genes encoding the Na.K-ATPase α- and β-subunits are not acutely regulated by aldosterone, although increased levels are part of the response to chronic aldosterone administration.

ENaC is a key component of the response to aldosterone and therefore an obvious candidate for regulation (51). The genes encoding the ENaC β- and γ-subunits in the distal colon are regulated by aldosterone (53, 71). The gene encoding the α-subunit, but not the β- and γ-subunits of ENaC, is similarly upregulated in the kidney (54). However, the time course of this response and the magnitude of the change are inadequate to explain the increased amiloride-sensitive Na^+ flux that occurs in response to aldosterone (71).

Probably the best characterized AIP is sgk (73, 74). This protein is rapidly upregulated by aldosterone in the colon and distal nephron (1, 32). Two studies (33, 75) have demonstrated the ability of sgk to interact with the ubiquitin ligase Nedd 4-2

and, through that interaction, to inhibit the action of Nedd 4-2, thereby prolonging the half-life of the ENaC channels in the apical membrane. The molecular characterization of the monogenetic hypertension syndrome or Liddle's syndrome (72) has shown the importance of the degradation of the ENaC channels as part of their regulation (75). Nedd 4-2 plays an important role in this process. When the interaction between Nedd 4-2 and the C-terminus of the ENaC β- and γ-subunits is compromised, the channels exhibit a prolonged half-life, resulting in increased Na^+ flux (75).

Work on amphibian systems has shown that *KRAS2*, particularly the 2A isoform, is acutely upregulated by aldosterone (75, 76). It is possible that the interaction might involve the phosphatidylinositol 3-kinase pathway, which is responsible for the phosphorylation of sgk (66).

The other well characterized aldosterone-induced gene, *FXYD4* (77), is regulated in the distal colon but not the kidney (78, 79). It is an acute primary transcriptional event (74). Although the initial studies of channel inducing factor (CHIF) (77) suggested that it might interact with a K^+ channel, recent information from the same group has demonstrated an interaction with Na.K-ATPase (80). CHIF belongs to the FXYD family of small transmembrane proteins, which includes the γ-subunit of Na.K-ATPase; this subunit is not upregulated by aldosterone in the distal colon (71). CHIF has the reverse effect of the γ-subunit in that it increases the affinity of the pump for Na^+ and therefore increases flux through the pump (80). This is a probable mechanism through which aldosterone increases the activity of the basolateral pump.

Regulation of Aldosterone Production

Aldosterone represents the primary mineralocorticoid produced by the adrenal gland and specifically within the outer adrenocortical cells of the glomerulosa layer. Aldosterone is synthesized in the glomerulosa from cholesterol through the successive actions of four enzymes (Figure 10). Cholesterol side-chain cleavage (CYP11A1), 21-hydroxilase (CYP21) and aldosterone synthase (CYP11B2) are members of the cytochrome P450 family of enzymes. CYP11A1 are localized to the inner mitochondrial membrane, while CYP21 is found in the endoplasmic reticulum. These enzymes are P450 heme-containing proteins that accept electrons from

NADPH via accessory proteins and utilize molecular oxygen hydroxylations (CYP21 and CYP11B2) or other oxidative conversions (CYP11A1). The fourth enzyme, type 2 3β-hydroxysteroid dehydrogenase (HSD3B2), is a member of the short-chain dehydrogenase family and is localized to the endoplasmatic reticulum.

Historically, the regulation of aldosterone biosynthesis has been divided into two main phases. Acutely (minutes after a stimulus), aldosterone production is controlled by rapid signalling pathways that increase the movement of cholesterol into the mitochondria (Figure 12). This has been called the “early regulatory step” and, is mediated by increased expression and phosphorylation of StAR protein (81). Chronically (hours to days), aldosterone production is regulated at the level of expression of the enzymes involved in the synthesis of aldosterone (82). This has been called the “late regulatory step” and is particularly dependent on increased transcription and expression of CYP11B2 (Figure 13).

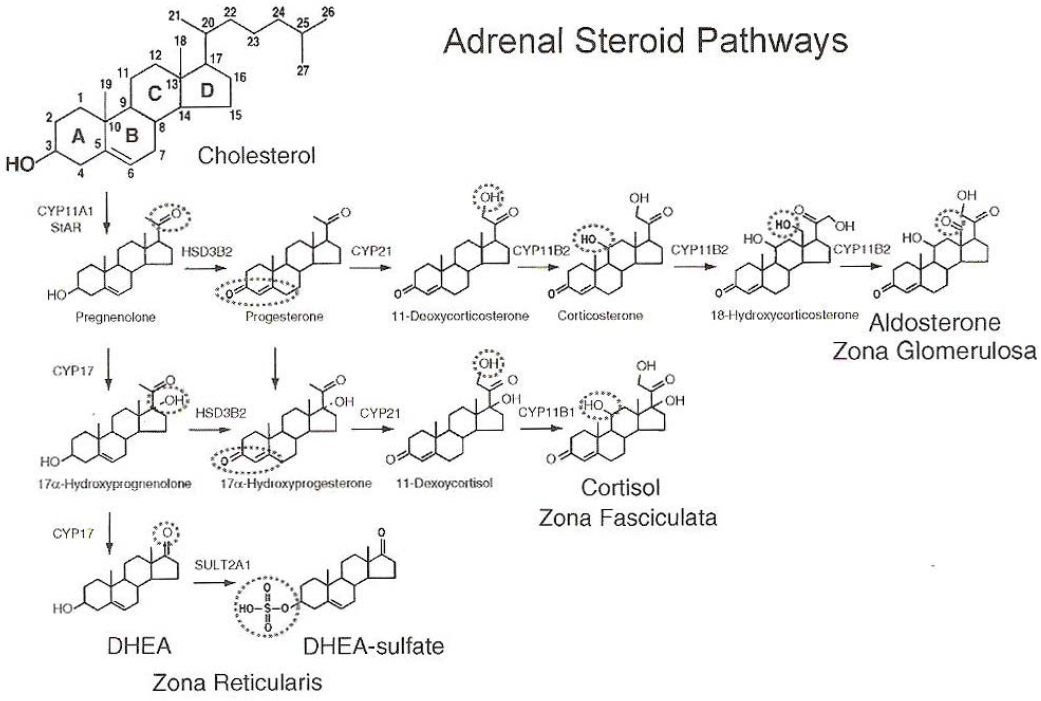

Figure 10- Adrenal steroid pathways leading to mineralocorticoid, glucocorticoids and adrenal androgens. Enzymes involved include side-chain cleavage (CYP11A1), 3β-hydroxysteroid dehydrogenase type 2 (HSD3B2),17α-hydroxylase, 17,20 lyase (CYP17), 21-hydroxylase (CYP21), 11β-hydroxylase (CYP11B1), and aldosterone synthase (CYP11B2). Steroidogenic acute regulatory (StAR) protein is needed for the rate-limiting movement of cholesterol to CYP11A1 in the inner mitochondrial membrane (1).

Factors Regulating Aldosterone Production

The Renin-Angiotensin-Aldosterone System (RAAS)

Because the major function of aldosterone is to control body fluid volume by increasing sodium reabsorption by the kidneys, it is appropriate that the major regulator for aldosterone synthesis and secretion arises in the kidneys. Thus, the kidneys play the controlling role in the rennin-angiotensin-aldosterone feedback system (Figure 11). Renin is a protease produced and stored in the juxtaglomerular cells that surround the glomerular afferent arterioles. Renin release is controlled by at least three mechanisms. First, release is activated by a decrease in the perfusion pressure of blood traversing the renal afferent arterioles, which is sensed by the juxtaglomerular apparatus functioning as a baroreceptor. This reduction in perfusion pressure occurs as a result of a decrease in either systemic blood volume or blood pressure. Second, renin secretion can be stimulated by secretions from the macula densa as a result of a drop in sodium concentration in the distal tubule. Third, a drop in blood pressure will cause sympathetic stimulation of juxtaglomerular cells to stimulate both renin release and afferent arteriole constriction.

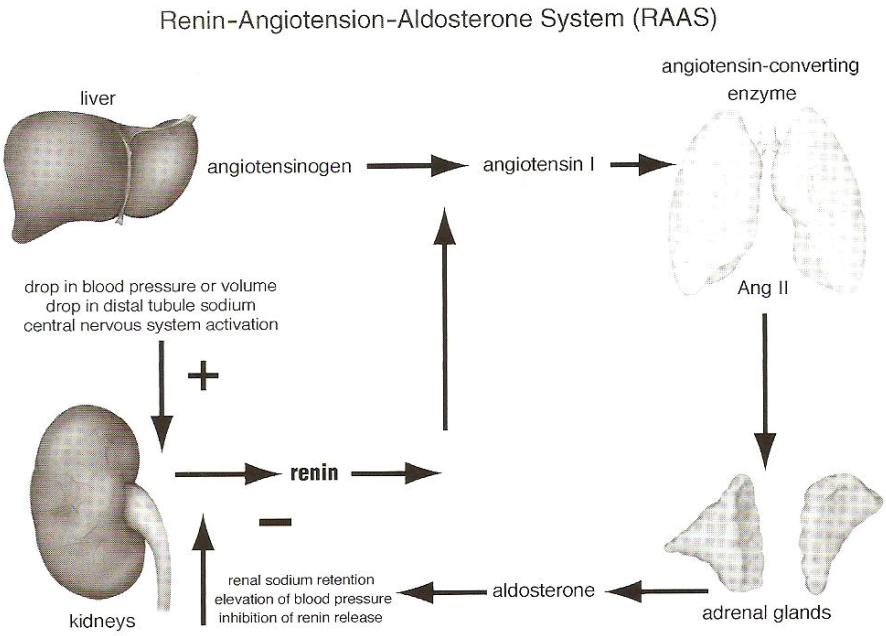

Figure 11- Aldosterone production is primarily regulated through a feedback loop that focuses on kidney production of renin. Once released, renin cleaves angiotensinogen to angiotensin I through the action of angiotensin-converting enzyme (ACE) to produce

angiotensin II. Angiotensin II is the primary hormonal regulator of adrenal aldosterone production. Aldosterone indirectly exerts negative feedback to decrease renin release through renal sodium retention and elevation in the blood pressure (1).

Acting in the blood, renin mediates the rate-limiting step in the production of angiotensin II (AngII), cleaving the circulating precursor angiotensinogen to release the 10-amino acid peptide, angiotensin I. Thereafter, inactive angiotensin I is rapidly converted to the potent octapeptide hormone AngII by the action of angiotensin-converting enzyme (ACE), which is found in the plasma membrane of vascular endothelial cells throughout the body. Circulating AngII is the arguably the most important regulator of adrenal glomerulosa aldosterone production.

Angiotensin II-Regulated Intracellular Glomerulosa Cell Signalling Pathways

In humans AngII has two G-protein-coupled receptors, type 1, (AT_1) and type 2 (AT_2), through which this hormone can elicit intracellular responses. AngII works primarily through AT_1 receptors to regulate aldosterone production (Figure 10). The expression of AT_1 receptors is highest in the glomerulosa, which localizes the action of this hormone to aldosterone-producing cells. AT_1 receptors activate a variety of signalling pathways including phosphoinositide-specific phopholipase C (PLC), which hydrolyzes phosphatylinositol 4,5-biphosphate (PIP_2) to generate the two second messengers, inositol 1,4,5-triphosphate (IP_3) and diacylglycerol (DAG) (83). IP_3 is thought to initiate aldosterone secretion by eliciting a transient increase in the cytosolic calcium concentration and activating calcium/calmodulin-dependent protein kinases (CaM kinase), whereas DAG increases protein kinase C (PKC) activity. PKC activity has been suggested to underlie sustained aldosterone secretion from glomerulosa cells (83).

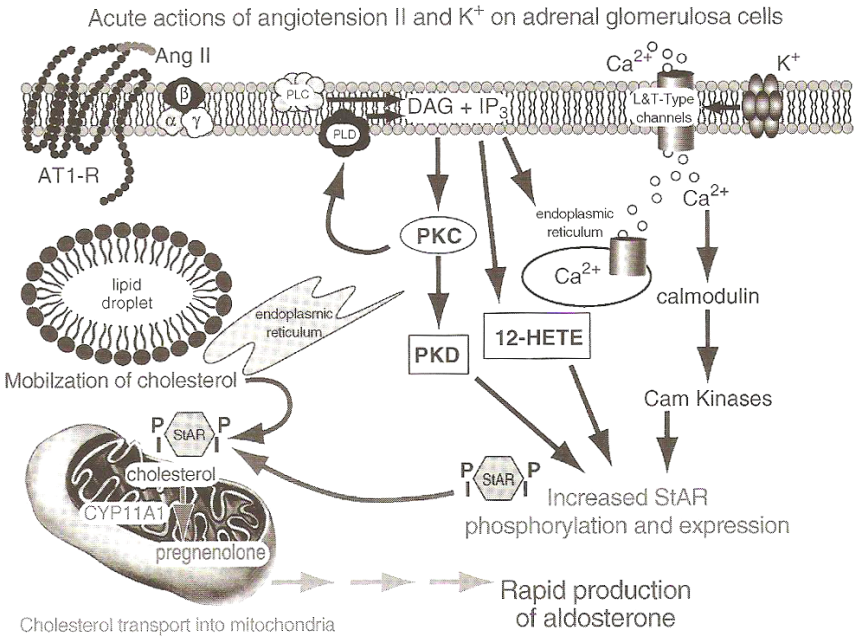

Figure 12- The acute regulation of aldosterone production is primarily regulated by AngII. AngII binds to AT_1 receptor (AT1-R) activating PLC to release DAG and IP_3. PLC activation also increases cellular levels of 12-HETE. DAG activates PKC, PKD and PLD. In turn, IP_3 causes release of intracellular calcium stores. CaM kinases, 12-HETE and PKD increase StAR protein levels and phosphorylation leading to increased cholesterol movement into the mitochondria. Within the mitochondria cholesterol is converted to pregnenolone by CYP11A1 which is then metabolized to aldosterone (1).

AngII also increases calcium influx in glomerulosa cells. Influx of extracellular calcium acts to increase PKC activity, enhance PKC-stimulated steroidogenesis and maintain aldosterone production (84). In addition to activating PKC, the DAG produced by AngII-stimulated phospholipid hydrolysis also serves as a precursor for other signals regulating aldosterone secretion. Thus, arachidonic acid can be released by DAG lipase and is then metabolized by 12-lipoxygenase to generate 12-hydroxyeicosatetraenoic acid (12-HETE) (85). 12-HETE appears to play an important role in mediating AngII-induced aldosterone secretion since blocking its production or metabolism reduces AngII-induced steroidogenesis (85).

The second and rate-limiting step of steroidogenesis involves transfer of the mobilized cholesterol from the outer mitochondrial membrane to the inner membrane, where CYP11A1 is localized and initiates steroid production. StAR seems to be

responsible for that role but the mechanism by which StAR induces cholesterol movement is not clear. Several hypothesis have been proposed, none of which seem entirely satisfactory. The molten globule model suggests that near the mitochondrial membrane, a high concentration of protons converts a structured tertiary conformation of the StAR carboxy terminus into a semi-ordered molten globule, which as secondary but not tertiary structure (86). However, whether the pH is sufficiently low to trigger this transition or whether such a relatively unstructured domain could efficiently transport cholesterol is unclear. Other models have similar shortcomings, such that the mechanism of StAR's action remains unclear. Nevertheless, StAR is clearly required for the translocation of cholesterol from the outer to the inner mitochondrial membrane and this rate-limiting step is controlled by signalling pathways that are activated by aldosterone secretagogues.

Chronic Effects of Angiotensin II

Chronically, AngII increases adrenal aldosterone production through two major actions. First, AngII increase expression of the enzymes needed to produce aldosterone, particularly CYP11B2. Second, AngII causes hypertrophy and hyperplasia of the adrenal glomerulosa, thus increasing the number of aldosterone-producing cells. *In vivo* studies have provided strong evidence that sodium restriction increases renin/AngII levels causing an induction of glomerulosa CYP11B2 expression (87, 88).

The increase in CYP11B2 expression appears to result from increased transcription of the gene (89). Activation of the transcription appears to rely on the activation of transcription factors that bind to a cyclic AMP response element (CRE) found in the proximal region of the CYP11B2 promoter (90). In addition, both AngII and potassium rapidly induce the expression of the nuclear hormone receptor NR4A3, which also binds the promoter and activates CYP11B2 transcritption (82).

AngII regulation of long-term aldosterone relies on other signalling pathways. AngII treatment activates adrenal cell protein kinase D (PKD) and this activation is associated with increased CYP11B2 expression, suggesting that this pathway may be involved in CYP11B2 regulation. Further, AngII-induced PKD activation is dependent upon PKC (91). However, PKD is known to phosphorylate and stimulate transcriptional activity of the cAMP response element binding (CREB) protein

transcription factor (92, 93). The promoter region is highly dependent on CREB response elements (89), suggesting that this PKD-mediated CREB activation may be important in regulating chronic aldosterone synthetic capacity.

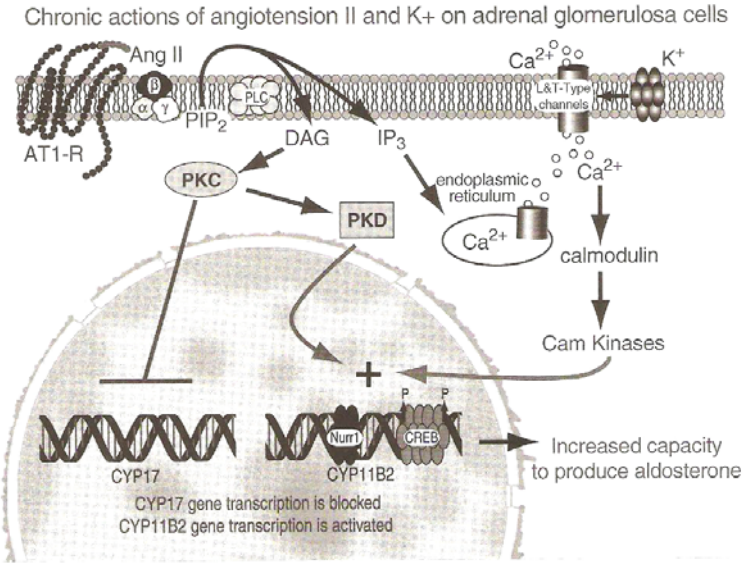

Figure 13- The chronic regulation of aldosterone production is mainly due to angiotensin II and potassium. Angiotensin II binds to AT_1 receptors (AT1-R) to activate PLC activity, which releases DAG and IP_3. DAG activates PKC and PKD, and IP_3 causes intracellular calcium release. PKC activation inhibits the transcription of CYP17, while calcium and PKD increase transcription of CYP11B2. This occurs through increased expression and phosphorylation of specific transcription factors. The increase in CYP11B2 increases the capacity to produce aldosterone (1).

The role of potassium in the regulation of aldosterone production is often underestimated. Infusion of potassium will cause an acute increase in aldosterone production and a high potassium diet will increase aldosterone levels as well as the capacity of the adrenal to produce aldosterone. The mechanism by which potassium regulates aldosterone production relies on the extreme sensitivity of the glomerulosa cell membrane to small increases in potassium concentrations. Indeed, small increases in potassium stimulate calcium influx, via depolarization of the plasma membrane and activation of voltage-dependent calcium channels. As with AngII stimulation, this influx is also thought to activate CaM kinase (94) and is required for elevated potassium-induced aldosterone secretion, since inhibition of calcium influx abolishes the elevated potassium-stimulated secretory response (83).

ALDOSTERONE EFFECTS

Kidney

The kidney plays the primary role in salt and water homeostasis, maintaining osmolarity and volume in the extracellular space within a very narrow range despite wide variations in fluid and salt intake. Aldosterone plays a significant role in the maintenance of mammalian sodium, potassium, water and acid-base balance, primarily through effects on renal electrolyte excretion. Aldosterone promotes stimulation of Na^+ absorption, potassium and hydrogen secretion by tight epithelia that display high transepithelial electrical resistance and amiloride-sensitive sodium transport. This epithelium is found in distal segments of the nephron, bladder, distal parts of the colon and rectum and in the ducts of exocrine glands (salivary, sweat glands) (95).

Sodium transport across the epithelia is driven by an electrochemical potential difference across the apical membrane allowing for passive movement of ions and water and by an active transport of ions across the basolateral membrane. The apical-membrane step is mediated by the opening of the amiloride-sensitive sodium channels that are sodium-selective. The basolateral extrusion of sodium is mediated by activation of a ouabain-sensitive sodium potassium ATPase (96).

Vectorial sodium transfer induced by aldosterone occurs mainly in the distal nephron and distal colon. Sodium entry in the cell at the apical membrane is regulated by the amiloride-sensitive epithelial sodium channel (ENaC). Efflux of sodium from the epithelial cell at the basolateral membrane is energy-dependent and is mediated by the sodium-potassium ATPase (Na^+-K^+ ATPase). Aldosterone stimulates Na^+ transport by activating pre-existing sodium channels (96).

ENaC is composed of three subunits α, β, γ, which are regulated by corticosteroids in a tissue specific manner, however, this is not the principal mechanism by which aldosterone regulates ENaC activity (76). More importantly aldosterone can alter ENaC subunit turnover (degradation) and increase the number of channels located in the plasma membrane. Turnover of ENaC is mediated by ubiquitin protein ligase, Nedd4-2 (75).

Under Na^+ replete conditions, when aldosterone levels are low, ENaC is mainly in an intracellular location (77). Na^+ absorption in response to aldosterone increases before any changes in mRNA for the subunits are observed (78) suggesting that aldosterone first induces the transcritption of proteins that modulate ENaC trafficking or function. One aldosterone-induced protein is SGK, a member of the serine-threonine kinase family. Sgk1 overexpression results n a large increase in Na^+ current, but has no effect on K^+ channel activity, due to an increase in the number of ENaC channels at the cell surface (74). Sgk1 phosphorylates Nedd4-2, decreasing its binding to ENaC and resulting in ENaC surface expression. Aldosterone stimulation results in a rapid increase in Sgk1 which peaks 1-2 hours after exposure (79).

The late phase of aldosterone regulation of ENaC involves the increase in the expression of αENaC mRNA and protein in the kidney with no changes in the β or γ subunits (80, 97).

Nongenomic effects of aldosterone

Nongenomic effects of aldosterone which occur too rapidly to be mediated by gene transcription, insensitive to inhibitors of transcription (actinomycin D) or translation (cyclohexamide) have been postulated to be mediated by a membrane receptor different from the soluble MR (98-100). Some membrane MR effects may be inhibited by classical MR antagonist, but not others.

Nongenomic effects of aldosterone on ion transport proteins have been studied. Aldosterone has been show to regulate the Na^+/K^+ exchange isoforms (NHE) NHE1 and NHE3. The Maldin-Darby canine kidney cells (MDCK cells) have properties corresponding to collecting duct intercalated cells and demonstrate nongenomic responses to aldosterone. At physiologic concentrations, aldosterone had rapid (1-2 minutes) nongenomic stimulatory effects N^+/H^+ exchange in these cells as determined by increases in pH and Na^+ concentration (101, 102). The rapid effects were not prevented by actinomycin D, cyclohexamide or spironolactone and resulted from an increase in affinity of the exchanger for intracellular H^+. The rapid stimulation of N^+/H^+ exchange by aldosterone depends on an increase in intracellular Ca^+, as well as rapid phosphorylation of the extracellular signal-regulated kinase (ERK1/2) (101).

Cardiovascular System

In recent years, our understanding of aldosterone has changed from considering it to be a hormone mainly responsible for fluid and electrolyte balance to a hormone with widespread cardiovascular and metabolic effects. A large body of literature demonstrates that activation of the mineralocorticoid receptor by aldosterone increases oxidative stress, inflammation, insulin resistance and vascular dysfunction, leading to renovascular and cardiovascular injury and stroke. Further, clinical studies using the selective MR antagonist, eplerenone, or the non-selective antagonist, spironolactone, have demonstrated beneficial cardiovascular and renovascular effects in patients with heart failure, diabetes and hypertension. The adverse cardiovascular actions of MR involve both genomic and nongenomic mechanisms.

- *Heart*

Approximately 50 years after the discovery of aldosterone, several large-scale clinical studies revealed potent beneficial effects of MR antagonist on the heart. The Randomized Aldalactone Evaluation Study (RALES) was designed to test the effect of an MR antagonist in addition to standard therapy, including angiotensin-converting enzyme (ACE) inhibitors, on mortality in patients with severe heart failure secondary to systolic left ventricular dysfunction with ejection fraction $\leq$ 35% (103). Spironolactone treatment had clear benefits with a 30% reduction in relative risk of death. Hospitalization rate for worsening heart failure was 35% lower in the spironolactone group than in the placebo group. In addition, spironolactone caused a significant improvement in the symptoms of heart failure. Further, the beneficial effect of spironolactone was observed without significant effects on blood pressure.

The benefit of MR blockade in heart disease was confirmed in the Eplerenone Post-Acute Myocardial Infarction Heart Failure Efficacy and Survival Study (EPHESUS). This study was designed to test the effect of eplerenone, a selective MR antagonist, on mortality and hospitalization rates in patients with left ventricular dysfunction and heart failure after acute myocardial infarction (104). During a mean follow-up of 16 months, there was a 15% relative risk reduction in overall mortality

and 17% relative risk reduction in cardiovascular mortality. Hospitalization rates were also significantly lower in the eplerenone group.

Two small clinical studies suggest a beneficial effect of MR blockade on diastolic dysfunction. Treatment for 6 months with MR antagonist canrenone improved diastolic function, as compared to placebo treatment, in patients with hypertension and left ventricular diastolic dysfunction on ACE inhibitor and calcium channel blockade therapy (105). The improvements in diastolic function with canrenone were not mediated by changes in blood pressure or left ventricular mass, suggesting that MR blockade has a direct beneficial effect on diastolic function. In another study in patients with dilated cardiomyopathy, 12 months of treatment with spironolactone led to decreased myocardial collagen content, decreased myocardial stiffness and ameliorated diastolic dysfunction (106).

Thus, available clinical data demonstrate benefits of MR blockade in the treatment of heart failure, left ventricular hypertrophy and diastolic dysfunction. The potential mechanisms for these beneficial effects have been investigated using cell culture systems and animal models of cardiovascular injuries.

Animal models of cardiac injury have clearly demonstrated an adverse effect of mineralocorticoids on the heart and vasculature. Activation of the MR for 8 weeks through administration of aldosterone or deoxycorticosterone led to hypertension and cardiac fibrosis in uninephrectomized rats on a moderately high sodium diet (1% NaCl in drinking water) and MR blockade prevented this damage (107, 108). In a short-term (14 day) rodent model of hypertension and cardiovascular injury, rats receiving a nitric oxide synthase (NOS) inhibitor, AngII and a moderately high sodium diet developed coronary artery injury, myocardial necrosis and inflammation in both right and left ventricles (109, 110). Vascular injury was characterized by increased expression of plasminogen activator inhibitor (PAI-1), inflammation, intimal thickening and vascular wall necrosis with surrounding granulation tissue. Treatment with eplerenone or spironolactone to block the actions of aldosterone or adrenalectomy to reduce circulating aldosterone levels prevented the injury, while injury recurred when adrenalectomized animals were infused with aldosterone. In this model, there was minimal cardiac fibrosis suggesting that vascular injury is an early event in aldosterone-mediated cardiovascular injury leading secondarily to myocardial ischemia and necrosis followed by repair and fibrosis.

Several investigators demonstrated that activation of MR by administration of aldosterone, deoxycorticosterone acetate or an inhibitor of 11βHSD2, increased coronary vascular expression of pro-inflammatory molecules, cyclo-oxygenase 2 (COX-2), monocyte chemoattractant protein-1 (MCP1) and osteopontin in uninephrectomized rats on a moderately high sodium diet (111, 112). These vascular changes preceded the development of cardiac fibrosis. In these pre-clinical studies of cardiovascular injury, the beneficial effects of blocking the MR or reducing aldosterone via adrenalectomy appeared to be independent of effects on volume homeostasis and blood pressure as vascular injury was ameliorated without reductions in blood pressure (110, 111).

Thus, vascular injury and dysfunction appeared to play a key role in the pathophysiology of aldosterone-induced cardiac injury. However, aldosterone's adverse vascular effects are not limited to the heart but, extend to brain, kidney and peripheral vasculature.

- *Renal disease*

Aldosterone blockade has been shown to reduce albuminuria in hypertensive patients independent of an effect on blood pressure itself (113, 114). Eplerenone caused a reduction in 35% of urinary albumin excretion. Similarly, in older patients with isolated systolic hypertension, eplerenone reduced microalbuminuria to a much greater extent than amlodipine (a drug used to treat for this condition). One mechanism for the apparent increase in mineralocorticoid-mediated renal injury may involve increased renal expression of MR. Renal biopsies of patients with renal disease demonstrated a marked increase in renal expression of the MR in individuals with high albuminuria, compared to those with lesser amounts of albuminuria (115).

MR blockade also reduces renal injury in non-diabetic animal models. In rodents on a moderately high sodium diet, administration of a NOS inhibitor and AngII caused proteinuria and renal arteriopathy that was prevented by administration of eplerenone or adrenalectomy (110). The injury was again present when adrenalectomized rats were infused with aldosterone, demonstrating that aldosterone is required for the induction of AngII renal injury in this model. Similarly, blockade of the MR or adrenalectomy reduced proteinuria and renal arteriopathy in other hypertensive rodent models of AngII-mediated renal injury (116).

Potential mechanisms mediating the cardiovascular effects of aldosterone

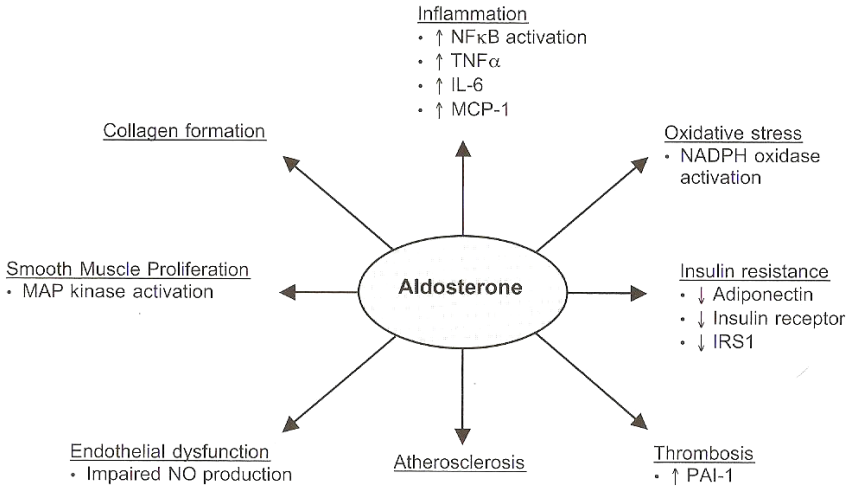

Figure 14- potential mechanisms of aldosterone-induced adverse cardiovascular effects (1).

- *Effect of Aldosterone on Intracellular Signalling Pathways*

In addition to aldosterone's well characterized effects on gene transcription, aldosterone has rapid nongenomic effects that appear to involve cross-talk between the MR and other signalling cascades, many of which are associated with cardiovascular injury. A research group led by Grossman demonstrated that aldosterone increased phosphorylation of ERK through a process dependent on aldosterone-mediated increases in c-Src phosphorylation and transactivation of epidermal growth factor receptor (EGFR) (117, 118). Further, they identified the c-terminal EF domain of the MR, which includes the ligand binding region, as the region that mediates these nongenomic actions of aldosterone on ERK activation (119). Other investigators reported that aldosterone interacts synergistically with angiotensin II to increase ERK activation (120). Aldosterone-mediated phosphorylation of c-Src also leads to increased activation of MAP kinases and NADPH oxidase in rat vascular smooth muscle cells (121). In endothelial cells, aldosterone increased superoxide generation via activation of Src, NADPH oxidase and the small GTP-binding protein Rac-1 (122).

Thus, aldosterone has effects on multiple intracellular processes including activity of EGFR and angiotensin II receptor, oxidative stress and activity of ERK, c-Src and MAP kinase signalling pathways. Activation of these pathways may mediate some of the adverse effects of aldosterone. For example, aldosterone stimulation of MAPK1 led to increased vascular smooth muscle proliferation (122).

- *Vascular Function*

Aldosterone affects vasoconstriction and vasodilation. In mesenteric resistance vessels, aldosterone potentiated phenylephrine-mediated constriction through a nongenomic process involving PI3K and PKC, but not ERK activation (123). In rabbit preglomerular arterioles, aldosterone promoted vasoconstriction through these same pathways, but also stimulated vasodilation through increases in endothelial-derived nitric oxide (NO) (124). In intact aortic rings, the vasodilatory effects of aldosterone appeared to dominate. However, when the endothelium was removed from the aortic ring, aldosterone reversed the effect, indicating dominance of aldosterone's vasoconstrictive properties under these conditions (125).

Additional studies suggest that aldosterone may reduce endothelial NO. In human umbilical vein endothelial cells (HUVEC), MR activation increased generation of oxygen reactive species, which can inactivate NO, and decreased NOS expression (126). Also, aldosterone was shown do decrease endothelial glucose-6-phosphate dehydrogenase (G6PDH) expression and activity leading to increased oxidative stress, decreased NO and impaired vascular reactivity (127). In conclusion, while aldosterone has both vasodilatory and vasoconstrictive actions, most preclinical studies supported an adverse effect on vascular function. In disease states, such as heart failure, the adverse vascular effects of aldosterone also appear dominant.

- *Inflammation*

Studies in animal models of cardiac and renal injury, have clearly demonstrated the pro-inflammatory effects of aldosterone. *In vitro* studies, suggest that these inflammatory effects are due in part to direct pro-inflammatory actions of aldosterone. In human coronary artery smooth muscle cells, aldosterone increased gene expression of pro-inflammatory molecules as well as those involved in fibrosis and calcification (128). Aldosterone increased N-κB transcriptional activity and MCP-1 expression in cultured mesangial and proximal tubule cells (129, 130) and increased TNF-α, IL-6 and MCP-1 in adipocytes cultures (131, 132). These pro-inflammatory effects of aldosterone are also observed in humans (133).

- *Insulin sensitivity*

Obesity is often associated with hypertension and one of the mechanisms of obesity-induced hypertension involves increased mineralocorticoid activity (134).

Increased aldosterone levels were associated with an increase in insulin resistance (135). The underlying mechanism for aldosterone overproduction in obesity is not clear. Some studies linked increased production of aldosterone to mineralocorticoid releasing factors from the adipocytes (136). Another hypothesis suggests the role of hepatic intermediaries in the stimulation of adrenal aldosterone by fatty acids produced by visceral adipocytes (137).

The mechanism of aldosterone-induced insulin resistance may involve effects of aldosterone on the adipose tissue. MR has been shown to mediate corticosteroid-induced adipocyte differentiation (138). Furthermore, aldosterone increased expression of pro-inflammatory factors, decreased expression of adiponectin and PPAR-γ and reduced insulin-stimulated glucose uptake in culture adipocytes (131, 132). *In vivo* studies in the *db/db* mouse model of obesity and diabetes demonstrated that the blockade of the MR reduced adipose tissue inflammation, decreased adipose tissue expression of pro-inflammatory factors, increased adipose tissue expression of adiponectin and PPAR-γ and improve measures of insulin sensitivity (131).

- *Dietary Sodium*

In animal models, dietary sodium intake has been shown to have a profound effect on aldosterone-mediated cardiovascular injury. A low dietary sodium intake prevented the development of cardiac and renal injury uninephrectomized rats infused with deoxycorticosterone acetate for 8 weeks, whereas the animals developed profound cardiac and perivascular fibrosis when consuming a high sodium diet (139). Also, rats receiving a NOS inhibitor and AngII developed vascular and cardiac injury when on a moderately high sodium diet. However, a low sodium diet prevented this injury despite markedly elevated blood levels of aldosterone (107). These studies suggest that increases in circulating aldosterone that are appropriate for the level of sodium consumption, i.e. elevated aldosterone levels in individuals consuming a low sodium diet, may not result in cardiovascular injury. Rather, cardiovascular injury occurs when aldosterone is elevated relative to dietary sodium intake (140). In contrast to dietary sodium, modulation of dietary potassium does not have a major effect on aldosterone-mediated cardiovascular injury (141).

The estrogen receptor

17β-Estradiol (E2) is the main ligand to the estrogen receptor (ERα/β) (Figure 15). E2 is secreted into the bloodstream by the adrenal cortex and gonads and plays a prominent role in mediating sexual development and behaviour, reproductive functions, proliferation and differentiation of various tissues via ER. For example, E2/ERα interaction is responsible for E2-induced proliferation of breast and uterine tissue.

ERα was first isolated in 1962, the corresponding gene cloned in the same year (142) and subsequently located to the long arm of chromosome 6 (6q24-q27; today 6q25.1) (143). Three decades later, in 1993, the first ERα knockout mouse was created and led to the discovery that development was possible without ERα (144). At that time, ERα was thought to be the only receptor mediating responses to E2, but in 1996 ERβ was cloned (145).

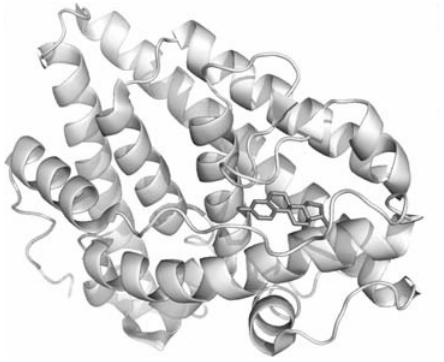

Figure 15- Molecular structure of ERα bound to E2. Ligand Domain of ERα complexed to E2. Image based on X-ray structures (3).

E2 binds with a high affinity to ER, whereas metabolic products of E2, like estrone or estriol, bind with a much lower affinity. Estrogenic action can be influenced pharmacologically by anti-estrogens and selective estrogen receptor modulators called SERMs. The first SERM clinically tested was tamoxifen in the 1970s and still today tamoxifen is used, with very good results, for the reduction of breast cancer incidence in high-risk premenopausal and postmenopausal women (146).

Estrogen receptor protein structure

Steroid hormone receptors share a high level of homology, conservation of three dimensional structure and protein domains (Figure 16).

A/B-domain (amino acids 1-180)

The A/B domain is also called activation function 1 (AF1). Concerning ERs, different splice variants of AF1 may modulate transcriptional activity by repressing AF1-mediated transactivation upon heterodimerization with full-length ER. Interestingly, in contrast to ERα, ERβ AF1 contains a repressor domain that decreases overall receptor transcriptional activity by masking transactivation of the amino terminal domain and it only functions in the context of a full length receptor (147).

Figure 16- Estrogen receptor domains. The ER is composed of a variable N-terminal domain (A/B), an AF1 protein domain which is weakly conserved (<15%) among NR members and a highly conserved DNA-binding domain (DBD) or C-domain (96%), which in the case of ERα/β binds EREs. The palindromic character of this sequence supports ER binding as a dimer. The receptors also have a flexible hinge region (D) and a C-terminal E-domain, containing the ligand-dependent AF2 region. ERα and ERβ contain an additional F-domain at their carboxy-terminal ends. Numbers on the right represent the length of each receptor protein in amino acids (148).

C-domain (amino acids 181-263)

The C-domain of ER consists of a DNA-binding domain (DBD), which is highly homologous. It features two zinc-finger motifs, which are not only responsible for DNA-binding, but also for the dimerization of the receptors, allowing the formation of homo- and heterodimers. In addition to the zinc fingers, there are also two alpha-helical motifs within the DBD, where the first helix directly interacts with the DNA major groove, while the second helix stabilizes the complex. ERα and ERβ dimmers

bind DNA with comparable affinities as either homo- or heterodimers to the same estrogen response elements (EREs) and regulate similar sets of genes.

D-domain (amino acids 264-302)

The D-domain is also referred to as the Hinge-region and contains a serine residue (S305) that can be phosphorylated in ERs.

E and F-domains (amino acids 303-552 and 553-595)

The carboxy terminal E-domain (also called AF2) represents a ligand binding domain (LBD) and an interaction site co-activators and co-repressors. The carboxy terminal F-domain represents the last 45 amino acids in ERα and approximately the last 30 amino acids in ERβ where it possibly functions to internally restrain dimerization of ER, thus protecting against improper ligand activation (149).

ER isoforms

With eight total ERα coding exons, up to five different ERα transcript isoforms/variants have been detected in humans due to alternative usage of eight 5' untranslated exons, exonic duplications, alternative splicing and intronic exons (150). The length of human ERα correlates mainly with 595 amino acids, where in different cell lines protein variants derived from mRNA splice products have been confirmed, e.g. human ERα-36 (ERα-36 kDa), ERα-46 kDa and ERα-66 kDa (151, 152). Interestingly, the ERα-36 lacks both transcriptional activation domains (AF1+2) and contains an exon coding for myristoylation sites, thus predicting an interaction with the plasma membrane (152).

Like ERα, ERβ also displays several transcriptional isoforms/variants, including seven untranslated 5' exons, alternative exonic splicing and intronic exons (150).

Co-activators and Co-repressors

SRC-1 was the first co-activator identified and has been shown to interact with different nuclear receptors (153). SRC-2, also termed glucocorticoid receptor-interacting protein 1 (GRIP1), transcriptional intermediary factor 2 (TIF2) or nuclear receptor co-activator 2 (NCoA2), binds to AF2 of specific nuclear receptors. Although not considered a real co-activator, the MUC1 oncoprotein not only binds directly to ERα, but also increases the recruitment of SRC-1 and SRC-2, thus enhancing ER mediated transcription following E2 stimulation of breast cancer cells (154).

The third member of the SRC family, SRC-3, was identified and described as retinoic acid receptor interacting protein (RAC3), mouse homolog CBP-interacting protein (p/CIP), hRARβ-stimulatory protein (ACTR) and TR-interacting protein (TRAM1). p/CIP and the human isoforms are involved in cellular proliferation, differentiation, migration and up-regulated in breast cancer (155). The demonstration of an interaction of SRC family members (also called the p160 family) with the CREB binding protein (CBP) and its homolog p300 has provided further insight into the molecular mechanisms. Importantly, co-activators exert their functions in at least two ways: on the one hand interacting with components of the transcription machinery (153), and on the other hand recruiting p300/CBP, which possesses both intrinsic and associated histone acetyltransferase (HAT) activities (156), thus promoting transcription by opening the chromatin structure.

In 2001, a novel co-activator PELP1 (proline, glutamic acid and leucine-rich protein), not related to the SRC family was identified (157). PELP1 also interacts with CBP and p300 to enhance transcription, and additionally affects cell cycle progression. PELP1 was also described to be involved in histone modification, especially in the displacement of H1 (158).

Evidence supports that antagonist-mediated inhibition of ERα not only blocks co-activator recruitment but also facilitates the recruitment of a variety of co-repressors to ERα (159). The nuclear receptor co-repressor (NCoR1) and silencing mediator for retinoic and thyroid receptor (SMRT or NCoR2) are found in complexes with histone-deacetylases supporting their role in chromatin modification into a transcriptionally less active state (160). Interestingly, ER does not interact with co-

repressors in the absence of a ligand, but only interacts when antagonists or modulators of estrogenic action (e.g. tamoxifen) are bound (161).

Estrogen receptor signalling

The most well-characterized steroid hormone receptor signalling occurs via a cellular genomic response where lipophilic ligands diffuse through the cellular membrane, bind to ER, induce a conformational change and release heat shock proteins (hsp) (Figure 17). Upon unveiling a nuclear localization signal (NLS), ligand bound receptor dimmers translocate to the nucleus and along with a variety of cofactors bind to specific response elements know as estrogen response elements (EREs) located in the promoters of target genes resulting in a transcriptional regulation of such target genes. In addition to freely diffusing steroids, Hames et al. demonstrated that megalin, an endocytic receptor in reproductive tissues, may provide an active transport mechanism for cellular uptake of biologically active androgens and estrogens (162). Also mediated by ligand binding and even independent of ligands, activation of membrane associated steroid hormone receptors can signal via a rapid cellular but nongenomic response occurring in seconds or minutes where activation of signal transduction pathways or second messenger signalling results in target gene activation.

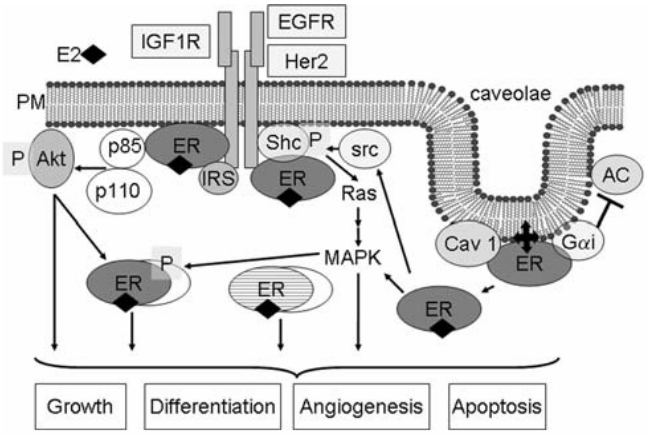

Figure 17- Model of ER-signalling: the main ER-signalling in cells occurs via a genomic response after binding of steroid hormones or analogues. Following ligand binding and release from the chaperones hsp70 and/or hsp90 (163), ER dimers (*middle grey striped oval circle*) translocate to the nucleus where they regulate target genes, resulting in specific

cellular outcomes. In addition, membrane associated ER can signal via a rapid response leading to cellular fates. ER membrane association can occur following different membrane receptor activations, like IGF-1R, EGFR or Her2 via PI3-K (p85 and p110) (*grey stick receptor*) and lead to further signal transduction of AKT or with Shc via MAPK pathway. In addition, palmitoylated was also found at specific membrane domains, called caveolae (*far right*) associated with caveolin 1 (CAV_1), which inhibits adenocyclase (AC) via $G_{\alpha 1}$ and results in ER dissociation from the membrane after ligand binding through de-palmitoylation (164). *Black diamond* E2, *cross* palmitoylation, *P* phosphorylation*, IRS* Insulin receptor substrate, *PM* plasma membrane (148).

Nongenomic estrogen signalling

The model of nongenomic responses arose from studies demonstrating that E2 repeatedly exerted effects that were too fast to be based on transcriptional events. The ER membrane form is predicted to be a full length ER (165), an isoform (166), or a completely distinct receptor (167). ERs harbour neither transmembrane nor intrinsic kinase domains, which could explain membranous signalling events, thus specific modifications like myristoylation, palmitoylation and protein interactions are most likely involved to target and maintain ER at the plasma membrane. The adaptor protein Shc and the Insulin-like growth factor 1 receptor (IGF-1R) were shown necessary for membrane localization of ER by siRNA knock-down assays (168).

In endothelial cells, as in other cell types, ER was shown to target lipid rafts within the plasma membrane (caveolae) by interaction with caveolin-1, where it activates endothelial nitric oxide synthase (eNOS) through protein kinase-mediated phosphorylation (169). Caveolae facilitate signal transduction by providing a location for various signalling molecules (170).

Activation of ER by phosphorylation was demonstrated in a hormone-dependent as well as hormone-independent manner and is an integral regulatory mechanism of nongenomic responses (Figure 15). Martin et al. demonstrated for the first time the involvement of AKT, also called Protein Kinase B, in phosphorylation of ERα (171). AKT becomes activated by growth factors binding to tyrosine-kinase receptors which signal via phosphatidylinositol 3-kinase (PI3K). Major regulatory proteins for AKT regulation in the signalling pathway are phosphatase with tensin

homology (PTEN) and target of Rapamycin (mTOR). PTEN is a lipid phosphatase specific for 3'phosphorylated inositol phosphates and inhibits AKT, whereas the mTOR kinase is essential for AKT phosphorylation (172). Upon phosphorylation and activation AKT functions in two ways, on the one hand augments transcription of ERα, and on the other hand increases ER activity by phosphorylating AF1 on different residues. Increased protein phosphorylation of both AKT and PTEN along with *PTEN* gene mutations, deletions or loss of expression have been detected in hormone responsive tumours, which would lead to an enhancement of ER signalling.

Protein Kinase A (PKA) is also involved in regulating ERα transcriptional activity by phosphorylation of ER S236 in one zinc finger of the DBD, this modification was found to inhibit dimerization and DNA-binding and had attenuating effects. Cholera toxin, a G-protein activator, in combination with 3-isobutyl-1-methylxanthine, a phosphodiesterase inhibitor, and Dopamine have all been demonstrated to increase intracellular cAMP levels and activate PKA (173).

Caveolins

Caveolin proteins are primary structural components of caveolae, which form 50-100nm plasma membrane invaginations in various cell types (174). Caveolae are involved in several cellular processes including cholesterol homeostasis, vesicular transport and regulation of signal transduction (175). There are three known caveolin proteins caveolin-1 (CAV_1) (176), caveolin-2 (CAV2) (177), and caveolin-3 (CAV3) (178). CAV_1 and CAV2 are expressed in a variety of tissues, including endothelial (179), epithelial (180), and neuronal (181), and have overlapping expression in most tissues. CAV3 is expressed mainly in skeletal and smooth muscles (178) and the nervous system (181). While ablation of CAV_1 and CAV3 resulted in a complete loss of caveolae formation (182, 183), disruption of CAV2 did not seem to affect caveolae formation (184).

The plasma membrane invagination structure of caveolae supports functional protein-protein interactions and cluster of several discrete signalling pathways. Thus, caveolae are thought to integrate interactions of receptors and signalling molecules in the plasma membrane, resulting in rapid and specific signal transduction (175). The caveolin scaffolding domain (CSD) of CAV_1 binds numerous signalling

molecules, including Src family kinases, c-Neu, H-Ras, EGFR, eNOS, and G-protein coupled receptors (GPCRs). Interaction of the CSD domain with these signalling molecules holds them in an inactive state, which is released upon activation by the appropriate stimuli (185).

The ability of CAV_1 to hold and orchestrate the spatio-temporal pairing of membrane localized ERα with its effectors makes CAV_1 an important scaffolding protein mediating membrane ERα actions. CAV_1 is required for estrogen-mediated ERα-dependent eNOS production in endothelial cells (186). In MCF-7 breast cancer cells and in vascular smooth muscle cells, overexpression of CAV_1 increases estrogen-dependent ERα translocation to the cell membrane and potentiates nuclear ERα-mediated gene expression (187).

More recently, CAV_1 has also been shown to interact with the WD-repeat protein striatin, which has been shown to be a key intermediary of the effects of steroid receptors, specifically estrogen receptor-α (ERα) (188). Lu et al provided evidence that striatin´s N-terminal segment interacts with the DNA binding domain of ERα in the immortalized human endothelial cell line, EA.hy926 cells. This interaction organizes the ERα-eNOS membrane signalling leading to rapid nongenomic activation of downstream signalling pathways including ERK and eNOS in endothelial cells.

WD-repeat proteins: Striatin, Zinedin and SG2NA

The WD-repeat-containing family of proteins is defined by two main characteristic features: a lack of intrinsic catalytic activity and repeated units of beta-sheet motifs that are arranged into a beta-propeller structure to form a platform on which multiple protein complexes can dynamically assemble. In this way WD repeat containing proteins play a major role in cellular events by mediating important protein-protein interactions by providing a permissive scaffold for the anchorage of several diverse molecules that are important in cellular signalling, cytoskeletal assembly and vesicular trafficking.

Striatin, zinedin and SG2NA are three distinct but structurally related WD-repeat proteins that share high protein sequence homology within both C- and N-terminal domains.

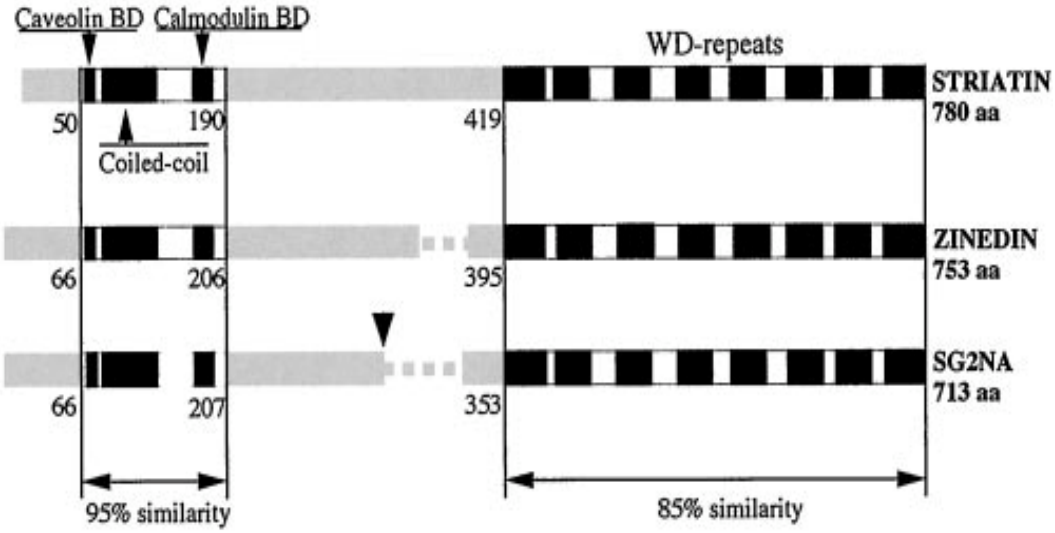

Figure 18. Schematic representation of protein-protein interaction domains present in the WD-repeat proteins, striatin, zinedin and SG2NA. Percentage homology within the mapped interaction domains (black boxes) are indicated. Gray boxes represent poorly conserved regions between the three proteins and may contribute to differential functions of these molecules. The respective amino acid length of each protein is also noted. The arrow head indicates the position of an additional amino acid present in SG2NA (189).

Striatin, which comprises 780 amino acids and weighs 110 kDa, was first isolated from brain synaptomes as a calmodulin-binding protein. It contains at least four protein-protein interaction domains (see Figure 18), including caveolin-binding, coiled-coil, and Ca^{2+}-calmodulin (CaM) binding at the N-terminus, and a series of eight WD repeat domains at the C-terminus (190). Overexpression of striatin in endothelial cells resulted in an increase in ERα localization within membrane-enriched fractions containing EGFR and IGF-1 receptor and a slight decrease in the presence of nuclear ERα suggesting that it plays a role in the cellular distribution of ERα bringing it in close proximity to membrane receptors where it can potentially be involved in cellular signalling (188). In this way, the N-terminus of striatin (amino acids 1-203) has been found interact with the N-terminus of ERα (amino acids 185-253) while the C-terminal WD repeat domain binds the GPCR ($G_{\alpha i}$) complex. Therefore, striatin serves as a scaffold directing ERα to the plasma membrane and bridges ERα with the GPCR ($G_{\alpha i}$) complex to facilitate assembly of a membrane signalling complexes required for rapid estrogen extra-nuclear activation of MAPK,

Akt, and eNOS in endothelial cells (188). Interestingly, disruption of the striatin-ERα interaction had no effect on estrogen-mediated gene transcription suggesting that striatin specifically mediates ERα extra-nuclear signalling independent of ERα nuclear actions.

Phylogenetic analysis of the WD proteins striatin, zinedin and SG2NA suggest that are derived from an ancestral gene through gene duplication to explain their similar gene and protein characteristics. Furthermore, tissue expression; at least in the mouse, overlap and appear to be localized within the same tissue types. In this way, these three WD protein members may potentially play an important and functional role in mediating steroid receptor dependent signalling.

Materials and Methods

Cell Lines and Cell Culture

During the course of this work two cell lines were used: EA.hy926 and IMR90.

EA.hy926

Immortalized endothelial cell lines are very often used as a model of endothelium for studies of various processes connected with its functions. Among the hybrid cells, the EA.hy926 cell line, derived by the fusion of HUVECs with the continuous human lung carcinoma cell line A549, is presently the best characterized macro-vascular endothelial cell line (191). The EA.hy926 cells used in these experiments were a kind gift from Dr. Cora J Edgell and were obtained from the Tissue Culture Facility at the University of North Carolina Lineberger Comprehensive Cancer Centre.

Cells were grown in Dulbecco's Modified Eagle's Medium (DMEM) media (DMEM 4,5g/L Glucose with L-Glutamine and sodium pyruvate by Cellgro, Manassas, USA) complemented with 10% Fetal Bovine Serum (FBS) (Gibco®, Invitrogen™, Carlsbad, USA) and 1% Pencilin/Streptomycin solution (100U/ml penicillin, 100μg streptomycin; Gibco®, Invitrogen™, Carlsbad, USA.

Cells were kept at low passages (1-13) due to informal reports by other groups, stating that the expression of certain proteins was lost or diminished if the cells were used past after passage 16. Cells were passaged at a 1 to 16 ratio (4500 cells/cm^2).

IMR90

The IMR90 cell line is a human diploid fibroblast strain derived by W.W. Nichols and associates from the lungs of a 16-week female foetus (192). The division potential, viral susceptibilities and other properties have been thoroughly studied such that the line may be considered as an alternate for WI-38 and other standard human lung cell strains. The cells have been reported to be capable of attaining 58 population doublings before the onset of senescence.

The IMR90 cells used were acquired from the American Type Culture Collection (catalogue number CCL-186™) (ATCC®, Manassas, VA, USA) and

maintained until population doubling (PDL) 48. IMR90 cells were grown and passaged in MCDB 131 media (Gibco®, Invitrogen™, Carlsbad, USA) complemented with 10% FBS and 1% Pencilin/Streptomycin solution. Cells were passaged at a 1 to 6 ratio (4000 cells/cm^2).

Primary Cell Culture

Primary cells are thus called because they are derived directly from a living organism. In the case of the work here presented healthy C57BL/6 mice were used to collect aortic endothelial cells.

The advantages of primary cultures are that the cells have not been "modified" in any way (other than the enzymatic or physical dissociation necessary to obtain them), and that allows for study conditions as close as possible to *in vivo*. The disadvantages of these cultures are the mixed nature of each preparation, limited lifespan of the culture and the potential contamination problems.

Mouse Aortic Endothelial Cells

Aortic endothelial cells were isolated under sterile conditions as previously described by Kobayashi *et al*. in 2005 (193).

The animals were sacrificed under deep inhalatory anaesthesia with isoflurane and cleaned with a 70% solution on ethanol. An incision was made vertically from the mid abdomen to the neck. The rib cage was cracked and removed as were the lungs to expose the aorta. Fat surrounding the aortic vase was removed using a scalpel. The lower extremity of the thoracic aorta was clipped to release the blood and subsequently perfused with 1 ml PBS (Gibco®, Invitrogen™, Carlsbad, USA) containing 1,000 U/ml heparin (Sigma-Aldrich, St. Louis, MO) from the left ventricle.

The heart was removed and a 23G needle was inserted in the aorta and the top part was tied using surgical thread. The aorta was perfused with DMEM media and the lower end equally tied using surgical thread. The aortas was then dissected out and placed in a Petri dish (no coating) containing 20% FBS-DMEM with 1000 U/ml heparin.

Using a syringe, the isolated aorta was washed in serum-free DMEM and filled with a 2 mg/ml collagenase II solution (Sigma-Aldrich, St. Louis, USA). The aorta was placed in a clean Petri dish that went in a 37ºC, 5% CO_2 incubator. After 45min incubation, endothelial cells were flushed into a conical tube with 5 ml of 20% FBS-DMEM.

The cells collected were then centrifuged (1200 rpm for 5 minutes), resuspended and cultured in 5 ml 20% FBS-DMEM in type I collagen-coated T25 flasks (Corning, New York, USA). Cells were incubated for 2 hr at 37ºC. The media was then removed and the cells resuspended in 20% FBS-DMEM containing: 100U/ml penicillin, 100μg streptomycin, 2mM L-glutamine (Gibco®, Invitrogen™, Carlsbad, USA), 1% MEM amino acids (Gibco®, Invitrogen™, Carlsbad, USA), 1% sodium pyruvate (Gibco®, Invitrogen™, Carlsbad, USA), 100 /ml heparin, 100 μg/ml endothelial cell growth supplements (Sigma-Aldrich, St. Louis, MO) and incubated in 5% CO2 at 37°C in a humidified atmosphere. The cells were used at passages 2-3. The purity of the primary cultures was confirmed by the specific monoclonal antibodies raised against vWF and PECAM-1.

FBS Selection and Growth Curve

As many scientists who work with cells on a regular basis know, there are some batches of FBS that seem to work better than others. FBS is not a man made product and hence its ingredients/components may vary not only in quality as in quantity. This way, and because the cells used for experiments revealed to be sensitive to such changes, it was decided to test different batches of FBS opting for one with which all of the necessary experiments would be ran.

Using the service Batch Testing with Reserves provided by Gibco®, which allows customers to obtain a sample for testing in their own application with a reserve held on that batch, 5 different serum lots were received and further tested:

Lot 1- 1355888
Lot 2- 1355891
Lot 3- 1389439
Lot 4- 1365490
Lot 5- 1385397

Seven T25 flasks were seeded with the same amount of cells for both the EA.hy926 and IMR90 cells. Counts were taken (at the same hour) everyday for 7 days using a Neubaüer counting chamber and Trypan Blue Stain (Gibco®, Invitrogen™, Carlsbad, USA) for cell viability purposes. Plating day was considered day 1. Cells were allowed to attach for three hours before the first count was taken. EA.hy926 cells were used at Passage 13 and IMR90 cells at PDL 26.

Immunofluorescence Staining

In order to confirm the endothelial nature and purity of the primary cell cultures used in this thesis specific monoclonal antibodies raised against different endothelial cell markers were used (Von Willebrand Factor (VWF, Santa Cruz #sc-8068) and CD31 (PECAM-1, BD Pharmingen #5502741.50)) in conjunction with immunofluorescence techniques.

Briefly EA.hy926, IMR90 and Mouse Aortic Endothelial Cells were grown in microscope coverslips. When cell confluence reached about 70% the coverslips were washed twice with PBS to remove any media residues. After the wash cells were fixed using 1ml of a 4% paraformaldehyde (Sigma-Aldrich, St. Louis, MO) solution prepared in PBS per slide and incubated for 15 minutes at room temperature. Following fixation, the slides were washed three times with PBS to remove any leftover paraformaldehyde residues.

In order for the antibodies to reach the cells, these have to be permeablized after fixated. A solution of 15% Triton X-100 (Sigma-Aldrich, St. Louis, MO) prepared in PBS was used. Cells were incubated at room temperature for 15 minutes, following a blocking step using a 1% BSA (Sigma-Aldrich, St. Louis, MO) solution prepared in PBS for 30 minutes again at room temperature.

After the cells were prepped the primary antibody was applied. The specific antibody was diluted in blocking solution (1% BSA in PBS) and left overnight at 4ºC. The following antibodies and dilutions were used:

- Purified Rat anti-mouse CD31 (PECAM-1) Monoclonal antibody; BD Pharmingen (San Diego, CA, USA) cat.no. 550274; 1:50 dilution.

- Von Willebrand Factor, Goat polyclonal anti-vWF (c-20) Santa Cruz Biotechnology Inc. (Santa Cruz, CA, USA) cat.no. sc8068; 1:100 dilution.
- 1E12 concentrate Iowa Hybridoma Bank Smooth Muscle Actin anti-mouse, 1:50 dilution.

Once the incubation time is over the coverslips are washed three times with a 0,1% Triton X-100 solution in PBS for 5 minutes per wash.

Since the primary antibody is not linked to any fluorochrome its necessary to apply a secondary antibody in order to be able to visualize the cell markers under the fluorescence microscope. The following secondary antibodies were respectively applied for 1 hour at 37ºC in blocking solution:

- Alexa Fluor® 488 donkey anti-rat IgG, Molecular Probes® #A-21208, 1:200 dilution.
- Alexa Fluor® 488 donkey anti-goat IgG, Molecular Probes® #A-11055, 1:200 dilution.
- Alexa Fluor® 568 goat anti-mouse IgG, Molecular Probes® #A-11004, 1:200 dilution.

Once the one hour incubation time is over the coverslips are again washed three times with a 0.1% Triton X-100 solution in PBS (5 minutes per wash). The final step consists on dipping the slides into water twice and letting them air dry.

Finally VECTASHIELD® Mounting Medium with DAPI (Vector Laboratories, Burlingame, USA) was applied to preserve fluorescence and counterstain DNA and the coverslips mounted on microscope slides (the coverslip was kept in place using nail polish). The Nikon Eclipse 90*i* Fluorescence Roper Scientific Microscope was used to analyze the resulting cell staining.

Electron Microscopy

After having confirmed the endothelial nature of the cells in use, electron microscopy was used to confirm the presence of caveolae in the cell membrane of the same cells. Both EA.hy926 and Mouse Aortic Endothelial Cells were tested as well as Mouse Aortic Endothelial Cells from a CAV_1 deficient animal.

Briefly, cells were fixed in 2.0% glutaraldehyde in 0.1 mol/L sodium cacodylate buffer, pH 7.4 (Electron Microscopy Sciences, Hatfield, PA) overnight at 4ºC. Cells were then rinsed in 0.1 mol/L sodium cacodylate buffer, post-fixed in 1.0% osmium tetroxide (in cacodylate buffer) for one hour at room temperature, rinsed in buffer again, then in distilled water and stained, en bloc, in an aqueous solution of 2.0% uranyl acetate for one hour at room temperature.

Cells were subsequently rinsed in distilled water and embedded in 2.0% agarose for ease of handling before being dehydrated through a graded series of ethanol to 100%. Cells were then infiltrated with Epon resin (Ted Pella, Redding, CA) in a 1:1 solution of Epon:ethanol. The following day they were placed in fresh Epon for several hours and then embedded in Epon overnight at 60 ºC. Thin sections were cut on a Reichert Ultracut E ultramicrotome, collected on formvar-coated grids, stained with uranyl acetate and lead citrate and examined in a JEOL JEM 1011 transmission electron microscope at 80 kV. Images were collected using an AMT digital imaging system (Advanced Microscopy Techniques, Danvers, MA).

Electron microscopy was performed in the Microscopy Core of the Centre for Systems Biology/Program in Membrane Biology, which is partially supported by an Inflammatory Bowel Disease Grant DK43351 and a Boston Area Diabetes and Endocrinology Research Centre Award DK57521.

Western Blot (Electrophoresis and Immunoblot)

Western blot, also know as protein immunoblot, is a widely used analytical technique used to detect specific proteins in a sample of tissue homogenate or cell extract. It uses gel electrophoresis to separate native proteins by 3D structure or denatured proteins by the length of the polypeptide. The proteins are then transferred to a membrane (typically nitrocellulose or PVDF), where they are probed (detected) using antibodies specific to the target protein (194, 195).

Tissue preparation

Samples can not be taken from whole tissue or from cell culture. Solid tissues are first broken down mechanically using a homogenizer and cells broken open by use of a sonicator. Assorted detergents, salts, and buffers are employed to

encourage lysis of cells and to solubilize proteins. Protease and phosphatase inhibitors are added to prevent the digestion of the sample by its own enzymes. Tissue preparation is done at cold temperatures to avoid protein denaturing and degradation.

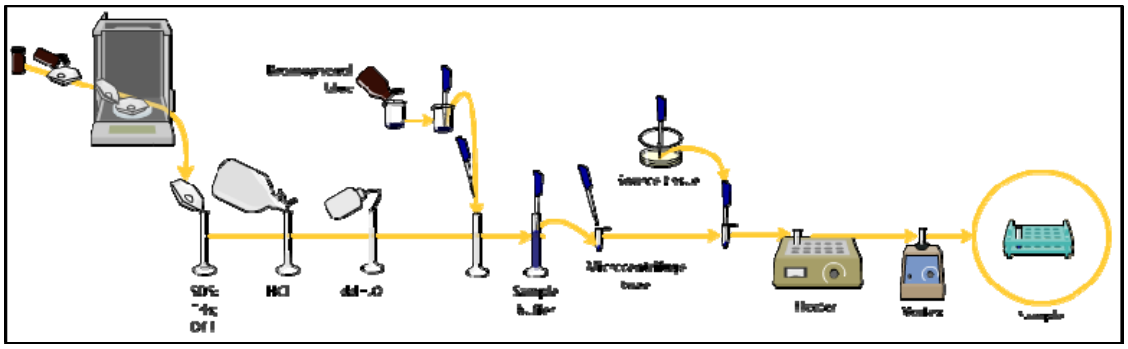

Figure 19 - Sample preparation for Western Blot technique.

In brief the cells/tissues were homogenized in RIPA (Radioimmunoprecipitation Assay) Lysis Buffer System (#sc-24948 Santa Cruz Biotechnology Inc, Santa Cruz, USA) containing Triton X-100 (detergent) and protease/phosphatase inhibitors (PMSF, sodium orthovanadate and protease inhibitor cocktail). If phospo-proteins were being studied PhosphoStop (Cat. No. 04 906 837 001, Roche, Mannheim, Germany) was added to the RIPA Buffer in order to inhibit phosphatase activity that would degrade the samples. When the sample of interest was a tissue sample (heart, aorta, etc) a homogenizer was used to break the collected tissue down but, in most cases, the samples were resultant from a cell based experiments. In this case, the cells were collected (scrapped) using the RIPA Lysis Buffer System and incubated on ice for 30 minutes. After the incubation, the cells were sonicated (30V, 10 seconds, 3 times) and spun down.

The resulting protein extracts were quantified using the Coomassie (Bradford) protein assay (#23200, Thermo Fisher Scientific, Rockford, USA). The Bradford assay is a colorimetric protein assay based on an absorbance shift of the dye Coomassie Brilliant Blue G-250, in which, under acidic conditions the red form of the dye is converted into its bluer form to bind to the protein being assayed. The binding of the protein stabilizes the blue form of the Coomassie dye; thus the amount of the complex present in solution is a measure for the protein concentration, and can be

estimated by use of an absorbance reading. The (bound) form of the dye has an absorption spectrum maximum historically held to be at 595 nm. The increase of absorbance at 595 nm is proportional to the amount of bound dye, and thus to the amount (concentration) of protein present in the sample.

Protein extracts (10-20 µg) were combined with an equal volume of 2X Laemmli Sample Buffer (Bio-Rad, Hercules, USA) (containing 5% 2-mercaptoethanol), boiled for 5 minutes at 95ºC, and size-fractionated by electrophoresis on 7.5%-12.5% SDS-polyacrylamide gels.

Gel Electrophoresis

The sample proteins are separated using gel electrophoresis. The most common type of gel electrophoresis employs polyacrylamide gels and buffers loaded with sodium dodecyl sulfate (SDS). SDS-PAGE (SDS polyacrylamide gel electrophoresis) maintains polypeptides in a denatured state once they have been treated with strong reducing agents (2-mercaptoethanol) to remove secondary and tertiary structure and thus allows separation of proteins by their molecular weight. Sampled proteins become covered in the negatively charged SDS and move to the positively charged electrode through the acrylamide mesh of the gel. Smaller proteins migrate faster through this mesh and the proteins are thus separated according to size (usually measured in kilodaltons, kDa). The concentration of acrylamide determines the resolution of the gel - the greater the acrylamide concentration the better the resolution of lower molecular weight proteins. The lower the acrylamide concentration the better the resolution of higher molecular weight proteins.

Samples are loaded into wells in the gel. One lane is usually reserved for a marker or ladder, a commercially available mixture of proteins having defined molecular weights, typically stained so as to form visible, coloured bands. Bio-rad kaleidoscope pre-stained standards (Bio-Rad, Hercules, USA) where use as control for molecular weight. When voltage is applied along the gel, proteins migrate into it at different speeds and separate into bands within each lane.

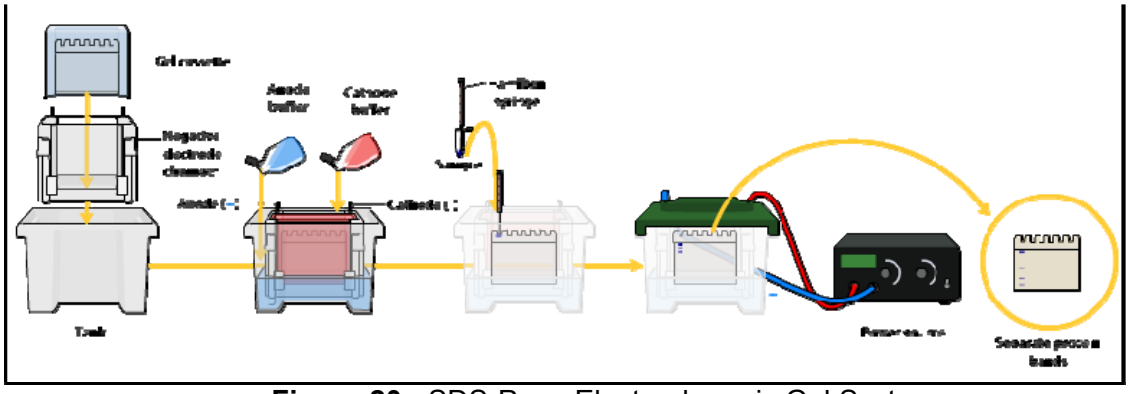

Figure 20 - SDS-Page Electrophoresis Gel System.

Transfer

In order to allow for antibody detection, the proteins are moved from within the gel onto a membrane made of cellulose. The membrane is placed on top of the gel carefully avoiding air bubbles to form and a stack of filter papers placed on top of that. The entire stack is then dipped in a buffer solution. The method used for transferring the proteins is called electroblotting and uses an electric current to pull proteins from the gel into the nitrocellulose membrane. The proteins move from within the gel onto the membrane while maintaining the organization they had in the gel. As a result of this "blotting" process, the proteins are exposed on a thin surface layer for detection (see below). Throughout the experiments 0.2 μm nitrocellulose membrane from Bio-rad (Bio-Rad, Hercules, USA) was used.

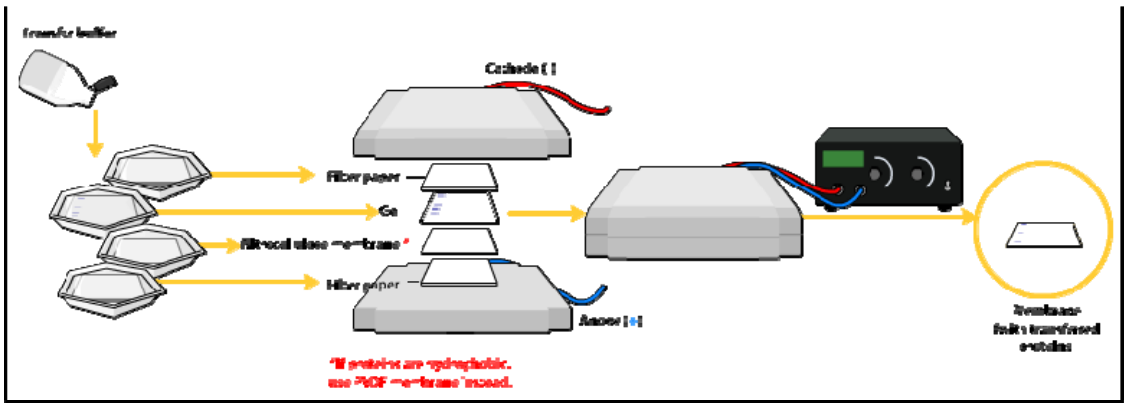

Figure 21 - Western Blot Transfer System (Electrobloting).

The uniformity and overall effectiveness of the transfer process was checked by staining the membrane with a Ponceau S dye (Sigma-Aldrich, St. Louis, MO, USA) solution (0,1% w/v in 5% acetic acid).

Blocking

Since the membrane has been chosen for its ability to bind protein and as both antibodies and the target are proteins, steps must be taken to prevent interactions between the membrane and the antibody used for detection of the target protein. Blocking of non-specific binding is achieved by placing the membrane in a dilute solution of protein - typically 3-5% Bovine serum albumin (BSA) or non-fat dry milk in Tris-Buffered Saline (TBS), with a minute percentage of detergent such as Tween 20 or Triton X-100. The protein in the dilute solution attaches to the membrane in all places where the target proteins have not attached. Thus, when the antibody is added, there is no room on the membrane for it to attach other than on the binding sites of the specific target protein. This reduces "noise" in the final product of the western blot, leading to clearer results, and eliminates false positives.

For the purpose of the experiments TBS-Tween (USB Corporation, Cleveland, OH) was used together with Blotting Grade Blocker Non Fat Dry Milk (Bio-Rad, Hercules, USA) usually in the form of a 5% solution employed for 1 hour at room temperature with gentle agitation.

Detection

During the detection process the membrane is "probed" for the protein of interest with a modified antibody which is linked to a reporter enzyme; when exposed to an appropriate substrate this enzyme drives a colorimetric reaction and produces a colour. This traditionally takes place in a two-step process.

Primary antibody

Primary antibodies are generated when a host species or immune cell culture is exposed to the protein of interest. Normally, this is part of the immune response, whereas here they are harvested and used as sensitive and specific detection tools that bind the protein directly. After blocking, a dilute solution of primary antibody is incubated with the membrane under gentle agitation. Typically, the solution is the

same as the one used for blocking the membrane. The antibody solution and the membrane can be sealed and incubated together for anywhere from 30 minutes to overnight. It can also be incubated at different temperatures, with warmer temperatures being associated with more binding, both specific (to the target protein, the "signal") and non-specific ("noise").

Primary antibodies were from BD Transduction Laboratories (San Diego, CA, USA): mouse anti- striatin (catalogue no. 610838, 1:1000), mouse anti-eNOS (catalogue no. 610297, 1:2500), anti-CAV_1 (clone 2297, catalogue no. 610406, 1:1000), and mouse anti-ERK1/2 (catalogue no. 610124, 1:5000); Cell Signalling Technology (Danvers, MA, USA): rabbit anti-phospho-eNOS (peNOS) (catalogue no. 9571, 1:1000), rabbit anti-phospho-p44/42 MAPK (pERK 1/2) (catalogue no 4377, 1:1000); and Santa Cruz Biotechnology Inc. (Santa Cruz, CA, USA) rabbit anti-MR (catalogue no. sc11412, 1:1000). Primary antibodies were typically left to incubate overnight at 4ºC with gentle agitation.

Secondary antibody

After rinsing the membrane to remove unbound primary antibody, the membrane is exposed to another antibody, directed at a species-specific portion of the primary antibody. Antibodies come from animal sources; anti-mouse secondary will bind to almost any mouse-sourced primary antibody, which allows some cost savings by allowing an entire lab to share a single source of mass-produced antibody, and provides far more consistent results. This is known as a secondary antibody, and due to its targeting properties, tends to be referred to as "anti-mouse," "anti-goat," etc. The secondary antibody is usually linked to biotin or to a reporter enzyme such as alkaline phosphatase or horseradish peroxidase. Most commonly, a horseradish peroxidase-linked secondary is used to cleave a chemiluminescent agent, and the reaction product produces luminescence in proportion to the amount of protein. A sensitive sheet of photographic film is placed against the membrane, and exposure to the light from the reaction creates an image of the antibodies bound to the blot.

Secondary antibodies used were from Sigma-Aldrich company (St. Louis, MO, USA): Anti-Mouse IgG (Fab specific)–Peroxidase antibody produced in goat (catalogue no. A9917, 1:10,000) and Anti-Rabbit IgG (whole molecule)–Peroxidase

antibody produced in goat (catalogue no. A0545, 1:10,000). Secondary antibodies were incubated for 1 hour at room temperature with gentle agitation.

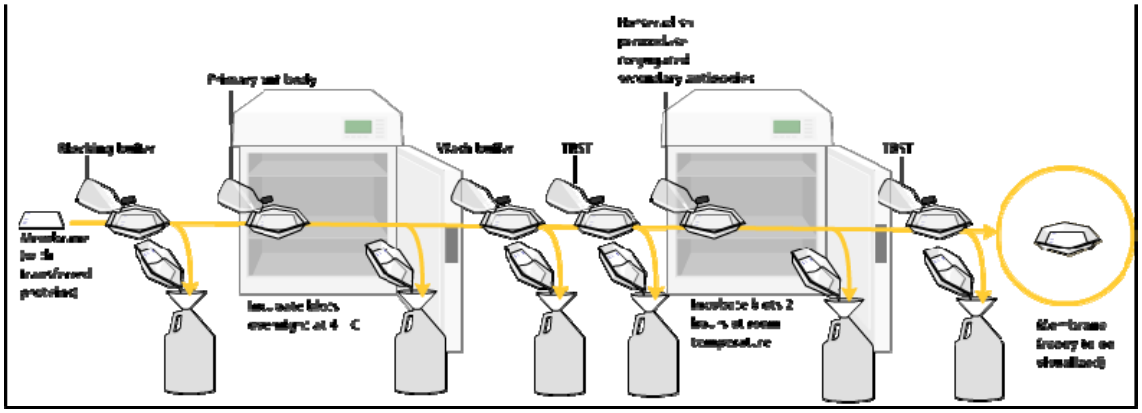

Figure 22 - Two step detection process for Western Blot analysis.

Analysis

After the unbound probes are washed away, the western blot is ready for detection of the probes that are labelled and bound to the protein of interest. In practical terms, not all westerns reveal protein only at one band in a membrane. Size approximations are taken by comparing the stained bands to that of the marker or ladder loaded during electrophoresis. The process is repeated for a structural protein, such as actin or tubulin, that should not change between samples. The amount of target protein is normalized to the structural protein to control between groups. This practice ensures correction for the amount of total protein on the membrane in case of errors or incomplete transfers.

After the initial detection of the target protein the membranes were stripped using Stripping Buffer (Boston BioProducts, Asland, MA, USA) and subsequently re-probed for β-actin. The results were normalized to β-actin to correct for loading. Quantitative data are presented as fold change relative to controls

Chemiluminescent detection

Chemiluminescent detection methods depend on incubation of the western blot membrane with a substrate that will luminesce when exposed to the reporter on the secondary antibody. The light is then detected by photographic film, and more recently by CCD cameras which capture a digital image of the western blot. The image is analysed by densitometry, which evaluates the relative amount of protein staining and quantifies the results in terms of optical density. Newer software allows further data analysis such as molecular weight analysis if appropriate standards are used.

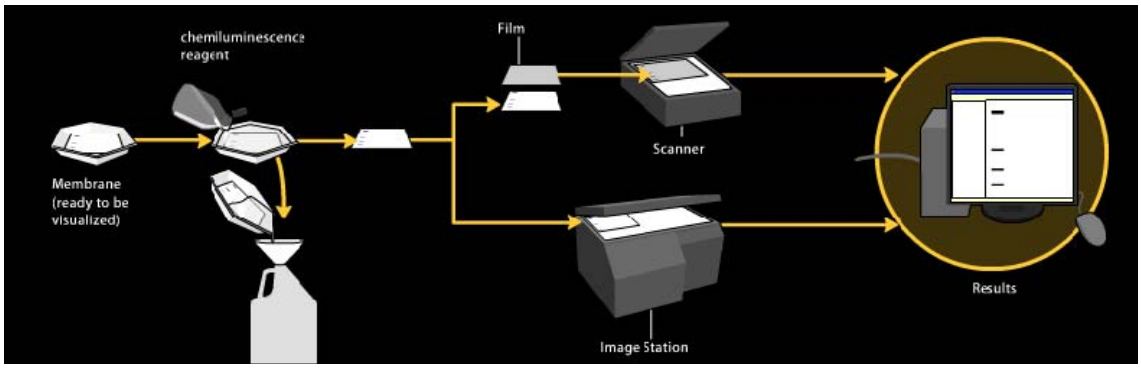

Figure 23 - Chemiluminescence detection used in Western Blot analysis. Enhanced Chemiluminescence Reagent (Perkin-Elmer Life Sciences, Boston, MA) was used before the membranes were exposed and developed on CL-XPosure Film (Thermo Scientific, Chicago, IL, USA).

Co-Immunoprecipitation (Co-IP)

Co-immunoprecipitation was used as a tool to try to establish if there were any protein-protein interactions or if the proteins were organized as protein complex.

Immunoprecipitation of intact protein complexes (i.e. antigen along with any proteins or ligands that are bound to it) is known as co-immunoprecipitation (Co-IP). Co-IP works by selecting an antibody that targets a known protein that is believed to be a member of a larger complex of proteins. By targeting this *known* member with an antibody it may become possible to pull the entire protein complex out of solution and thereby identify *unknown* members of the complex. This works when the proteins involved in the complex bind to each other tightly, making it possible to pull multiple

members of the complex out of solution by latching onto one member with an antibody. This concept of pulling protein complexes out of solution is sometimes referred to as a "pull-down".

Identifying the members of protein complexes may require several rounds of precipitation with different antibodies for a number of reasons:

- A particular antibody often selects for a subpopulation of its target protein that has the epitope exposed, thus failing to identify any proteins in complexes that hide the epitope.
- The first round of IP will often result in the identification of many new proteins that are putative members of the complex being studied. The researcher will then obtain antibodies that specifically target one of the newly identified proteins and repeat the entire immunoprecipitation experiment. This second round of precipitation may result in the recovery of additional new members of a complex. The identified proteins may not ever exist in a single complex at a given time, but may instead represent a network of proteins interacting with one another at different times for different purposes.
- Repeating the experiment by targeting different members of the protein complex allows the researcher to double-check the result. Each round of pull-downs should result in the recovery of both the original known protein as well as other previously identified members of the complex (and even new additional members). By repeating the immunoprecipitation in this way, the researcher verifies that each identified member of the protein complex was a valid identification. If a particular protein can only be recovered by targeting one of the known members but not by targeting other of the known members then that protein's status as a member of the complex may be subject to question.

In brief the cells were collected (scrapped) and homogenized in immunoprecipitation buffer (RIPA Buffer, Santa Cruz Biotechnology Inc.), the cell lysate sonicated for 20 seconds (30 Volts) and incubated for 30 min at 4 ºC. Next, the lysate was centrifuged at 10,000g for 10 minutes, and protein content determined by colorimetric assay (Micro BCA protein kit, Thermo Scientific, Chicago, IL, USA). The protein extract (500 μg) was incubated with 1-2 μg of monoclonal or polyclonal antibodies for 1-2 hours at 4 ºC together with 50-100 μl of protein G or A/G

MicroBeads (Miltenyi Biotec, Auburn, CA, USA). The Microbeads, antibody and cell lysate mix were separated using MACSmini columns and respective magnetic stand, according to the manufacturers protocol (described bellow). Finally the beads were washed with RIPA buffer and the bound immuno-complexes eluted using boiling loading dye and assessed by Western Blot analysis.

The antibodies used were from BD Transduction Laboratories (San Diego, CA): mouse anti- striatin (catalogue no. 610838), mouse anti-CAV_1 (catalogue no. 611338) and Santa Cruz Biotechnology Inc.: rabbit anti-MR (catalogue no. sc11412), rabbit anti- CAV_1 (catalogue no. sc 894). The specificity of the rabbit anti-MR was assessed by comparison by those provided by Dr. Gomez-Sanchez (University of Mississippi Medical Centre, Jackson, MS, USA) (196).

Immunopurification using µ Columns and µMACS™ Separator

Before starting the heating block was heated to 95ºC. The (Column is placed in the magnetic field of the µMACS™ Separator with a suitable waste container under it. The column is prepared by rinsing it with 200 (L of lysis buffer. The elution buffer is placed in the pre-heated block (90 (L should be pre-heated for each separation column). The cell lysate is applied onto the column and allowed to run through. The non-bound fraction can be collected in a fresh tube for analysis. Columns are “flow stop” and do not run dry. Magnetically labelled protein is retained in the µ Columns. The column is then rinsed with 4 x 200 (L of a suitable buffer (RIPA buffer). Finally, 20 µL of pre-heated (95 °C) 1× SDS gel loading buffer are applied onto the column matrix using a fresh pipette tip for each column and incubated for 5 minutes at room temperature (if a drop is present on the column tip, this should be removed by contacting the column tip with the waste tube or by using a fresh pipette tip). A fresh collection tube is placed under the µColumn and 50 µL of pre-heated (95 °C) SDS gel loading buffer are applied onto the column matrix using a fresh pipette tip for each column. If a drop is present on the column tip, this should also be collected by contacting the column tip with the tube or by using a pipette, ensuring thereby, a reproducible elution volume. The eluted immunoprecipitate can now be analyzed by SDS-PAGE.

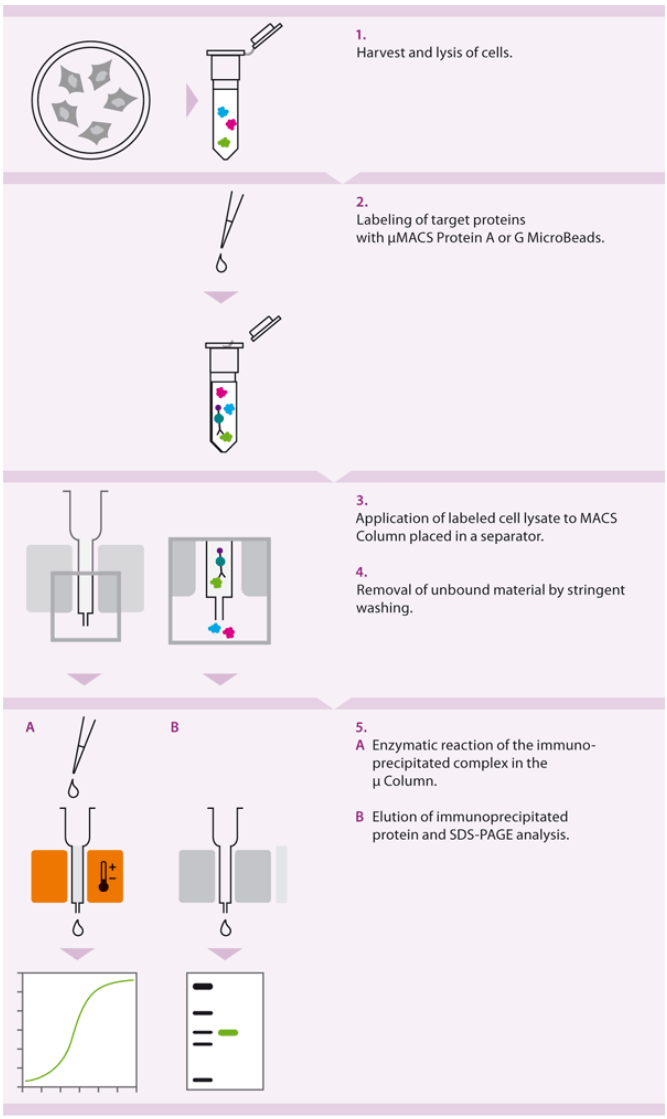

Figure 24 – Schematic protocol for Immunopurification using µ Columns and µMACS™ Separator.

MACS® Technology was selected for this application due to its sensitivity, specificity and speed. Immunoprecipitation with µMACS Protein A/G MicroBeads does not involve a centrifugation step. Instead, after a short incubation of cleared lysate with the MicroBeads- coated with the specific antibody- the magnetizable immune complex is passed over a separation column placed in the magnetic field of a MACS Separator. The labelled complex is retained within the column while other proteins are efficiently washed away. For SDS-PAGE analysis, the immunoprecipitated protein is eluted from the column with SDS gel loading buffer.

Alternatively, enzymatic reactions with the precipitated immune complex can be performed on the separation columns.

μMACS™ Protein A and μMACS Protein G MicroBeads are colloidal, super-paramagnetic MicroBeads, which are conjugated to Protein A or Protein G, respectively. Protein A is a 42 kDa protein component of the cell wall of *Staphylococcus aureus* while Protein G is a 33 kDa cell surface protein of the group G streptococci. Both of these proteins bind to the Fc region of IgG with high affinity and avidity, leaving the Fab region of the antibody free for interaction with its antigen; thus, resulting in the formation of multimeric complexes between antigen, antibody, and MicroBeads. The binding specificities of Protein A and G for immunoglobins differ depending on the subclass and origin of the antibody. The extremely small MicroBeads, 50 nm in diameter, allow fast reaction kinetics while the column technology provides effective washing steps to minimize contaminations.

RNA Extraction

Total RNA was extracted using the RNeasy Mini Kit (Qiagen Sciences, Valencia, CA, USA) following the manufacturer's instructions. The RNeasy procedure represents a well-established technology for RNA purification. This technology combines the selective binding properties of a silica-based membrane with the speed of microspin technology. A specialized high-salt buffer system allows up to 100 μg of RNA longer than 200 bases to bind to the RNeasy silica membrane. Biological samples are first lysed and homogenized in the presence of a highly denaturing guanidine-thiocyanate–containing buffer, which immediately inactivates RNases to ensure purification of intact RNA. Ethanol is added to provide appropriate binding conditions, and the sample is then applied to an RNeasy Mini spin column, where the total RNA binds to the membrane and contaminants are efficiently washed away. High-quality RNA is then eluted in 30–100 μl water. With the RNeasy procedure, all RNA molecules longer than 200 nucleotides are purified. The procedure provides an enrichment for mRNA since most RNAs <200 nucleotides (such as 5.8S rRNA, 5S rRNA, and tRNAs, which together comprise 15–20% of total RNA) are selectively excluded.

Protocol: Purification of Total RNA from Animal Cells Using Spin Technology

It is essential to use the correct amount of starting material in order to obtain optimal RNA yield and purity. The minimum amount is generally 100 cells, while the maximum amount of starting material should not exceed 1 x 10^7 cells. All steps of the procedure are performed at room temperature. Before starting the procedure it is recommended to add β-mercaptoethanol (β-ME) to Buffer RLT, 10 µl β-ME should be added per 1 ml of Buffer RLT.

For cells grown in a monolayer (EA.hy926 cells) and in a surface area of under 10 cm^2 (6 well plate) it is advised to lyse the cells directly in the cell culture vessel. The cell-culture medium should be removed using aspiration (without touching the cell layer) and the cells rinsed with PBS before lysis in order to remove any leftover media which could reduce the RNA yield. Cells are disrupted by adding 350 µl of Buffer RLT and scraping with an appropriate cell scrapper. The lysate is transferred to a microcentrifuge tube and vortexed to mix the cell pellet. No cell clumps should be visible before the homogenization step.

When processing a number of cells under $1x10^5$, homogenization can be achieved by vortexing the cell pellet at high speed for 1 minute. After this step, 350 µl of 70% Ethanol are added and mixed by pippeting up and down several times. This solution is transferred to an RNeasy spin column placed in a 2 ml collection tube and centrifuged for 15 seconds at 10,000 rpm. The resulting flow-through is discarded and the collection tube re-used. Next, 700 µl of Buffer RW1 are added to the spin column followed by centrifugation at 10,000 rpm for another 15 seconds. The flow-through is again discarded and the collection tube re-used. 500 µl RPE Buffer are added to the RNeasy spin column followed by centrifugation at 10,000 rpm 15 seconds. The flow-through is discarded and the step repeated with a 2 minute centrifugation to wash the spin column membrane before the final step.

After centrifugation, the RNeasy spin column is carefully removed from the collection tube so that the column does not contact the flow-through. The RNeasy spin column is placed in a new 1.5 ml collection tube and 30–50 µl RNase-free water is added directly to the spin column membrane. Next, the tube is centrifuged for one minute at 10,000 rpm to elute the RNA**.** The resulting RNA is pure enough to use for reverse-transcription.

Following extraction, the RNA yield was measured using spectrophotometric analysis. Nucleic acids absorb ultraviolet light in a specific pattern. In a spectrophotometer, a sample is exposed to ultraviolet light at 260 nm, and a photo-detector measures the light that passes through the sample. The more light absorbed by the sample, the higher the nucleic acid concentration in the sample. Using the Beer-Lambert Law it is possible to relate the amount of light absorbed to the concentration of the absorbing molecule. At a wavelength of 260 nm, the average extinction coefficient for single-stranded RNA it is 0.025 $(\mu g/ml)^{-1}$ cm^{-1} . Thus, an optical density (or "OD") of 1 corresponds to a concentration of 40 µg/ml for single-stranded RNA. This method of calculation is valid for up to an OD of at least 2 (197).

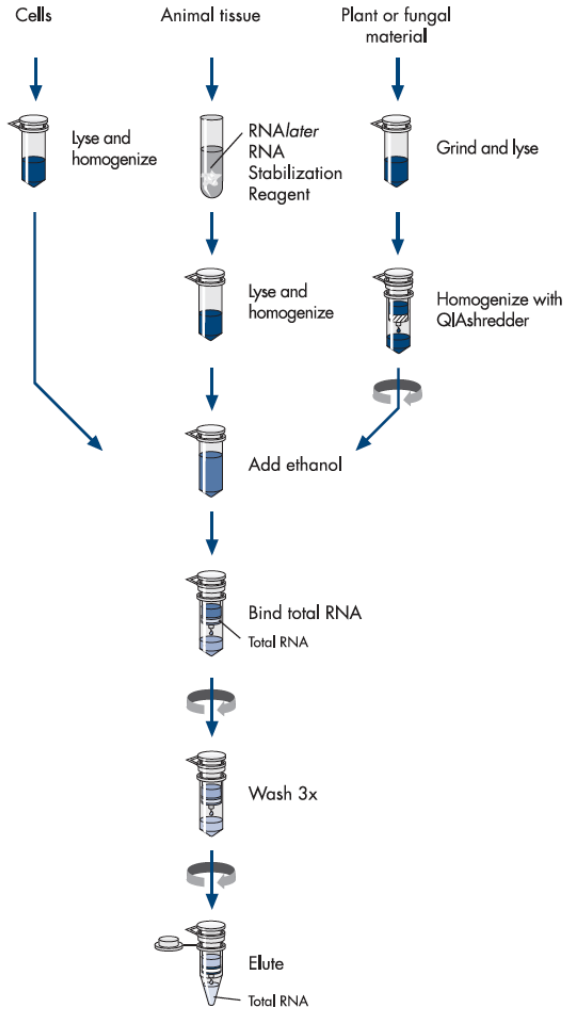

Figure 25 - Schematic protocol for RNA extraction using RNeasy Mini Kit.

Reverse Transcription (RT)

cDNA was synthesized from 3 μg total RNA with the First Strand cDNA Synthesis Kit (Amersham, Buckinghamshire, UK). Reverse transcription is a laboratory technique commonly used in molecular biology where a RNA strand is reverse transcribed into its DNA complement (*complementary DNA*, or *cDNA*) using the enzyme reverse transcriptase. First-strand cDNA synthesis is catalyzed by Moloney Murine Leukaemia Virus (M-MuLV) reverse transcriptase. The conditions of this reaction have been optimized to permit full-length transcription of RNAs 7 kilobases or more in length. The preassembled bulk firststrand cDNA reaction mixes require only the addition of DTT, RNA, and a primer of choice. The first-strand reaction may be primed with either of the primers provided with the kit: the *Not* I-d(T)18 bifunctional primer or pd(N)6 primer. Custom primers complementary to a specific mRNA sequence may also be used to prime first-strand synthesis. Following synthesis of the first-strand cDNA, the resulting doublestranded RNA:cDNA heteroduplex can be used directly for second-strand cDNA synthesis. Alternatively, the completed first-strand reaction may be amplified directly by PCR (198-200).

Depending on the intended use of the first-strand cDNA, synthesis may be performed using different volumes of bulk first-strand cDNA mix**,** and different types and amounts of primer and RNA. If the cDNA is to be amplified, either 5 μl or 11 μl of the bulk reaction mix may be used, and 1–5 μg of *total* RNA, or 20–150 ng of *mRNA*, are sufficient. For the purposes of the experiments conducted, 5 μl of bulk reaction mix were used together with 3 μg of total RNA diluted in a total of 8 μl of RNAse-free water.

The RNA sample is placed in a microcentrifuge tube and RNAse-free water added**,** if necessary, to bring the RNA to the appropriate volume (either 8 μl or 20 μl). The RNA solution is heated to 65ºC for 10 minutes and then chilled on ice. The bulk first-strand cDNA reaction mix is gently pipetted to obtain a uniform suspension and the appropriate volume of the bulk first-strand cDNA reaction mix (either 5 μl or 11 μl) is added to a sterile 1,5 or 0,5 ml microcentrifuge tube. To this tube are added 1 μl of DTT solution, 1 μl of primer at the appropriate concentration, and the heat-denatured RNA. The solution is pipetted up and down several times to mix and incubated at

37°C for 1 hour. The completed first-strand cDNA reaction product is now ready for immediate PCR amplification.

Quantitative Real-Time Polymerase Chain Reaction (qPCR)

In molecular biology, *quantitative real time polymerase chain reaction* (qPCR) is a technique based on PCR, which is used to amplify a targeted DNA sequence. For one or more specific sequences in a DNA sample, qPCR enables both detection and quantification. The quantity can either be an absolute number of copies or a relative amount when normalized to DNA input and/or additional normalizing genes.

The procedure follows the general principle of PCR; its key feature is that the amplified DNA is detected as the reaction progresses in real time. Two common methods for detection of products in real-time PCR are: (1) non-specific fluorescent dyes that intercalate with any double-stranded DNA, and (2) sequence-specific DNA probes consisting of oligonucleotides that are labelled with a fluorescent reporter which permits detection only after hybridization of the probe with its complementary DNA target.

A DNA-binding dye binds to all double-stranded (ds)DNA in PCR, causing fluorescence of the dye. An increase in DNA product during PCR therefore leads to an increase in fluorescence intensity and is measured at each cycle, thus allowing DNA concentrations to be quantified. However, dsDNA dyes such as SYBR Green will bind to all dsDNA PCR products, including non-specific PCR products (such as primer dimer). This can potentially interfere with, or prevent, accurate quantification of the intended target sequence.

Fluorescent reporter probes detect only the DNA containing the probe sequence; therefore, use of the reporter probe significantly increases specificity, and enables quantification even in the presence of non-specific DNA amplification. Fluorescent probes can be used in multiplex assays—for detection of several genes in the same reaction—based on specific probes with different-coloured labels, provided that all targeted genes are amplified with similar efficiency. The specificity of fluorescent reporter probes also prevents interference of measurements caused by primer dimers, which are undesirable potential by-products in PCR. The method relies on a DNA-based probe (e.g. Taqman probes) with a fluorescent reporter at one end and a quencher of fluorescence at the opposite end of the probe. The close

proximity of the reporter to the quencher prevents detection of its fluorescence; breakdown of the probe by the 5' to 3' exonuclease activity of the Taq polymerase breaks the reporter-quencher proximity and thus allows unquenched emission of fluorescence, which can be detected after excitation with a laser. An increase in the product targeted by the reporter probe at each PCR cycle therefore causes a proportional increase in fluorescence due to the breakdown of the probe and release of the reporter.

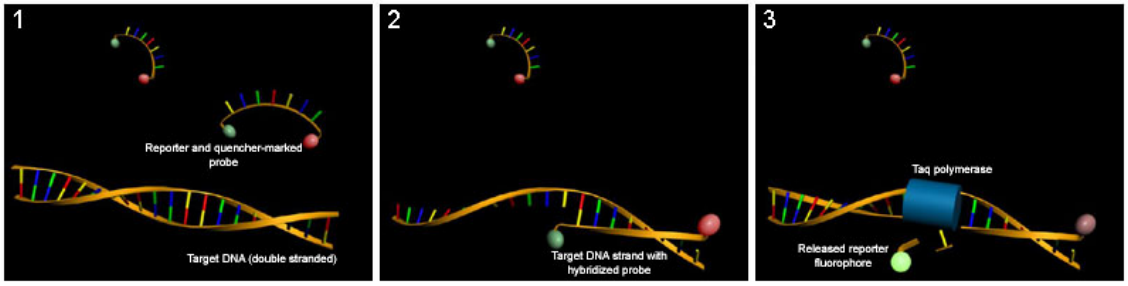

Figure 26 – DNA quantification using fluorescent reporter probes. (1) In intact probes, reporter fluorescence is quenched. (2) Probes and the complementary DNA strand are hybridized and reporter fluorescence is still quenched. (3) During PCR, the probe is degraded by the Taq polymerase and the fluorescent reporter released.

Real-time PCR can be used to quantify DNA sequences by two methods: relative quantification and absolute quantification. Relative quantification is based on internal reference genes to determine fold-differences in expression of the target gene. Absolute quantification gives the exact number of target DNA molecules by comparison with DNA standards (201). The general principle of DNA quantification by real-time PCR relies on plotting fluorescence against the number of cycles on a logarithmic scale. A threshold for detection of DNA-based fluorescence is set slightly above background. The number of cycles at which the fluorescence exceeds the threshold is called the cycle threshold, C_t. During the exponential amplification phase, the sequence of the DNA target doubles every cycle. For example, a DNA sample whose C_t precedes that of another sample by 3 cycles contained 2^3 = 8 times more template. However, the efficiency of amplification is often variable among primers and templates. Therefore, the efficiency of a primer-template combination is assessed in a titration experiment with serial dilutions of DNA template to create a standard curve of the change in C_t with each dilution. The slope of the linear

regression is then used to determine the efficiency of amplification, which is 100% if a dilution of 1:2 results in a C_t difference of 1. For commercially available probes such experiments are no longer necessary since the manufacturer has already optimized the performance of the primers for each target sequence.

To quantify gene expression, the C_t for an RNA or DNA from the gene of interest is divided by C_t of RNA/DNA from a housekeeping gene in the same sample to normalize for variation in the amount and quality of RNA between different samples. This normalization procedure is commonly called the *$\Delta\Delta C_t$-method* (202), and permits comparison of expression of a gene of interest among different samples. However, for such comparison, expression of the normalizing reference gene needs to be very similar across all the samples. Choosing a reference gene fulfilling this criterion is therefore of high importance, and often challenging, because only very few genes show equal levels of expression across a range of different conditions or tissues (203, 204).

Polymerase Chain Reaction amplification reactions were performed with Taqman gene expression assays in duplicate with the use of the ABI Prism 7000 Sequence Detection System (Applied Biosystems, Foster City Calif.). The $\Delta\Delta$ cycle (CT) threshold method was used to determine mRNA levels. Target gene expression was normalized to 18S rRNA levels. Probes used: zinedin (STRN4, Hs00183850_m1), SG2NA (STRN3, Hs00205827_m1), striatin (STRN, Hs00162404_m1), lysine deficient protein kinase 4 (WNK4, Hs00260769_m1), serum glucocorticoid regulated kinase 1 (SGK1, Hs00178612_m1), prostaglandin I2 (PTGIS, Hs00919949_m1) and prostaglandin-endoperoxide synthase 1 (PTGS1, Hs00168776_m1).

siRNA knockdown of striatin

Small interfering RNA (siRNA), sometimes known as short interfering RNA or silencing RNA, is a class of double-stranded RNA molecules, 20-25 nucleotides in length, that play a variety of roles in biology. The most notable role of siRNA is its involvement in the RNA interference (RNAi) pathway, where it interferes with the expression of a specific gene. In addition to its role in the RNAi pathway, siRNA also

acts in RNAi-related pathways, e.g., as an antiviral mechanism or in shaping the chromatin structure of a genome; the complexity of these pathways is only now being elucidated.

siRNAs were first discovered by David Baulcombe's group at the Sainsbury Laboratory in Norwich, England, as part of post-transcriptional gene silencing (PTGS) in plants. The group published their findings in Science in a 1999 paper titled "A species of small antisense RNA in posttranscriptional gene silencing in plants" (205). Shortly thereafter, in 2001, synthetic siRNAs were shown to be able to induce RNAi in mammalian cells by Thomas Tuschl, and colleagues in a paper published in Nature (206). This discovery led to a surge in interest in harnessing RNAi for biomedical research and drug development.

siRNAs have a well-defined structure: a short (usually 21-nt) double-strand RNA (dsRNA) with 2-nt 3' overhangs on either end:

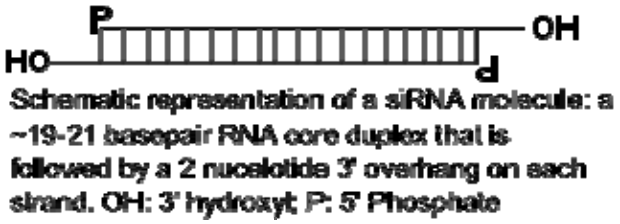

Figure 27- Schematic representation of a siRNA molecule.

Each strand has a 5' phosphatase group and a 3' hydroxyl (-OH) group. This structure is the result of processing by dicer, an enzyme that converts either long dsRNAs or small hairpin RNAs into siRNAs (207). siRNAs can also be exogenously (artificially) introduced into cells by various transfection methods to bring about the specific knockdown of a gene of interest. In essence, any gene whose sequence is known can, thus, be targeted based on sequence complementarity with an appropriately tailored siRNA. This has made siRNAs an important tool for gene function and drug target validation studies in the post-genomic era. Transfection of an exogenous siRNA can, sometimes, prove to be problematic because the gene knockdown effect is only transient, in particular, in rapidly dividing cells.

EA.hy926 cells were transfected with ON-TARGETplus siRNA pre-designed duplex specific for striatin (J-019572-09-0050) obtained from Dharmacon RNAi Technologies, Thermo Scientific (Chicago, IL, USA). Control/blank siRNA (D-001810-01-05) was transfected in parallel with striatin siRNA following the manufacturer's protocols and using the Dharmafect 1 siRNA Transfection Reagent (T-2001-03) from Dharmacon RNAi Technologies. The cells were then harvested for Western blot analysis 48 hours post-transfection.

siRNA Transfection Protocol

All steps of protocol should be performed in a laminar flow cell culture hood using sterile techniques. Cells were plated at a density of 700,000 cells per well of a six well plate in antibiotic-free media, the day before the experiment and left to incubate overnight at 37°C with 5 % CO_2. Before transfection, a 5 µM siRNA solution is prepared in 1X siRNA buffer.

In separate tubes, the siRNA (10 µl of siRNA, 5 µM per well) and the DharmaFECT transfection reagent (2 µl per well) are diluted with serum-free media to a total volume of 200 µl per well. The components of each tube are gently mixed by pipetting up and down followed by a 5 minute incubation at room temperature. The contents of tube 1 and 2 are added together and mixed by pipetting up and down, followed by 20 minutes incubation at room temperature.

The culture medium is removed from the cell culture well and 400 µl of the previous mixture are added. Another 1,6 ml of antibiotic-free media are added to each well to fulfil the 2 ml recommended volume per well. The plates are gently swirled to ensure appropriate distribution of the transfection reagents. The cells are incubated at 37°C in 5 % CO2 for 24–48 hours (for mRNA analysis) or 48–96 hours (for protein analysis). In order to reduce cytotoxicity, the transfection medium is replaced by regular culture medium after 24 hours of incubation.

Before selecting the concentrations of transfection reagents to use as well as which reagents to use several optimization experiments were conducted.

Animals

The present studies followed the guidelines approval from the Institutional Animal Care and Use Committee at Harvard Medical School and conforms to the *Guide for the Care and Use of Laboratory Animals* published by the US National Institutes of Health (NIH Publication No. 85-23, revised 1996). Male mice (C57Bl/6J) from Jackson Laboratory (Bar Harbour, ME) were selected for experiments. All animals were housed in a room lighted 12 h/day at an ambient temperature of 22 ± 1ºC. Animals were allowed 1-3 weeks to recover after arrival and had free access to Purina Lab Chow 5001 (Ralston Purina Co., St. Louis, MO) and tap water until the initiation of the experiment unless otherwise stated.

General Cell Culture Experimentation Protocol

EA.hy926 cells were maintained in DMEM with 10% FBS. Twelve hours before treatment, cells were switched to DMEM without FBS. At the time of treatment, cells were incubated with vehicle, aldosterone (10^{-8} mol/L; Acros Organics, Geel, Belgium), or aldosterone (10^{-8} mol/L) plus the MR antagonist canrenoate (10^{-6} mol/L; Sigma-Aldrich, St. Louis, USA) in DMEM without FBS. For the Estrogen experiments cells were grown is Estrogen Deficient (ED) phenol free media (Gibco) prepared with charcoal striped FBS (208). Twelve hours before treatment, cells were switched to DMEM without FBS. At the time of treatment, cells were incubated with vehicle, estrogen (5×10^{-8} mol/L; Sigma-Aldrich, St. Louis, USA), or estrogen (5×10^{-8} mol/L) plus aldosterone (10^{-8} mol/L) in DMEM without FBS.

Results

A significant part of the research shown here was based on cell culture of established immortalized cell lines and it is crucial to keep the culture conditions as homogenous as possible, so that, this is not one more variable that needs to be taken into account when analyzing the results of the experiments carried out with these cells. Since the culture media itself has a controlled formulation the major source of variation comes from additives that are not standardized such as, foetal bovine serum (FBS). To reduce such variation, FBS from a single manufacturer's lot was selected after rigorous screening, and subsequently used throughout the duration of the experimental phase of the work presented herein. As part of this screening cell number and viability were measured as well as the pERK protein response to aldosterone stimulation.

FBS is the sterile liquid that is obtained from the clotted blood of the bovine foetus. It contains numerous growth factors that are needed for the survival and propagation of mammalian cells in culture and for this reason was introduced early in cell biology research, subsequent to initial studies with hen and sheep sera (209-212). Already in the 1950s profound differences for cellular growth between human serum and FBS were described and first attempts were made to culture cells in serum-free media (212, 213). Despite advances in the fabrication of standardized serum-free media over the last decades (214), FBS still remains the most widely used cell culture medium supplement in cell biology.

FBS is commercially available from numerous manufacturers and researchers typically choose their sera batches based on price, good viability and function of their cell cultures, or cloning efficiency. However, few researchers study the composition of their FBS batches and these sera therefore remain a major black box in cellular experiments. It was previously reported that different sera contain distinct compositions of fatty acids, including arachidonic acid (215), and that these lipids can directly influence cellular experiments (216, 217). More recently, it was shown that

FBS can contain unknown factors that are able to inhibit Toll-like receptor (TLR) activation under certain circumstances (218). Although it is generally accepted that the composition of FBS may directly influence the outcome of cellular experiments, relatively little is known about the impact of lipids and other sera components.

FBS Selection and Growth Curve

Using the service Batch Testing with Reserves provided by Gibco®, 5 different lots of serum were tested:

Lot 1- 1355888
Lot 2- 1355891
Lot 3- 1389439
Lot 4- 1365490
Lot 5- 1385397

Seven T25 flasks were seeded with the same amount of cells for both the EA.hy926 and IMR90 cells. Counts were taken (at the same hour) everyday for 7 days using a Neubaüer counting chamber and Trypan Blue Stain (Sigma-Aldrich) for cell viability purposes. Plating day was considered day 1.

Table 1- EA.hy926 Cell Growth Study for FBS lot Selection.

Day	Cell number ($x10^5$)	Cell Viability (%)	Cell Density (%)	Lot
1	2.0×10^5	100%	10%	Lot 1- 135588
2	1.0×10^5	100%	20%	
3	2.0×10^5	100%	40%	
4	3.0×10^5	100%	40%	
5	2.0×10^5	100%	30%	
6	5.0×10^5	100%	60%	
7	8.0×10^5	100%	80%	

Day	Cell number ($x10^5$)	Cell Viability (%)	Cell Density (%)	Lot
1	2.0×10^5	100%	20%	Lot 2- 1355891
2	1.0×10^5	100%	20%	
3	2.0×10^5	100%	40%	
4	3.0×10^5	100%	40%	
5	8.0×10^5	87.5%	80%	
6	8.0×10^5	100%	100%	
7	20×10^5	100%	100%	
1	2.0×10^5	100%	15%	Lot 3- 1389439
2	1.0×10^5	100%	20%	
3	2.0×10^5	100%	30%	
4	5.0×10^5	100%	60%	
5	6.0×10^5	83.3%	70%	
6	9.0×10^5	88.9%	100%	
7	15×10^5	100%	100% (secondary)	
1	3.0×10^5	100%	20%	Lot 4- 1365490
2	2.0×10^5	100%	40%	
3	4.0×10^5	100%	60%	
4	8.0×10^5	100%	75%	
5	10×10^5	100%	90%	
6	15×10^5	100%	100% (secondary)	
7	20×10^5	85%	100% (secondary)	
1	2.0×10^5	100%	20%	Lot 5- 1385397
2	1.0×10^5	100%	30%	
3	3.0×10^5	100%	40%	
4	4.0×10^5	100%	60%	
5	7.0×10^5	100%	60%	
6	11.0×10^5	81.8%	90%	
7	14×10^5	100%	100%	

Before the FBS lot was selected, media samples were sent to a core facility part of Harvard University in order to measure the aldosterone levels present in each lot. After measurement aldosterone levels were considered too low to cause any

interference in the experiments being carried out with the FBS since they were not detectable using a sensitive radioactive assay.

Graphic 1- FBS Growth Study using EA.hy926 cells.

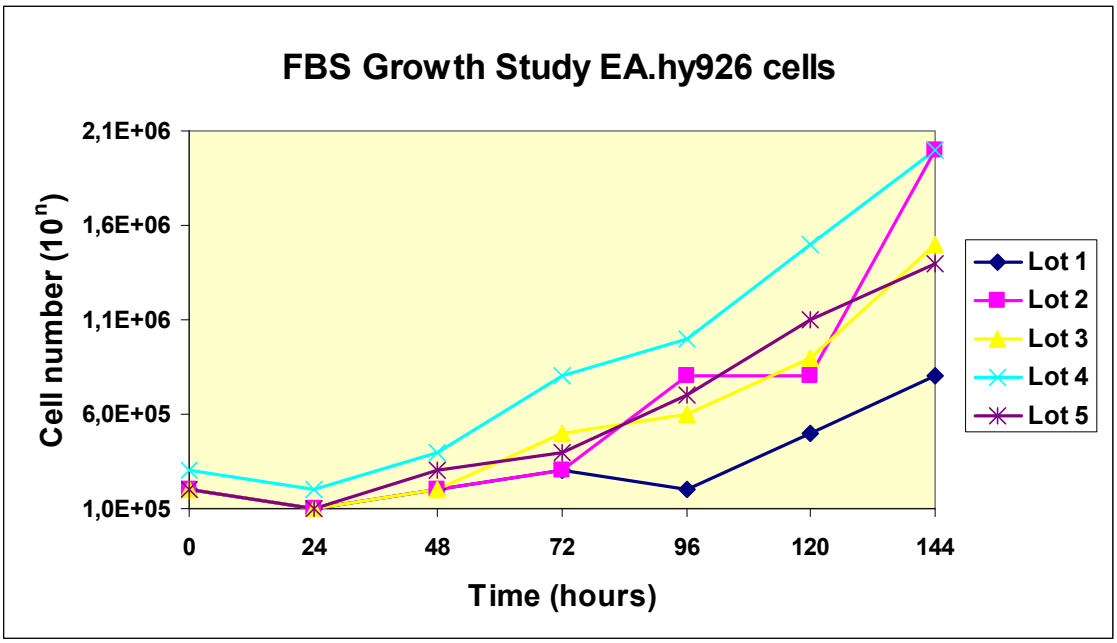

After analyzing the growth study results for all lots it became apparent that lot 1 did not present the necessary conditions for optimal growth of the cells due to poor cell growth, lots 2-4 showed consistent results with a exponential trend as desired but, lot number 4 did better overall not only showing a more consistent growth trend than the other lots but also a faster growth achieving full confluency sooner than other lots. Further testing was done to determine if this lot was suitable for the experiments planned although, at this stage, lot 4 was considered the most promising and the specific growth rate for these cells was calculated using data from lot number 4 growth curve.

The most well know form of the growth equation is as follows:

$$N = N_0.e^{\mu t}$$

This equation allows scientists to calculate the approximate number of cells (**N**) that will be present at a time **t**, provided that the initial number of cells plated (N_0) is

known. ***μ*** is termed the **specific growth rate** or often simply growth rate, (unit: d^{-1}, h^{-1}, or min^{-1}) and can be calculated using the following formula:

$$\mathbf{ln\ (x_2/x_1) = \mu(t_2-t_1)}$$

The specific growth rate for EA.hy926 cells using FBS lot number 4 was calculated to be 0.0289 h^{-1}. The doubling time for this cell line is between 24 and 48 hours depending on which phase of the growth curve the cells are in.

FBS lot 4 was the best choice for growing EA.hy926 cells but, what about IMR90 cells?

Table 2- IMR90 Cell Growth Study for FBS lot Selection.

Day	Cell number ($x10^5$)	Cell Viability (%)	Cell Density (%)	Lot
1	2.0×10^5	100%	10%	Lot 1- 1355888
2	1.0×10^5	100%	10%	
3	2.0×10^5	100%	15%	
4	3.0×10^5	100%	40%	
5	6.0×10^5	100%	50%	
6	7.0×10^5	100%	70%	
7	8.0×10^5	100%	70%	
1	2.0×10^5	50%	10%	Lot 2- 1355891
2	2.0×10^5	100%	15%	
3	3.0×10^5	100%	20%	
4	3.0×10^5	100%	40%	
5	7.0×10^5	100%	60%	
6	7.0×10^5	100%	70%	
7	7.0×10^5	100%	60%	
1	2.0×10^5	50%	10%	Lot 3- 1389439
2	3.0×10^5	66.7%	10%	
3	2.0×10^5	100%	20%	
4	6.0×10^5	83.3%	50%	
5	11.0×10^5	90.9%	50%	
6	8.0×10^5	100%	60%	
7	9.0×10^5	88.9%	70%	

Day	Cell number (x10^5)	Cell Viability (%)	Cell Density (%)	Lot
1	2.0 x 10^5	100%	10%	Lot 4- 1365490
2	2.0 x 10^5	100%	10%	
3	3.0 x 10^5	100%	30%	
4	4.0 x 10^5	100%	60%	
5	9.0 x 10^5	100%	60%	
6	7.0 x 10^5	100%	70%	
7	10 x 10^5	100%	70%	
1	2.0 x 10^5	100%	10%	Lot 5- 1385397
2	2.0 x 10^5	100%	20%	
3	2.0 x 10^5	100%	40%	
4	3.0 x 10^5	100%	40%	
5	4.0 x 10^5	100%	40%	
6	4.0 x 10^5	100%	50%	
7	6.0 x 10^5	100%	60%	

Graphic 2- FBS Growth Study using IMR90 cells.

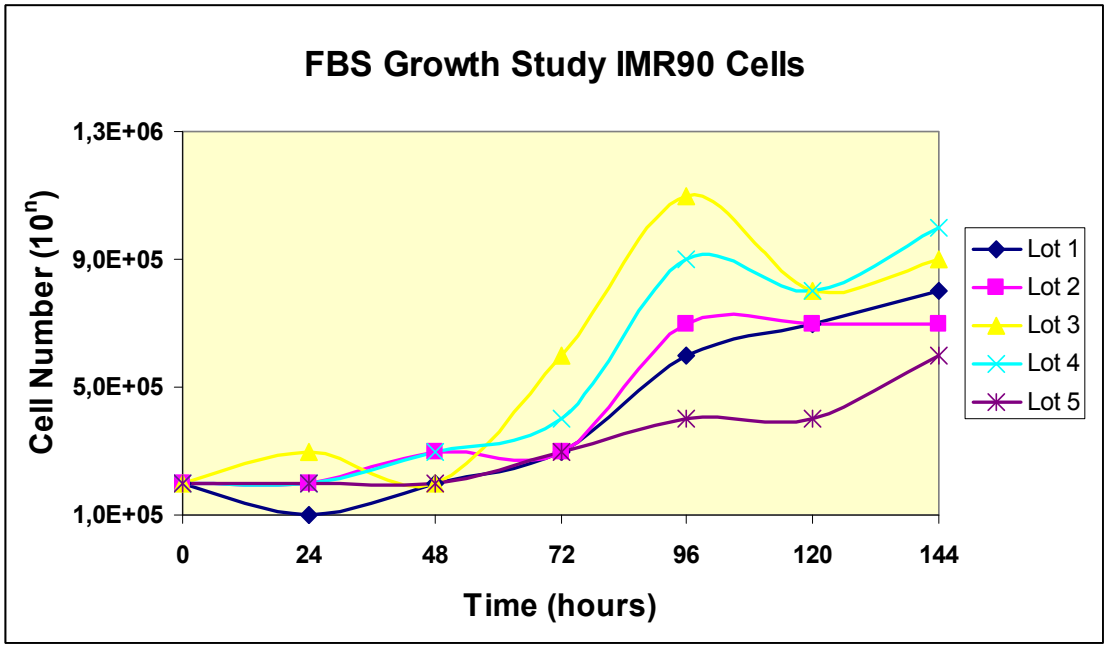

Analyzing the results shown on the table and graph depicted above it is easy to ascertain that the IMR90 cell line presents a very different growth pattern from the EA.hy926 cell line. The cell numbers achieve are lower and full confluency is never

achieved which is in keeping with the fact that these fibroblasts suffer from contact inhibition and hence need to be passaged before reaching full confluency. An example of that contact inhibition can be seen with lots 3 and 4 where cells peak at 96 hours but subsequently reduce in number. The growth also seems slower with a doubling time closer to 48 hours.

In terms of FBS batches, once again three different groups can be distinguished according with their general effectiveness. Lot number 5 was considered the worse FBS for culturing the IMR90 cell line due to a very poor growth rate. Lot number 1 and number 2 achieved better growth rates and could potentially be used but, it was lot number 3 and lot number 4 that delivered the best growth. Of all the lots tested, number 3 seems to have faired the best displaying a perfect exponential trend with higher number of cells. However, because this is not the only cell line used for experimental procedures and, furthermore, the main cell lines used are endothelial in nature, lot number 4 was elected the best fit for the work to be developed ahead, providing the best results for EA.hy926 cells and good results with IMR90 cells.

The specific growth rate for IMR90 cells using FBS lot number 4 was calculated to be 0.0338 h^{-1}. The doubling time for this cell line is between 24 and 48 hours depending on which phase of the growth curve the cells are in.

Endothelial Cell Phenotyping

Optimal cell culture conditions are very important to maintain the growing variables such as time and cell number present as stable as possible but, even more important is to make sure that the cells used have the right characteristics for the designed experiments. In the case of the experimental work developed for this thesis, the elected cell lines were selected in order to try and mimic the endothelial layer (endothelium) of the cells and arteries present in the cardiovascular system. As mentioned before and amongst the hybrid cells, the EA.hy926 cell line, derived by the fusion of HUVECs with the continuous human lung carcinoma cell line A549, is presently the best characterized macro-vascular endothelial cell line (191). Although these cells have been described it is still necessary to confirm its properties under

our culture conditions and also to make sure that the proteins of interest for this study are indeed present in these cells.

However, for the purpose of writing this thesis not only immortalized cell lines were used but also a primary cell line. The advantages of primary cultures are that the cells have not been "modified" in any way (other than the enzymatic or physical dissociation necessary to obtain them), and that allows for study conditions as close as possible to *in vivo*. The disadvantages of these cultures are the mixed nature of each preparation, limited lifespan of the culture and the potential contamination problems. For all of these reasons several tests have to be performed before any conclusions can be derived from the experiments designed using these cells.

Morphological Analysis

One of the first and easiest phenotypic analysis that can be performed is to evaluate the morphology of the experimental cells. The American Type Culture Collection (ATCC) is a non-profit bioresource centre which has been preserving, growing and distributing cultures for almost 80 years. ATCC is the largest biological resource centre in the world with the most comprehensive source of reference cultures and reagents. Since 1925, this company has set the standard for authentication and distribution of biological reference materials and it is easy to access its library to get the technical information relating to the cell type you might be working with. The following figures are representative images of EA.hy926 cells maintained and sold by ATCC that can be used as reference when evaluating the morphology of these cells.

EA.hy926 cells display a "triangular" shape at a low density and eventually evolve to cobblestone morphology when they are maintained in culture on a plastic support. They do not form multiple layers but a uniform cobblestone like monolayer at full confluency (219). Since the primary cultures used in these studies are also endothelial nature, it is expected they would exhibit a similar morphology and growth pattern to EA.hy926 cells.

Below are electron micrographs photos showing EA.hy926 cells (figure 29) used in the laboratory as well as Mouse Endothelial Cells (figure 30) at different culture densities.

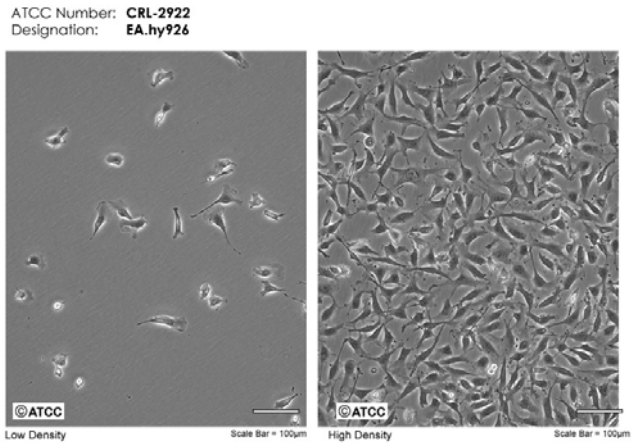

Figure 28- Light microscope photographs showing EA.hy926 cells at different culture densities.

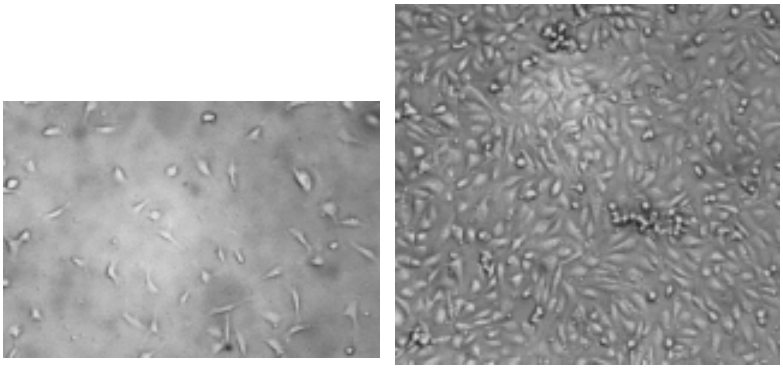

Figure 29- Light microscope photographs showing EA.hy926 used for experiments. Pictures taken using 200x magnification.

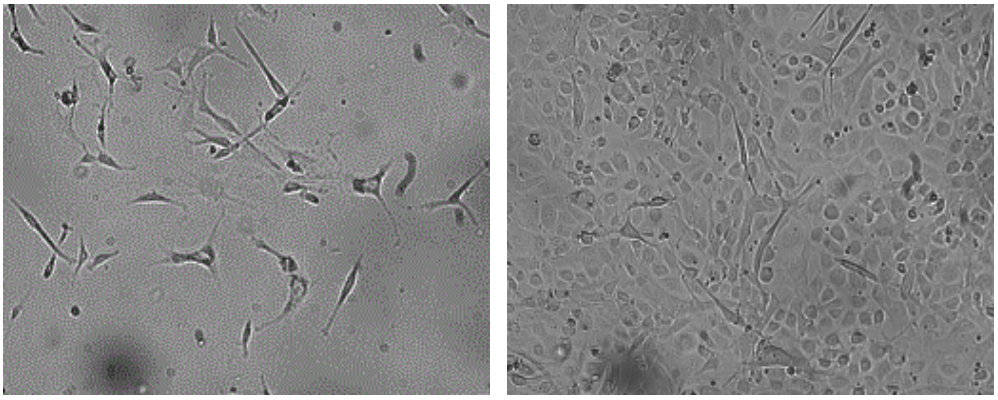

Figure 30- Light microscope photographs showing Mouse Aortic Endothelial Cells used for experiments. Pictures taken using 200x magnification.

Comparing the images supplied by ATCC (figure 28) to the images obtained by photographing the cells in culture in the laboratory (figure 29) it is easy to see morphological similarities. When the cells are less confluent it is possible to distinguish the triangular shape typical for these cells and, when the cells become confluent they evolve to form the monolayer cobblestone pattern as specified by ATCC.

Mouse Aortic Endothelial Cells electron micrographs depicted show a striking similarity to EA.hy926 cells. In low densities the cultured cells show several shapes ranging from fusiform to the typical more triangular shape. From observational studies it was possible to distinguish different stages of growth from the shape the cells take. When the cells first attach to the collagen matrix with which the flasks were treated they are spherical. After adhering onto the matrix, the cells start "stretching" and taking a more fusiform shape. On the next stage, pseudopods or "feet" start forming and evolve until the shape takes the more triangular and typical endothelial cell shape. At full confluency these cells show a tight cobblestone pattern similar to the EA.hy926 cells but it is also possible to see a couple scattered cells on top of the monolayer. All in all the primary cultures used for experiments show (through morphological analysis) a high degree of purity.

Immunofluorescence Staining

In order to confirm the endothelial nature and purity of the primary cell cultures used, specific monoclonal antibodies raised against different endothelial cell markers were used (Von Willebrand Factor (VWF) and CD31 (PECAM-1)) (220, 221) in conjunction with immunofluorescence techniques.

Briefly EA.hy926, IMR90 and Mouse Aortic Endothelial Cells were grown in microscope coverslips. When cell confluence reached about 70% the cells were fixed using paraformaldehyde and permeablized with a solution of 15% Triton X-100 detergent. After the cells were prepped the primary antibody was applied. The specific antibody was diluted in blocking solution (1% BSA in PBS) and left overnight at 4ºC. Since the primary antibody is not linked to any fluorochrome its necessary to apply a secondary antibody in order to be able to visualize the cell markers under the fluorescence microscope. Fluorescent green and red antibodies were used to label the VWF, CD31 and alpha smooth muscle actin (α-SMA), respectively.

VECTASHIELD® Mounting Medium with DAPI was applied to preserve fluorescence and counterstain DNA (stains the DNA blue) and the coverslips mounted on microscope slides. The Nikon Eclipse 90*i* Fluorescence Roper Scientific Microscope was used to analyze the resulting cell staining.

Both EA.hy926 and Mouse Aortic cells are expected to stain positive to endothelial cell markers CD31 and VWF but negative to α-SMA, whereas IMR90 cells, being fibroblasts are expected to stain positive to α-SMA (222), but negative to the other two markers.

EA.hy926 cells were used at passages 12 and 13, Mouse Aortic Endothelial cells were used at passages 3 and 4 and derived from different isolation experiments and finally IMR90 cells were used at different PDLs and were included in most immunofluorescence staining experiments as a negative control.

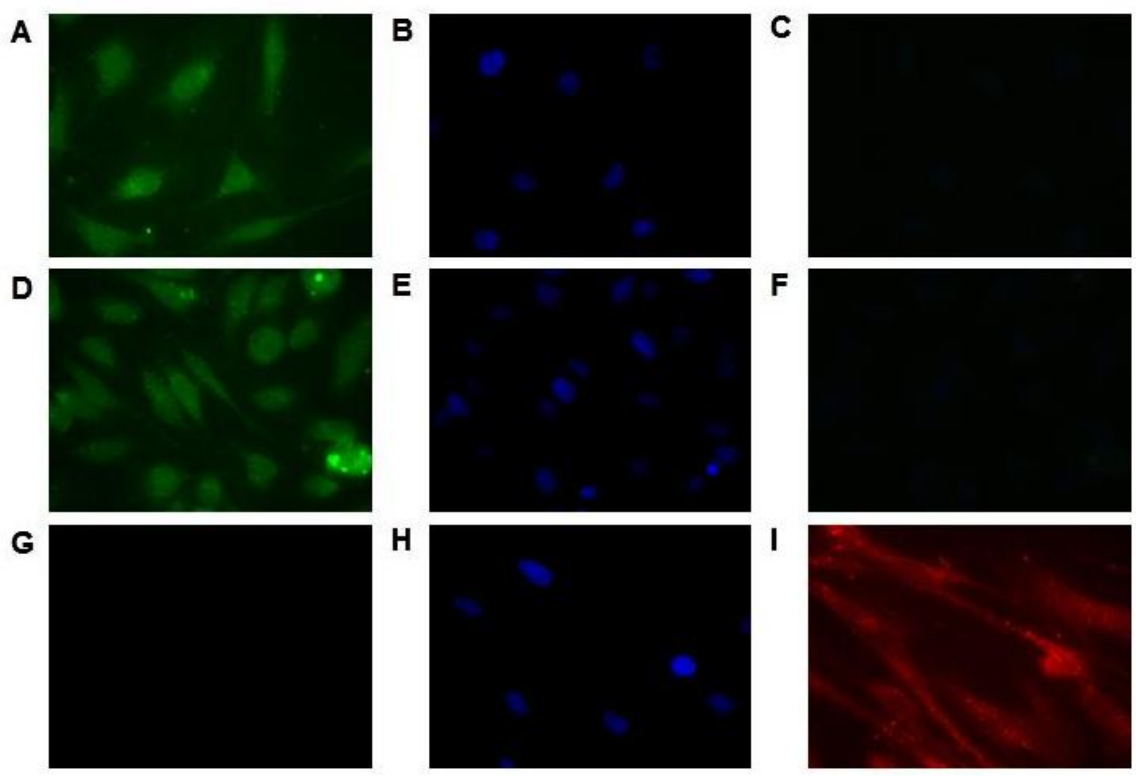

Figure 31- EA.hy926 and IMR90 cells stained with CD31 (green) or α-SMA (red) antibodies. Nuclear DNA stained blue with DAPI. Images shown with a 400x magnification (10x ocular, 40x lens) (A, D): EA.hy926 cells stained with CD31 antibody shown in green; (B, E): EA.hy926 cell nuclear DNA stained blue with DAPI; (C, F): EA.hy926 cells show negative staining for α-SMA (red). (G): IMR90 cells show negative staining for CD31 (green); (H): IMR90 cell nuclear stained blue with DAPI; (I): IMR90 cells stained with α-SMA shown in red.

Results shown above confirm that these cells are viable models t study cardiovascular function. EA.hy926 cells stained positive for CD31 confirming its endothelial nature. Further proof came from the negative staining for α-SMA. Contrary to EAhy.926 cells, IMR90 fibroblasts stained positive for α-SMA and negative to CD31. This result indicates that these cells are a good negative control and demonstrates that the immunofluorescence staining is extremely sensitive, with very low background and non-specific staining levels. Nuclear DNA staining, highlighted by DAPI shows that the cells have maintained their integrity and depict optimal levels of fixation and permeabilization as well as the quality of the mounting medium used.

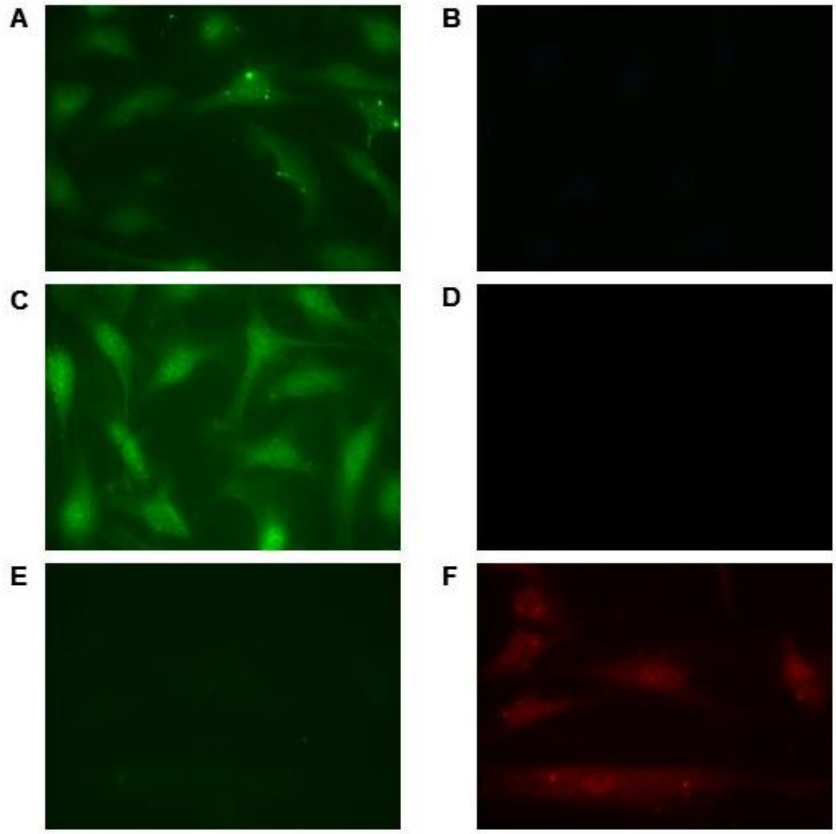

Figure 32- EA.hy926 and IMR90 cells stained with VWF (green) or α-SMA (red) antibodies. Images shown with a 400x magnification (10x ocular, 40x lens) (A, C): EA.hy926 cells stained with VWF antibody shown in green; (B, D): EA.hy926 cells show negative staining for α-SMA (red). (E): IMR90 cells show negative staining for VWF (green); (F): IMR90 cells stained with α-SMA shown in red.

Once again results shown above are in agreement with expectations. EA.hy926 cells stained positive for VWF confirming its endothelial nature with further proof derived from the negative staining for α-SMA. IMR90 fibroblasts stained positive for α-SMA and negative to VWF, again as expected.

Another piece of evidence demonstrating that the immunofluorescence staining was a success is the even distribution of the colour in the cells. This shows that the antibody displays little non-specific binding and the cells were prepared properly for the staining.

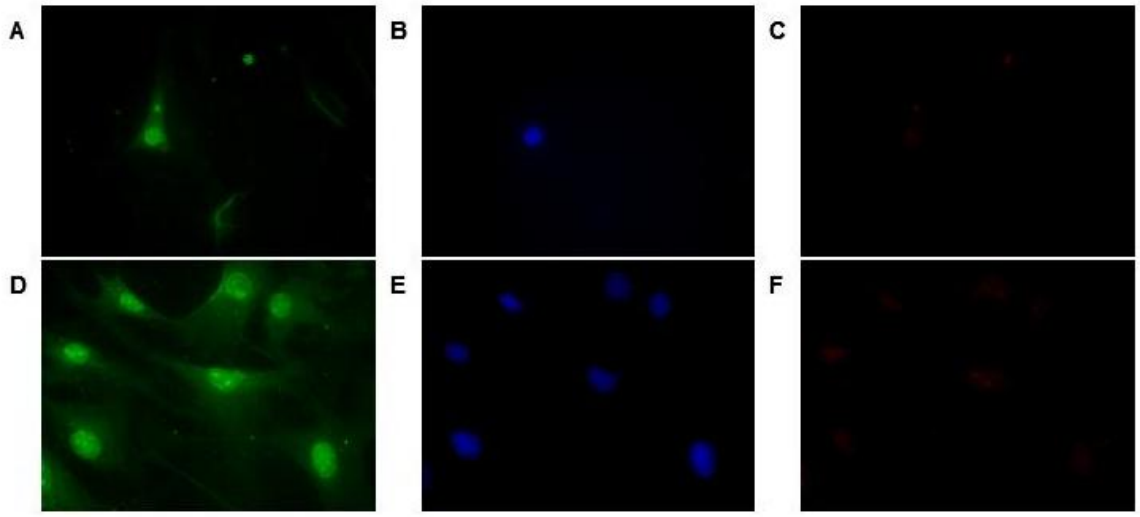

Figure 33- Mouse Aortic Endothelial cells stained with VWF (green) or α-SMA (red) antibodies. Nuclear DNA stained blue with DAPI. Images shown with a 400x magnification (10x ocular, 40x lens) (A, D): Mouse Aortic cells stained with VWF antibody shown in green; (B, E): Mouse Aortic cells nuclear DNA stained blue with DAPI; (C, F): Mouse Aortic cells show negative staining for α-SMA (red).

Due to the isolation method, these primary cells have a considerable chance of containing a mixture of more than one cell type, making the immunofluorescence staining results particularly important to determine if this is a viable method for future use in experimental procedures or if further purification of these primary cells is required.

Results depicted above point to the presence of a cell population of 100% endothelial cells suggesting that no further purification of these cells is required. Images show that even at higher levels of confluency all cells stain positive for VWF,

a specific marker for endothelial cells. Like EA.hy926 cells, Mouse Aortic Endothelial cells are also negative for α-SMA, confirming its endothelial nature. It is possible to see some background staining but comparatively to the staining seen in fibroblast cells, it is too low to be considered positive. Nuclear DNA, as measured by DAPI staining, indicates that these cells withstood fixation and permeabilization well and the primary antibodies were allowed to penetrate and stain the cell throughout.

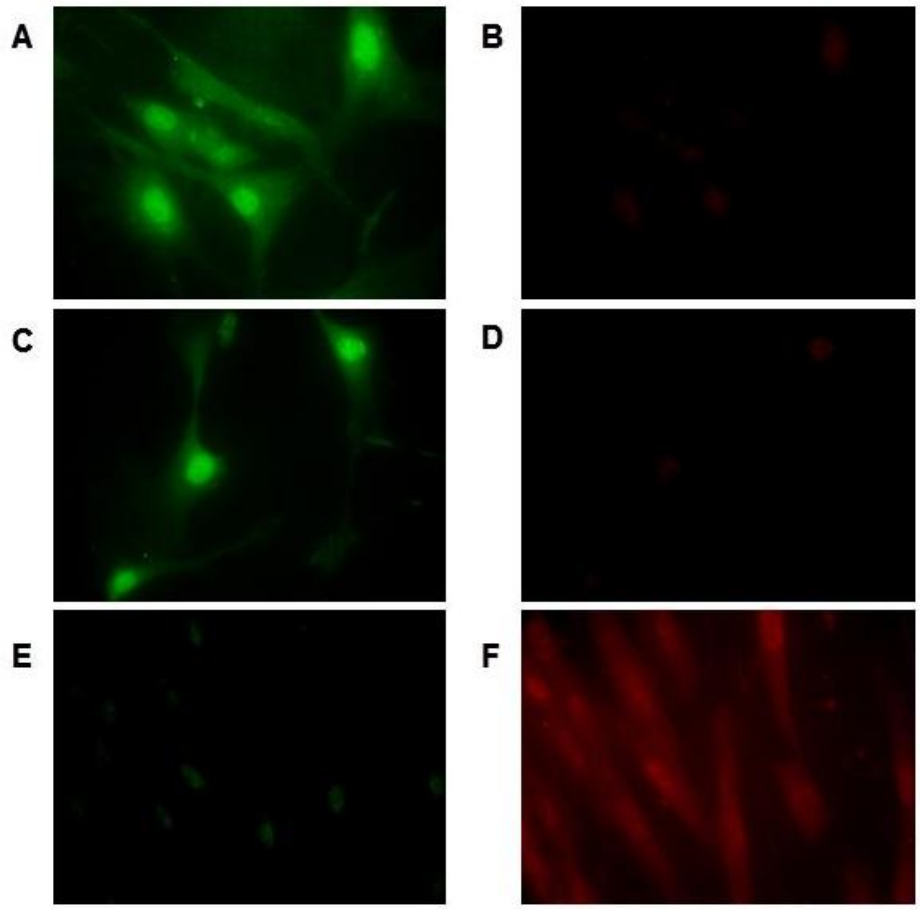

Figure 34- Mouse Aortic cells and IMR90 cells stained with CD31 (green) or α-SMA (red) antibodies. Images shown with a 400x magnification (10x ocular, 40x lens) (A, C): Mouse Aortic cells stained with CD31 antibody shown in green; (B, D): Mouse Aortic cells show negative staining for α-SMA (red). (E): IMR90 cells show negative staining for CD31 (green); (F): IMR90 cells stained with α-SMA shown in red.

Results shown above are in agreement with what was observed in EA.hy926 cells. Mouse Aortic cells stained positive for CD31 antibody confirming its endothelial nature with further proof derived from the negative staining for α-SMA. Also as expected, IMR90 fibroblasts stained positive for α-SMA and negative to CD31.

These results, together with the VWF staining results, indicate that the Mouse Aortic cells are indeed endothelial and, therefore, can be used for further experiments without any concerns for purity. Both isolation experiments resulted in a pure endothelial cell population viable for experimentation.

As mentioned previously in the introductory chapter, in endothelial cells ER was shown to target lipid rafts within the plasma membrane (caveolae) by interaction with caveolin-1, where it activates endothelial nitric oxide synthase (eNOS) through protein kinase-mediated phosphorylation (169). Caveolae facilitate signal transduction by providing a location for various signalling molecules (170). Activation of ER by phosphorylation has been demonstrated to occur in both a hormone-dependent as well as hormone-independent manner and is an integral regulatory mechanism of nongenomic responses.

The plasma membrane invagination structure of caveolae supports functional protein-protein interactions and cluster of several discrete signalling pathways. Thus, caveolae are thought to integrate interactions of receptors and signalling molecules in the plasma membrane, resulting in rapid and specific signal transduction (175). The caveolin scaffolding domain (CSD) of CAV_1 binds numerous signalling molecules, including Src family kinases, c-Neu, H-Ras, EGFR, eNOS, and G-protein coupled receptors (GPCRs). The ability of CAV_1 to hold and orchestrate the spatio-temporal pairing of membrane localized ERα with its effectors makes CAV_1 an important scaffolding protein mediating membrane ERα actions. CAV_1 is required for estrogen-mediated ERα-dependent eNOS production in endothelial cells (186).

More recently, CAV_1 has also been shown to interact with the protein striatin, which has been shown to be a key intermediary of the effects of steroid receptors, specifically estrogen receptor-α (ERα) (188). Lu et al provided evidence that striatin´s N-terminal segment interacts with the DNA binding domain of ERα in the immortalized human endothelial cell line, EA.hy926 cells. This interaction organizes

the ERα-eNOS membrane signalling leading to rapid nongenomic activation of downstream signalling pathways including ERK and eNOS in endothelial cells. Interestingly, disruption of the striatin-ERα interaction had no effect on estrogen-mediated gene transcription suggesting that striatin specifically mediates ERα extra-nuclear signalling independent of ERα nuclear actions.

Results demonstrated for ERα by other groups and mentioned above served as the basis for this thesis. Being part of the same family of steroid receptors and having in common its method of action it is possible that MR also shares this form of nongenomic/rapid signalling with ERα. Having established the endothelial nature of both the EA.hy926 and mouse aortic primary cells, the next logical step was to make sure that the proteins of interest (MR, striatin and caveolin 1) were present in the cells to be used in experimental studies.

Protein Determination by Western Blot Analysis

Since the subject of this study is the nongenomic action of MR, it is only natural to investigate MR expression in EA.hy926 and mouse aortic cells. According to the proteomic information repository website UniProtKB/Swiss-Prot, MR protein is expected to have a molecular weight of 107 kDa. **UniProt** is a comprehensive, high-quality and freely accessible database of protein sequence and functional information, many entries being derived from genome sequencing projects. It contains a large amount of information about the biological function of proteins derived from the research literature and is a good place to look for reliable information on molecular weights and protein isoforms.

The antibody selected for this study was Santa Cruz's rabbit polyclonal antibody raised against amino acids 1-300 of the human MR protein (catalogue number sc-11412). The main reason for selecting this antibody was the fact that it had been used before in the laboratory (223), providing consistent results. Below is the image provided by the manufacturer for the band size to expect.

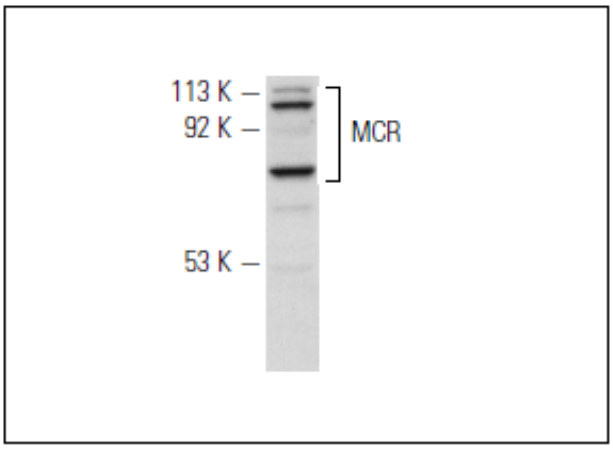

MCR (H-300): sc-11412. Western blot analysis of MCR expression in K-562 whole cell lysate.

Figure 35 – Image provided by Santa Cruz Technology for cat. no. sc-11412 MR antibody.

Analyzing the image it is possible to see several bands. One faint band over 113 kDa which one can speculate might either be non specific or, due to post-translational modification of the MR protein. The strong intensity band at around 107 kDa can be assumed to be MR and finally, an even stronger intensity band at around 75-80 kDa which could potentially be an MR isoform that lacks steroid-binding activity and acts as ligand-independent transactivator (52). Bearing in mind that the manufacturer itself does not offer any explanation for the multiple bands present, this explanation is only one of many possible.

Both Mouse Aortic Endothelial cells (MAEC) and EA.hy926 cells were tested for MR protein. Mouse heart tissue was also used to ascertain if there was any MR present in this tissue.

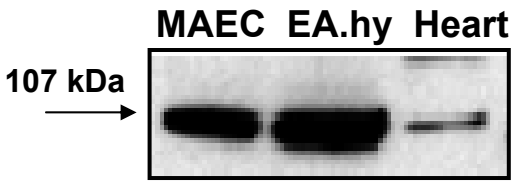

Figure 36 – Western blot membrane showing the presence of MR protein in Mouse Aortic Endothelial cells (MAEC), EA.hy926 cells (EA.hy) and Mouse heart tissue (Heart).

The size of the bands shown in this western blot membrane was estimated from the relative position of the bands to the Kaleidoscope Precision western blot marker manufactured by BioRad. The bands were positioned slightly above the 100 kDa marker, making the 107 kDa a very likely weight.

Results show a strong presence of the protein in both MAEC and EA.hy926 cells, being the later where the highest abundance can be found. There are several reports pointing to the presence of MR in cardiac tissue (224, 225). It has also been established that the presence of MR in cardiac tissue tends to increase with inflammation and fibrosis, being higher in disease models (226). Western blot results above show the presence of MR in mouse cardiac tissue although not in very high amounts as seen in the endothelial cells tested alongside in the same membrane. These results are consistent with the literature and would indicate a healthy rodent. The different bands seen in the image provided by the manufacturer were not present in the western blots carried out with our samples.

The next protein that was looked at was striatin since it plays a key role in the nongenomic actions of ERα and may possibly be involved in the nongenomic actions of MR if the initial hypothesis for this work is correct.

The UniProtKB/Swiss-Prot website predicts the molecular weight of the striatin protein to be around 86 kDa. The antibody selected for this study was BD Bioscience's mouse monoclonal antibody raised against amino acids 450-600 of the rat striatin protein (catalogue number 610838). Below is the image provided by the manufacturer for the band size to expect.

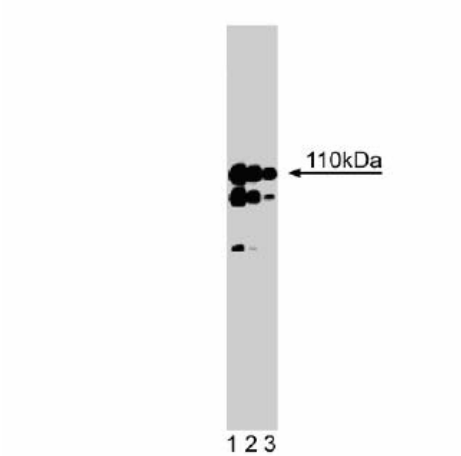

Western blot analysis of Striatin on a rat cerebrum lysate. *Lane 1: 1:1000, lane 2: 1:2000, lane 3: 1:4000 dilution of the mouse anti-Striatin antibody.*

Figure 37 – Image provided by BD Biosciences for cat. no. 610838 striatin antibody.

The expected molecular weight differs significantly from the predicted weight but, it is in accordance with results obtained for other antibodies available in the market which strongly points to the possibility that striatin undergoes a post-translational modification. In light of the available information on this protein, the most probable modification appears to be phosphorylation and there is some evidence in the literature (227) that seems to corroborate this hypothesis. Unfortunately, there isn't a commercially available antibody that can be used to prove such a theory.

Again, both endothelial cell lines were tested for striatin protein, alongside mouse heart tissue. Results obtained are depicted below.

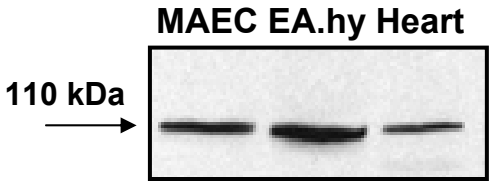

Figure 38 – Western blot membrane showing the presence of striatin protein in Mouse Aortic Endothelial cells (MAEC), EA.hy926 cells (EA.hy) and Mouse heart tissue (Heart).

Once again, the size of the bands shown in this western blot membrane was estimated from the relative position of the bands to the Kaleidoscope Precision western blot marker. The bands were positioned a little above the 100 kDa marker, pointing to the 110 kDa weight.

Results show the presence of the protein in all the samples tested, MAEC, EA.hy926 cells and Mouse heart tissue. Samples show an even amount of striatin protein present, although the strongest band can be seen for the EA.hy926 cell line, making it an ideal cell line to study this thesis hypothesis.

Finally, the samples were tested for the presence of the protein caveolin 1.The UniProtKB/Swiss-Prot website predicts the molecular weight of the caveolin 1 protein to be around 20/21 kDa, having an alpha and a beta isoform. The antibody chosen for this study was BD Transduction Laboratories mouse monoclonal antibody developed using amino acids 1-178 of Rous Sarcoma Virus Transformed-Chick Embryo Fibroblasts (RSV-CEF) and purified from tissue culture supernatant or ascites using affinity chromatography (catalogue number 610406). Below is the image provided by the manufacturer for the western blot results that can be expected.

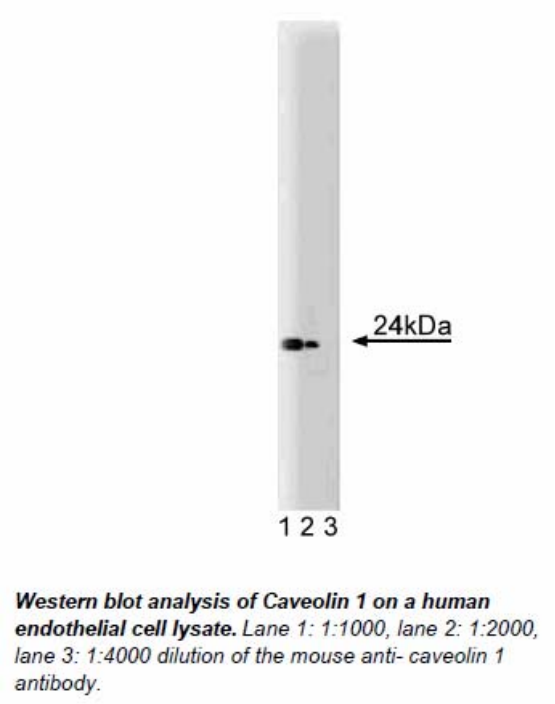

Figure 39 – Image provided by BD Transduction Laboratories for cat. no. 610406 caveolin 1. antibody.

The manufacturers western blot results show a single band which they place at 24 KDa. This result is in agreement with the expected molecular weight for the alpha isoform of this protein (20/21 KDa). Although there is a discrepancy, the variation does not seem to indicate that there is any post-translational modification or that it can be a different protein.

Both endothelial cell lines used in this study were tested as well as a mouse heart sample. Western blot was carried out using the standard protocol for the laboratory and following the manufacturer's instructions. Results obtained are depicted below.

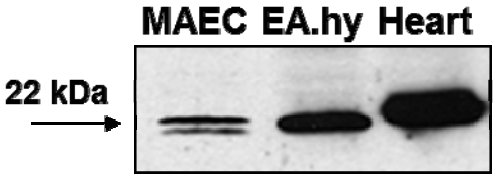

Figure 40 – Western blot membrane showing the presence of caveolin 1 protein in Mouse Aortic Endothelial cells (MAEC), EA.hy926 cells (EA.hy) and Mouse heart tissue (Heart).

Results obtained in the lab show the presence of one or two bands around the 22/24 KDa weight. It is also possible that there were two bands for EA.hy926 cells and/or heart tissue but, there is so much of the protein that the potential two bands appear as one. The bands all came under the 25 KDa Kaleidoscope weight marker. Mouse endothelial cells show 2 distinct bands which were attributed to a possible phosphorylated form of the protein. Results seen are in line with what the manufacturer predicts. The highest level of caveolin 1 protein is seen in the mouse heart tissue sample, followed by the EA.hy926 endothelial cell line.

The results from all the western blot tests carried out confirm the choice of the EA.hy926 immortalized endothelial cell line as a good model to study this work's hypothesis.

In addition to western blot analysis, the presence of MR and striatin protein in mouse aortic endothelial cells was also detected using immunofluorescence techniques.

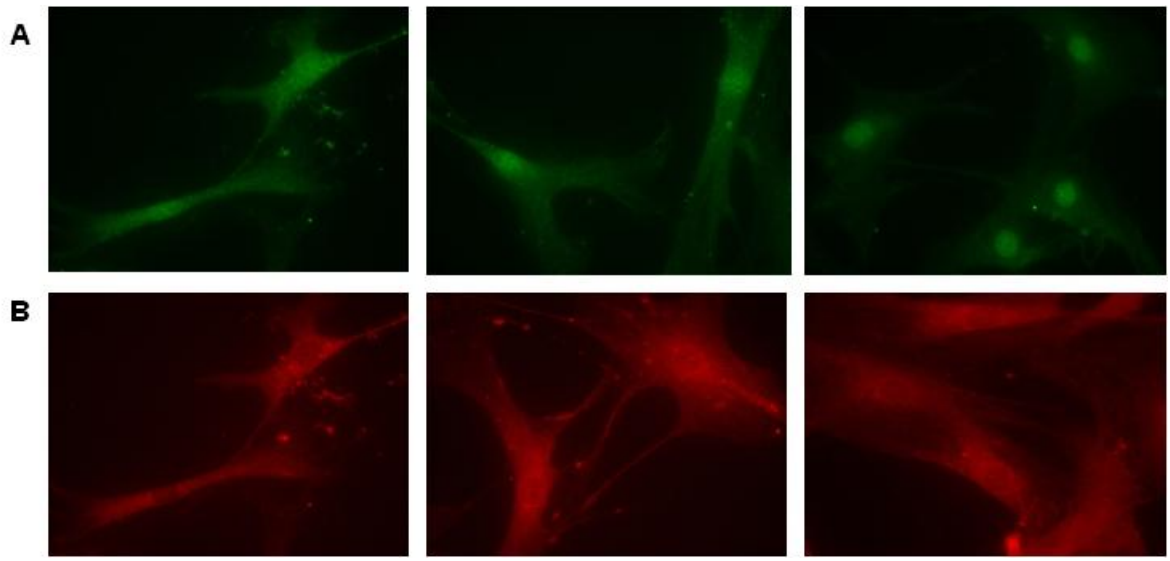

Figure 41 – Mouse Aortic Endothelial cells stained with striatin (green, A) antibody and MR (red, B) antibody. Cells were used at passage 4. Images shown with a 400x magnification.

The presence of the protein caveolin 1 in the cell lines studied is a good indication of the existence of *caveolae* rafts in the cell membrane but, in order to be sure of their presence and, because it's a fundamental point in the hypothesis, it was

decided to send the cells to be tested by electron microscopy to confirm the presence or absence of the *caveolae*.

Determination of the Presence/Absence of caveolae rafts by Electron Microscopy

The plasma membrane is a biological membrane that separates the interior of all cells from the outside environment. It is selectively permeable to ions and organic molecules and controls the movement of substances in and out of cells, protecting them from outside sources. But, the plasma membrane is not a homogenous structure. Specifically, the plasmalemma typically contains numerous small lipid patches enriched for cholesterol and glycosphingolipids, commonly referred to as lipid rafts. Lipid rafts may function to bring different proteins into proximity and thus promote interactions between receptors and signalling proteins and among different signalling receptors, allowing for receptor cross-talk (228). In certain cell types, plasmalemmal lipid rafts can be clustered and organized by a scaffolding composed of the intracytoplasmatic cholesterol-binding proteins caveolin 1, 2, or (in muscle cells) 3 into 50- to 100-nm flask shaped invaginations called *caveolae* (229). These organelles were originally discovered in the early 1950s by electron microscopic analysis of vascular endothelial cells (230) and of bladder epithelium (231). *Caveolae* have since been observed in many cell types although adipocytes, fibroblast, muscle cells and endothelial cells show the greatest abundance. *Caveolae* function to permit transcytosis of macromolecules across an endothelial cell barrier such as that found in brain capillaries. More recently, it has been appreciated that *caveolae* may also play a key role in cell signalling. This is because caveolins, especially caveolin 1, can bind to several types of plasma membrane receptor proteins and concentrate these molecules within the *caveolae* (232). This clustering of disparate receptor types further facilitates receptor cross-talk, allowing one type of ligand-occupied receptor to activate the downstream signalling pathways normally initiated by a different receptor type (185, 229). In other words, in addition to their role in transcytosis, *caveolae* appear to function as highly efficient lipid rafts.

It is know that *caveolae* are abundant in endothelial cells (ECs) *in situ* but markedly diminished in cultured cells, making it difficult to assess their role in signalling. For the particular immortalized cell line used in this study (EA.hy926) there

is some preliminary data that demonstrates the presence of *caveolae* on the cell membrane of these cells (see figure 42). D'Alessio *et al (229)*, used Transmission Electron Microscopy (Phillips CM 100 electron microscope at an accelerating voltage of 80 kV) to demonstrate the presence of these structures in EA.hy926 cells.

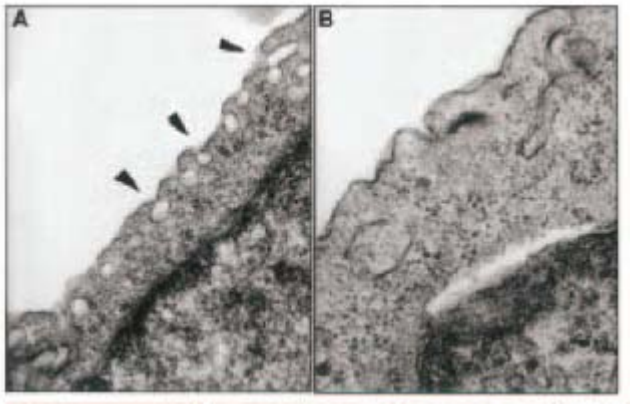

Figure 42- A: Transmission electron microscopy reveals *caveolae*, indicated by **arrowheads**, in resting EA.hy926 cells.
B: Electron Microscopy analysis of methyl-β-cyclodextrin (MβCD) treated cells showing the disappearance of caveolae network (28).

Results obtained by this group show the presence of *caveolae* in resting EA.hy926 cells that, disappear when these cells are treated with methyl-β-cyclodextrin which acts as a disruptor of lipids rafts. These results are a very good indication of what can be expected from the cells used in this thesis sent for EM analysis.

EA.hy926 cells were sent for EM analysis together with mouse aortic endothelial cells (wild type and caveolin 1 knock-out) and a potentially negative cell line (HEPG2 liver hepatocyte cell line). After fixation in the laboratory, thin sections were cut on a Reichert Ultracut E ultramicrotome, collected on formvar-coated grids, stained with uranyl acetate and lead citrate and examined in a JEOL JEM 1011 transmission electron microscope at 80 kV. Images were collected using an AMT digital imaging system (Advanced Microscopy Techniques, Danvers, MA). Electron microscopy was performed in the Microscopy Core of the Centre for Systems Biology/Program in Membrane Biology at the Massachusetts General Hospital in Boston. Results obtained can be seen in the figures presented below.

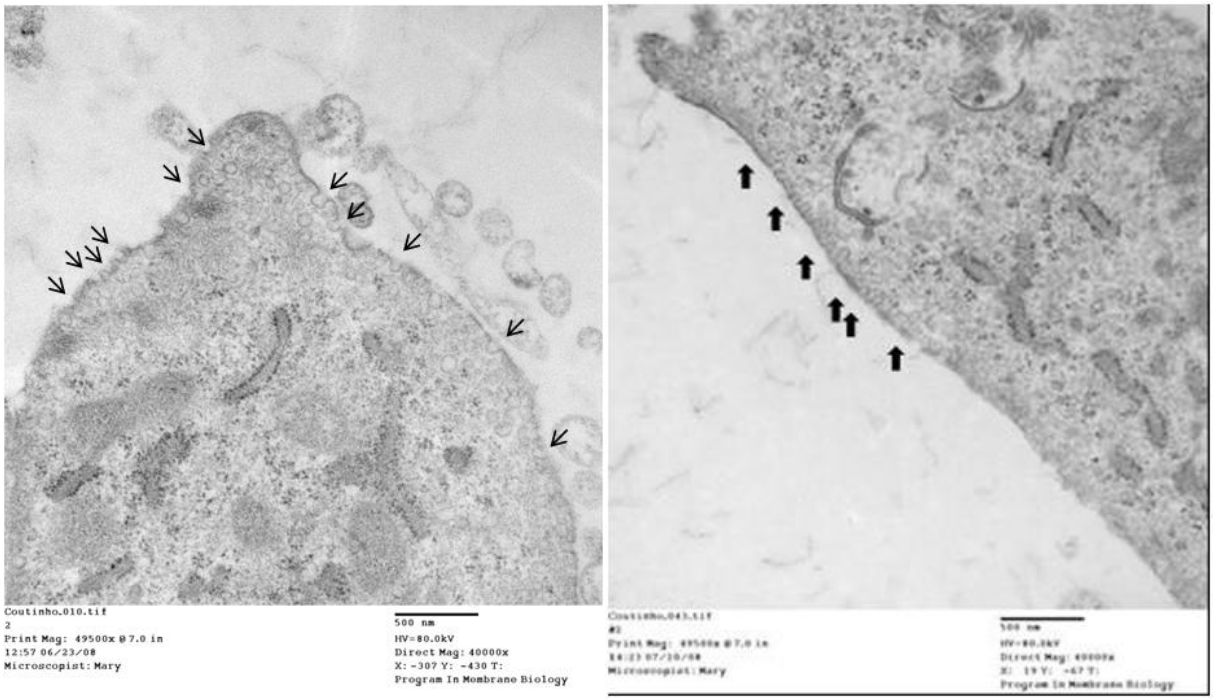

Figure 43 – Transmission electron micrographs depicting EA.hy926 cells. *Caveolae* can be seen on the cell membrane (refer to **arrows**). Images shown at 40000x magnification. Scale bar shown on right bottom below the image.

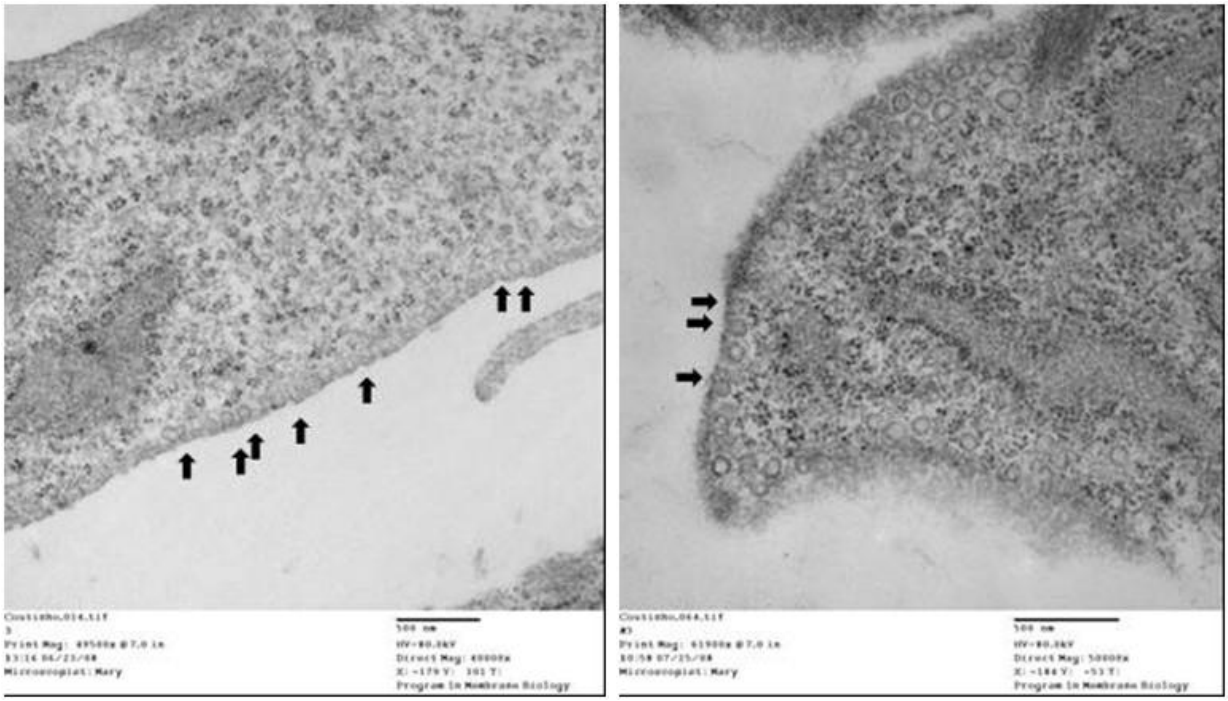

Figure 44 – Transmission electron micrographs depicting mouse aortic endothelial cells. *Caveolae* can be seen on the cell membrane (refer to **arrows**). Images shown at 40000x magnification. Scale bar shown on right bottom below the image.

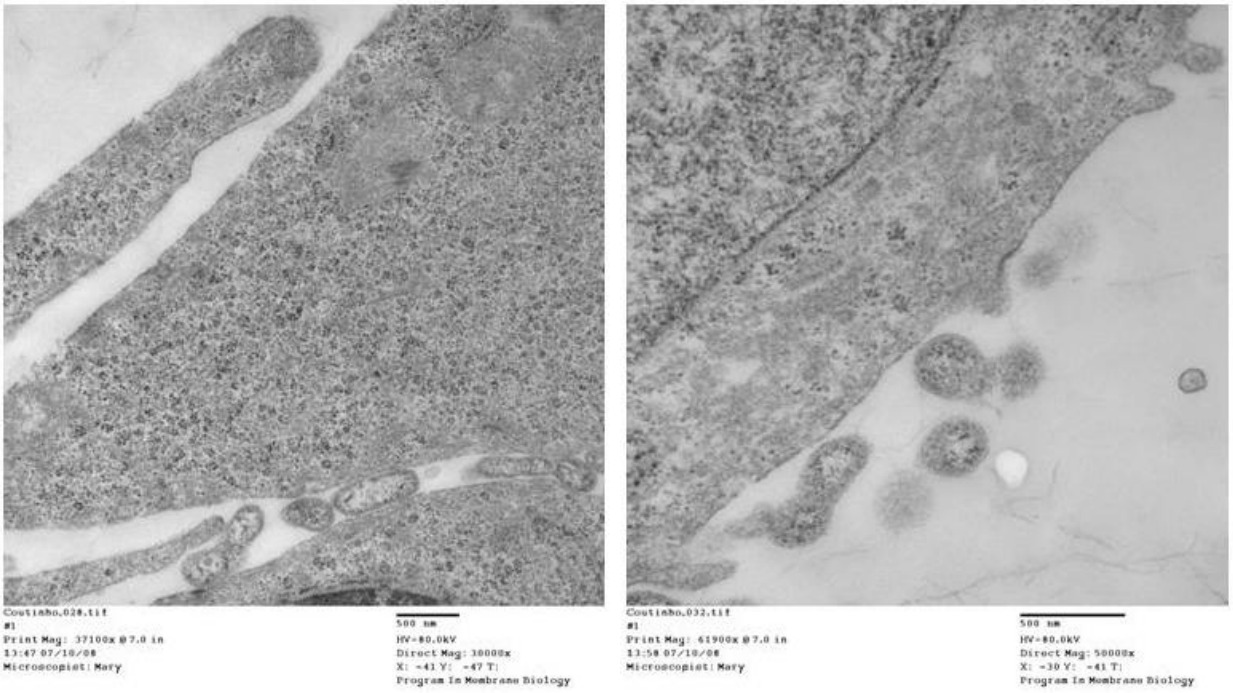

Figure 45 – Transmission electron micrographs depicting HEPG2 hepatocyte cells. No c*aveolae* can be seen on the cell membrane. Images shown at 40000x magnification. Scale bar shown on right bottom below the image.

EA.hy926 cells shown in figure 43 clearly show the presence of *caveolae* in the cell membrane. The flask-shape invaginations are present all along the cell membrane of different cells and are accompanied by signs of endocytosis. There are several endocytic vesicles in the vicinity of the cell membrane thought to be result of the intake of molecules by the *caveolae* to be transported to different locations in the cell, namely the nucleus. The results depicted are very similar to what had been published before (229) not only in the number and shape of the *caveolae* seen but are also in keep with the expected size of 50- to 100 nm.

Mouse aortic endothelial cells were collected from animal vessels and perpetuated in culture for several passages. Although they are closer to the *in vivo* conditions, it is still possible for them to lose characteristics when placed in culture conditions, hence it is very important to look for *caveolae* presence in these cells before proceeding to more experiments. Results shown in figure 44 are very similar to the ones observed for EA.hy926 cells. Cell membranes show a high number of invaginations consistent with the presence of *caveolae* in these cells together with

endocytic vesicles concurrent with the engulfing of molecules from the outside environment of the cells to be “delivered” to different destinations within the cellular milieu. The main differences that can be seen between the mouse aortic endothelial cells and the immortalized endothelial cell line EA.hy926 are that the size of the *caveolae* appears to be smaller in the mouse cells and these also appear to be more distant between themselves. It is difficult to discern if this is result of culturing the cells or a characteristic intrinsic to the cells. What can be said is that the presence of the endocytic vesicles is a positive sign of the working order of the *caveolae* present and hence makes these cells adequate for further experiments on the potential function of the caveolae in cell signalling.

Contrary to the endothelial cells seen in figure 43 and 44, the hepatocyte cell line HEPG2 electron micrographs shown on figure 45 depict a very smooth cell membrane without any invaginations resembling the shape of *caveolae* seen before. There are also no endocytic vesicles which is in keep with the lack of endocytosis carried out by the *caveolae*. It is possible to discern a few “dimples” on the cell membrane that show heavy staining. These are clathrin-coated pits which tend to be bigger than the *caveolae* and are present in virtually every type of cells. These pits are also present in the endothelial cells shown and can be easily differentiated from the *caveolae* due to their heavy staining and bigger size, they also do not have the flask shape associated with the *caveolae*.

All in all these results are very positive, endothelial cells shown, both immortalized and primary cultures, depict a strong caveolae presence on their cell membrane confirming their promise as a good study tool to potentially answer the questions asked during this experimental project.

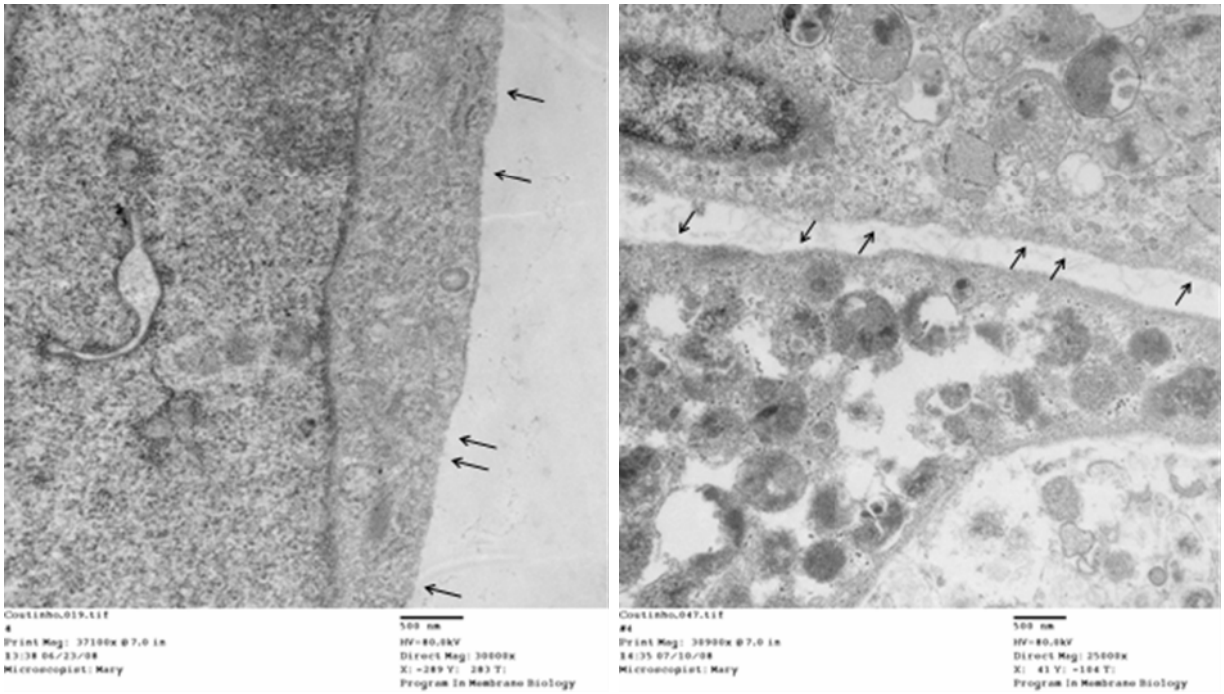

Figure 46 – Transmission electron micrographs depicting mouse aortic endothelial cells from CAV_1 WT animals. *Caveolae* can be seen on the cell membrane (refer to arrows). Images shown at 40000x magnification. Scale bar shown on right bottom below the image.

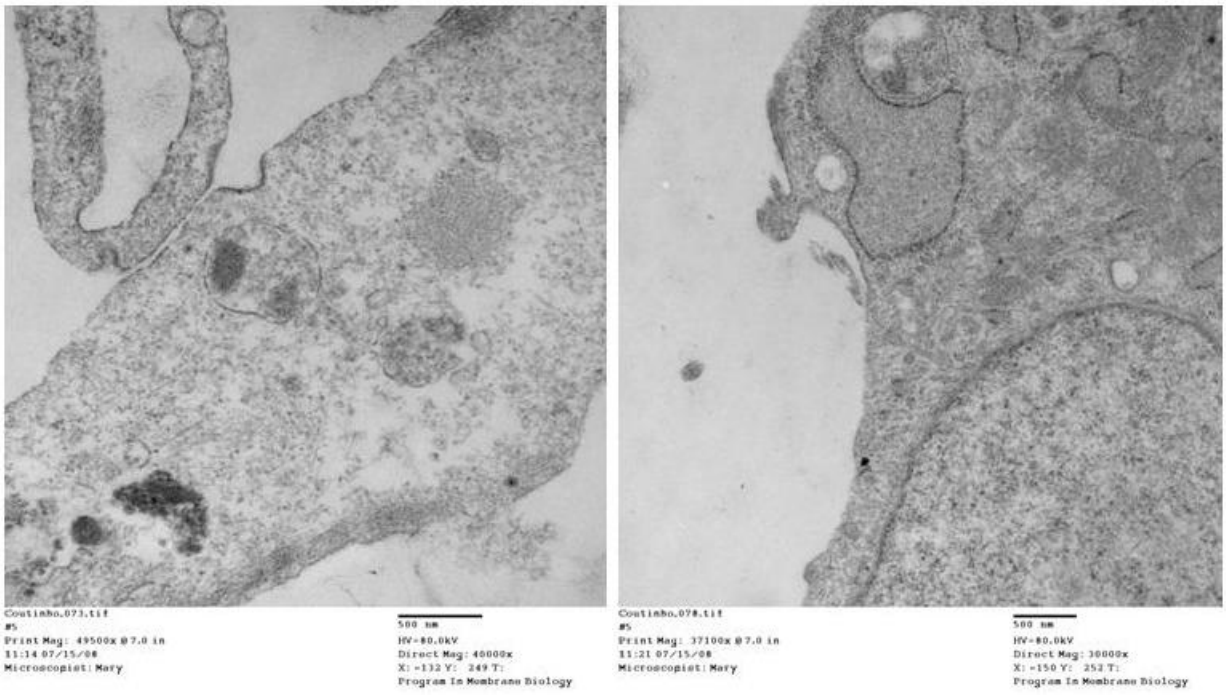

Figure 47 – Transmission electron micrographs depicting mouse aortic endothelial cells from CAV_1 KO animals. No c*aveolae* can be seen on the cell membrane. Images shown at 40000x magnification. Scale bar shown on right bottom below the image.

Figures 46 and 47 show electron micrographs of mouse aortic endothelial cells resultant from primary cell culture of aortic cells collected from CR57BL6 mice that lack the caveolin 1 gene (CAV_1 KO animals) or their wild type counterparts. The reason why we look at the wild type mouse once again is due to the fact that different species were being used. Whereas the original mouse aortic endothelial cells were collected from CD1 mice (the regular white or brown laboratory mouse), which is a cheaper animal model, the CAV_1 KO wild type animal comes from a different species of mouse, the black 6 model that has some genetic differences. Hence the only way to make sure that the cells collected from these different animals displayed the same basic characteristics was to submit both cell cultures to be analyzed by electron transmission microscopy and compare the photographic results obtained.

Looking at figure 46 it is easy to spot differences between these cells and the ones shown in figure 44. The *caveolae* are present but are more difficult to spot on the cell membrane due to their size. The membrane has the same general reticulated aspect as the previous mouse aortic endothelial cells but the invaginations themselves are much smaller in size making them harder to distinguish against the general background of the cell cytoplasm. There is some evidence of endocytic vesicles but again not as pronounce as what was observed before. Figure 47 derives from a CAV_1 KO animal and shows smoother cell surface with clathrin-coated pits visible but no apparent caveolae or endocytic vesicles.

Although the results are in keeping with what was expected, they are not believed to be very clear. The size of the *caveolae* is much smaller than what was observed before and they are difficult to distinguish in the cell membrane. In this way judgment was reserved until further experiments were undertaken about the presence/absence of caveolae in these cells.

Aldosterone-Response Studies

This work is based on the premise that aldosterone rapid signalling via the mineralocorticoid receptor may function in a similar way to what has been described for the estrogen receptor alpha (188). To explore this hypothesis it is important to select a signalling molecule to focus on and test in order to investigate whether the action of this molecule is enhanced when the cells are stimulated with aldosterone. The authors of the paper mentioned above, used mitogen activated protein kinases (MAPK), specifically ERK1/2 kinases as target molecules and tested if its phosphorylation was enhanced when the cells were stimulated with estrogen. After careful consideration, literature review and previous results analyzed, it was decided to study ERK1/2 from the MAPK family as possible important players in the aldosterone nongenomic signalling cascade. This decision was greatly aided by the literature where several sources referred to an increase in pERK activity (118, 233, 234) but also by previous results observed within the research group (235).

Male C57BL/6 on a 3% NaCl (salt) diet were injected intraperitoneally with either 10 μg/kg of aldosterone (experimental group) or vehicle (control group) and killed at different time points after injection (0, 0.5, 1, 2, 3, 4, 5 and 12h). Plasma aldosterone levels reached a peak (290 ng/dl) at 30 minutes, returning to baseline at 3 hours. Total RNA was extracted from whole hearts and used in microarray studies to analyze the gene expression profiles in the heart. Animal models of mineralocorticoid excess demonstrate cardiac damage (107, 236, 237), and human clinical trials offer evidence that blockade of the mineralocorticoid receptor can decrease morbidity and mortality in patients with heart failure (103, 104). The experiment was designed to focus on the genetic effects of aldosterone that could potentially mediate empirically observed myocardial injury. In rodent models, uninephrectomy and high-salt diet are necessary for demonstration of mineralocorticoid-mediated cardiac damage (107, 110, 111). Whereas the duration of this particular experiment was too short to observe myocardial injury, experimental conditions were designed to replicate the physiological conditions that have been shown to lead to cardiac damage. Several of the genes whose expression level was affected by aldosterone are known to play a role in steroid signalling: dual specificity phosphatase 7 dephosphorylates ERK (238), and protein phosphatase 5 may be

involved in glucocorticoid receptor signalling (239). Several groups have reported an increase in phosphorylation of ERK1/2 within several minutes after aldosterone administration that is not blocked by inhibitors of transcription and translation (240, 241), implying a nongenomic mechanism. These findings possibly indicate a second, genomic pathway leading to ERK1/2 phosphorylation (by decreasing the expression of the enzyme responsible for ERK1/2 dephosphorylation), after a longer period of time.

With reports of increases in phosphorylation as early as 5 minutes after stimulation with aldosterone, it was felt that the best course of action was a short-time aldosterone stimulation study to pinpoint when the endothelial cells used in the laboratory achieve a peak in ERK1/2 phosphorylation.

Graph 3: Aldosterone short-time stimulation study.

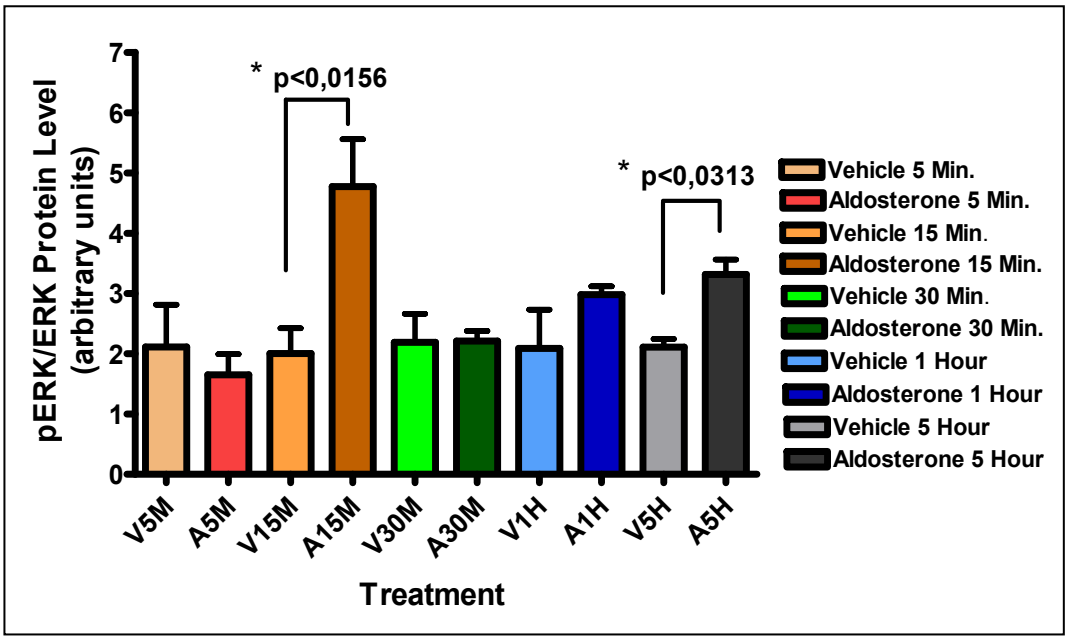

EA.hy926 cells were grown in 10% FBS DMEM media until reaching about 70% confluency. At that stage the cells were stepped-down to 0,4% FBS DMEM to keep the environment stimulation to a minimum. Although the aldosterone levels in FBS were measured and considered to be negligent, this is still a very rich media and it is difficult to assess if the growth factors and cytokines present influence the signalling pathway under study, hence by keeping their levels to the minimum to ensure cell viability the chance of external factors influencing the outcome of the

experiments is highly diminished. Cells were kept in the step-down media overnight and then stimulated with 10 nM aldosterone or vehicle (ethanol solution used to dissolve the aldosterone chemical) for different periods of time. Cells were then washed in PBS and collected in RIPA buffer for western blot analysis. Phosphorylated ERK1/2 protein levels were measured and normalized to ERK1/2. Results are shown on graph 3 and it is easy to identify two distinct peaks of activity for phospho-ERK after EA.hy926 cells are stimulated with aldosterone. The first peak is quite steep and observed at 15 minutes of aldosterone treatment. Although the short length of time of treatment leads to the very tempting conclusion that this might be a nongenomic effect of aldosterone signalling, it is not possible to correctly ascertain if this is the case without performing further experiments. The second peak can be seen at 5 hours of treatment. Due to the relatively long period of time of treatment, this peak is believed to be due to genomic effects of aldosterone and further experiments were undertaken to confirm this hypothesis. Statistical results shown on graph 3 were obtained by one-way ANOVA followed by *post-hoc* Mann-Whitney *t*-test comparison for selected time-points.

Graph 4: Aldosterone short-time stimulation study.

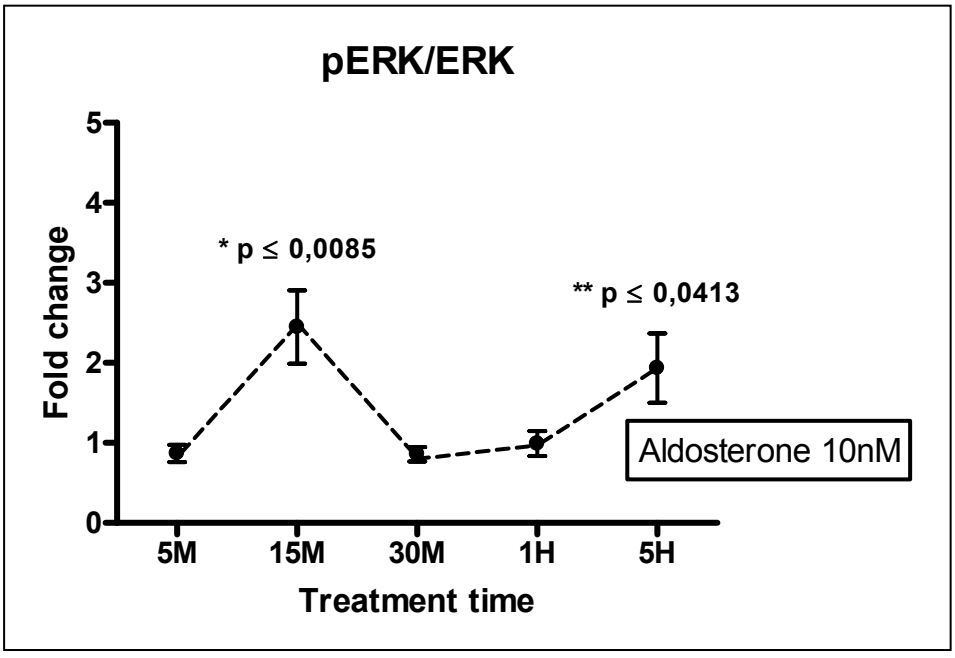

In order to make results clearer and the graph easier to read, pERK/ERK results achieved through aldosterone were normalized to vehicle results and presented as fold change in graph 4. Again the two peaks are evident at 15 minutes

and 5 hours with the highest being at 15 minutes with an almost doubling of ERK phosphorylation. Once more, statistical results shown on graph 4 were obtained by one-way ANOVA followed by *post-hoc* Mann-Whitney *t*-test comparison for selected time-points.

When it comes to what aldosterone dose to use for cell stimulation authors seem to be divided. When looking at the literature it is possible to find values going from 0,1 to 100nM of aldosterone being used to stimulate cells. For the first experiments carried out with the EA.hy926 cells, 10nM aldosterone was the selected concentration for time course studies. Although cells responded well to this concentration, it was felt that a dose response study was necessary to determinate if this was the best concentration to use with these cells.

Graph 5: Aldosterone dose response study.

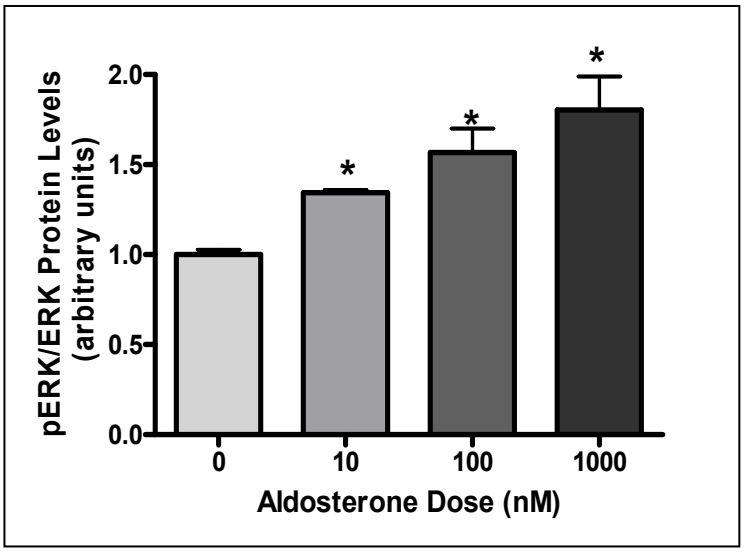

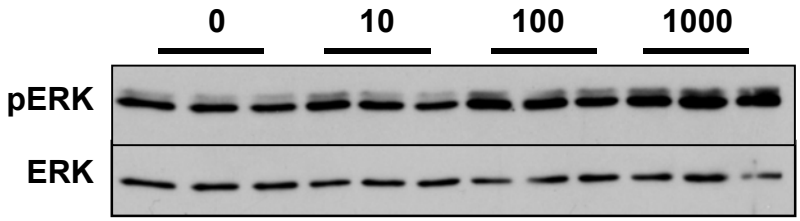

Figure 48 – Western blot depicting the results shown on graph 5.
Numbers shown above the photo represent the aldosterone dose in nM.

Results show a nice increasing response, as expected for a dose response curve, with around 1,5 increase (30%) in ERK phosphorylation with a 10nM

aldosterone dose at 15 minutes of stimulation leading up to a 2-fold response when a 1μM aldosterone dose is used. * represents a $p < 0,05$ when compared to vehicle (0 nM). Although it is tempting to select the dose that delivers the highest response in terms of ERK phosphorylation and, hence, cell signalling, it is important to consider the physiological relevance of the dose used in cell experiments, making it possible to compare to situations of high aldosterone levels in medical science.

Primary hyperaldosteronism (PHA) is recognized as the most common endocrine form of secondary hypertension (242-247) with an estimated prevalence between 5% and 15% in the hypertensive population (248). Primary aldosteronism, also known as primary hyperaldosteronism, is characterized by the overproduction of aldosterone by the adrenal glands without the expected excessive renin secretion, making the ratio of plasma aldosterone concentration to plasma renin activity the most common screening test for this condition. Aldosterone causes increase in sodium and water retention and potassium excretion in the kidneys, leading to arterial hypertension. PHA has many causes, including adrenal hyperplasia and adrenal carcinoma. When it occurs due to a solitary aldosterone-secreting adrenal carcinoma (a type of benign tumour), it is known as Conn's syndrome (249). Plasma aldosterone levels vary considerably, even for normotensive individuals. A study conducted in 76 healthy individuals and 28 confirmed PHA patients resulted in plasma aldosterone values of 0,033 to 1,930 nM for healthy subjects and 0,158 to 5,012 nM for PHA patients (250).

These values, especially the top value for PHA patients seems to validate the choice of 10nM aldosterone as a valid one both for cell studies as for a possible comparison with pathophysiological states in humans as it is within the same order of magnitude, although higher. This way although 10nM aldosterone cannot be called a pathophysiological dose, it is still an acceptable pharmacological dose for comparison with disease states in humans. In addition, clinical results collected by other investigators in the group over the past 30 years (HyperPATH cohort) show that in 828 hypertensive subjects the circulating aldosterone levels ranged between 0,05 and 11,53 nmol/L (Mean= 1,37 ± 0,94 nmol/L [Std Dev]; Median 1,13 nmol/L). Furthermore, aldosterone levels over 100 nmol/L have been observed in heart failure patients (251, 252), reinforcing the fact that high levels of aldosterone play a part in the pathophysiology of cardiovascular failure.

Aldosterone's nongenomic effects

Having focused on making sure that everything is in place for the key experiments, the aldosterone short-time study was repeated with cells grown in the selected FBS batch media and a mineralocorticoid receptor inhibitor. EA.hy926 cells were grown until about 70% confluency in 10% FBS media and then stepped-down to 0,4% FBS media overnight before the experiments took place. Each treatment was applied in triplicate and each experiment repeated three times.

Potassium canrenoate is the potassium salt of canrenoic acid, an antagonist of aldosterone action. Like spironolactone, it is a prodrug, which is metabolized to canrenone in the body. Spironolactone and its active metabolites canrenone and potassium canrenoate are normally used as hypertensive drugs but, their mechanism

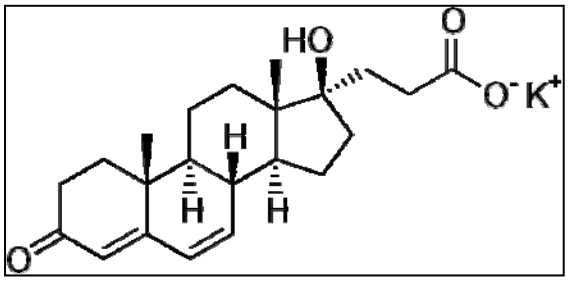

Figure 49 – Potassium canrenoate. Systematic IUPAC name: potassium 3-[(8*R*,9*S*,10*R*,13*S*,14*S*,17*R*)-17-hydroxy-10,13-dimethyl – 3 – oxo - 2, 8, 9, 11, 12, 14, 15, 16 – octahydro - 1*H* – cyclopenta [a] phenanthren -17-yl] propanoate.

of action is not fully understood. It is known that it initially inhibits sodium reabsorption and secondarily potassium excretion in the distal tubule of nephrons but little is known about how it acts in the cardiovascular system. A study conducted in aortic rings suggests that canrenoate might exert this action through an inhibition of voltage-dependent Ca2+ channels (253).

There were several reasons for selecting canrenoic acid as the inhibitor of choice for aldosterone in these studies, most of them due to practicality. Canrenoic acid is readily available from chemical suppliers like Sigma-Aldrich whereas eplerenone and especially spironolactone are more difficult to get hold of in pure form. Canrenoic acid is also water soluble making it a perfect inhibitor for use in cell based assays. In contrast, both spironolactone and eplerenone need to be dissolved in ethanol making them more toxic for cells.

As previously described, cells were plated in 6 well plates at a density of 5 x 10^5 cells/well and allowed to reach 70% confluency before the media was

changed from DMEM 10% FBS (selected batch) to DMEM 0,4% FBS and left overnight. Canrenoic acid was used at a concentration of 1µM (100 times the aldosterone concentration) to ensure an efficient inhibition.

Graph 6: Aldosterone short-time course with antagonist.

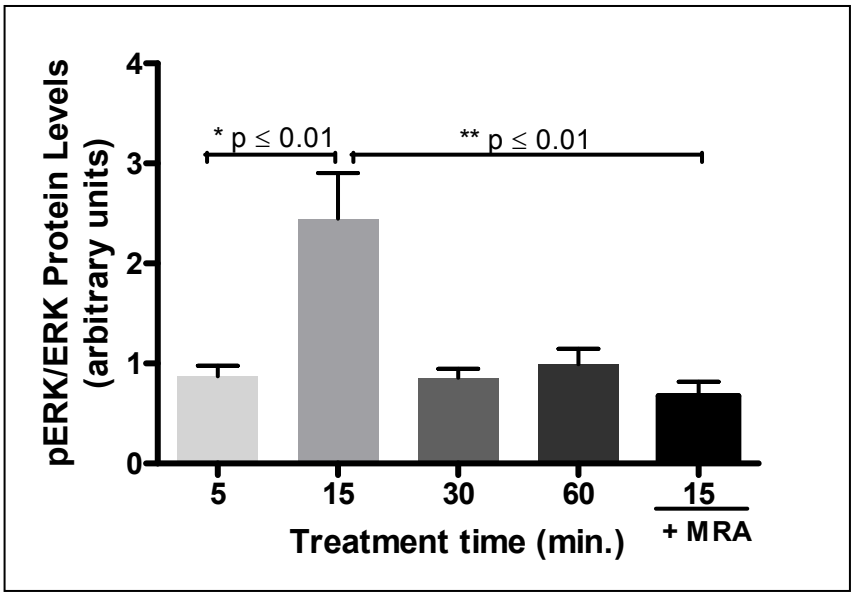

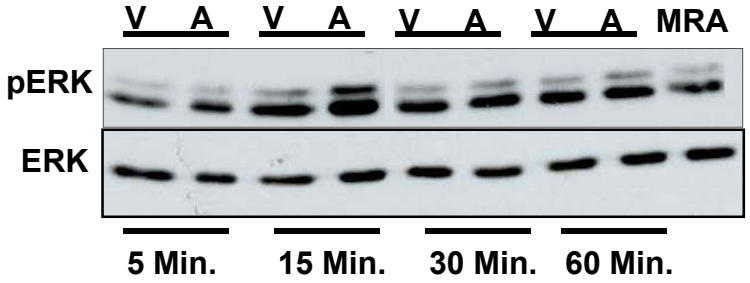

Figure 50 – Western blot illustrating the results shown on graph 6.
Letters shown above the photo represent the treatment
(V- vehicle, A- aldosterone, MRA- mineralocorticoid antagonist).

Just as seen before, EA.hy926 cells show an increase in ERK1/2 phosphorylation when stimulated with 10nM aldosterone for 15 minutes. This result is in agreement with has been observed before with these cells with a 2,5 fold increase in pERK ($p \leq 0,01$ when compared to 5 minutes). When the mineralocorticoid antagonist canrenoic acid (MRA) is used in conjunction with the aldosterone treatment, the increase in ERK phosphorylation is abrogated, thus confirming that the

increase in pERK observed is indeed due to an effect of aldosterone acting through the mineralocorticoid receptor.

This result is by itself promising, especially because it is consistent with previous experiments and thus would appear to be a true biological observation and not an artefact of the experimental paradigm. Although promising, more experiments are necessary before claiming any physiological significance for this result. One of the easiest critiques is that the cell line used is not only an immortalized cell line but also not of cardiovascular origin, making the conclusions drawn from these results of lesser interest and significance in the study of cardiovascular relevance of aldosterone nongenomic actions. In order to add relevance to the results observed in EA.hy926 cells, experiments were repeated using early culture mouse aortic endothelial cells collected from healthy mice. Cells were isolated from the pulmonary section of mice aortas and grown in DMEM, 20% FBS with the addition of 1% MEM amino acids, 1% sodium pyruvate, 100 /ml heparin, 100 μg/ml endothelial cell growth supplements (Sigma-Aldrich, St. Louis, MO) and incubated in 5% CO2 at 37°C in a humidified atmosphere. The cells were used at passages 2-3. The purity of the primary cultures was confirmed by the specific monoclonal antibodies raised against VWF and PECAM-1 previous to use in experiments.

Because each individual aorta yields a small number of cells, it was necessary to combine cells from more than one aorta for these experiments. All aortas were collected at the same time and processed using the same experimental protocol and reagents. Cells were cultured in collagen coated 6 well plates till confluency and then passaged to collagen coated t-flasks to expand previous to use in aldosterone experiments. Cells were first used at passage 2 and for no longer than 4 passages total. As with EA.hy926 cells, mouse aortic endothelial cells were stepped-down previous to use in experiments. Due to the fact that these cells are grown in double the amount of FBS as the EA.hy926 cells it took to stepping-down phases, from 20% FBS to 10% FBS and then to 0,4% FBS, to allow the cells to get used to less nutrients without entering senescence.

Graph 7: Aldosterone short-time stimulation study using Mouse Aortic Endothelial cells.

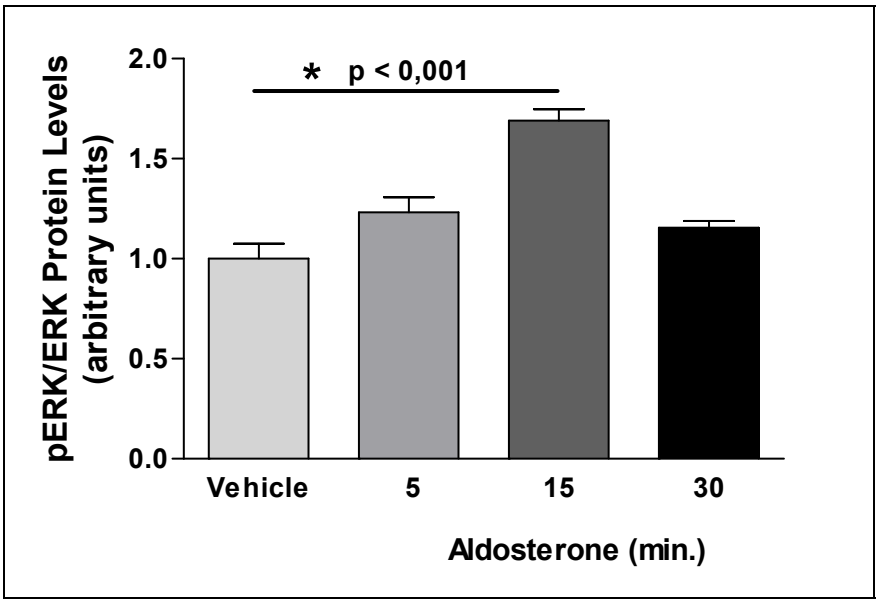

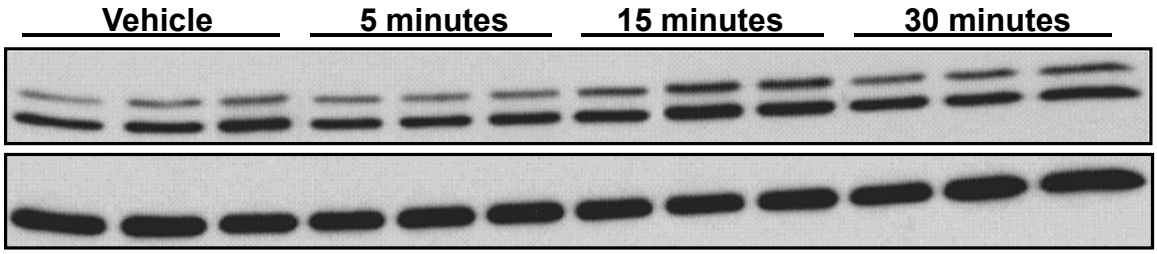

Figure 51 – Western blot illustrating the results shown on graph 7. Treatments were done in triplicate using 10nM aldosterone for different periods of time.

Each treatment was done in triplicate and the experiment itself repeated at least 3 times. 6 mice were sacrificed per experiment and the cells collected pooled together in order to have the necessary number of cells per experiment.

Results show a significant increase in pERK protein levels at 15 minutes of aldosterone, confirming previous observations with the EA.hy926 cells line. The magnitude of the increase in protein levels is smaller than the one observed before but more consistent between experiments as indicated by a smaller error bar (see graphs 6 and 7). Seeing that these cells were isolated from the aorta of healthy rodents, the results observed are in all probability closer to physiological relevance in humans. They also confirm that the EA.hy926 cell line as a good model for endothelial cell action.

Combined together, the results from short-time aldosterone stimulation studies with EA.hy926 endothelial cells and mouse aortic endothelial cells start to piece together a convincing amount of evidence pointing to a newly described nongenomic action of aldosterone in endothelial cells. Although the observed results can be considered as a rapid action of aldosterone, in order to call it a nongenomic action, first it is necessary to demonstrate that no gene translation is occurring in the 15 minutes of aldosterone action.

EAhy.926 cells were stimulated with 10nM aldosterone for 15 minutes and 5 hours and then collected for mRNA extraction. After mRNA was purified and quantified, a reverse-transcription kit was used to obtain cDNA that was then used in Real-Time PCR gene expression experiments. The 5 hour time-point was used as a measure of positive genomic action. Aldosterone is known to change the expression of several different genes being it by increasing or reducing it (254). 4 different genes were selected for quantification in aldosterone stimulated EA.hy926 cells but only 2 showed the expected results with an increase/decrease at 5 hours and no change at 15 minutes. Although all the genes studied showed no change at 15 minutes, NOS and aldolase, did not show a sufficient change at 5 hours to make it significant evidence of a genomic effect of aldosterone, only being slightly elevated when compared to control.

The mechanisms behind aldosterone action have been extensively characterized, particularly in the kidney collecting duct (CD). In intact CD or cultured CD cells, the response to aldosterone can be divided into main phases- early and late –that differ significantly, although both require changes in gene transcription (255). The principal early action of aldosterone in CD cells (after 30-45 minutes) is to increase apical membrane permeability by increasing Na^+ transport through ENaC (96). In most cases, the ENaC-mediated early effect of aldosterone accounts for more than 60% of the total increase in Na^+ current and, importantly without changes in ENaC gene transcription (77). These observations suggest that MR regulates the transcription of a regulatory protein that increases the plasma membrane localization and/or activity of existing ENaC protein. The early effects of aldosterone are potent, rapid and largely limited to changes in ENaC-mediated Na^+ transport, with other effects such as proliferation, occurring later (256). Thus, the mRNA levels of a

mediator of the early response should increase markedly and rapidly and the mediator of the early response should, in turn, strongly stimulate ENaC activity. SGK1 (Serum/glucocorticoid regulated kinase 1) has been shown to be such an aldosterone-stimulated regulator of ENaC activity (79, 257, 258).

SGK1 mRNA is rapidly increased by aldosterone and, when expressed in *Xenopus* oocytes, SGK1 strongly and selectively stimulates ENaC-mediated Na^+ transport in addition to localizing ENaC to the membrane (255). Most studies regarding aldosterone action concern the renal system where its action is most important, indeed, one study using cardiomyocytes has shown that some of the genes whose expression is affected by aldosterone in the collecting duct are also increased in the cardiovascular system. Results of this study showed a 2.5 fold increase in SGK1 mRNA (259), other genes were found to be up-regulated by aldosterone action, including several connected to inflammation and fibrosis like PAI-1 and ADAMTS1.

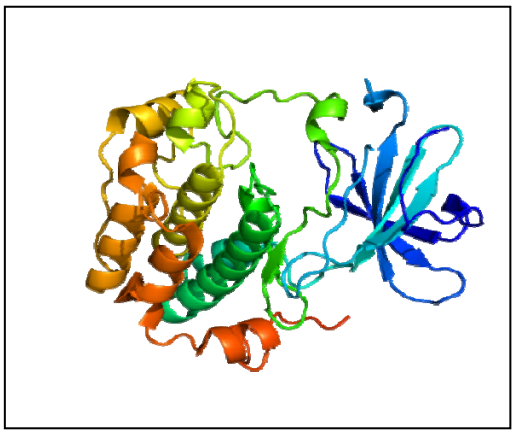

Figure 52- Crystal structure of Serum Glucocorticoid Regulated Kinase 1, adapted from the Protein Data Base (PDB 2R5T).

Graph 8: SGK1 mRNA levels in EA.hy926 cells after stimulation with aldosterone.

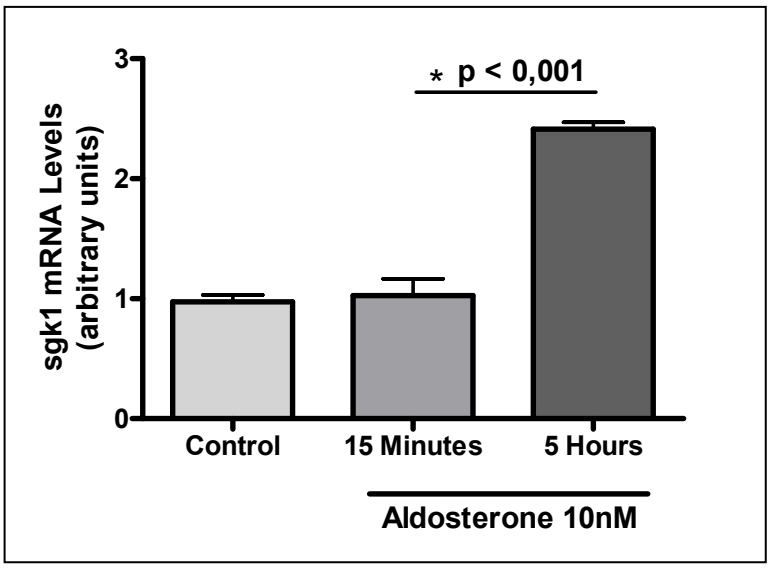

Consistent with the observations for cardiomyocytes, EA.hy926 cells stimulated with aldosterone showed an increase in SGK1 mRNA levels. SGK1 went up by about 2,5 fold after 5 hours of 10nM aldosterone treatment ($p \leq 0{,}001$ when compared to 15 minutes). Contrary to the 5 hour time-point that displays a classic genomic action of aldosterone with a significant increase in SGK1 mRNA levels, the 15 minute time-point did not show any significant change supporting the hypothesis that the increase in pERK protein levels is indeed a nongenomic effect of aldosterone action at this time-point. In order to take into account differences between samples, SGK1 mRNA levels were normalized using the housekeeping ribosomal gene 18S.

Graph 9: WNK4 mRNA levels in EA.hy926 cells after stimulation with aldosterone.

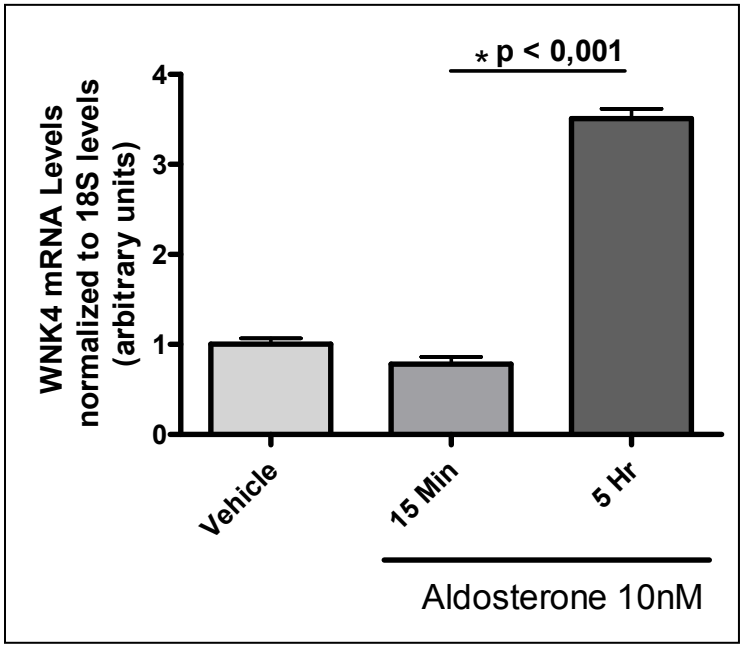

Serine/threonine-protein kinase WNK4 also known as WNK lysine deficient protein kinase 4 or WNK4, is an enzyme that in humans is encoded by the *WNK4* gene (260). The WNK4 gene encodes a serine-threonine kinase expressed in distal nephron. Its primary role in renal physiology is as a molecular switch between the angiotensin II-aldosterone mediated volume retention and the aldosterone mediated potassium wasting. This is achieved by regulating the sodium-chloride symporter (NCC), that is uniquely expressed in the distal nephron and is sensitive to thiazide type diuretics (261). Under basal conditions (low circulating Ang II and low Aldosterone), WNK4 will inhibit NCC function. It has been proposed that in the event

of hyperkalemia and an increased secretion of aldosterone (which will upregulate both ENaC and the renal outer medullary potassium channel (ROMK)), this inhibition of NCC, will allow an increase in the arrival of sodium to the distal nephron (rich in ENaC and ROMK) which will allow the exchange of sodium for potassium ions, thereby reducing plasma potassium levels, without increasing sodium chloride retention (which is always accompanied by volume expansion). Mutations in NCC regulators WNK1 and WNK4 cause Type II pseudohypoaldosteronism (PHA2), also known as Gordon's syndrome, an autosomal dominant disease in which there is an increase in NCC activity leading to short stature, increased blood pressure, increased serum K^+ levels, increased urinary calcium excretion and hyperchloremic metabolic acidosis.

It was thought that aldosterone required the presence of angiotensin II to activate the WNK4 regulator but, recently, it was shown that in the presence of losartan (an angiotensin II inhibitor), aldosterone was still capable of increasing total and phosphorylated NCC twofold to threefold. The kinases WNK4 and SPAK (STE20/SPS1-related proline/alanine-rich kinase) also increased with aldosterone and losartan. Furthermore, a dose-dependent relationship between aldosterone and NCC, SPAK and WNK4 was identified, suggesting that these are aldosterone-sensitive proteins (262).

In keeping with these observations, EA.hy926 cells stimulated with aldosterone showed an increase in WNK4 mRNA levels. WNK4 increased by about 3.5 fold after 5 hours of 10nM aldosterone treatment ($p \leq 0{,}001$ when compared to 15 minutes). Although the 5 hour time-point displayed a classic genomic action of aldosterone with a significant increase in WNK4 mRNA levels, the 15 minute time-point again did not show any significant change reinforcing the idea that the increase in pERK protein levels is a nongenomic effect of aldosterone action. In order to take into account differences between samples, WNK4 mRNA levels were normalized using the housekeeping ribosomal gene 18S.

Aldosterone's genomic effects

Having so far concentrated on the nongenomic effects of aldosterone and having established that there is a significant increase of pERK due to aldosterone stimulation both in EA.hy926 cells and mouse aortic endothelial cells, it was necessary to investigate if striatin and the *caveolae* play a role in this action as seen for estrogen's nongenomic actions.

The first question asked was if aldosterone influences striatin in any way and in order to answer that question, EA.hy926 cells were stimulated with 10nM aldosterone for different periods of time conducive to a potential genomic effect. As before cells were stepped-down the day before the experiment. After stimulation, cells were collected for western blot analysis and striatin protein levels measured.

Graph 10: Striatin protein levels in EA.hy926 cells after stimulation with aldosterone (ALDO).

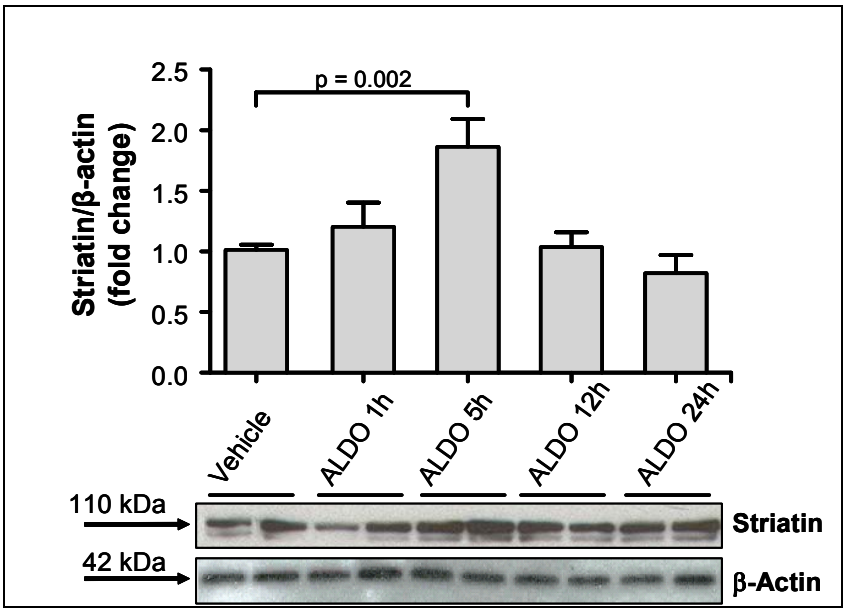

Results showed a significant increase in striatin protein at 5 hours of aldosterone stimulation, consistent with the second increase in ERK1/2 phosphorylation observed before, leading to the possibility that these two effects might, somehow, be linked. This result was unexpected, since striatin is believed to be a chaperone protein, facilitating the interactions between different signalling proteins. The increase in striatin takes place at 5 hours of aldosterone stimulation which, as shown before, is in agreement of other genomic actions of aldosterone.

However, this increase seems to be an acute event that occurs only at 5 hours of stimulation and is not sustained further. Striatin protein levels were normalized to β-actin to account for possible variations in the amount of protein loaded in each well.

In order to determine if this is indeed an effect of mineralocorticoid activation, further experiments were carried out using the MR antagonist canrenoic acid. EA.hy926 cells were treated with, vehicle, 10nM aldosterone or 1μM canrenoic acid for 5 and 24 hours.

Graph 11: Striatin protein levels in EA.hy926 cells after MR activation/inhibition.

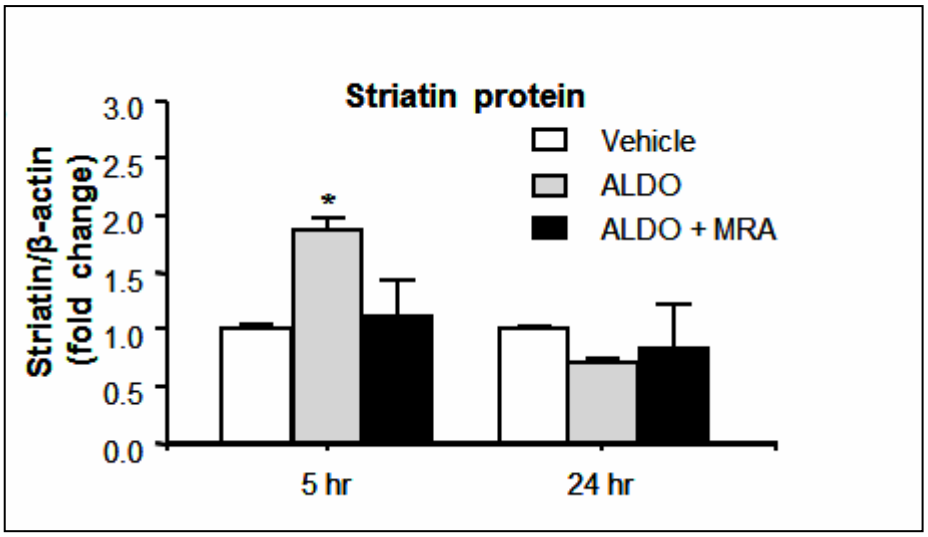

Results show that the aldosterone-induced increases in striatin expression are mediated via the activation of the mineralocorticoid receptor in EA.hy926 cells since canrenoic acid effectively inhibited the increase in striatin protein levels. Consistent with the previous experiments, striatin protein levels (after normalization to β-actin) went up by about two fold (*$p < 0.05$ vs. vehicle-treated cells). In the graph ALDO stands for 10nM aldosterone treatment and MRA for 1μM canrenoic acid treatment.

Although it was established that the observed effect is a consequence of mineralocorticoid receptor activation, it is still to be determined if this is in fact a genomic action of aldosterone. To determine if this is the case, EA.hy926 cells were stimulated with 10nM aldosterone ± canrenoic acid for 5 and 24 hours. After stimulation, cells were harvested for mRNA isolation and quantification of striatin mRNA using Real-Time PCR.

Graph 12: Striatin mRNA levels in EA.hy926 cells after MR activation/inhibition.

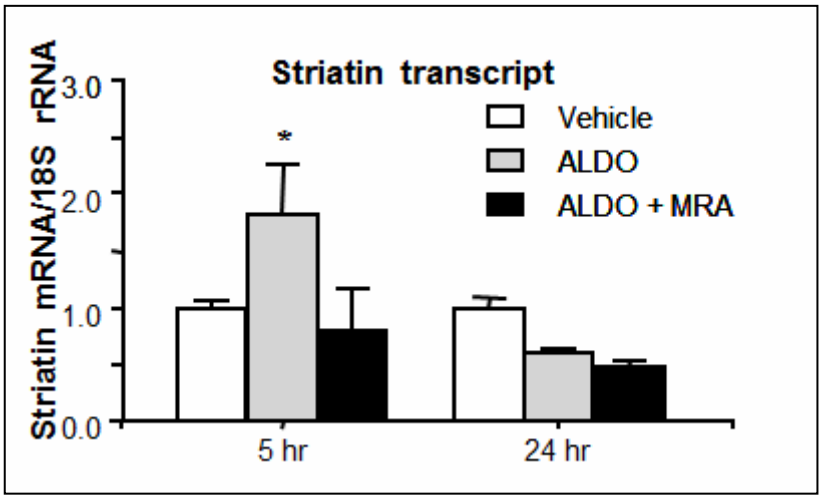

Results observed are consistent with the observed increase in striatin protein levels seen at 5 hours of aldosterone stimulation and supports the hypothesis that aldosterone is exerting a genomic effect on the EA.hy926 cells studied and that striatin is an aldosterone-sensitive protein. Striatin mRNA levels (after normalization to 18S) went up by about two fold (*$p < 0.05$ vs. vehicle-treated cells). In the graph ALDO stands for 10nM aldosterone treatment and MRA for 1μM canrenoic acid treatment.

Because the increase in striatin protein was an unexpected find, experiments were repeated using mouse aortic endothelial cells to ensure that this was not an artefact due to using an immortalized cell line as a model. As before cells were stepped-down to 0,4% FBS media and left overnight to quiesce. The following day cells were treated with 10nM aldosterone in the presence/absence of the mineralocorticoid inhibitor canrenoic acid (1μM). After 5 hours of treatment, cells were rinsed and collected in RIPA buffer for subsequent western blot analysis. Each treatment was carried out in triplicate wells and, every experiment executed three times for statistical analysis.

Graph 13: Striatin protein levels in MAEC cells after MR activation/inhibition.

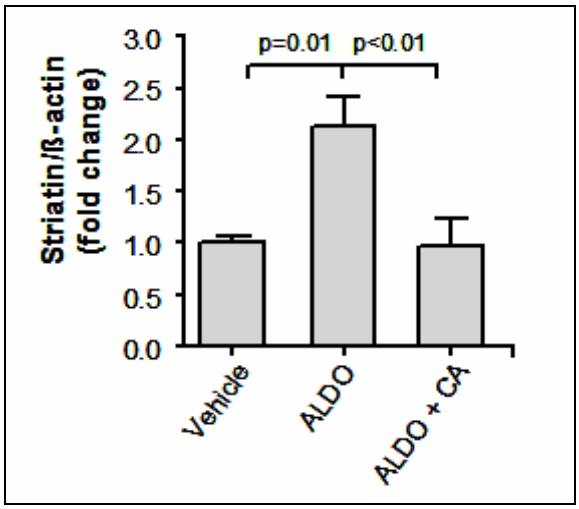

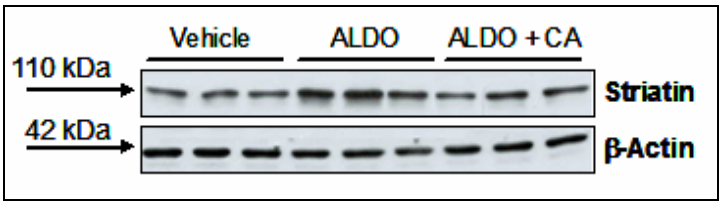

Figure 53 – Western blot illustrating the results shown on graph 13. ALDO stands for 10nM aldosterone treatment and CA for 1µM canrenoic acid.

Results obtained with MAEC are very similar to previous observations with EA.hy926 cells. Striatin protein levels went up by about two-fold confirming that striatin is indeed an aldosterone-sensitive protein and leading to more questions about the consequences of this discovery. Although striatin protein was increased at five hours in these cells, there wasn't an increase in the mRNA levels, leading us to believe that the peak of stimulation does not occur at the same time as was observed with EA.hy926 cells or the increase in mRNA levels is not as noticeable as with EA.hy926 cells making the differences more difficult to detect.

Results obtained in animal studies seem to confirm the observations from the cell experiments carried out. An experimental study with animals showed that dietary sodium restriction increased striatin levels in mouse hearts and aorta. A sodium restricted mouse model was studied which is known to have increased aldosterone levels (263). Mice were given a low sodium (LS) diet for 11 days which led to a significantly higher plasma aldosterone level (64,18 ± 14,30 ng/dl; (*n*=6)) than their cohort study companions on a (HS) high sodium diet (34,26 ± 4,99 ng/dl (*n*=7)) for

the same amount of time. Heart tissue as well as aorta was isolated upon animal sacrifice and protein isolated and measured by western blot analysis. Striatin levels were significantly higher in mice on a low sodium diet than the mice on higher sodium levels.

Graph 14: Heart tissue striatin protein levels in mice on a high sodium or low sodium diet.

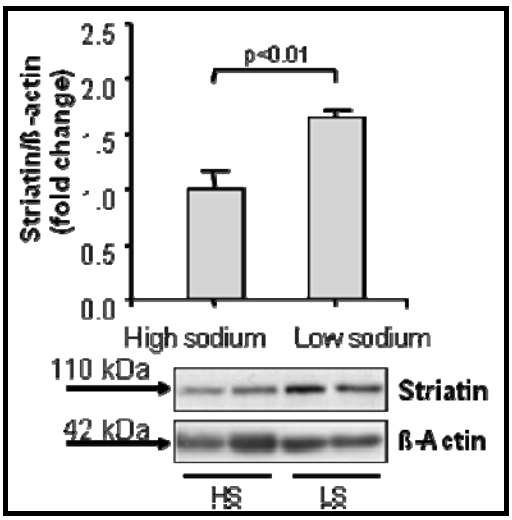

Results show on graph 14 depict a near two-fold increase in striatin protein levels in animals on a low sodium diet, consistent with the higher plasma aldosterone levels and previous results obtained in experimental endothelial cell studies. Higher striatin protein levels were also observed in aortic tissue collected from these animals.

Graph 15: Aorta striatin protein levels in mice on a high sodium or low sodium diet.

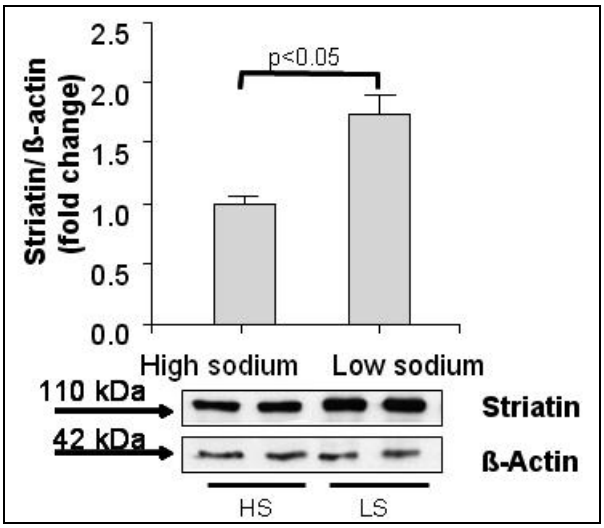

As with heart tissue, striatin protein levels were significantly higher in aortas from LS mice when compared to HS mice by about two-fold once again, consistently with the higher striatin protein levels observed in mouse aortic endothelial cells treated with aldosterone. Blood pressure levels were also measured in these animals using the tail cuff method (264). As shown previously under these conditions, low sodium was associated with lower blood pressure than high sodium (108,8 ± 2,8 mm Hg vs. 114,7 ± 3,1 mm Hg, LS vs. HS respectively, mean ± standard deviation, p < 0,03) (264).

In order to characterize the *in vivo* relevance of these findings, the effects of aldosterone on striatin levels was studied in mouse heart by using additional models of mineralocorticoid activation. The effects of an acute in vivo aldosterone administration on striatin levels in the heart were analysed. A vehicle injection was included at each time point in order to distinguish the effects caused by the injection from the ones due to a response to aldosterone stimulation. Male C57BL/6 mice on a 3% NaCl diet were injected intraperitoneally (IP) with either 10 µg/kg of aldosterone or vehicle and sacrificed at the following time-points after injection: 0 hours (no injection), 1, 2 and 3 hours. Five mice were sacrificed in each group at each individual time-point.

Graph 16: Striatin protein levels in mice injected with aldosterone or vehicle.

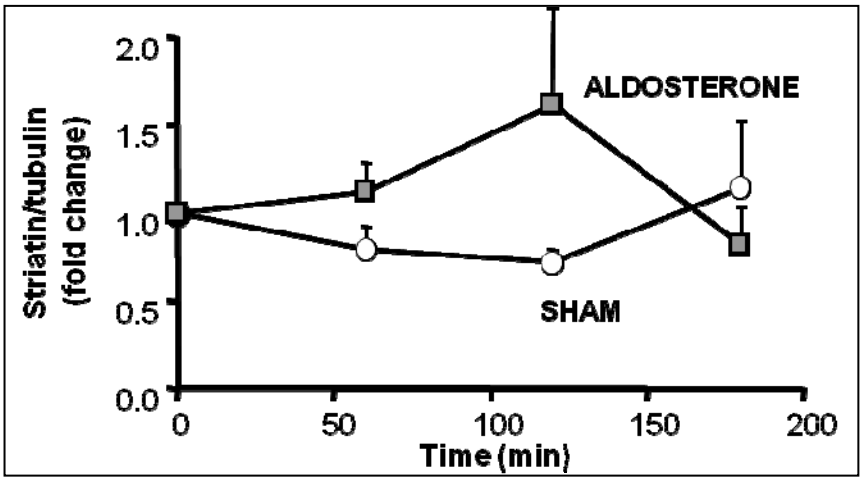

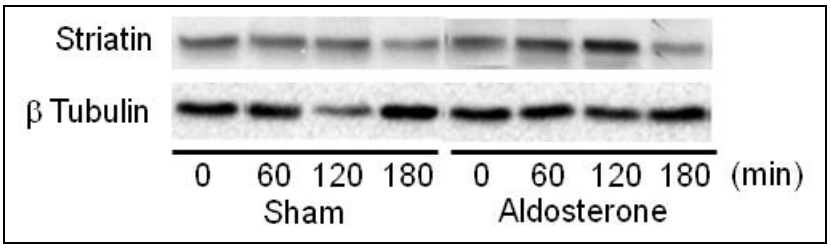

Figure 54 – Western blot illustrating the results shown on graph 16. Sham stands for vehicle injection.

It was observed (in heart tissue) that striatin levels increased in aldosterone-treated mice when compared to vehicle injected animals (sham). Plasma aldosterone concentrations were determined in each animal as reported previously (235) and, as expected, plasma aldosterone levels only increased in the aldosterone injected group, reaching its highest level at 30 minutes with a concentration of 280 ng/dl. Although the results shown are not statistically significant due to high error values, the overall result confirms previous results obtained and adds physiological relevance to them. The big difference being that, in the case of an acute injection it seems that the increase in striatin protein occurs more quickly than in *in vitro* studies. This can be due to many factors but it is believed to be mainly due to the fact that we are working with a bigger mass of cells as well as interactions (including feedback mechanisms) and crosstalk of other tissue types that are intact within the whole animal, instead of a monolayer of cultured endothelial cells.

Finally, a previous studied animal model of acute, generalized, multiple organ injury secondary to vascular inflammation (109, 110) was used to assess the interaction of mineralocorticoid activation on striatin. In this model, animals are treated with the nitric oxide synthase inhibitor, L-NG-Nitroarginine Methyl Ester (L-NAME), in combination with angiotensin II. The treatment induces myocardial damage initiated at the vascular level which can be prevented by MR blockade or by adrenalectomy (109, 110). Knowing this, the AngII/L-NAME model was used as a "stressor" model to ascertain if an increase in mineralocorticoid activation would also lead to an increase in striatin levels.

Results show that AngII/L-NAME treatment is associated with increased striatin levels both in heart and kidney tissues when compared to vehicle treated control. In these studies, AngII/L-NAME treatment increased aldosterone circulating

levels (122,1 ± 34,1 ng/dl (*n*= 6)) when compared to vehicle treatment (34,26 ± 4,99 ng/dl (*n* =7); *p*= 0,008). In addition, blood pressure levels were also measured in these animals and, as shown previously, AngII/L-NAME treatment was associated with increased blood pressure levels vs. vehicle treated mice (120 ± 3,8 mm Hg vs. 161 ± 23 mm Hg, vehicle vs. AngII/L-NAME respectively, mean ± standard deviation, *p* < 0,04) (265).

Graph 17: Heart striatin protein levels in mice treated with AngII/L-NAME or vehicle.

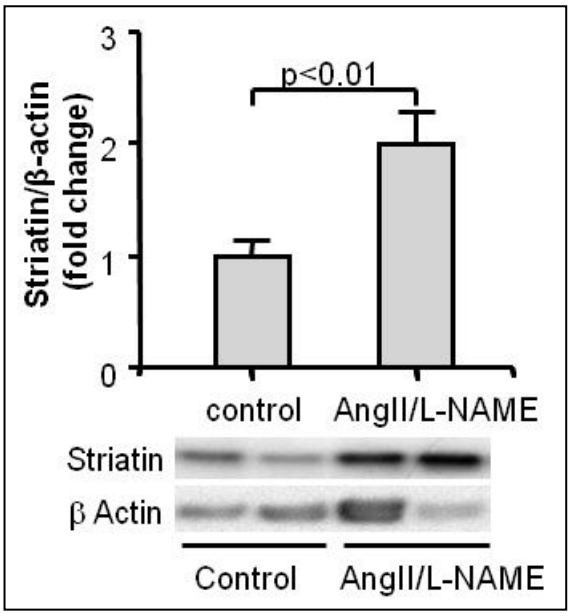

Graph 18: Kidney striatin protein levels in mice treated with AngII/L-NAME or vehicle.

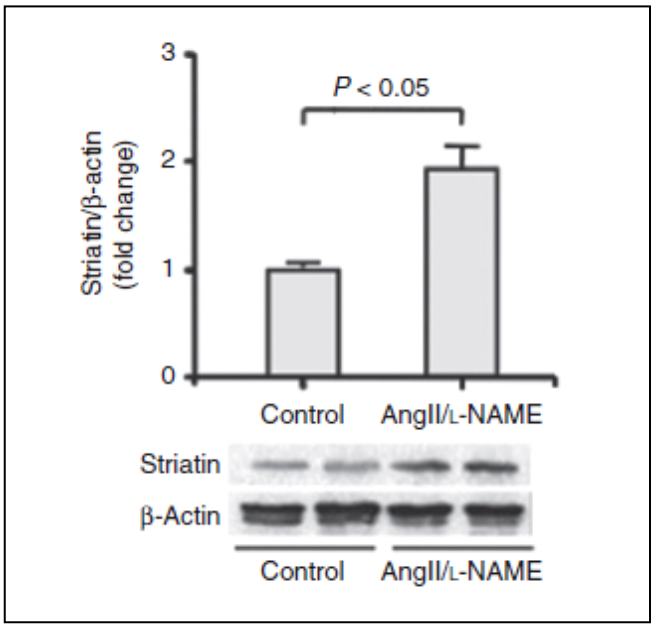

All the data obtained from these different animal experiments consolidates the previous results generated by the endothelial cell studies. Although unexpected, the finding that aldosterone levels seem to influence striatin protein levels is an important one and might change the way this protein is viewed by other investigators as well as add to its functions.

After establishing that aldosterone has both genomic and nongenomic effects in the endothelial cells studied and, the presence of striatin in the same cells, it is now necessary to ascertain if the presence of striatin is necessary for the nongenomic effects to occur and, if higher striatin levels will change the way the mineralocorticoid signalling occurs in these cells. In order to establish if striatin is a necessary player in the nongenomic rise of pERK levels in the endothelial cells studied it was decided to employ siRNA technology to knock-down striatin in these cells followed by aldosterone stimulation to confirm if the nongenomic effects had changed in any way.

Striatin knock-down using siRNA

Small interfering RNA (siRNA), sometimes known as short interfering RNA or silencing RNA, is a class of double-stranded RNA molecules, 20-25 nucleotides in length, that play a variety of roles in biology. The most notable role of siRNA is its involvement in the RNA interference (RNAi) pathway, where it interferes with the expression of a specific gene. In addition to its role in the RNAi pathway, siRNA also acts in RNAi-related pathways, e.g., as an antiviral mechanism or in shaping the chromatin structure of a genome; the complexity of these pathways is only now being elucidated.

siRNAs have a well-defined structure: a short (usually 21-nt) double-strand RNA (dsRNA) with 2-nt 3' overhangs on either end. Each strand has a 5' phosphatase group and a 3' hydroxyl (-OH) group. siRNAs can also be exogenously (artificially) introduced into cells by various transfection methods to bring about the specific knockdown of a gene of interest. In essence, any gene whose sequence is known can, thus, be targeted based on sequence complementarity with an appropriately tailored siRNA. This has made siRNAs an important tool for gene function and drug target validation studies in the post-genomic era. Transfection of

an exogenous siRNA can, sometimes, prove to be problematic because the gene knockdown effect is only transient, in particular, in rapidly dividing cells.

EA.hy926 cells were transfected with ON-TARGETplus siRNA pre-designed duplex specific for striatin obtained from Dharmacon RNAi Technologies in parallel with Control/blank siRNA following the manufacturer's protocols and using the Dharmafect 1 siRNA Transfection Reagent. The cells were then harvested for Western blot analysis 48 hours post-transfection.

The goal for the siRNA experiments was to significantly decrease the amount of striatin protein being produced in these cells without affecting the normal functioning of the cells. Because it was the first time this technology was employed in the laboratory, there were several rounds of optimization experiments before the suitable conditions were achieved.

Since each cell line reacts differently to a siRNA duplex, it was decided to order 4 different duplexes and test which one functioned better with the EA.hy926 endothelial cell line. Transfection was executed according to the manufacturer's protocols. Cells were transfected for 24 hours for mRNA collection and 48 hours for western blot analysis. Each time transfection media was replaced by normal growth media after 24 hours to prevent cell toxicity and death. Different transfection conditions like solution concentrations and transfection length were also optimized but are not shown here.

Graph 19: Striatin mRNA levels in EA.hy926 cells transfected with siRNA duplexes.

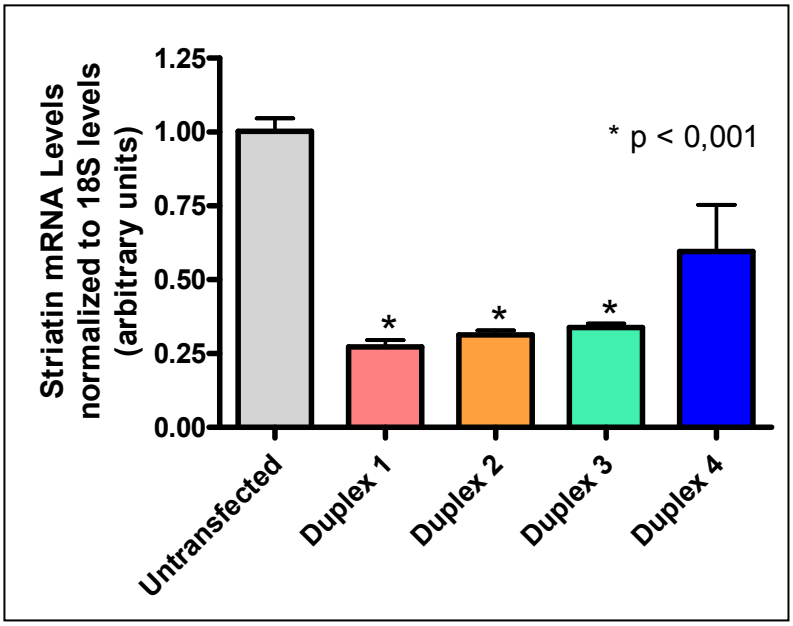

Real-time PCR results showed that transfection with duplexes 1-3 resulted in a significant decrease in striatin mRNA levels to about 25% when compared to an untransfected control. Each experiment was carried out in triplicate wells.

Since a decrease in mRNA is not sufficient proof that striatin protein was indeed reduced, experiments were repeated and the transfection extended to 48 hours to induce protein reduction. Cells were then collected for western blot analysis.

Graph 20: Striatin protein levels in EA.hy926 cells transfected with siRNA duplexes.

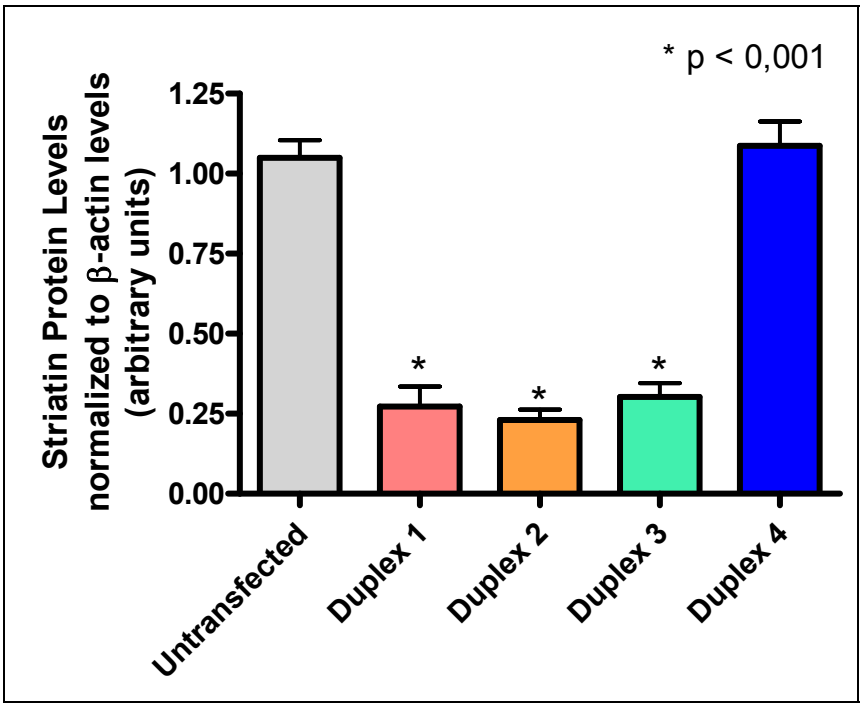

Western blot results confirmed that there was a significant reduction in striatin protein levels by about 75% compared to untransfected control when duplexes 1-3 where employed. Again duplex 4 did not knockdown striatin protein levels with respect to control, confirming that each cell line reacts differently and reinforcing the need to perform optimization steps prior to experimentation. Different combinations of two duplexes where also tried but not shown here. Results obtained where very similar to the ones yielded by individual duplexes and therefore not an improvement and was not pursued further.

Striatin is not the only member of its family; Zinedin and SG2NA are two other family members with similar structure and sequence homology which could

potentially be affected by the siRNA gene expression inhibition. In this way cells transfected with the 4 duplexes for 24 hours where analysed by Real-Time PCR quantification to determine if other family members, besides striatin, had their mRNA levels significantly reduced.

Graph 21: SG2NA mRNA levels in EA.hy926 cells transfected with siRNA duplexes.

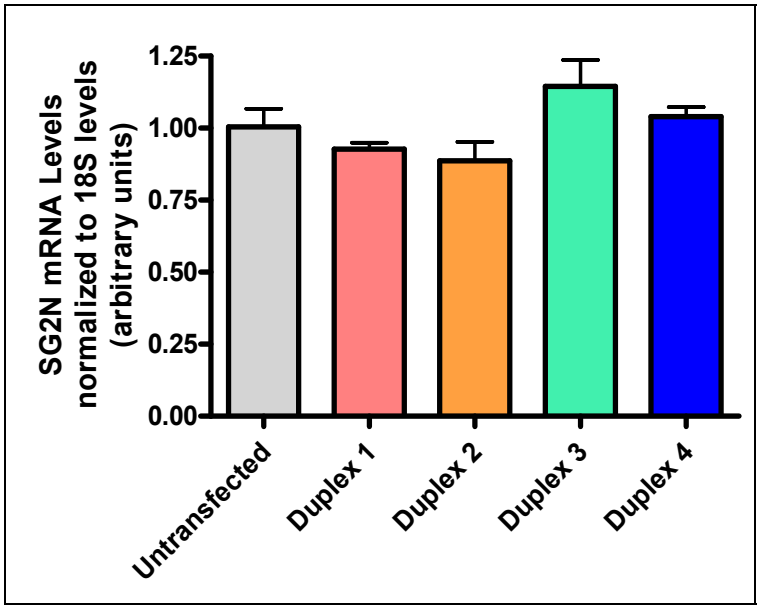

Graph 22: Zinedin mRNA levels in EA.hy926 cells transfected with siRNA duplexes.

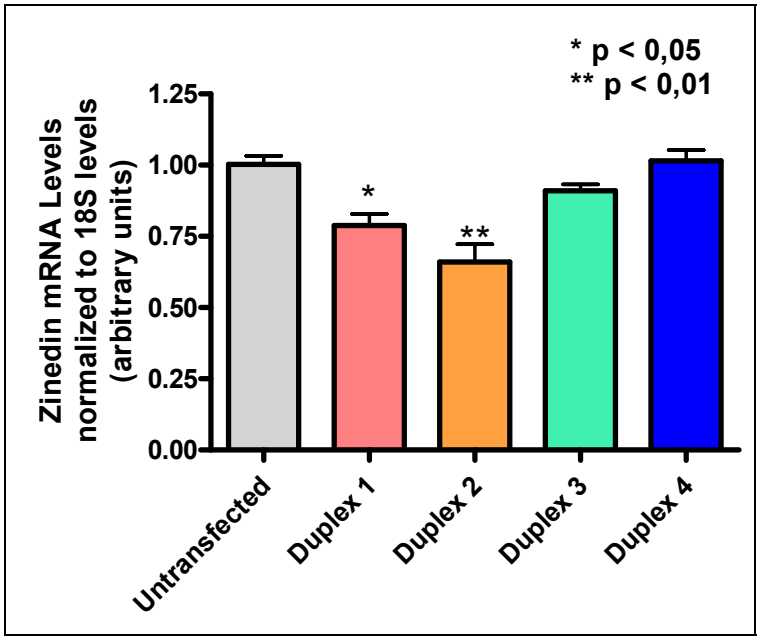

Results showed that SG2NA levels did not seem to be affected by the transfection with siRNA duplexes designed to interfere with striatin gene expression but, it was a different case with Zinedin. Duplex 1 and 2 where significantly reduced after 25 hours of transfection, making then unviable reagents to use in future experiments due to the fact that more than one striatin family member is being affected and, in this way, making conclusions about the specific role of striatin in future siRNA experiments limited.

After all the results where analysed it was decided to selected duplex 3 for use in future experimental paradigms since it complied with all the necessary requirements, specifically targeted knockdown of striatin expression without off target effects of related family proteins.

Having established the optimal conditions for striatin knock-down experiments using siRNA technology, previous experiments where now repeated. Before employing the siRNA technology to the cells, the first critical experiment was once more repeated to ensure consistency of the results and also to use the same cell batch and passage for all of the knock-down experiments.

Graph 23: ERK protein phosphorylation levels in EA.hy926 cells stimulated with aldosterone.

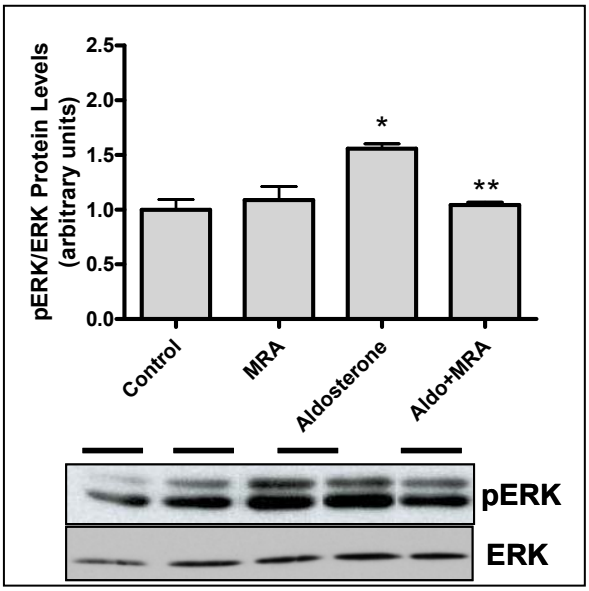

Untransfected EA.hy926 cells show an increase in the pERK/ERK ratio, following incubation with aldosterone (10nM) for 15 minutes (* $p < 0.05$ vs. Control,

**p < 0.05 vs. Aldosterone). MRA stands for mineralocorticoid receptor antagonist and represents treatment with 10μM canrenoic acid. These results are consistent with what was previously shown and demonstrate that the cells are responsive to aldosterone stimulation.

Graph 24: ERK protein phosphorylation levels in EA.hy926 cells transfected with striatin siRNA and subsequently stimulated with aldosterone.

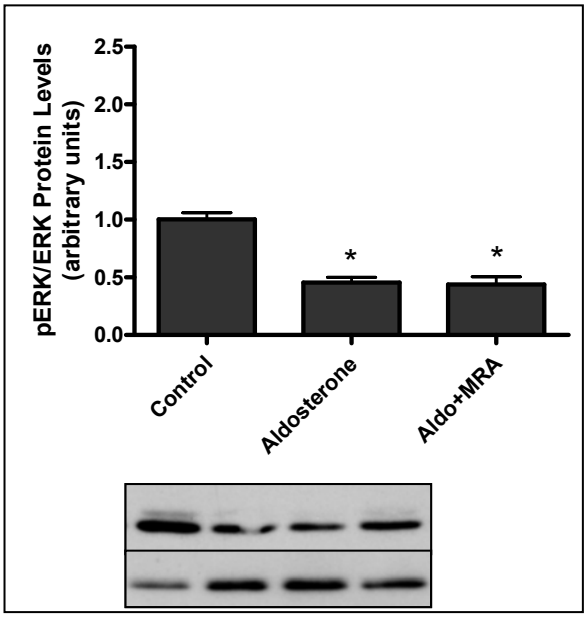

The rapid increase in pERK levels, observed in the previous graphic, is abolished when the EA.hy926 cells are transfected with striatin siRNA (* p < 0.01 vs. Control). Control represents untransfected cells, all of the "transfection" procedure was carried out but the duplex was absent from the mix effectively making it a mock transfection. MRA stands for mineralocorticoid receptor antagonist and represents treatment with 10μM canrenoic acid. Results show that the rapid rise in pERK levels is abolished but also, the overall phosphorylation levels seem to be lower in the transfected cells. By comparison, though, ERK protein levels seem to be elevated in the transfected cells, perhaps justifying the decrease in phosphorylation levels as it is showed has a ratio between pERK and total ERK.

In order to establish that the scrambled (control) sequence does not affect the cell signalling, the first experiment was repeated in cells transfected with the control duplex and results compared.

Graph 25: ERK protein phosphorylation levels in EA.hy926 cells transfected with striatin control siRNA and subsequently stimulated with aldosterone.

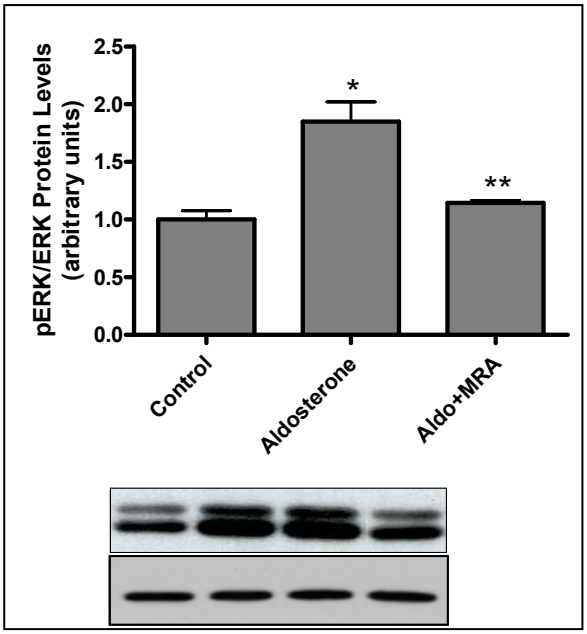

Cells transfected with scrambled siRNA show a significant increase in ERK phosphorylation levels (* p < 0,05 vs. Control; **p < 0,05 vs. Aldosterone). Results shown on graph 25 clearly confirm that the scrambled control sequence does not affect the way these cells signal. The rapid increase in ERK phosphorylation is present in comparable levels to what has been shown previously and is abrogated when the cells are treated with canrenoic acid (MRA).

Graph 26: WNK4 mRNA levels in EA.hy926 cells transfected/untransfected with striatin siRNA and subsequently stimulated with aldosterone.

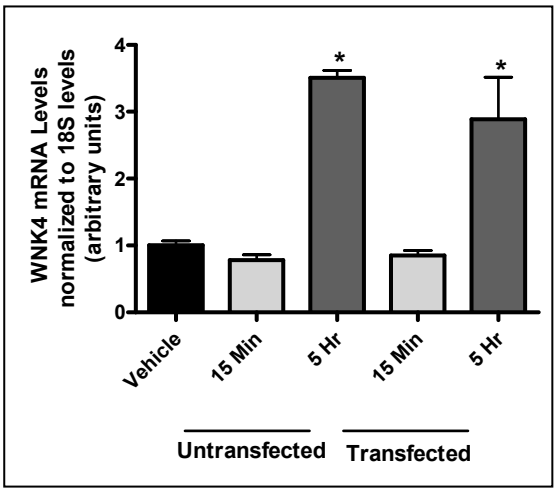

Finally, EA.hy926 cells, transfected with striatin siRNA or controls (untransfected) were treated with aldosterone (10nM) and mRNA levels of WNK4 and SGK1 were measured to establish if a decrease in striatin gene expression influenced aldosterone's known genomic responses. Results show that in both cases the genomic signalling is not affected, there is no significant change between transfected and untransfected cells while, at 5 hours of aldosterone stimulation, a genomic effect is still visible and significant (WNK4, $p< 0,05$ vs. control and SGK1, $p<0,001$ vs. control).

Graph 27: SGK1 mRNA levels in EA.hy926 cells transfected/untransfected with striatin siRNA and subsequently stimulated with aldosterone.

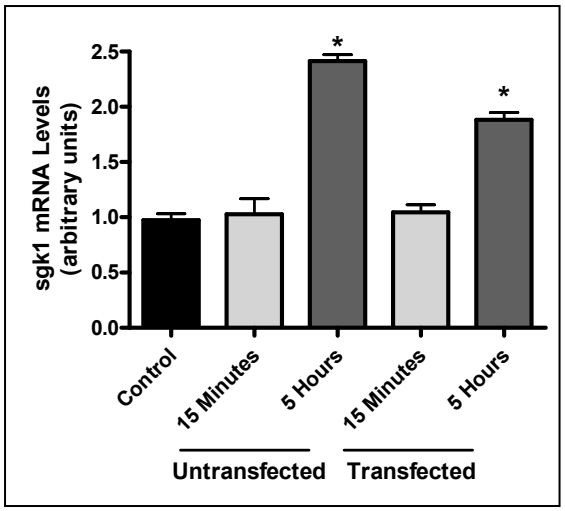

All combined these results indicate that striatin is a necessary player in aldosterone's nongenomic effects and that when it is not present such effects (increase in ERK phosphorylation levels at 15 minutes) do not occur. They also indicate that striatin does not seem to be necessary for the classical, genomic effects to occur, pointing to the possibility that different pathways are in play here.

Having established that striatin is a key player in aldosterone's nongenomic effects via the mineralocorticoid receptor it remains to study the importance of the *caveolae* in this process. It is known that striatin contains four protein-protein interaction domains, including a caveolin-binding domain (190) and that, CAV_1 has been shown to interact with the protein striatin.

Striatin seems to be a key intermediary of the effects of steroid receptors, specifically estrogen receptor-α (ERα) (188). Lu et al provided evidence that striatin´s N-terminal segment interacts with the DNA binding domain of ERα in EA.hy926 cells. This interaction organizes the ERα-eNOS membrane signalling leading to rapid nongenomic activation of downstream signalling pathways including ERK and eNOS in endothelial cells. Taking these previous observations into account it is important to investigate the possible connection between MR, striatin and caveolin 1.

Interactions between MR, Striatin and CAV_1

In order to detect any possible interaction between these 3 proteins of interest it was decided to employ co-immunoprecipitation (Co-IP) as a tool to try to establish if there were any protein-protein interactions or if they were organized as protein complex. Co-IP works by selecting an antibody that targets a known protein that is believed to be a member of a larger complex of proteins. By targeting this *known* member with an antibody it may become possible to pull the entire protein complex out of solution and thereby identify *unknown* members of the complex. This works when the proteins involved in the complex bind to each other tightly, making it possible to pull multiple members of the complex out of solution by latching onto one member with an antibody. This concept of pulling protein complexes out of solution is also referred to as a "pull-down".

If MR, striatin and CAV_1 are interacting closely, it will be possible to “pull” one of these proteins down and use a different antibody to detect the other protein. In brief, endothelial cells were collected (scrapped) and homogenized in RIPA Buffer and protein content determined by colorimetric assay. The protein extract (500 μg) was incubated with 1-2 μg of monoclonal or polyclonal antibodies for 1-2 hours at 4 ºC together with 50-100 μl of protein G or A/G MicroBeads. The Microbeads, antibody and cell lysate mix were separated using MACSmini columns and respective magnetic stand, according to the manufacturers protocol. Finally the beads were washed with RIPA buffer and the bound immuno-complexes eluted using boiling loading dye and assessed by Western Blot analysis.

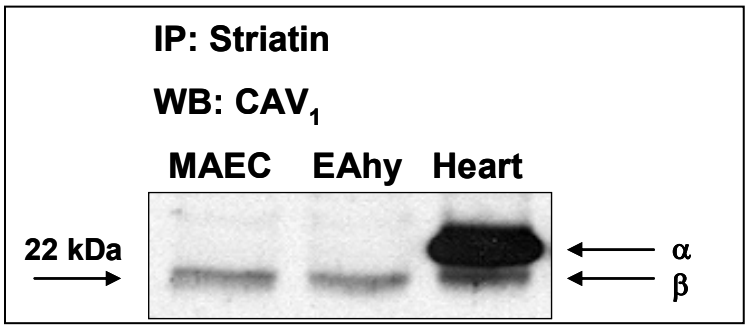

Figure 55 – Western blot illustrating the presence of CAV_1 protein after striatin "pull-down". MAEC stands for mouse aortic endothelial cells and EAhy for EA.hy926 cells.

In the first Co-IP, striatin was targeted to be pulled down and the resulting elution studied for the presence of CAV_1 protein. Results show that there seems to be an interaction between striatin and caveolin 1 in mouse aortic endothelial cells, EA.hy926 cells and mouse heart tissue. This result was not unexpected since it is known that striatin has a caveolin-binding domain but, it was necessary to establish such a fact in our cells of interest and it also goes to demonstrate that the Co-IP technique chosen to look at possible interactions is an efficient study tool.

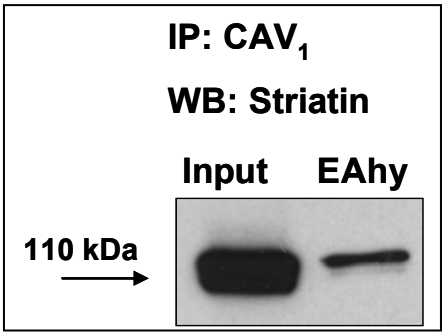

Figure 56 – Western blot illustrating the presence of striatin protein after CAV_1 "pull-down". Input stands unprecipitated cell extract and EAhy for EA.hy926 cells.

To prevent any possible artefacts resulting from the technique used, the reverse Co-IP was always performed. The figure shows that when CAV_1 is the target of the "pull-down", striatin is presence is detected in the resulting cell elution. This confirms the previous result and demonstrates a close interaction between caveolin 1 and striatin proteins. Input represents a cell extract that did not go through the Co-IP process, and serves as a control for the antibody used in western-blot analysis since it hadn't been used in Co-IP studies previously.

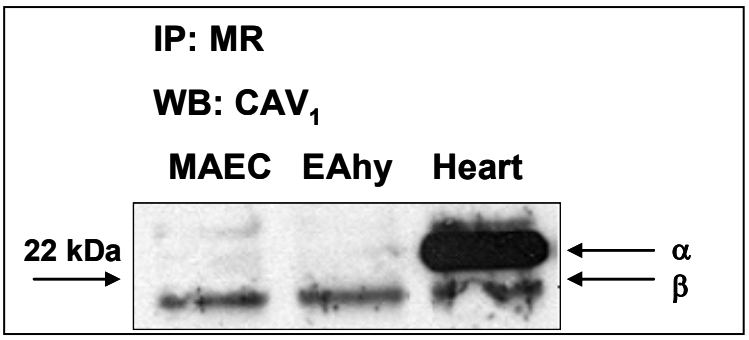

Figure 57 – Western blot illustrating the presence of CAV_1 protein after MR "pull-down". MAEC stands for mouse aortic endothelial cells and EAhy for EA.hy926 cells.

The next round of Co-IPs connects the mineralocorticoid receptor to caveolin 1 and the *caveolae.* When the MR is captured by the beads treated with MR-specific antibody it is possible to detect the presence of CAV_1 in the resulting elution. This means that MR and CAV_1 have a close interaction and potentially places the mineralocorticoid in the *caveolae* structure located in the cell membrane. Results shown for heart tissue depict two different bands that correspond to the alpha and beta isoforms of caveolin 1, known to be expressed in cardiomyocytes (266).

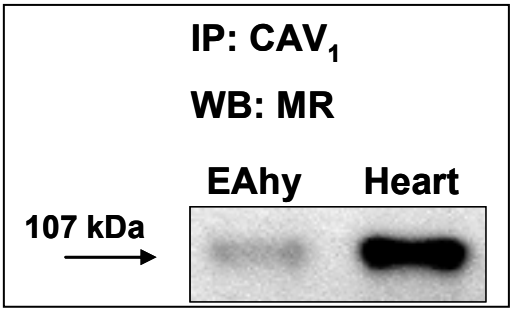

Figure 58 – Western blot illustrating the presence of MR protein after CAV_1 "pull-down". EAhy stands for EA.hy926 cells.

Once again, the reverse Co-IP confirms the results shown before and points to the presence of the mineralocorticoid receptor in the cell membrane in the *caveolae* structures or connected to them via CAV_1 protein. Due to a smaller amount of CAV_1 protein present in the EA.hy926 cells when compared to whole heart tissue, the resulting MR band appears faint but with enough definition to be considered a positive result.

The next possible interaction studied was that between striatin and MR. It was already known that MR needs striatin to exert its nongenomic effects so this interaction is expected to be strong.

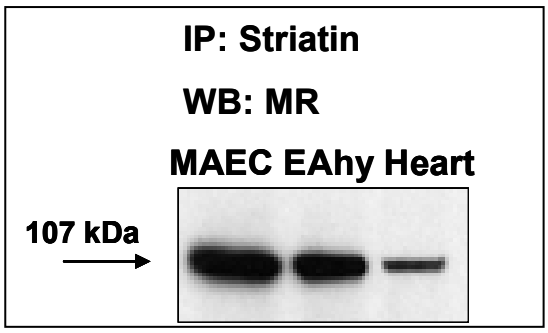

Figure 59 – Western blot illustrating the presence of MR protein after striatin "pull-down". MAEC stands for mouse aortic endothelial cells and EAhy for EA.hy926 cells.

As expected, when striatin is precipitated with A/G beads conjugated to striatin antibody, the resulting elution contains a high amount of mineralocorticoid receptor, demonstrating and confirming the predicted close interaction between the two proteins.

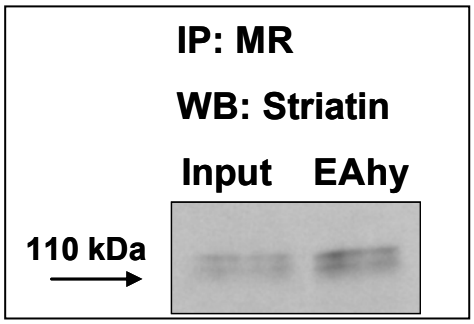

Figure 60 – Western blot illustrating the presence of striatin protein after MR "pull-down". Input stands for unprecipitated cell extract and EAhy for EA.hy926 cells.

The reverse Co-IP confirms the interaction between striatin and MR and seems to point to the presence of two striatin isoforms in EA.hy926 cells. According to Swiss-Prot striatin has two different isoforms although isoform I is the one that is commonly reported and referred to. Isoform I has 780 amino acid and weighs about 86.13 KDa, whereas isoform II has 731 amino acids and weighs about 80.76 KDa. The different in expected weight and the results obtained with the antibody used might be due to a post-translational modification as has been referred previously when phenotyping the EA.hy926 cells.

These Co-IP results show a strong interaction between MR, striatin and CAV_1 and seem to indicate the formation of a possible triple complex between these three proteins, most likely modulated by CAV_1 since it has a known role in binding the

striatin protein and would likely also serve to anchor the MR to the cell membrane, keeping it in place for further interactions with other molecules to occur and leading to rapid, nongenomic effects of MR activation. To test this hypothesis mouse aortic endothelial cells were collected from wild-type and CAV_1 knock-out animals. These cells were expended and used at passage 3 and 4. Just like the previous studies, cells were collected in RIPA buffer, processed and used for Co-IP studies.

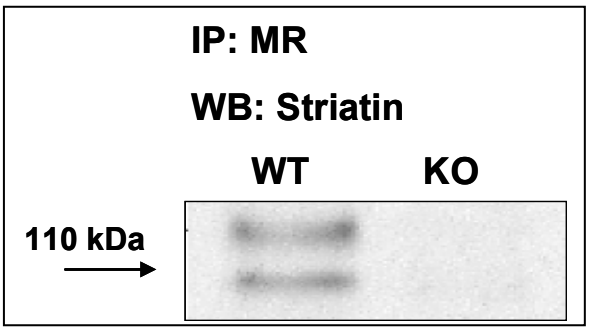

Figure 61 – Western blot illustrating the presence/absence of striatin protein after MR "pull-down" in MAEC. WT stands for wild-type animals and KO for knock-out.

Results show that in the absence of CAV_1, the mineralocorticoid receptor does not seem to interact with striatin or, there interaction is weakened and cannot be detected using co-immunoprecipitation techniques. The reverse Co-IP was also executed in order to confirm this theory.

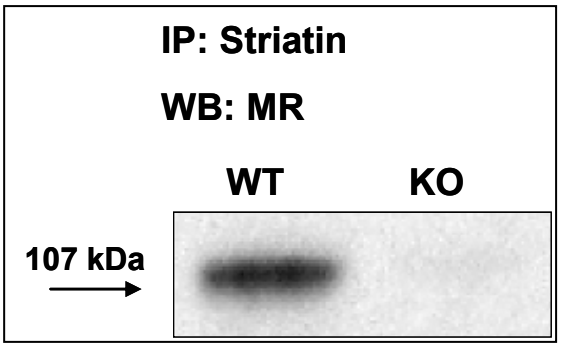

Figure 62 – Western blot illustrating the presence/absence of MR protein after striatin "pull-down" in MAEC. WT stands for wild-type animals and KO for knock-out.

Likewise and, as expected, the reverse Co-IP showed that in the absence of CAV_1 Striatin does not seem to interact with the mineralocorticoid receptor. These results are very important and seem to strengthen the existence of a triple complex between MR, striatin and CAV_1, with caveolin 1 as the intermediary between the

other the proteins. These results also point to an important role being played by the *caveolae* in providing a prime spot for protein interactions and cell signalling to take place. To test if the *caveolae* are indeed pivotal in MR activation and aldosterone's nongenomic signalling, EA.hy926 cells were treated with lipid-raft disruptors (cyclodextrin and β-Methylcyclodextrin) and subsequently treated with 10nM aldosterone for 15 minutes.

Graph 28: ERK phosphorylation levels in EA.hy926 cells treated with lipid raft disrupting chemicals and subsequently stimulated with aldosterone.

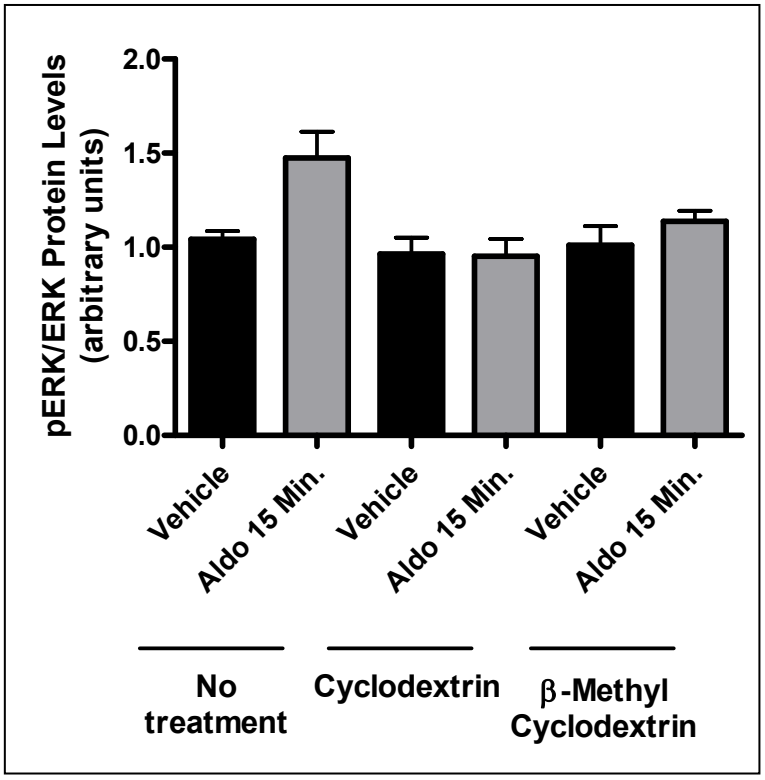

EA.hy926 cells were pre-incubated overnight with two lipid raft disrupting chemicals and then treated with 10nM aldosterone for 15 minutes. As is shown in the above graphic, aldosterone had no effect on pERK in the presence of either chemical. Although these results are not quite significant due to a low number of repeats, the general trend which they demonstrate seems to confirm the *caveolae* as having a facilitating role is aldosterone's nongenomic effects by providing a place for MR to interact with other players in this cell signalling pathway.

Further experiments (results not shown) carried out with mouse aortic endothelial cells collected form wild-type and CAV_1 knock-out animals seemed to indicate that the lack of caveolin 1 did not affect the genomic effects of aldosterone with a visible peak in striatin protein levels still being observed after 5 hours of aldosterone stimulation. This result, albeit not significant, might indicate that aldosterone and striatin are playing more than one role in these endothelial cells and the striatin protein peak observed at 5 hours of aldosterone might prove to be important on its own.

Aldosterone's influence on Estrogen's nongenomic actions

Lu *et al* identified striatin as a scaffold protein that promotes localization of ERα to the plasma membrane and assembly of the signalling complex of ERα and G_i that is required for ERα-dependent activation of MAPK, phosphatidylinositol 3–Akt kinase, and eNOS, a critical regulator of many physiologic and pathophysiological processes (188). Their results show a peak in eNOS phosphorylation at 15 minutes of estrogen stimulation that is abrogated if striatin is disrupted (using a blocking peptide). They also show that overexpression of striatin markedly changes the distribution of ERα by substantially increasing the proportion of ERα that is distributed along the plasma membrane. These results combined with the information that the binding of estrogen (E_2) to the membrane has been confirmed, in addition to the presence of ERα and caveolin in plasmalemmal caveolae and, their connection to nongenomic and short-term effect of E_2 on endothelial NO release (186) led to the possibility of a an interaction/cross-talk relationship between aldosterone and estrogen signalling in endothelial cells.

The first step taken was to ascertain if, like aldosterone, estrogen treatment stimulated the production of striatin protein. EA.hy926 cells were treated with either 10nM aldosterone or 50nM estrogen for 5 hours. Aldosterone but not estrogen treatment increases striatin protein levels. Cells used for experiments with estrogen stimulation were grown in Estrogen-Deficient media which is achieved by charcoal-stripping the FBS used in the media preparation.

Graph 29: Striatin protein levels in EA.hy926 cells treated with aldosterone (10nM) or estrogen (50nM) for 5 hours.

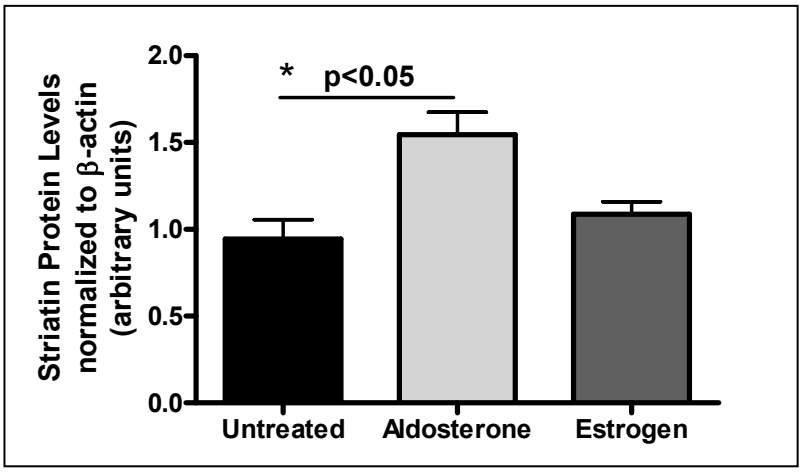

Results show that the increase in striatin protein seems to be specific to aldosterone's MR activation and does not occur with estrogen stimulation. The next logical step was then to reproduce the estrogen action previously observed by Lu *et al* and introduce aldosterone in the mix to determine if the presence of more striatin protein at a given time in these cells affected the way nongenomic actions of estrogen occurred.

Graph 30: eNOS phosphorylation levels in EA.hy926 cells treated with estrogen (50nM) for short periods of time with/without aldosterone (10nM) pre-treatment for 5 hours.

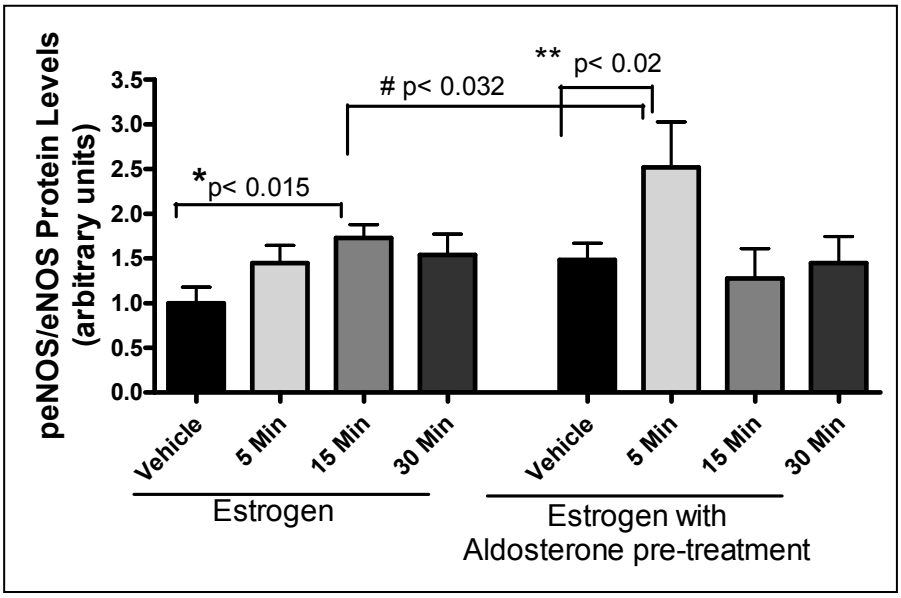

EA.hy926 cells were pre-treated with or without aldosterone (10nM) for 5 hours. peNOS/eNOS levels were then measured in response to estrogen (50nM) stimulation were measured at 5, 15 and 30 minutes. Pre-treatment with aldosterone enhanced estrogen's nongenomic response.

The graphic depicted above shows that results previously obtained by Lu *et al* were successfully replicated. There was a peak in eNOS phosphorylation which occurred at 15 minutes of estrogen stimulation (*p<0,015 vs. vehicle). This peak is smaller than previously observed and the estrogen dose employed higher which can be justified by the absence of overexpression of striatin protein in cells used.

When an aldosterone pre-treatment is added to the treatment conditions, a very interesting event occurs. There is a shift in the peNOS peak observed; it not only increases its levels but it also occurs sooner (#p<0,032 vs. 15 minutes with no pre-treatmen; **p<0,02 vs. vehicle). This is not an experimental artefact as this experiment was repeated six times always in triplicate wells and the results obtained consistent with some variation in the peNOS levels achieved.

This is a novel result and might prove to change the way steroid signalling is viewed, adding a new level of complexity concerning crosstalk between different receptors. Although Lu *et al* had already showed that the peak observed in eNOS phosphorylation disappears when striatin action is blocked by a specifically designed peptide; they had not attempted to knock-down striatin levels to confirm this conclusion.

Graph 31: peNOS levels in EA.hy926 cells transfected with striatin scramble/siRNA and treated with estrogen for 15 minutes with/without aldosterone pre-treatment.

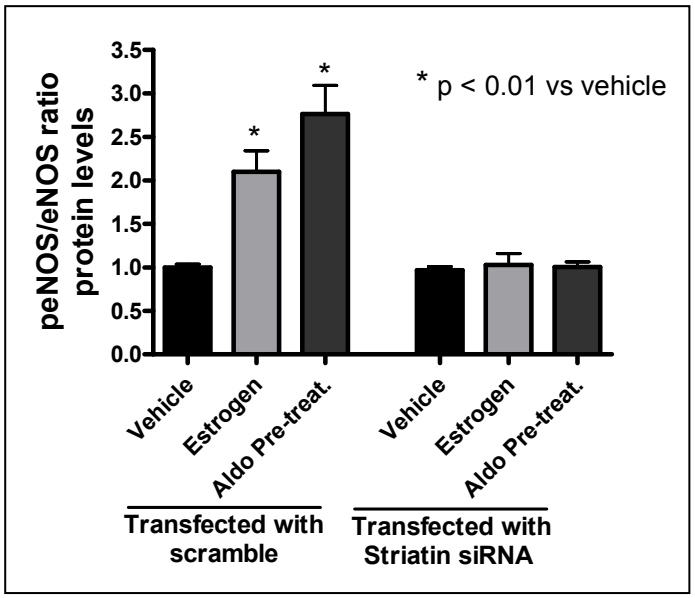

EA.hy926 cells grown in estrogen deprived media were transfected with striatin scrambled sequence or striatin siRNA for a period of 48 hours. After transfection cells were made quiescent by stepping-down serum levels to 0,4% FBS overnight. Cells were then treated with 50nM estrogen for 15 minutes with/without a pre-treatment with 10nM aldosterone for a period of 5 hours. Results shown confirm the previous observations and confirm striatin has a key player in estrogen signalling. Cells transfected with striatin scrambled sequence (control) show a 2 fold peak in eNOS phosphorylation levels at 15 minutes of estrogen treatment. This peak increases when the same cells were subjected to a 5 hour pre-treatment step with 10nM aldosterone. When the cells are transfected with striatin siRNA, the response to estrogen stimulation is completely abrogated, even when pre-treatment with aldosterone is employed.

Because the results showed so far indicate a potential cross-talk between estrogen and aldosterone signalling pathways, it was important to study the effect of estrogen on ERK phosphorylation. Since aldosterone pre-treatment enhances eNOS phosphorylation levels when cells are stimulated with estrogen, it is possible that estrogen pre-treatment might influence ERK phosphorylation levels when cells are stimulated with aldosterone.

Graph 32: ERK phosphorylation levels in EA.hy926 cells treated with aldosterone (10nM) for short periods of time with/without estrogen (50nM) pre-treatment for 5 hours.

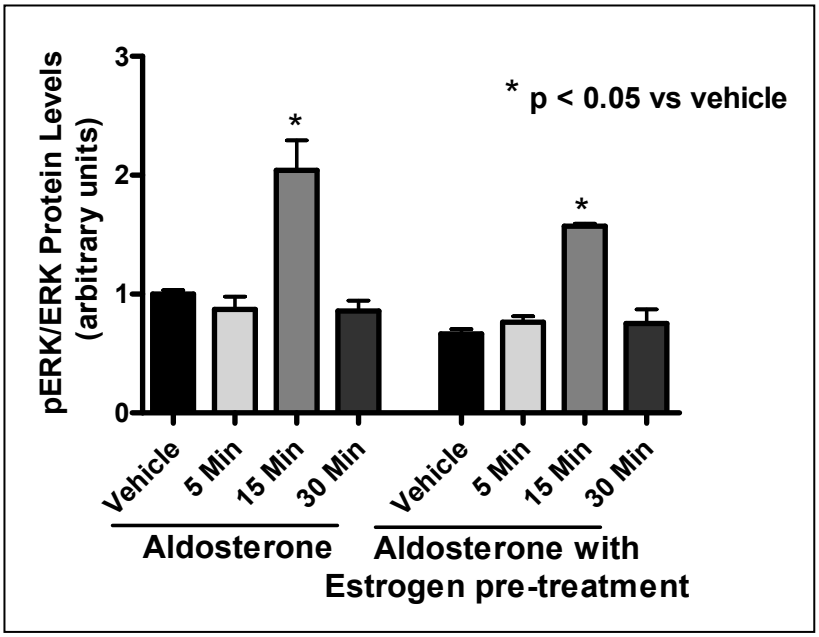

Results show that, contrary to what was observed with aldosterone, estrogen pre-treatment does not increase pERK levels in EA.hy926 cells. Aldosterone stimulation for 15 minutes caused a peak in pERK levels, consistent with has been shown here before but, pre-treatment with 50nM estrogen for 5 hours did not increase this peak, showing no significant change from cells untreated with estrogen.

Striatin has been proven to be involved in rapid signalling events in the cells studied but, results observed so far do not seem to indicate that the same is true for the more classical genomic effects of steroid action. Striatin siRNA did not damper the genomic effects of aldosterone stimulation but, it remains to be seen if the same is true for estrogen action. PTGIS or prostaglandin I2 (prostacyclin) synthase, together with PTGS1 or prostaglandin-endoperoxide synthase 1 were selected as targets to study the effects of striatin knock-down on estrogen's genomic actions.

Prostaglandin-I synthase (EC 5.3.99.4) also known as prostaglandin I2 (prostacyclin) synthase (PTGIS) or CYP8A1 is an enzyme involved in prostanoid biosynthesis that in humans is encoded by the PTGIS gene (267). This enzyme belongs to the family of cytochrome P450 isomerases. This endoplasmic reticulum membrane protein catalyzes the conversion of prostaglandin H_2 to prostacyclin (prostaglandin I_2), a potent vasodilator and inhibitor of platelet aggregation. An imbalance of prostacyclin and its physiological antagonist thromboxane A_2 contribute to the development of myocardial infarction, stroke, and atherosclerosis (268). Recent studies have shown that in human umbilical vein endothelial cells (HUVEC), treatment with estrogen (1-100nM) caused a dose-dependent increase in prostaglandin I2 synthase protein production, up to 50% and PTGIS gene expression levels were also increased by 50% after exposure to estrogen (269).

PTGIS expression levels were measured by Real-Time PCR in EA.hy926 cells transfected/untransfected with striatin siRNA and subsequently treated with 50nM estrogen for 15 minutes and 5 hours.

Graph 33: PTGIS mRNA levels in EA.hy926 cells transfected/untransfected with striatin siRNA and stimulated with 50nM estrogen for 15 minutes and 5 hours.

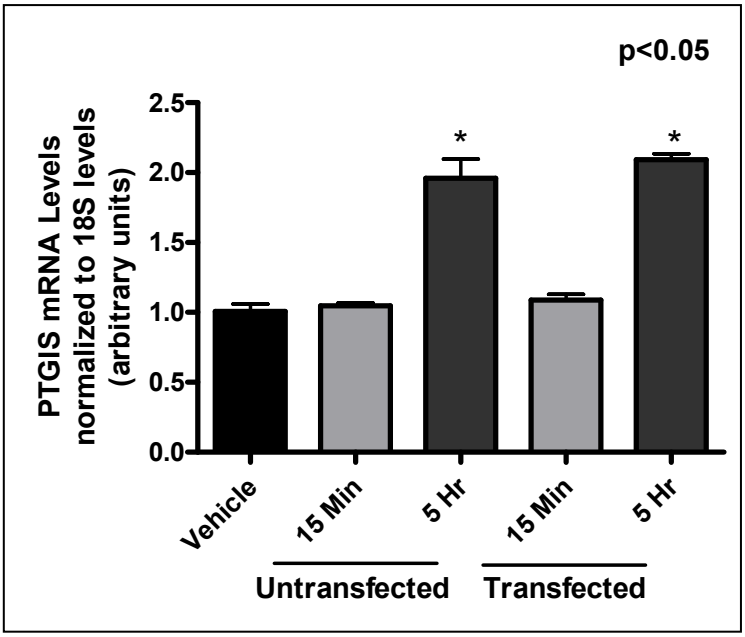

Results show that, as expected and described in the literature, treatment with estrogen stimulated PTGIS expression in the endothelial cells studied (p<0,05 vs. vehicle). Transfection with striatin siRNA, did not affect this genomic action, with similar levels of mRNA observed for both untransfected and transfected cells.

Graph 34: PTGS1 mRNA levels in EA.hy926 cells transfected/untransfected with striatin siRNA and stimulated with 50nM estrogen for 15 minutes and 5 hours.

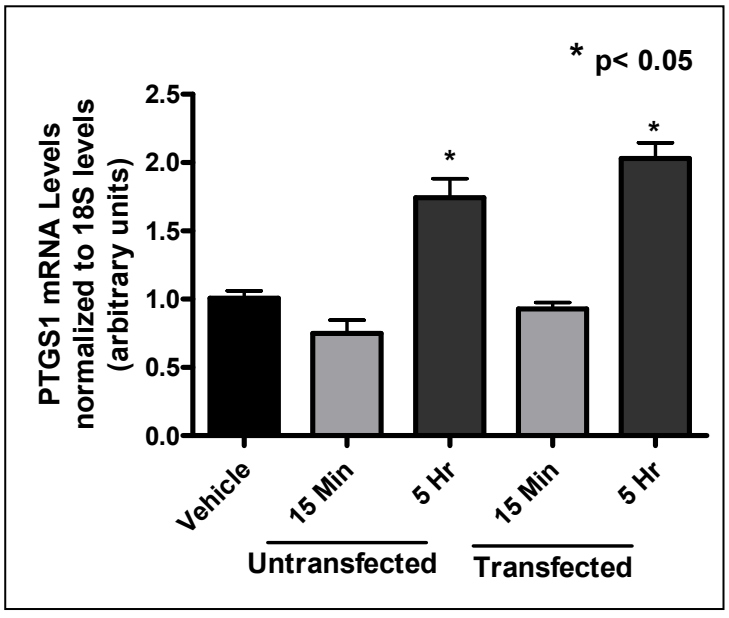

Cyclooxygenase-1 (COX-1), also known as prostaglandin G/H synthase 1, prostaglandin-endoperoxide synthase 1 or prostaglandin H2 synthase 1, is an enzyme that in humans is encoded by the PTGS1 gene (270, 271). Prostaglandin-endoperoxide synthase (PTGS), also known as cyclooxygenase (COX), is the key enzyme in prostaglandin biosynthesis. It converts free arachidonic acid, released from membrane phospholipids to prostaglandin (PG) H2. There are two isozymes of COX encoded by distinct gene products: a constitutive COX-1 (this enzyme) and an inducible COX-2, which differ in their regulation of expression and tissue distribution. The PTGS1 gene encodes COX-1, which regulates angiogenesis in endothelial cells. COX-1 is normally present in a variety of areas of the body, including not only the stomach but any site of inflammation and is inhibited by nonsteroidal anti-inflammatory drugs (NSAIDs) such as aspirin. Estrogen is known to increase the expression of the PTGS1 gene in endothelial cells (272, 273).

Results show that treatment with estrogen stimulated PTGS1 expression in the endothelial cells studied ($p<0,05$ vs. vehicle), consistent with the literature. Transfection with striatin siRNA, did not affect this genomic action in anyway, with similar levels of mRNA observed for both untransfected and transfected cells.

The fact that aldosterone has been shown to increase eNOS phosphorylation in EA.hy926 cells stimulated with estrogen might be viewed as a consequence of the use of an immortalized endothelial cell line as a study tool, this way previous key experiments were repeated in mouse aortic endothelial cells in an attempt to bring the results shown close to physiological relevance.

Mouse aortic endothelial cells were collected from healthy animals and allowed to expand until passage 2 when a high enough number of cells was achieve in order to proceed with the cell studies. Cells were grown in estrogen deprived media and stepped-down to 0,4% FBS the night before in order to avoid the occurrence of any potential secondary stimulation by factors still present in the FBS.

Graph 35: eNOS phosphorylation levels in EA.hy926 cells treated with estrogen (50nM) for short periods of time.

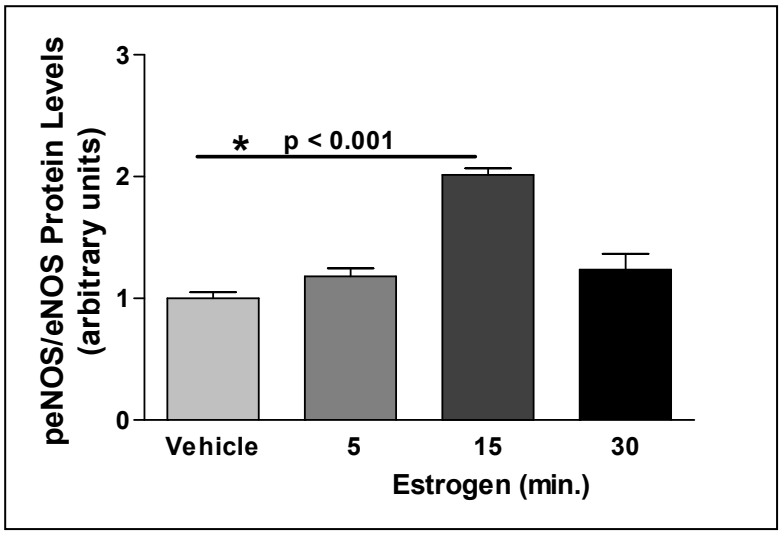

Graph 36: eNOS phosphorylation levels in EA.hy926 cells treated with estrogen (50nM) for short periods of time with aldosterone (10nM) pre-treatment for 5 hours.

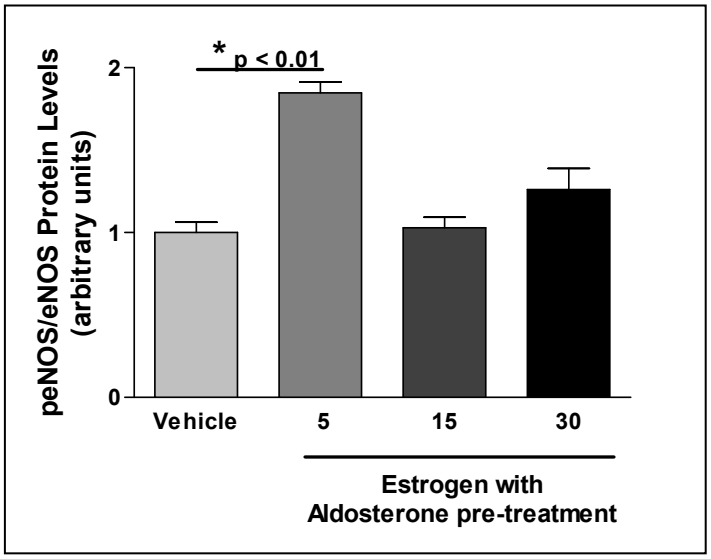

Just as seen with EA.hy926 cells, pre-treatment with aldosterone enhanced estrogen's nongenomic response. Graphic 33, depicted above, begins by showing that the results previously obtained in EA.hy926 cells where replicated. There was a peak in eNOS phosphorylation which occurred at 15 minutes of estrogen stimulation. The levels of phosphorylation achieved are also very similar to what as previously been observed for EA.hy926 cells (p<0,001 vs. vehicle).

When an aldosterone pre-treatment is added to the treatment conditions, there is, once more, a shift in the peNOS peak observed. In the case of mouse aortic endothelial cells there doesn't seem to be an increase in peNOS levels (as observed before) but, the nongenomic response to 5 minutes of estrogen stimulation is confirmed ($p<0,01$ vs. vehicle). Total protein lysates were immunoblotted for phospho-eNOS (peNOS) and normalized for the amount of total eNOS. These ratios were normalized to one for the vehicle-treated cells.

Discussion

Aldosterone and MR: classic physiology and pathophysiology

Aldosterone was first isolated in 1953 and characterized as the major mineralocorticoid hormone on the basis of its potent effects on unidirectional transepithelial sodium transport (274). It is commonly thought that the major stimulus to its secretion is angiotensin (275, 276) and that the physiologic actions of aldosterone are homeostatic, preserving fluid and electrolyte status via a negative feedback loop - depletion of sodium or circulating volume leading to increased renin secretion, and the consequently increased angiotensin generation raising aldosterone secretion, which in turn increases Na^+ and water retention via epithelial mineralocorticoid receptor (MR) activation to restore the status quo.

The MR is a member of a close subfamily, with glucocorticoid receptors, androgen receptors, and progesterone receptors. This receptor was first studied in classic aldosterone target tissues, such as the kidney, distal colon and salivary gland; subsequently, identical receptors were described in nonepithelial tissues such as hippocampus and heart, not commonly considered to be physiologic aldosterone target tissues (35, 277). In addition to the effects on gene expression, such receptors have increasingly been shown to have additional rapid nongenomic effects; although rapid nongenomic effects of aldosterone via MR activation have been clearly demonstrated experimentally, their physiologic roles remain to be established (278).

Primary aldosteronism (Conn's syndrome) was first reported in 1954 by Dr Jerome Conn, who diagnosed aldosterone overproduction in a young woman with hypertension and hypokalemia, reversed by surgical removal of the affected adrenal (279). Inappropriately elevated aldosterone levels drive sodium and water retention, which increases circulatory volume and cardiac output; the latter, in turn, by reflex normalized by vasoconstriction, resulting in hypertension.

Recently, evidence has been accumulating that aldosterone elicits additional, nonclassical effects. Besides experimental data, clinical studies like RALES, EPHESUS, and 4E (103, 104) convincingly demonstrate that aldosterone receptor (i.e. MR) antagonism protects against cardiovascular and renal remodelling independently of major alterations in blood pressure or NaCl homeostasis. The

model derived from these clinical trials and experimental animal studies suggests that activated mineralocorticoid receptor induces an inflammatory milieu with enhanced formation of reactive oxygen species and matrix proteins in the vasculature (107, 111, 280, 281). Subsequently, this vasculopathy leads to cardiac and renal damage. Although this model is now widely accepted, the individual steps in this pathophysiological network are only incompletely understood.

Rapid, nongenomic actions of aldosterone

After almost 30 years of research, the existence of nongenomic steroid actions is no longer disputed. The classical pathway of steroid action focuses on intracellular steroid receptors which modulate gene transcription by interacting with a transcription initiation complex and transcription factors (282); in addition, a direct interaction of steroids with nuclear DNA has been demonstrated (283). Besides these transcriptional actions, steroids mediate multiple other effects, through nongenomic mechanisms.

The main feature of nongenomic steroid actions is the quick onset of their effects. Nongenomic effects have been assumed to originate at the cell membrane as most of the second messenger generating systems or the early steps in the kinase cascades, which are involved in rapid steroid actions, are organized and localized here to form functional signalling units. For the classical estrogen, glucocorticoid, androgen and progesterone receptors (ER, GR, AR and PR), localization at membranes has already been shown (284-286). In contrast to these receptors, the MR does not contain a palmitoylation motif which is usually involved in the membrane anchoring of steroid receptors. Interestingly, an interaction of the classical MR with the epidermal growth factor receptor (EGFR) at the membrane has been shown (287).

At the cellular level, these rapid effects of aldosterone have not only been reported in renal and intestinal cells but also in cells from the cardiovascular system (278). In 1984, Moura and Worcel (288) showed a biphasic effect of aldosterone on Na efflux from arterial smooth muscle with a rapid component which they interpreted to be nongenomic, marking the beginning of the research on the nongenomic mechanisms of aldosterone. In vascular smooth muscle and endothelial cells,

activation of the above-described signalling pathways and the Na+/H+ exchanger has now been described by various studies (278, 289), although the functional significance has not yet been clarified. For cardiomyocytes, different rapid effects have been reported, including PKCε-mediated direct inhibition of Na^+/K^+-ATPase activity (278). Furthermore, activation of ERK1/2 had been observed after 30 minutes (233).

Aldosterone-Response Studies

The work presented here is based on the hypothesis that nongenomic actions of the MR may function in a similar way to what has been described for the ERα (188). To explore this hypothesis it was decided to study ERK1/2 from the MAPK family as a possible player in the aldosterone nongenomic signalling cascade. This decision was greatly aided by the literature where several sources referred to an increase in pERK levels suggesting higher MAPK activity (118, 233, 234) but also by previous results observed within the research group (235). Several groups have reported an increase in phosphorylation of ERK1/2 within several minutes after aldosterone administration that is not blocked by inhibitors of transcription and translation (240, 241), implying a nongenomic mechanism. With reports of increases in ERK phosphorylation as early as 5 minutes after stimulation with aldosterone, it was felt that the best course of action was a short-time aldosterone stimulation study to pinpoint when the endothelial cells used in the laboratory achieve a peak in ERK1/2 phosphorylation.

Two different types of endothelial cells were used in experiments EA.hy926 and MAEC cells, both of which were extensively phenotyped. In addition, before each experiment cells were stepped-down to 0,4% FBS DMEM to keep the environment stimulation to a minimum, since it is impossible to determine which potential stimulating factors are present in the FBS.

In order to select the adequate aldosterone dosage to use in experimentation, a dose response curve was generated. Results showed a dose-dependent response, with around 1,5 increase (30%) in ERK phosphorylation with a 10nM aldosterone dose at 15 minutes of stimulation leading up to a 2-fold response when a 1μM

aldosterone dose is used. Bearing in mind the potential physiological relevance of future results, 10nM aldosterone was the elected concentration for ensuing studies. Plasma aldosterone levels vary considerably. A study conducted in 76 healthy individuals and 28 confirmed primary hyperaldosteronism (PHA) patients resulted in plasma aldosterone values of 0,033 to 1,930 nM for healthy subjects and 0,158 to 5,012 nM for PHA patients (250). In addition, clinical results collected by other investigators in the group over the past 30 years (HyperPATH cohort) show that in 828 hypertensive subjects the circulating aldosterone levels ranged between 0.05 and 11,53 nmol/L. Furthermore, aldosterone levels over 100 nmol/L have been observed in heart failure patients (251, 252). These values, especially the top value for PHA patients seems to validate the choice of 10nM aldosterone as a valid one both for cell studies as for a possible comparison with pathophysiological states in humans.

A short-term study revealed two distinct peaks of activity for pERK after cells were stimulated with aldosterone. The first peak is observed at 15 minutes of aldosterone treatment and the second peak can be seen at 5 hours of treatment. These results were true for both cell lines used in the experimental design. Statistical results were obtained by one-way ANOVA followed by *post-hoc* Mann-Whitney *t*-test comparison for selected time-points.

Aldosterone's nongenomic effects

The short length of time of treatment needed to obtain the first peak in pERK lead to the hypothesis that this could be part of a nongenomic effect of aldosterone signalling. The second peak, seen at 5 hours of treatment was believed to be involved in genomic effects of aldosterone.

Before further conclusions could be drawn, an antagonist of aldosterone action, potassium canrenoate, was used to ensure that the previously observed effects were due to MR activation and not an experimental artefact. Canrenoic acid was selected as inhibitor of choice for aldosterone due to practicality. Canrenoic acid is readily available from chemical suppliers is also water soluble making it a perfect inhibitor for use in cell based assays.

EA.hy926 stimulated with aldosterone with/without MR antagonist (MRA) showed an increase in ERK1/2 phosphorylation at 15 minutes of treatment, consistently with what has been observed before with these cells. When canrenoic acid was used in conjunction with the aldosterone treatment, the increase in ERK phosphorylation was abrogated, thus confirming that the increase in pERK observed is indeed due to an effect of aldosterone acting, at least in part, through MR. Put together, the results from short-time aldosterone stimulation studies point to a newly described nongenomic action of aldosterone in endothelial cells but, in order to call it a nongenomic action it was necessary to demonstrate that no gene translation was occurring in the 15 minutes of aldosterone action.

EAhy.926 cells were stimulated for 15 minutes and 5 hours and collected for mRNA extraction. After reverse-transcription, cDNA obtained was used for Real-Time PCR, the 5 hour time-point was used as a positive control for genomic action, based on previously published data. Aldosterone is known to increase or reduce the expression of several different genes (254), SGK1 has been shown to be one of these genes with a 2.5 fold increase in SGK1 mRNA after aldosterone stimulation (259) in cardiomyocytes. The kinase WNK4 has also been shown to have a dose-dependent relationship with aldosterone, suggesting that it might be an aldosterone-sensitive gene (262).

Consistent with the observations for cardiomyocytes, EA.hy926 cells stimulated with aldosterone showed an increase in SGK1 mRNA levels of 2.5 times after 5 hours of aldosterone treatment. WNK4 mRNA levels also showed an increase of about 3.5 fold after 5 hours of treatment. Contrary to the 5 hour time-point that displays a classic genomic action of aldosterone with a significant increase in mRNA levels, the 15 minute time-point did not show any significant change supporting the hypothesis that the increase in pERK protein levels is indeed a nongenomic effect of aldosterone action at this time-point. In order to take into account differences between samples, mRNA levels were normalized using the housekeeping ribosomal gene 18S.

Aldosterone's genomic effects

Having established that there is a significant nongenomic increase of pERK due to aldosterone stimulation in endothelial cells, it was investigated if striatin and the *caveolae* played a role in this action as seen in estrogen's nongenomic actions. To answer if aldosterone influenced striatin in any way, EA.hy926 cells were stimulated with aldosterone for periods of time conducive to a potential genomic effect. Results showed a significant increase in striatin protein at 5 hours of aldosterone stimulation, consistent with the second increase in pERK previously seen, hinting at the possibility that the two effects might be linked.

This result was unexpected because striatin is believed to be a chaperone protein, facilitating the interactions between different signalling proteins. The increase in striatin took place at 5 hours of aldosterone treatment, similarly to other genomic actions of aldosterone. However, this increase seems to be an acute event occurring at 5 hours of stimulation. To determine if it was an effect of MR activation, experiments were carried out using canrenoic acid which, effectively inhibited the increase in striatin protein levels, thus establishing that the observed effect is a consequence of MR activation.

Confirming the rise in striatin protein levels as a genomic consequence of MR activation, striatin mRNA levels (after normalization to 18S) went up by about two fold and did not occur in the presence of canrenoic acid. This result constitutes a novel genomic action of aldosterone and may have several implications linked to steroid hormone signalling, since striatin has been described as a necessary component in other steroid hormone pathways like estrogen (188). The increase in striatin protein levels at five hours of aldosterone treatment was confirmed in MAEC cells but, not the raise in mRNA levels, leading us to belief that the peak of stimulation does not occur at the same time as was observed with EA.hy926 cells or the increase is not as noticeable, making the differences more difficult to detect.

Results obtained in animal studies strengthened the observations derived from endothelial cell studies. An experimental study with animals showed that dietary sodium restriction increased striatin levels in mouse hearts and aorta. Striatin levels were significantly higher in mice on a low sodium diet; characterized as having higher

plasma aldosterone levels, than the mice on higher sodium levels. An acute in vivo aldosterone administration (IP) lead to an increase of striatin protein levels in mouse heart when compared to vehicle injected animals. Finally, animals treated with L-NAME, in combination with AngII; treatment which induces myocardial damage that can be prevented by MR blockade; showed increased striatin levels both in heart and kidney tissues when compared to vehicle treated control.

Striatin and its family members zinedin and SG2NA are three distinct but structurally related WD-repeat proteins that share high protein sequence homology. The WD-repeat-containing family of proteins is defined by two main characteristic features: a lack of intrinsic catalytic activity and repeated units of beta-sheet motifs that are arranged into a beta-propeller structure to form a platform on which multiple protein complexes can dynamically assemble. In this way WD repeat containing proteins play a major role in cellular events by mediating important protein-protein interactions by providing a permissive scaffold for the anchorage of several diverse molecules that are important in cellular signalling, cytoskeletal assembly and vesicular trafficking.

Striatin, which comprises 780 amino acids and weighs 110 kDa, was first isolated in the brain as a calmodulin-binding protein. It contains at least four protein-protein interaction domains (see Figure 18), including caveolin-binding, coiled-coil, and Ca^{2+}-calmodulin (CaM) binding at the N-terminus, and a series of eight WD repeat domains at the C-terminus (190). The N-terminus of striatin (amino acids 1-203) has been found interact with the N-terminus of ERα (amino acids 185-253) while the C-terminal WD repeat domain binds the GPCR ($G_{\alpha i}$) complex. In this context, striatin acts as a scaffold directing ERα to the plasma membrane and bridges ERα with the GPCR ($G_{\alpha i}$) complex to facilitate assembly of a membrane signalling complexes required for rapid estrogen extra-nuclear activation of MAPK, Akt, and eNOS in endothelial cells (188).

Outside the brain, not much is known about striatin function apart from its connection to ERα and, in the literature it is always viewed as a scaffolding protein that facilitates the interaction between different intervenients in a signalling cascade. It is proven that it binds to CAV_1 (290) and that it assembles signalling complexes in

the vicinity of the cell membrane but it is the first time that a steroid hormone has been shown to influence its levels.

Having shown that aldosterone has nongenomic effects in the endothelial cells studied and, the presence of striatin in the same cells, it is was important to ascertain if the presence of striatin is necessary for the effects to occur and, if higher striatin levels changed the way MR signalling occurs in these cells. To explore these possibilities, striatin was knocked-down using siRNA technology and MR activation studies repeated in transfected cells.

Through several rounds of optimization, ideal conditions for striatin knock-down experiments using siRNA technology were established. Striatin gene expression and protein production was reduced to 25% when compared to untransfected cells and the oligonucleotide selected was shown not to affect the expression of the other two striatin family members.

In order to ensure the consistency of the results, the same cell batch was used for all of the knock-down experiments. Untransfected EA.hy926 cells were once more stimulated with aldosterone in the presence/absence of MRA to determine if the cells are responsive to aldosterone stimulation and the baseline levels of ERK phosphorylation. Consistently with what was previously shown EA.hy926 cells showed an 1,5 fold increase in the pERK/ERK ratio, following incubation with aldosterone for 15 minutes, which was abrogated with MRA.

When the cells were transfected with striatin siRNA, the rapid increase in pERK levels was abolished. The controls for these experiments were mock transfected cells. Results showed that the rapid rise in pERK levels is abolished but also, the overall phosphorylation levels were lower in the transfected cells. The first important point in these results is the fact that the controls used were, in fact, untransfected cells. Although this does not invalidate the conclusions, it would have been more adequate to use cells transfected with the scrambled control sequence instead. This way, the transfection effects on the cells would have been fully controlled for, including any potential changes in the levels of ERK phosphorylation.

Another point worth mentioning is the fact that pERK levels were lower in transfected cells when compared to mock transfected cells. The fact that untransfected cells are being compared to transfected ones might, very well, account for this difference and also, ERK protein levels seem to be more elevated in the transfected cells, which, due to the way the results are shown would in part justify the decrease in phosphorylation levels. Despite these possibilities, it is necessary to assume that this might also be a real biological find and look for possible explanations.

One possible explanation is linked to the already described actions of striatin. The serine/threonine protein phosphatases are targeted to specific subcellular locations and substrates in part via interactions with a wide variety of regulatory proteins. Understanding these interactions is thus critical to understanding phosphatase function. Protein phosphatase 2A (PP2A) is a multifunctional serine/threonine phosphatase that is critical to many cellular processes including development, neuronal signalling, cell cycle regulation, and viral transformation. PP2A has been implicated in Ca2+-dependent signalling pathways, but how PP2A is targeted to these pathways was not understood until striatin was found to form a stable complex with the PP2A A/C heterodimer (291). Striatin, binds to CaM in a Ca2+-dependent manner. In addition to CaM and PP2A, several other proteins stably associate with the striatin-PP2A and SG2NA-PP2A complexes. Thus, one mechanism of targeting and organizing PP2A with components of Ca2+-dependent signalling pathways may be through the molecular scaffolding proteins striatin and SG2NA (291).

Other proteins found in complexes with striatin family members include, but are not limited to, Mob3/phocein (227, 292), which is involved in vesicular trafficking (292-294); Mst3, Mst4, and STK25 (295), members of the Germinal Centre Kinase-III (GCK-III) subfamily of sterile 20-like kinases recently implicated in control of cell migration, cell cycle, Golgi assembly, and cell polarity (296-299); cerebral cavernous malformation 3 (CCM3) protein (295), which is required for stabilization of the GCK-III kinases and thus for their function (297); and striatin-interacting proteins (STRIP) 1 and 2 (295).

Considering that, in most of the described interactions, striatin functions as a chaperone protein “taking” proteins where they need to go, it was hypothesized that lower levels of striatin might influence signalling molecules that come before ERK in the pathway and, in that way, inhibit its phosphorylation, this way it would make sense that the overall phosphorylation levels in transfected cells were lower than in cells that retain all its striatin.

In order to establish that the scrambled (control) sequence did not affect the cell signalling, the short-time aldosterone treatment was repeated in cells transfected with the control duplex. Cells transfected with scrambled siRNA showed a significant increase in ERK phosphorylation levels confirming that the scrambled control sequence does not affect the way these cells signal. pERK levels were similar to what was shown previously and was abrogated by MRA.

Finally, EA.hy926 cells, transfected with striatin siRNA or controls (untransfected) were treated with aldosterone and mRNA levels of WNK4 and SGK1 measured to establish if a decrease in striatin gene expression influenced aldosterone’s known genomic responses. Results show that in both cases the genomic signalling was not affected.

The above mentioned results indicate that striatin is a necessary player in aldosterone’s nongenomic effects and in its absence (or when in reduced levels) such effects (increase in ERK phosphorylation levels at 15 minutes) do not occur. They also indicate that striatin does not seem to be necessary for the classical, genomic effects to occur, suggesting that pathways independent of striatin, are more important or that the genomic aldosterone action in these cells is less sensitive to reduced striatin levels.

Taking into account that striatin has a major role in aldosterone’s nongenomic effects via the MR and that it is know to associate with CAV_1 (190), the importance of the *caveolae* in this process was also analysed.

Interactions between MR, Striatin and CAV_1

Co-immunoprecipitation (Co-IP) was used in order to explore possible protein-protein interactions between the MR, striatin and CAV_1. If proteins interact closely, it is possible to "pull" one of these proteins down (known) and use a different antibody to detect the other protein (unknown). This would support the notion that MR, striatin and CAV_1 are involved in a reciprocal cellular mechanism.

To determine if the technique was working, striatin was targeted to be pulled down and the resulting elution studied for the presence of CAV_1 protein. Results showed an interaction between striatin and CAV_1 in MAEC, EA.hy926 cells and mouse heart tissue. The result was expected and demonstrated that the technique chosen is an efficient study tool. To prevent any possible artefacts, the reverse Co-IP was always performed and in this case, CAV_1 was shown to interact with striatin.

The next round of Co-IPs connected MR to CAV_1 and, as CAV_1 is an integral caveolar protein, the presence of MR in the *caveolae.* Results point to a close interaction between MR and CAV_1 and, potentially place MR in the *caveolae* structure located in the cell membrane. Results shown for heart tissue depict two different bands that correspond to the alpha and beta isoforms of CAV_1, known to be expressed in cardiomyocytes (266).

The next possible interaction studied was that between striatin and MR. It was already known that MR needs striatin to exert its nongenomic effects so this interaction was expected to be strong. As expected, when striatin was precipitated with A/G beads conjugated to striatin antibody, the resulting elution contained a high amount of MR, confirming the predicted interaction between the two proteins. The reverse Co-IP confirmed this interaction and showed the presence of two striatin isoforms in EA.hy926 cells.

Co-IP results show a strong interaction between MR, striatin and CAV_1 and seem to indicate the formation of a possible triple complex.

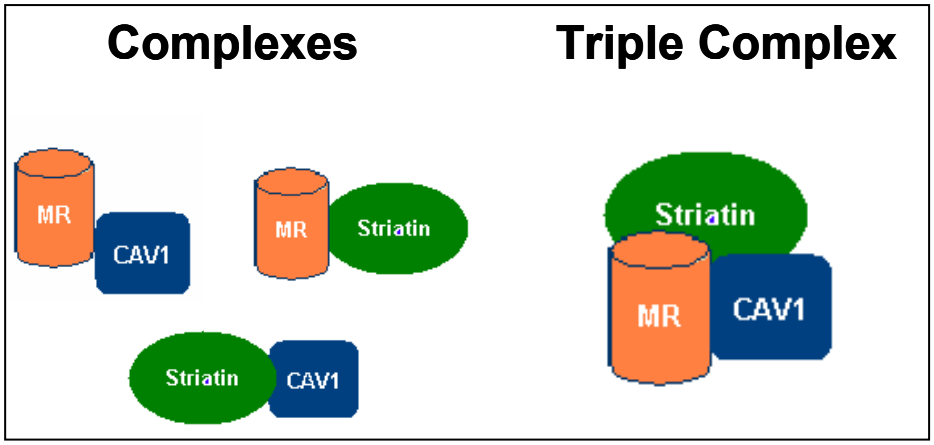

Figure 63- Individual complexes shown on the left represent the results obtained in the Co-IP studies. On the right is represented the posited, potential triple complex between MR, striatin and CAV_1.

Considering the role of CAV_1 in binding striatin protein it was proposed that caveolin could be acting as an intermediary in this complex, most likely serving as an anchor for MR in the cell membrane and keeping it in place for further interactions with other molecules, leading to rapid, nongenomic effects of MR activation. To test this hypothesis MAEC from wild-type and CAV_1 knock-out animals were used for Co-IP studies. Results showed that in the absence of CAV_1, the MR does not seem to interact with striatin or, the interaction is weakened and cannot be detected using co-immunoprecipitation techniques.

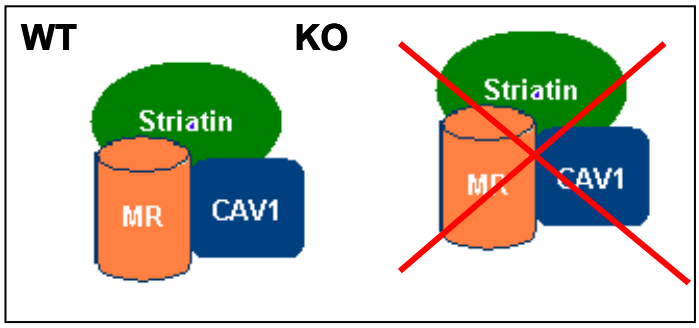

Figure 64- Diagram representing CAV_1 WT/KO MAEC Co-IP study results. In the absence of CAV_1 protein there doesn't seem to be an interaction between MR and striatin.

Such results are very important and strengthen the existence of a triple complex, with CAV_1 as the intermediary between the other the proteins. These results are consistent with *caveolae* playing a role in providing a platform for protein interactions and cell signalling to occur. To test this hypothesis, EA.hy926 cells were treated with lipid-raft disruptors, which inhibit *caveolae* formation, and subsequently stimulated with aldosterone. EA.hy926 cells were pre-incubated overnight with two lipid raft disrupting chemicals and then treated with 10nM aldosterone for 15 minutes. Results showed that aldosterone had no effect on pERK in the presence of either chemical. Results were not statistically significant but, the general trend seems to confirm that *caveolae* have a facilitating role in nongenomic aldosterone effects by providing a platform for MR to interact with other players to mediate subsequent cell signalling cascades.

Originally *caveolae* were given the exclusive electron microscopic description of membrane invaginated “smooth” vesicles of 50 to 100 nm in size (as opposed to the more electron-dense and larger “coated” vesicles- i.e., clathrin-coated pits). However, with further investigation the definition of *caveolae* has expanded to also include vesicles detached from the plasma membrane, associated in groups as grape-like clusters or rosettes, and in fused form as elongated tubules or *trans*-cellular channels (Figure 65).

The discovery of caveolin, the original member of the three-protein caveolin family, and its relationship to caveolae was converged upon by investigators from different fields with disparate research interests. In an antibody screen for tyrosine-phosphorylated substrates in Rous sarcoma virus-transformed fibroblasts, four predominant proteins were isolated (300).

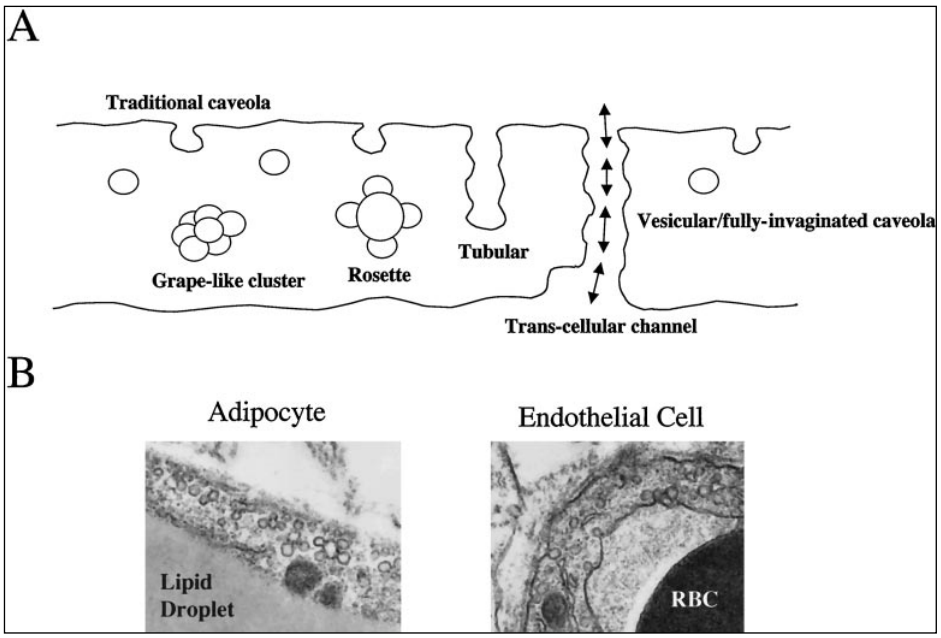

Figure 65- Different types of *caveolae* morphology (A). (B), two electron micrographs (16000x), an adipocyte (on the left) and an endothelial cell (on the right). Caveolar rosettes are frequently observed in adipoctyes, and endothelial cells are often found with caveolae in all states of membrane association- from membrane bound to fully invaginated (185).

Antibodies raised against one of the proteins showed punctuated staining on the plasma membrane (174, 300). This distribution was curiously similar to that observed for flask-shaped *caveolae* and led to experiments linking this 22-kDa protein and *caveolae* (174). *Caveolae* were shown to be composed of a series of concentric striated rings that stained with antibodies directed against the 22-kDa protein. Moreover, treatment of cells with cholesterol binding agents, led to flattening of the vesicles and dissociation of the 22-kDa protein rich striations. Because this protein was so intimately associated with the structural components of *caveolae*, it was named caveolin (174).

The subsequent cloning of the caveolin gene led to yet another surprise about the possible functions of the protein (176, 301). In an attempt to identify the cellular machinery involved in the differential sorting of vesicles to the apical or basolateral surface of polarized epithelial cells, VIP-21 (vesicular integral protein of 21 kDa) had been cloned (302). As it turned out, the caveolin sequence was identical to that of VIP-21, thereby showing that the same protein could possibly serve as a structural

component of plasma membrane caveolae, as well as have roles in oncogenesis and vesicular trafficking- all at the same time (301).

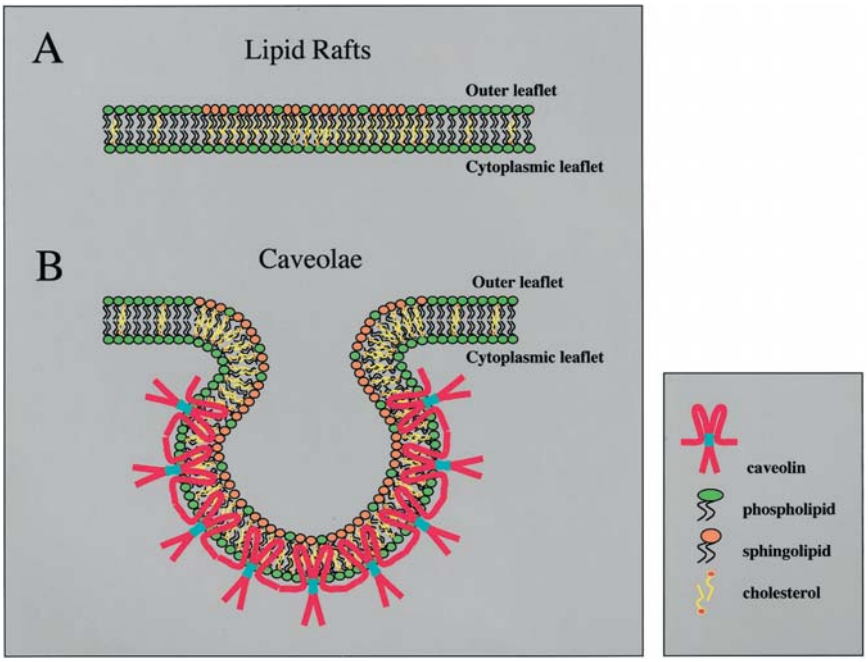

Figure 66- Detailed organization of lipid rafts and caveolae membranes. (A) lipid rafts. (B) caveolae. (185)

Caveolin-1 was not only the first protein to be localized to caveolae but due to its apparent involvement in the structural integrity of caveolae was also the first caveolar "marker protein" (174). Caveolar resident proteins were identified using sucrose gradients. Of the numerous proteins identified in this manner, it was surprising to find that a large majority were signal transduction molecules, some at concentrations manifold higher than the bulk plasma membrane (179, 303). This observation led to the "caveolae/raft signalling hypothesis": the compartmentalization of such molecules has distinct advantages as it provides a mechanism for the regulation of subsequent signalling events and explains *cross-talk* between different signalling pathways (232). Since this initial observation, an array of proteins (ranging from receptor tyrosine kinases, G-protein-coupled receptors, ion channels, adaptor proteins, and structural proteins) has now been reported to be preferentially localized to *caveolae* (185). This is a growing list but, nevertheless, it is clear that *caveolae* are involved in the compartmentalization of various signalling pathways and can be considered specialized signalling organelles.

Several lines of evidence now suggest that the caveolins might also act as scaffolding proteins by directly interacting with and modulating the activity of *caveolae*-localized signalling molecules. Residues 82-101 form a region termed the caveolin scaffolding domain (CSD) where G-proteins but also a host of other signalling proteins bind to. Caveolin-interacting molecules have caveolin binding domains (CBDs). Striatin is one of those molecules and it has been shown to modulate nongenomic actions of another steroid hormone, estrogen (188). Due to this last connection it was felt that it was necessary to investigate a possible connection between aldosterone and estrogen effects since aldosterone increases striatin levels in endothelial cells.

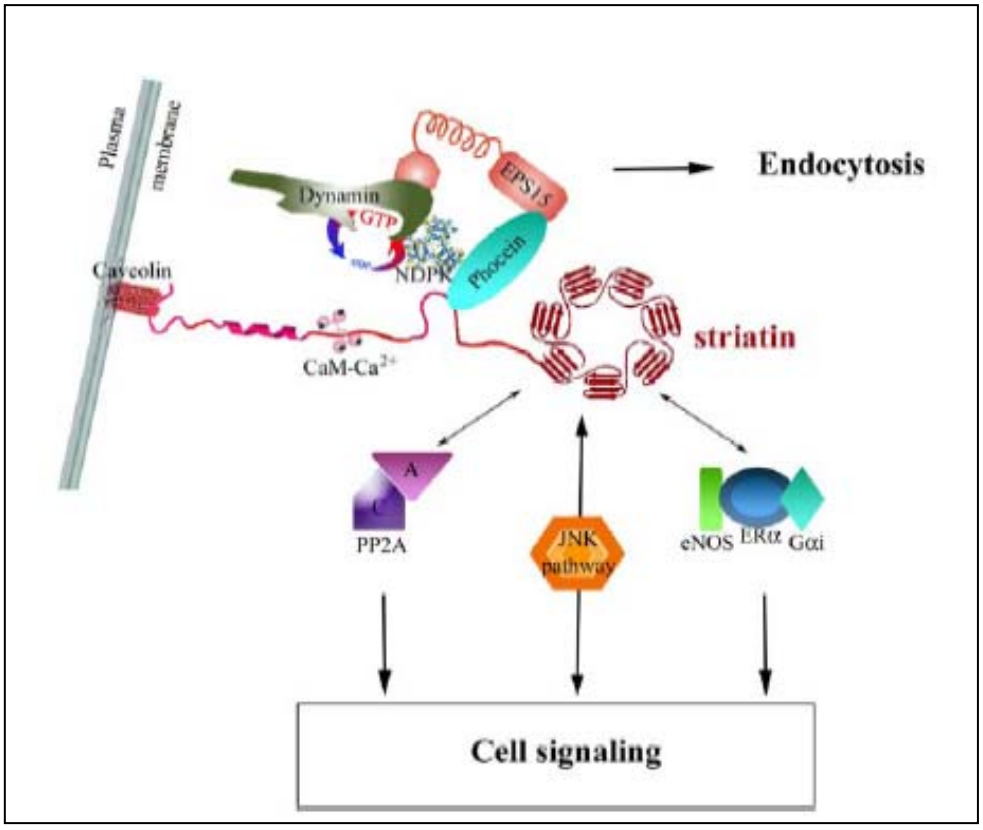

Figure 67- Diagram depicting the interaction between striatin and caveolin proteins.

Aldosterone's influence on Estrogen's nongenomic actions

Lu *et al* identified striatin as a scaffold protein that promotes localization of ERα to the plasma membrane and assembly of the signalling complex of ERα and G_i that is required for ERα-dependent activation of MAPK, phosphatidylinositol 3–Akt kinase, and eNOS, a critical regulator of many physiologic and pathophysiological processes (188). Their results show a peak in eNOS phosphorylation at 15 minutes of estrogen stimulation that is abrogated if striatin is disrupted. They also show that overexpression of striatin increases the proportion of ERα that is distributed along the plasma membrane. These results combined with the information that the binding of estrogen (E_2) to the membrane has been confirmed, in addition to the presence of ERα and caveolin in plasmalemmal caveolae and, their connection to nongenomic and short-term effect of E_2 on endothelial NO release (186) led to the possibility of a an interaction/cross-talk relationship between aldosterone and estrogen signalling in endothelial cells.

The first step taken was to ascertain if, like aldosterone, estrogen treatment stimulated the production of striatin protein. EA.hy926 cells were treated with either 10nM aldosterone or 50nM estrogen for 5 hours. Aldosterone but not estrogen treatment increases striatin protein levels. Results show that the increase in striatin protein seems to be specific to aldosterone's MR activation.

Because the experimental design used was different from aforementioned studies it was necessary to replicate the results already published. EA.hy926 cells were stimulated with estrogen (50nM) for 5, 15 and 30 minutes, with or without aldosterone (10nM) pre-treatment for 5 hours. peNOS/eNOS levels were then measured by western blot analysis. Results obtained successfully replicated the findings of Lu *et al*, exhibiting a peak in eNOS phosphorylation occurring at 15 minutes of estrogen stimulation. This peak is smaller than previously observed and the estrogen dose employed higher which can be justified by the absence of overexpression of striatin protein in the present study.

When the aldosterone pre-treatment was added to the experimental paradigm, a very interesting event occurred; there was a shift in the pattern of the peNOS

activity; peNOS levels were not only increased compared to estrogen treatment alone but it also occurred sooner.

This is a novel result and might prove to change the way steroid signalling is viewed, adding a new level of complexity concerning cross-talk between different steroid receptors and subsequent downstream signalling cascades and cellular events.

In order to confirm that this effect is dependent on striatin, EA.hy926 cells were transfected with striatin scrambled sequence or striatin siRNA. Cells were then treated with estrogen for 15 minutes with or without aldosterone pre-treatment. Results confirmed published observations and implicated striatin as a key player in estrogen signalling. Cells transfected with the scrambled sequence display a peak in peNOS levels at 15 minutes of estrogen treatment, which increases when the cells are subjected to aldosterone pre-treatment. When the cells are transfected with striatin siRNA, the response to estrogen stimulation is completely abrogated, even when pre-treatment with aldosterone is employed.

With the mounting evidence of a potential cross-talk between estrogen and aldosterone signalling pathways, it was important to study the effect of estrogen on ERK phosphorylation. Results showed that, contrary to what was observed with aldosterone, estrogen pre-treatment does not increase pERK levels in EA.hy926 cells.

Striatin siRNA did not damper the genomic effects of aldosterone stimulation but, the same had to be shown for estrogen. PTGIS, together with PTGS1 were selected as targets to study the effects of striatin knock-down on estrogen's genomic actions. PTGIS and PTGS1 expression levels were measured by Real-Time PCR in EA.hy926 cells transfected/untransfected with striatin siRNA and subsequently treated with 50nM estrogen for 15 minutes and 5 hours. Results showed that, as described in the literature, treatment with estrogen stimulated PTGIS and PTGS1 expression in the endothelial cells studied. Transfection with striatin siRNA, did not affect these genomic actions in anyway, with similar levels of mRNA observed for both untransfected and transfected cells.

In an attempt to bring the results shown close to physiological relevance, MAEC were used in repeat experiments with estrogen stimulation with/without aldosterone pre-treatment. Just as seen with EA.hy926 cells, pre-treatment with aldosterone enhanced estrogen's nongenomic response. There was a peak in eNOS phosphorylation at 15 minutes of estrogen stimulation with levels of phosphorylation very similar to previously observed for EA.hy926 cells. When an aldosterone pre-treatment was added to the treatment conditions, there was, once more, a shift in the peNOS peak observed. In the case of MAEC there was no apparent increase in peNOS levels but, the nongenomic response at 5 minutes of estrogen stimulation was confirmed.

Estrogen is a complex hormone with pleiotropic effects. Aging and estrogen loss are indelibly linked. Aging is associated with inflammation (304), with increased oxidative stress and a blunting of the protective heat shock response (305). In the cardiovascular system, aging is accompanied by increased stiffness, increased fibrosis, and loss of contractile reserve, increased ROS and endothelial dysfunction. All of these factors contribute to cardiovascular dysfunction. Estrogen, which is an antioxidant through indirect upregulation of antioxidant gene expression and increasing eNOS activity while decreasing superoxide production, is lost through menopause and may underlie such cardiovascular diseases that are often observed in postmenopausal women.

Membrane associated ERα, when bound by estrogen, can activate a signalling cascade that includes PI3K and Akt, as well as ERK 1/2, JNK and p38 (306). This signalling cascade protects the cell from injury, except for JNK, which increases apoptosis. The signalling mediated by membrane associated ERα has been termed nongenomic signalling and has recently been shown to provide cardiovascular protection without increasing uterine or breast cancer growth in mice (307). Also, without rapid signalling, this apparent protective effect is lost (308). This supports the idea that the increased risk of cancer with estrogen therapy is related to estrogen's classical nuclear effects.

These facts combined with the findings here presented could potentially lead to two very different possible biological outcomes. Based on the data generated by experimental work herein, a general signalling model can be proposed.

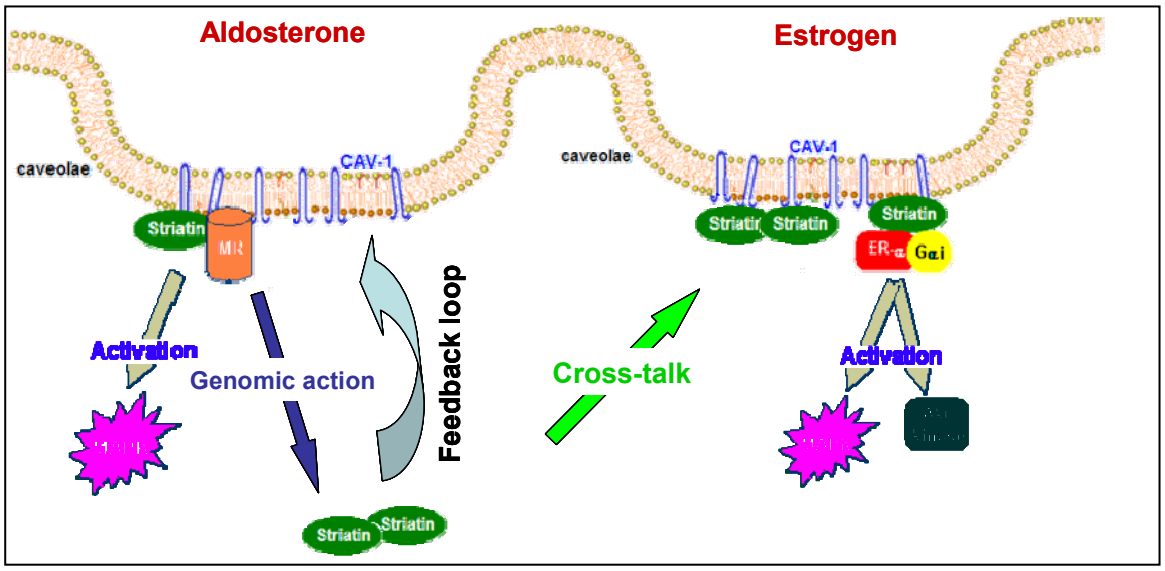

Figure 68- Diagram depicting the general conclusions drawn from the experimental studies here presented.

The left panel of the diagram shows the nongenomic and genomic actions of aldosterone that were described in this thesis. Aldosterone activates the MR that can be found at the cell membrane level in the form of a triple complex with striatin and CAV_1. MR activation for a short period of time (15 minutes) leads to the nongenomic increase in phosphorylation of ERK1/2. When MR is activated for a longer period of time (5 hours), striatin protein expression levels are increased, which constitutes a genomic effect of aldosterone action.

In the right panel the nongenomic signalling pathway for estrogen action is depicted, as previously described (188). This panel also illustrates the potential cross-talk between the two steroid hormones with the increased striatin levels brought about by aldosterone's genomic action.

MR blockade has important effects on reno-cardiovascular remodelling and fibrosis, autonomic balance, fibrinolysis, oxidative stress, and activation of proinflammatory and profibrotic pathways (309). These are the adverse effects of aldosterone action. However, a very important aspect of the "ugly" actions of aldosterone is the fact that this hormone *per se* is incapable of eliciting damage but requires a certain pathological milieu, and only when correct conditions are met (Figure 69) does this leads to pathophysiological MR activation resulting in this adverse or ugly action. In 1992, Brilla and Weber reported that in the presence of

enhanced sodium intake, but not with sodium deprivation, chronic administration of aldosterone is associated with cardiac fibrosis and hypertrophy (107). Further *in vivo* studies confirmed that the damaging effect of aldosterone in reno-cardiovascular tissue depends on a high salt diet (310-315), which could be followed by a milieu characterized in part by enhanced reactive oxygen stress (ROS) and prevented by a low salt diet (314, 316-319).

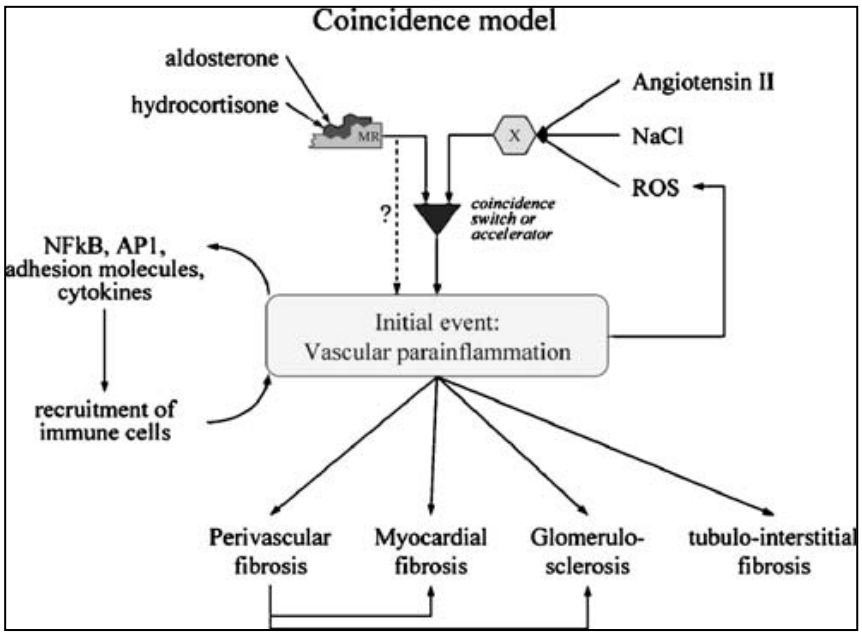

Figure 69- Hypothetical coincidence model of the signalling events, leading to damaging actions of MR-stimulation (320).

Adding this information to what has already been stated about nongenomic actions of estrogen there are two possible conclusions that can be drawn from the experimental studies herein. The first conclusion is that the cross-talk between aldosterone and estrogen, through striatin is of potential therapeutic significance, because it increases the anti-oxidative action of estrogen. This is only true when there is no evident, pre-existing, cardiovascular damage. In the case that there is already some inflammation due to age or a different initiating agent, the increase in striatin protein by aldosterone might be adverse to cardiovascular health and may preclude disease by, facilitating further MR activation, leading to more damage in the cardiovascular system.

Conclusion

Cellular responses to steroids are mediated by two general mechanisms: genomic and rapid/nongenomic effects. Identification of the mechanisms underlying aldosterone's nongenomic actions has been difficult to study and is still not clearly understood. In the presented thesis, the hypothesis that striatin is a critical intermediary of the rapid/nongenomic effects of aldosterone was explored.

In human and mouse endothelial cells, aldosterone promoted an increase in pERK that peaked at 15 minutes. Striatin was shown to be a critical mediator in this process as reducing striatin levels with siRNA technology prevented the rise in pERK levels. In contrast, reducing striatin did not significantly affect two well-characterized genomic responses to aldosterone. Down regulation of striatin with siRNA produced similar effects on estrogen's actions – reducing nongenomic, but not the genomic actions investigated and, aldosterone, but not estrogen, increased striatin levels. When endothelial cells were pre-treated with aldosterone, the rapid/nongenomic response to estrogen on peNOS/eNOS ratio was enhanced and accelerated significantly. Importantly, pre-treatment with estrogen did not enhance aldosterone's nongenomic response on pERK.

In conclusion, these results indicate that striatin is a novel mediator for both aldosterone's and estrogen's rapid and nongenomic mechanisms of action on pERK and peNOS, respectively, thereby providing evidence for a synergistic effect between the mineralocorticoid receptor and the estrogen receptor.

Multiple studies *in vivo* and *in vitro* have indicated that estrogen has the ability to either confer cardiovascular protection or increase cardiovascular risk. For example, in the Women's Health Initiative the overall findings support the concept that estrogen increases cardiovascular risk in post-menopausal females (321). However, a secondary analysis suggests that depending on the women's age, estrogen can reduce or increase cardiovascular risk (322). Since aldosterone levels also vary with age (323), the results of the present study may provide one mechanistic explanation for these findings- varying striatin levels. Thus, these results suggest a unique level of interactions between steroids on the cardiovascular system that may have broad application for the treatment of cardiovascular diseases.

Future Directions

The experimental work described in this thesis is by no means concluded and some of the conclusions described not fully investigated. Additional studies need to be performed to prove the posited triple complex and its relevance to Aldosterone/MR and estrogen/ERα signaling. The absence of an animal model lacking striatin hampers the ability to assess the physiological relevance of these findings. It has also been assumed that the mechanism observed is mediated by the classical MR since it is blocked by canrenoic acid. However, the possibility that ALDO is interacting with a recently proposed non-genomic regulator of ALDO function, GPR30 (324) cannot be excluded.

In the future, one of the most significant experiments necessary is to assess the physiological relevance of striatin by employing a striatin KO animal model (heterozygous), especially relative to salt sensitivity and aldosterone-mediated cardiovascular damage. Some experiments are already underway connected to the salt sensitivity of the blood pressure (Hight Salt vs Low Salt in the Heterozydous vs Wild Type) and results seem promising.

The physiological relevance in humans, is also to be assessed by looking at SNPs (Single Nucleotide Polymorphism) in the striatin gene, and by using the carefully phenotyped HyperPATH cohort already studied within the group.

Another interesting avenue would be the interaction between gender (i.e. estrogen) and the effects of aldosterone, which could be assessed in the animal or even humans.

Finally, other nongenomic events following aldosterone stimulation need to be clarified in order to build a clearer signalling pathway model. Akt phosphorylation is known to associate with ERK1/2 and would be a good first target.

Aknowledgements

EA.hy926 cells were kindly provided by the Tissue Culture Facility at the University of North Carolina Lineberger Comprehensive Cancer Centre. Electron microscopy was performed in the Microscopy Core of the Centre for Systems Biology/Program in Membrane Biology (Massachusetts General Hospital), which was partially supported by an Inflammatory Bowel Disease Grant DK43351 and a Boston Area Diabetes and Endocrinology Research Centre Award DK57521.

I would like to thank Doctor José Romero for the opportunity to work in a highly stimulating and competitive atmosphere such is Harvard Medical School and, for all his guidance during my doctoral work. I would also like to thank Doctor Gordon Williams for all the shared knowledge and valuable lessons in how to write papers and grants.

A big thank you for all the William's and Romero's Lab members, that taught me the experimental techniques, and helped me throughout my time there. In special: Lumi, Tham and Paul. Also Susan for all the Chinese food to keep us going!

I would also like to thank my supervisor, Professor Margarida Meireles for bearing with me and helping to expedite my thesis.

Lastly, thank you to my husband that proofread this thesis and put up with me while writing it.

Bibliography

1. 2009. *Textbook of Nephro-Endocrinology*: Elsevier. 522 pp.
2. 1989. IUPAC-IUB Joint Commission on Biochemical Nomenclature (JCBN). The nomenclature of steroids. Recommendations 1989. *Eur J Biochem* 186:429-458.
3. Gangloff, M., Ruff, M., Eiler, S., Duclaud, S., Wurtz, J.M., and Moras, D. 2001. Crystal structure of a mutant hERalpha ligand-binding domain reveals key structural features for the mechanism of partial agonism. *J Biol Chem* 276:15059-15065.
4. Shibata, H., Spencer, T.E., Onate, S.A., Jenster, G., Tsai, S.Y., Tsai, M.J., and O'Malley, B.W. 1997. Role of co-activators and co-repressors in the mechanism of steroid/thyroid receptor action. *Recent Prog Horm Res* 52:141-164; discussion 164-145.
5. Bain, D.L., Heneghan, A.F., Connaghan-Jones, K.D., and Miura, M.T. 2007. Nuclear receptor structure: implications for function. *Annu Rev Physiol* 69:201-220.
6. Aranda, A., and Pascual, A. 2001. Nuclear hormone receptors and gene expression. *Physiol Rev* 81:1269-1304.
7. Lavery, D.N., and McEwan, I.J. 2005. Structure and function of steroid receptor AF1 transactivation domains: induction of active conformations. *Biochem J* 391:449-464.
8. Germain, P., Staels, B., Dacquet, C., Spedding, M., and Laudet, V. 2006. Overview of nomenclature of nuclear receptors. *Pharmacol Rev* 58:685-704.
9. Jensen, E.V., Greene, G.L., Closs, L.E., DeSombre, E.R., and Nadji, M. 1982. Receptors reconsidered: a 20-year perspective. *Recent Prog Horm Res* 38:1-40.
10. O'Malley, B.W. 1995. Thirty years of steroid hormone action: personal recollections of an investigator. *Steroids* 60:490-498.
11. MacGregor, J.I., and Jordan, V.C. 1998. Basic guide to the mechanisms of antiestrogen action. *Pharmacol Rev* 50:151-196.
12. Notides, A., and Gorski, J. 1966. Estrogen-induced synthesis of a specific uterine protein. *Proc Natl Acad Sci U S A* 56:230-235.
13. O'Malley, B.W., and Schrader, W.T. 1972. Progesterone receptor components: identification of subunits binding to the target-cell genome. *J Steroid Biochem* 3:617-629.
14. Chang, C.H., Rowley, D.R., Lobl, T.J., and Tindall, D.J. 1982. Purification and characterization of androgen receptor from steer seminal vesicle. *Biochemistry* 21:4102-4109.
15. Chong, M.T., and Lippman, M. 1980. Purification of estrogen receptors from MCF-7 human breast cancer cells. *Cancer Res* 40:3172-3176.
16. Lazar, G., Pagano, M., and Agarwal, M.K. 1990. Purification and characterization of the activated mineralocorticoid receptor from rat myocardium. *Biochim Biophys Acta* 1033:41-48.
17. Arriza, J.L., Weinberger, C., Cerelli, G., Glaser, T.M., Handelin, B.L., Housman, D.E., and Evans, R.M. 1987. Cloning of human mineralocorticoid receptor complementary DNA: structural and functional kinship with the glucocorticoid receptor. *Science* 237:268-275.

18. O'Malley, B.W., and Tsai, M.J. 1992. Molecular pathways of steroid receptor action. *Biol Reprod* 46:163-167.

19. Metzger, D., Berry, M., Ali, S., and Chambon, P. 1995. Effect of antagonists on DNA binding properties of the human estrogen receptor in vitro and in vivo. *Mol Endocrinol* 9:579-591.

20. Joab, I., Radanyi, C., Renoir, M., Buchou, T., Catelli, M.G., Binart, N., Mester, J., and Baulieu, E.E. 1984. Common non-hormone binding component in non-transformed chick oviduct receptors of four steroid hormones. *Nature* 308:850-853.

21. Sanchez, E.R., Toft, D.O., Schlesinger, M.J., and Pratt, W.B. 1985. Evidence that the 90-kDa phosphoprotein associated with the untransformed L-cell glucocorticoid receptor is a murine heat shock protein. *J Biol Chem* 260:12398-12401.

22. Jensen, E.V. 1996. Steroid hormones, receptors, and antagonists. *Ann N Y Acad Sci* 784:1-17.

23. Brinkmann, A.O. 1994. Steroid hormone receptors: activators of gene transcription. *J Pediatr Endocrinol* 7:275-282.

24. Sanchez, E.R., Meshinchi, S., Tienrungroj, W., Schlesinger, M.J., Toft, D.O., and Pratt, W.B. 1987. Relationship of the 90-kDa murine heat shock protein to the untransformed and transformed states of the L cell glucocorticoid receptor. *J Biol Chem* 262:6986-6991.

25. Savouret, J.F., Chauchereau, A., Misrahi, M., Lescop, P., Mantel, A., Bailly, A., and Milgrom, E. 1994. The progesterone receptor. Biological effects of progestins and antiprogestins. *Hum Reprod* 9 Suppl 1:7-11.

26. Giangrande, P.H., Kimbrel, E.A., Edwards, D.P., and McDonnell, D.P. 2000. The opposing transcriptional activities of the two isoforms of the human progesterone receptor are due to differential cofactor binding. *Mol Cell Biol* 20:3102-3115.

27. Graham, J.D., Bain, D.L., Richer, J.K., Jackson, T.A., Tung, L., and Horwitz, K.B. 2000. Nuclear receptor conformation, coregulators, and tamoxifen-resistant breast cancer. *Steroids* 65:579-584.

28. Simpson, S.A., Tait, J.F., Wettstein, A., Neher, R., Von Euw, J., and Reichstein, T. 1953. [Isolation from the adrenals of a new crystalline hormone with especially high effectiveness on mineral metabolism]. *Experientia* 9:333-335.

29. Watson, J.D., and Crick, F.H. 1953. Molecular structure of nucleic acids; a structure for deoxyribose nucleic acid. *Nature* 171:737-738.

30. Feldman, D., Funder, J.W., and Edelman, I.S. 1972. Subcellular mechanisms in the action of adrenal steroids. *Am J Med* 53:545-560.

31. Fuller, P.J., and Funder, J.W. 1976. Mineralocorticoid and glucocorticoid receptors in human kidney. *Kidney Int* 10:154-157.

32. Liu, W., Wang, J., Sauter, N.K., and Pearce, D. 1995. Steroid receptor heterodimerization demonstrated in vitro and in vivo. *Proc Natl Acad Sci U S A* 92:12480-12484.

33. Liu, W., Wang, J., Yu, G., and Pearce, D. 1996. Steroid receptor transcriptional synergy is potentiated by disruption of the DNA-binding domain dimer interface. *Mol Endocrinol* 10:1399-1406.

34. Tsai, M.J., and O'Malley, B.W. 1994. Molecular mechanisms of action of steroid/thyroid receptor superfamily members. *Annu Rev Biochem* 63:451-486.

35. Krozowski, Z.S., and Funder, J.W. 1983. Renal mineralocorticoid receptors and hippocampal corticosterone-binding species have identical intrinsic steroid specificity. *Proc Natl Acad Sci U S A* 80:6056-6060.

36. White, P.C., Mune, T., and Agarwal, A.K. 1997. 11 beta-Hydroxysteroid dehydrogenase and the syndrome of apparent mineralocorticoid excess. *Endocr Rev* 18:135-156.

37. Rogerson, F.M., Dimopoulos, N., Sluka, P., Chu, S., Curtis, A.J., and Fuller, P.J. 1999. Structural determinants of aldosterone binding selectivity in the mineralocorticoid receptor. *J Biol Chem* 274:36305-36311.

38. Rogerson, F.M., Brennan, F.E., and Fuller, P.J. 2004. Mineralocorticoid receptor binding, structure and function. *Mol Cell Endocrinol* 217:203-212.

39. Williams, S.P., and Sigler, P.B. 1998. Atomic structure of progesterone complexed with its receptor. *Nature* 393:392-396.

40. Sack, J.S., Kish, K.F., Wang, C., Attar, R.M., Kiefer, S.E., An, Y., Wu, G.Y., Scheffler, J.E., Salvati, M.E., Krystek, S.R., Jr., et al. 2001. Crystallographic structures of the ligand-binding domains of the androgen receptor and its T877A mutant complexed with the natural agonist dihydrotestosterone. *Proc Natl Acad Sci U S A* 98:4904-4909.

41. Bledsoe, R.K., Montana, V.G., Stanley, T.B., Delves, C.J., Apolito, C.J., McKee, D.D., Consler, T.G., Parks, D.J., Stewart, E.L., Willson, T.M., et al. 2002. Crystal structure of the glucocorticoid receptor ligand binding domain reveals a novel mode of receptor dimerization and coactivator recognition. *Cell* 110:93-105.

42. Kauppi, B., Jakob, C., Farnegardh, M., Yang, J., Ahola, H., Alarcon, M., Calles, K., Engstrom, O., Harlan, J., Muchmore, S., et al. 2003. The three-dimensional structures of antagonistic and agonistic forms of the glucocorticoid receptor ligand-binding domain: RU-486 induces a transconformation that leads to active antagonism. *J Biol Chem* 278:22748-22754.

43. Morrison, N., Harrap, S.B., Arriza, J.L., Boyd, E., and Connor, J.M. 1990. Regional chromosomal assignment of the human mineralocorticoid receptor gene to 4q31.1. *Hum Genet* 85:130-132.

44. Bloem, L.J., Guo, C., and Pratt, J.H. 1995. Identification of a splice variant of the rat and human mineralocorticoid receptor genes. *J Steroid Biochem Mol Biol* 55:159-162.

45. Zennaro, M.C., Keightley, M.C., Kotelevtsev, Y., Conway, G.S., Soubrier, F., and Fuller, P.J. 1995. Human mineralocorticoid receptor genomic structure and identification of expressed isoforms. *J Biol Chem* 270:21016-21020.

46. Kwak, S.P., Patel, P.D., Thompson, R.C., Akil, H., and Watson, S.J. 1993. 5'-Heterogeneity of the mineralocorticoid receptor messenger ribonucleic acid: differential expression and regulation of splice variants within the rat hippocampus. *Endocrinology* 133:2344-2350.

47. Zennaro, M.C., Farman, N., Bonvalet, J.P., and Lombes, M. 1997. Tissue-specific expression of alpha and beta messenger ribonucleic acid isoforms of the human mineralocorticoid receptor in normal and pathological states. *J Clin Endocrinol Metab* 82:1345-1352.

48. Wickert, L., Watzka, M., Bolkenius, U., Bidlingmaier, F., and Ludwig, M. 1998. Mineralocorticoid receptor splice variants in different human tissues. *Eur J Endocrinol* 138:702-704.

49. Wickert, L., and Selbig, J. 2002. Structural analysis of the DNA-binding domain of alternatively spliced steroid receptors. *J Endocrinol* 173:429-436.

50. Wickert, L., Selbig, J., Watzka, M., Stoffel-Wagner, B., Schramm, J., Bidlingmaier, F., and Ludwig, M. 2000. Differential mRNA expression of the two mineralocorticoid receptor splice variants within the human brain: structure analysis of their different DNA binding domains. *J Neuroendocrinol* 12:867-873.

51. Zhou, M.Y., Gomez-Sanchez, C.E., and Gomez-Sanchez, E.P. 2000. An alternatively spliced rat mineralocorticoid receptor mRNA causing truncation of the steroid binding domain. *Mol Cell Endocrinol* 159:125-131.

52. Zennaro, M.C., Souque, A., Viengchareun, S., Poisson, E., and Lombes, M. 2001. A new human MR splice variant is a ligand-independent transactivator modulating corticosteroid action. *Mol Endocrinol* 15:1586-1598.

53. Alnemri, E.S., Maksymowych, A.B., Robertson, N.M., and Litwack, G. 1991. Overexpression and characterization of the human mineralocorticoid receptor. *J Biol Chem* 266:18072-18081.

54. Galigniana, M.D. 1998. Native rat kidney mineralocorticoid receptor is a phosphoprotein whose transformation to a DNA-binding form is induced by phosphatases. *Biochem J* 333 (Pt 3):555-563.

55. Piwien-Pilipuk, G., and Galigniana, M.D. 1998. Tautomycin inhibits phosphatase-dependent transformation of the rat kidney mineralocorticoid receptor. *Mol Cell Endocrinol* 144:119-130.

56. Le Moellic, C., Ouvrard-Pascaud, A., Capurro, C., Cluzeaud, F., Fay, M., Jaisser, F., Farman, N., and Blot-Chabaud, M. 2004. Early nongenomic events in aldosterone action in renal collecting duct cells: PKCalpha activation, mineralocorticoid receptor phosphorylation, and cross-talk with the genomic response. *J Am Soc Nephrol* 15:1145-1160.

57. Massaad, C., Houard, N., Lombes, M., and Barouki, R. 1999. Modulation of human mineralocorticoid receptor function by protein kinase A. *Mol Endocrinol* 13:57-65.

58. Mihailidou, A.S., Mardini, M., and Funder, J.W. 2004. Rapid, nongenomic effects of aldosterone in the heart mediated by epsilon protein kinase C. *Endocrinology* 145:773-780.

59. Poukka, H., Karvonen, U., Janne, O.A., and Palvimo, J.J. 2000. Covalent modification of the androgen receptor by small ubiquitin-like modifier 1 (SUMO-1). *Proc Natl Acad Sci U S A* 97:14145-14150.

60. Tian, S., Poukka, H., Palvimo, J.J., and Janne, O.A. 2002. Small ubiquitin-related modifier-1 (SUMO-1) modification of the glucocorticoid receptor. *Biochem J* 367:907-911.

61. Chauchereau, A., Amazit, L., Quesne, M., Guiochon-Mantel, A., and Milgrom, E. 2003. Sumoylation of the progesterone receptor and of the steroid receptor coactivator SRC-1. *J Biol Chem* 278:12335-12343.

62. Tirard, M., Almeida, O.F., Hutzler, P., Melchior, F., and Michaelidis, T.M. 2007. Sumoylation and proteasomal activity determine the transactivation properties of the mineralocorticoid receptor. *Mol Cell Endocrinol* 268:20-29.

63. Pascual-Le Tallec, L., Simone, F., Viengchareun, S., Meduri, G., Thirman, M.J., and Lombes, M. 2005. The elongation factor ELL (eleven-nineteen lysine-rich leukemia) is a selective coregulator for steroid receptor functions. *Mol Endocrinol* 19:1158-1169.

64. Silverstein, A.M., Galigniana, M.D., Kanelakis, K.C., Radanyi, C., Renoir, J.M., and Pratt, W.B. 1999. Different regions of the immunophilin FKBP52 determine its

association with the glucocorticoid receptor, hsp90, and cytoplasmic dynein. *J Biol Chem* 274:36980-36986.

65. Galat, A. 2003. Peptidylprolyl cis/trans isomerases (immunophilins): biological diversity--targets--functions. *Curr Top Med Chem* 3:1315-1347.

66. Dahmer, M.K., Housley, P.R., and Pratt, W.B. 1984. Effects of molybdate and endogenous inhibitors on steroid-receptor inactivation, transformation, and translocation. *Annu Rev Physiol* 46:67-81.

67. Rousseau, G.G. 1984. Structure and regulation of the glucocorticoid hormone receptor. *Mol Cell Endocrinol* 38:1-11.

68. Galigniana, M.D., Radanyi, C., Renoir, J.M., Housley, P.R., and Pratt, W.B. 2001. Evidence that the peptidylprolyl isomerase domain of the hsp90-binding immunophilin FKBP52 is involved in both dynein interaction and glucocorticoid receptor movement to the nucleus. *J Biol Chem* 276:14884-14889.

69. Piwien Pilipuk, G., Vinson, G.P., Sanchez, C.G., and Galigniana, M.D. 2007. Evidence for NL1-independent nuclear translocation of the mineralocorticoid receptor. *Biochemistry* 46:1389-1397.

70. Galigniana, M.D., Harrell, J.M., Murphy, P.J., Chinkers, M., Radanyi, C., Renoir, J.M., Zhang, M., and Pratt, W.B. 2002. Binding of hsp90-associated immunophilins to cytoplasmic dynein: direct binding and in vivo evidence that the peptidylprolyl isomerase domain is a dynein interaction domain. *Biochemistry* 41:13602-13610.

71. Rogerson, F.M., and Fuller, P.J. 2000. Mineralocorticoid action. *Steroids* 65:61-73.

72. Wilson, F.H., Disse-Nicodeme, S., Choate, K.A., Ishikawa, K., Nelson-Williams, C., Desitter, I., Gunel, M., Milford, D.V., Lipkin, G.W., Achard, J.M., et al. 2001. Human hypertension caused by mutations in WNK kinases. *Science* 293:1107-1112.

73. Chen, S.Y., Bhargava, A., Mastroberardino, L., Meijer, O.C., Wang, J., Buse, P., Firestone, G.L., Verrey, F., and Pearce, D. 1999. Epithelial sodium channel regulated by aldosterone-induced protein sgk. *Proc Natl Acad Sci U S A* 96:2514-2519.

74. Alvarez de la Rosa, D., Zhang, P., Naray-Fejes-Toth, A., Fejes-Toth, G., and Canessa, C.M. 1999. The serum and glucocorticoid kinase sgk increases the abundance of epithelial sodium channels in the plasma membrane of Xenopus oocytes. *J Biol Chem* 274:37834-37839.

75. Snyder, P.M. 2002. The epithelial Na+ channel: cell surface insertion and retrieval in Na+ homeostasis and hypertension. *Endocr Rev* 23:258-275.

76. Muller, O.G., Parnova, R.G., Centeno, G., Rossier, B.C., Firsov, D., and Horisberger, J.D. 2003. Mineralocorticoid effects in the kidney: correlation between alphaENaC, GILZ, and Sgk-1 mRNA expression and urinary excretion of Na+ and K+. *J Am Soc Nephrol* 14:1107-1115.

77. Masilamani, S., Kim, G.H., Mitchell, C., Wade, J.B., and Knepper, M.A. 1999. Aldosterone-mediated regulation of ENaC alpha, beta, and gamma subunit proteins in rat kidney. *J Clin Invest* 104:R19-23.

78. Garty, H., and Palmer, L.G. 1997. Epithelial sodium channels: function, structure, and regulation. *Physiol Rev* 77:359-396.

79. Naray-Fejes-Toth, A., Canessa, C., Cleaveland, E.S., Aldrich, G., and Fejes-Toth, G. 1999. sgk is an aldosterone-induced kinase in the renal collecting duct. Effects on epithelial na+ channels. *J Biol Chem* 274:16973-16978.

80. Escoubet, B., Coureau, C., Bonvalet, J.P., and Farman, N. 1997. Noncoordinate regulation of epithelial Na channel and Na pump subunit mRNAs in kidney and colon by aldosterone. *Am J Physiol* 272:C1482-1491.

81. Cherradi, N., Brandenburger, Y., and Capponi, A.M. 1998. Mitochondrial regulation of mineralocorticoid biosynthesis by calcium and the StAR protein. *Eur J Endocrinol* 139:249-256.

82. Bassett, M.H., White, P.C., and Rainey, W.E. 2004. The regulation of aldosterone synthase expression. *Mol Cell Endocrinol* 217:67-74.

83. Barrett, P.Q., Bollag, W.B., Isales, C.M., McCarthy, R.T., and Rasmussen, H. 1989. Role of calcium in angiotensin II-mediated aldosterone secretion. *Endocr Rev* 10:496-518.

84. Kojima, I., Kojima, K., Kreutter, D., and Rasmussen, H. 1984. The temporal integration of the aldosterone secretory response to angiotensin occurs via two intracellular pathways. *J Biol Chem* 259:14448-14457.

85. Natarajan, R., Stern, N., Hsueh, W., Do, Y., and Nadler, J. 1988. Role of the lipoxygenase pathway in angiotensin II-mediated aldosterone biosynthesis in human adrenal glomerulosa cells. *J Clin Endocrinol Metab* 67:584-591.

86. Miller, W.L. 2007. StAR search--what we know about how the steroidogenic acute regulatory protein mediates mitochondrial cholesterol import. *Mol Endocrinol* 21:589-601.

87. Adler, G.K., Chen, R., Menachery, A.I., Braley, L.M., and Williams, G.H. 1993. Sodium restriction increases aldosterone biosynthesis by increasing late pathway, but not early pathway, messenger ribonucleic acid levels and enzyme activity in normotensive rats. *Endocrinology* 133:2235-2240.

88. Tremblay, A., Parker, K.L., and Lehoux, J.G. 1992. Dietary potassium supplementation and sodium restriction stimulate aldosterone synthase but not 11 beta-hydroxylase P-450 messenger ribonucleic acid accumulation in rat adrenals and require angiotensin II production. *Endocrinology* 130:3152-3158.

89. Clyne, C.D., Zhang, Y., Slutsker, L., Mathis, J.M., White, P.C., and Rainey, W.E. 1997. Angiotensin II and potassium regulate human CYP11B2 transcription through common cis-elements. *Mol Endocrinol* 11:638-649.

90. Bassett, M.H., Zhang, Y., White, P.C., and Rainey, W.E. 2000. Regulation of human CYP11B2 and CYP11B1: comparing the role of the common CRE/Ad1 element. *Endocr Res* 26:941-951.

91. Romero, D.G., Plonczynski, M.W., Gomez-Sanchez, E.P., Yanes, L.L., and Gomez-Sanchez, C.E. 2006. RGS2 is regulated by angiotensin II and functions as a negative feedback of aldosterone production in H295R human adrenocortical cells. *Endocrinology* 147:3889-3897.

92. Johannessen, M., Delghandi, M.P., Rykx, A., Dragset, M., Vandenheede, J.R., Van Lint, J., and Moens, U. 2007. Protein kinase D induces transcription through direct phosphorylation of the cAMP-response element-binding protein. *J Biol Chem* 282:14777-14787.

93. Johannessen, M., and Moens, U. 2007. Multisite phosphorylation of the cAMP response element-binding protein (CREB) by a diversity of protein kinases. *Front Biosci* 12:1814-1832.

94. Ganguly, A., and Davis, J.S. 1994. Role of calcium and other mediators in aldosterone secretion from the adrenal glomerulosa cells. *Pharmacol Rev* 46:417-447.

95. Pearce, D., Bhargava, A., and Cole, T.J. 2003. Aldosterone: its receptor, target genes, and actions. *Vitam Horm* 66:29-76.

96. Verrey, F. 1999. Early aldosterone action: toward filling the gap between transcription and transport. *Am J Physiol* 277:F319-327.

97. Stokes, J.B., and Sigmund, R.D. 1998. Regulation of rENaC mRNA by dietary NaCl and steroids: organ, tissue, and steroid heterogeneity. *Am J Physiol* 274:C1699-1707.

98. Boldyreff, B., and Wehling, M. 2003. Non-genomic actions of aldosterone: mechanisms and consequences in kidney cells. *Nephrol Dial Transplant* 18:1693-1695.

99. Koppel, H., Christ, M., Yard, B.A., Bar, P.C., van der Woude, F.J., and Wehling, M. 2003. Nongenomic effects of aldosterone on human renal cells. *J Clin Endocrinol Metab* 88:1297-1302.

100. Losel, R.M., Falkenstein, E., Feuring, M., Schultz, A., Tillmann, H.C., Rossol-Haseroth, K., and Wehling, M. 2003. Nongenomic steroid action: controversies, questions, and answers. *Physiol Rev* 83:965-1016.

101. Gekle, M., Golenhofen, N., Oberleithner, H., and Silbernagl, S. 1996. Rapid activation of Na+/H+ exchange by aldosterone in renal epithelial cells requires Ca2+ and stimulation of a plasma membrane proton conductance. *Proc Natl Acad Sci U S A* 93:10500-10504.

102. Gekle, M., Silbernagl, S., and Oberleithner, H. 1997. The mineralocorticoid aldosterone activates a proton conductance in cultured kidney cells. *Am J Physiol* 273:C1673-1678.

103. Pitt, B., Zannad, F., Remme, W.J., Cody, R., Castaigne, A., Perez, A., Palensky, J., and Wittes, J. 1999. The effect of spironolactone on morbidity and mortality in patients with severe heart failure. Randomized Aldactone Evaluation Study Investigators. *N Engl J Med* 341:709-717.

104. Pitt, B., Remme, W., Zannad, F., Neaton, J., Martinez, F., Roniker, B., Bittman, R., Hurley, S., Kleiman, J., and Gatlin, M. 2003. Eplerenone, a selective aldosterone blocker, in patients with left ventricular dysfunction after myocardial infarction. *N Engl J Med* 348:1309-1321.

105. Grandi, A.M., Imperiale, D., Santillo, R., Barlocco, E., Bertolini, A., Guasti, L., and Venco, A. 2002. Aldosterone antagonist improves diastolic function in essential hypertension. *Hypertension* 40:647-652.

106. Izawa, H., Murohara, T., Nagata, K., Isobe, S., Asano, H., Amano, T., Ichihara, S., Kato, T., Ohshima, S., Murase, Y., et al. 2005. Mineralocorticoid receptor antagonism ameliorates left ventricular diastolic dysfunction and myocardial fibrosis in mildly symptomatic patients with idiopathic dilated cardiomyopathy: a pilot study. *Circulation* 112:2940-2945.

107. Brilla, C.G., and Weber, K.T. 1992. Mineralocorticoid excess, dietary sodium, and myocardial fibrosis. *J Lab Clin Med* 120:893-901.

108. Young, M., Fullerton, M., Dilley, R., and Funder, J. 1994. Mineralocorticoids, hypertension, and cardiac fibrosis. *J Clin Invest* 93:2578-2583.

109. Oestreicher, E.M., Martinez-Vasquez, D., Stone, J.R., Jonasson, L., Roubsanthisuk, W., Mukasa, K., and Adler, G.K. 2003. Aldosterone and not plasminogen activator inhibitor-1 is a critical mediator of early angiotensin II/NG-nitro-L-arginine methyl ester-induced myocardial injury. *Circulation* 108:2517-2523.

110. Rocha, R., Stier, C.T., Jr., Kifor, I., Ochoa-Maya, M.R., Rennke, H.G., Williams, G.H., and Adler, G.K. 2000. Aldosterone: a mediator of myocardial necrosis and renal arteriopathy. *Endocrinology* 141:3871-3878.

111. Rocha, R., Rudolph, A.E., Frierdich, G.E., Nachowiak, D.A., Kekec, B.K., Blomme, E.A., McMahon, E.G., and Delyani, J.A. 2002. Aldosterone induces a vascular inflammatory phenotype in the rat heart. *Am J Physiol Heart Circ Physiol* 283:H1802-1810.

112. Young, M.J., Moussa, L., Dilley, R., and Funder, J.W. 2003. Early inflammatory responses in experimental cardiac hypertrophy and fibrosis: effects of 11 beta-hydroxysteroid dehydrogenase inactivation. *Endocrinology* 144:1121-1125.

113. White, W.B., Duprez, D., St Hillaire, R., Krause, S., Roniker, B., Kuse-Hamilton, J., and Weber, M.A. 2003. Effects of the selective aldosterone blocker eplerenone versus the calcium antagonist amlodipine in systolic hypertension. *Hypertension* 41:1021-1026.

114. Williams, G.H., Burgess, E., Kolloch, R.E., Ruilope, L.M., Niegowska, J., Kipnes, M.S., Roniker, B., Patrick, J.L., and Krause, S.L. 2004. Efficacy of eplerenone versus enalapril as monotherapy in systemic hypertension. *Am J Cardiol* 93:990-996.

115. Quinkler, M., Zehnder, D., Eardley, K.S., Lepenies, J., Howie, A.J., Hughes, S.V., Cockwell, P., Hewison, M., and Stewart, P.M. 2005. Increased expression of mineralocorticoid effector mechanisms in kidney biopsies of patients with heavy proteinuria. *Circulation* 112:1435-1443.

116. Rocha, R., Chander, P.N., Khanna, K., Zuckerman, A., and Stier, C.T., Jr. 1998. Mineralocorticoid blockade reduces vascular injury in stroke-prone hypertensive rats. *Hypertension* 31:451-458.

117. Grossmann, C., Benesic, A., Krug, A.W., Freudinger, R., Mildenberger, S., Gassner, B., and Gekle, M. 2005. Human mineralocorticoid receptor expression renders cells responsive for nongenotropic aldosterone actions. *Mol Endocrinol* 19:1697-1710.

118. Grossmann, C., Krug, A.W., Freudinger, R., Mildenberger, S., Voelker, K., and Gekle, M. 2007. Aldosterone-induced EGFR expression: interaction between the human mineralocorticoid receptor and the human EGFR promoter. *Am J Physiol Endocrinol Metab* 292:E1790-1800.

119. Grossmann, C., Freudinger, R., Mildenberger, S., Husse, B., and Gekle, M. 2008. EF domains are sufficient for nongenomic mineralocorticoid receptor actions. *J Biol Chem* 283:7109-7116.

120. Min, L.J., Mogi, M., Li, J.M., Iwanami, J., Iwai, M., and Horiuchi, M. 2005. Aldosterone and angiotensin II synergistically induce mitogenic response in vascular smooth muscle cells. *Circ Res* 97:434-442.

121. Callera, G.E., Touyz, R.M., Tostes, R.C., Yogi, A., He, Y., Malkinson, S., and Schiffrin, E.L. 2005. Aldosterone activates vascular p38MAP kinase and NADPH oxidase via c-Src. *Hypertension* 45:773-779.

122. Iwashima, F., Yoshimoto, T., Minami, I., Sakurada, M., Hirono, Y., and Hirata, Y. 2008. Aldosterone induces superoxide generation via Rac1 activation in endothelial cells. *Endocrinology* 149:1009-1014.

123. Michea, L., Delpiano, A.M., Hitschfeld, C., Lobos, L., Lavandero, S., and Marusic, E.T. 2005. Eplerenone blocks nongenomic effects of aldosterone on the Na+/H+ exchanger, intracellular Ca2+ levels, and vasoconstriction in mesenteric resistance vessels. *Endocrinology* 146:973-980.

124. Arima, S., Kohagura, K., Xu, H.L., Sugawara, A., Uruno, A., Satoh, F., Takeuchi, K., and Ito, S. 2004. Endothelium-derived nitric oxide modulates vascular action of aldosterone in renal arteriole. *Hypertension* 43:352-357.

125. Liu, S.L., Schmuck, S., Chorazcyzewski, J.Z., Gros, R., and Feldman, R.D. 2003. Aldosterone regulates vascular reactivity: short-term effects mediated by phosphatidylinositol 3-kinase-dependent nitric oxide synthase activation. *Circulation* 108:2400-2406.

126. Nagata, D., Takahashi, M., Sawai, K., Tagami, T., Usui, T., Shimatsu, A., Hirata, Y., and Naruse, M. 2006. Molecular mechanism of the inhibitory effect of aldosterone on endothelial NO synthase activity. *Hypertension* 48:165-171.

127. Leopold, J.A., Dam, A., Maron, B.A., Scribner, A.W., Liao, R., Handy, D.E., Stanton, R.C., Pitt, B., and Loscalzo, J. 2007. Aldosterone impairs vascular reactivity by decreasing glucose-6-phosphate dehydrogenase activity. *Nat Med* 13:189-197.

128. Jaffe, I.Z., and Mendelsohn, M.E. 2005. Angiotensin II and aldosterone regulate gene transcription via functional mineralocortocoid receptors in human coronary artery smooth muscle cells. *Circ Res* 96:643-650.

129. Han, K.H., Kang, Y.S., Han, S.Y., Jee, Y.H., Lee, M.H., Han, J.Y., Kim, H.K., Kim, Y.S., and Cha, D.R. 2006. Spironolactone ameliorates renal injury and connective tissue growth factor expression in type II diabetic rats. *Kidney Int* 70:111-120.

130. Han, S.Y., Kim, C.H., Kim, H.S., Jee, Y.H., Song, H.K., Lee, M.H., Han, K.H., Kim, H.K., Kang, Y.S., Han, J.Y., et al. 2006. Spironolactone prevents diabetic nephropathy through an anti-inflammatory mechanism in type 2 diabetic rats. *J Am Soc Nephrol* 17:1362-1372.

131. Guo, C., Ricchiuti, V., Lian, B.Q., Yao, T.M., Coutinho, P., Romero, J.R., Li, J., Williams, G.H., and Adler, G.K. 2008. Mineralocorticoid receptor blockade reverses obesity-related changes in expression of adiponectin, peroxisome proliferator-activated receptor-gamma, and proinflammatory adipokines. *Circulation* 117:2253-2261.

132. Kraus, D., Jager, J., Meier, B., Fasshauer, M., and Klein, J. 2005. Aldosterone inhibits uncoupling protein-1, induces insulin resistance, and stimulates proinflammatory adipokines in adipocytes. *Horm Metab Res* 37:455-459.

133. Luther, J.M., Gainer, J.V., Murphey, L.J., Yu, C., Vaughan, D.E., Morrow, J.D., and Brown, N.J. 2006. Angiotensin II induces interleukin-6 in humans through a mineralocorticoid receptor-dependent mechanism. *Hypertension* 48:1050-1057.

134. Hiramatsu, K., Yamada, T., Ichikawa, K., Izumiyama, T., and Nagata, H. 1981. Changes in endocrine activities relative to obesity in patients with essential hypertension. *J Am Geriatr Soc* 29:25-30.

135. Goodfriend, T.L., Egan, B., Stepniakowski, K., and Ball, D.L. 1995. Relationships among plasma aldosterone, high-density lipoprotein cholesterol, and insulin in humans. *Hypertension* 25:30-36.

136. Ehrhart-Bornstein, M., Lamounier-Zepter, V., Schraven, A., Langenbach, J., Willenberg, H.S., Barthel, A., Hauner, H., McCann, S.M., Scherbaum, W.A., and

Bornstein, S.R. 2003. Human adipocytes secrete mineralocorticoid-releasing factors. *Proc Natl Acad Sci U S A* 100:14211-14216.

137. Goodfriend, T.L., Egan, B.M., and Kelley, D.E. 1998. Aldosterone in obesity. *Endocr Res* 24:789-796.

138. Caprio, M., Feve, B., Claes, A., Viengchareun, S., Lombes, M., and Zennaro, M.C. 2007. Pivotal role of the mineralocorticoid receptor in corticosteroid-induced adipogenesis. *Faseb J* 21:2185-2194.

139. Hitomi, H., Kiyomoto, H., Nishiyama, A., Hara, T., Moriwaki, K., Kaifu, K., Ihara, G., Fujita, Y., Ugawa, T., and Kohno, M. 2007. Aldosterone suppresses insulin signaling via the downregulation of insulin receptor substrate-1 in vascular smooth muscle cells. *Hypertension* 50:750-755.

140. Martinez, D.V., Rocha, R., Matsumura, M., Oestreicher, E., Ochoa-Maya, M., Roubsanthisuk, W., Williams, G.H., and Adler, G.K. 2002. Cardiac damage prevention by eplerenone: comparison with low sodium diet or potassium loading. *Hypertension* 39:614-618.

141. Young, M., Head, G., and Funder, J. 1995. Determinants of cardiac fibrosis in experimental hypermineralocorticoid states. *Am J Physiol* 269:E657-662.

142. Greene, G.L., Gilna, P., Waterfield, M., Baker, A., Hort, Y., and Shine, J. 1986. Sequence and expression of human estrogen receptor complementary DNA. *Science* 231:1150-1154.

143. Gosden, J.R., Middleton, P.G., and Rout, D. 1986. Localization of the human oestrogen receptor gene to chromosome 6q24----q27 by in situ hybridization. *Cytogenet Cell Genet* 43:218-220.

144. Lubahn, D.B., Moyer, J.S., Golding, T.S., Couse, J.F., Korach, K.S., and Smithies, O. 1993. Alteration of reproductive function but not prenatal sexual development after insertional disruption of the mouse estrogen receptor gene. *Proc Natl Acad Sci U S A* 90:11162-11166.

145. Kuiper, G.G., Enmark, E., Pelto-Huikko, M., Nilsson, S., and Gustafsson, J.A. 1996. Cloning of a novel receptor expressed in rat prostate and ovary. *Proc Natl Acad Sci U S A* 93:5925-5930.

146. Jordan, V.C. 2007. Chemoprevention of breast cancer with selective oestrogen-receptor modulators. *Nat Rev Cancer* 7:46-53.

147. Hall, J.M., and McDonnell, D.P. 1999. The estrogen receptor beta-isoform (ERbeta) of the human estrogen receptor modulates ERalpha transcriptional activity and is a key regulator of the cellular response to estrogens and antiestrogens. *Endocrinology* 140:5566-5578.

148. Ellmann, S., Sticht, H., Thiel, F., Beckmann, M.W., Strick, R., and Strissel, P.L. 2009. Estrogen and progesterone receptors: from molecular structures to clinical targets. *Cell Mol Life Sci* 66:2405-2426.

149. Yang, J., Singleton, D.W., Shaughnessy, E.A., and Khan, S.A. 2008. The F-domain of estrogen receptor-alpha inhibits ligand induced receptor dimerization. *Mol Cell Endocrinol* 295:94-100.

150. Hirata, S., Shoda, T., Kato, J., and Hoshi, K. 2003. Isoform/variant mRNAs for sex steroid hormone receptors in humans. *Trends Endocrinol Metab* 14:124-129.

151. Flouriot, G., Brand, H., Denger, S., Metivier, R., Kos, M., Reid, G., Sonntag-Buck, V., and Gannon, F. 2000. Identification of a new isoform of the human estrogen receptor-

alpha (hER-alpha) that is encoded by distinct transcripts and that is able to repress hER-alpha activation function 1. *EMBO J* 19:4688-4700.

152. Wang, Z., Zhang, X., Shen, P., Loggie, B.W., Chang, Y., and Deuel, T.F. 2005. Identification, cloning, and expression of human estrogen receptor-alpha36, a novel variant of human estrogen receptor-alpha66. *Biochem Biophys Res Commun* 336:1023-1027.

153. Ikeda, M., Kawaguchi, A., Takeshita, A., Chin, W.W., Endo, T., and Onaya, T. 1999. CBP-dependent and independent enhancing activity of steroid receptor coactivator-1 in thyroid hormone receptor-mediated transactivation. *Mol Cell Endocrinol* 147:103-112.

154. Wei, X., Xu, H., and Kufe, D. 2006. MUC1 oncoprotein stabilizes and activates estrogen receptor alpha. *Mol Cell* 21:295-305.

155. McKenna, N.J., Lanz, R.B., and O'Malley, B.W. 1999. Nuclear receptor coregulators: cellular and molecular biology. *Endocr Rev* 20:321-344.

156. Ogryzko, V.V., Schiltz, R.L., Russanova, V., Howard, B.H., and Nakatani, Y. 1996. The transcriptional coactivators p300 and CBP are histone acetyltransferases. *Cell* 87:953-959.

157. Vadlamudi, R.K., Wang, R.A., Mazumdar, A., Kim, Y., Shin, J., Sahin, A., and Kumar, R. 2001. Molecular cloning and characterization of PELP1, a novel human coregulator of estrogen receptor alpha. *J Biol Chem* 276:38272-38279.

158. Nair, S.S., Mishra, S.K., Yang, Z., Balasenthil, S., Kumar, R., and Vadlamudi, R.K. 2004. Potential role of a novel transcriptional coactivator PELP1 in histone H1 displacement in cancer cells. *Cancer Res* 64:6416-6423.

159. Cottone, E., Orso, F., Biglia, N., Sismondi, P., and De Bortoli, M. 2001. Role of coactivators and corepressors in steroid and nuclear receptor signaling: potential markers of tumor growth and drug sensitivity. *Int J Biol Markers* 16:151-166.

160. Nagy, L., Kao, H.Y., Chakravarti, D., Lin, R.J., Hassig, C.A., Ayer, D.E., Schreiber, S.L., and Evans, R.M. 1997. Nuclear receptor repression mediated by a complex containing SMRT, mSin3A, and histone deacetylase. *Cell* 89:373-380.

161. Edwards, D.P. 2000. The role of coactivators and corepressors in the biology and mechanism of action of steroid hormone receptors. *J Mammary Gland Biol Neoplasia* 5:307-324.

162. Hammes, A., Andreassen, T.K., Spoelgen, R., Raila, J., Hubner, N., Schulz, H., Metzger, J., Schweigert, F.J., Luppa, P.B., Nykjaer, A., et al. 2005. Role of endocytosis in cellular uptake of sex steroids. *Cell* 122:751-762.

163. Chambraud, B., Berry, M., Redeuilh, G., Chambon, P., and Baulieu, E.E. 1990. Several regions of human estrogen receptor are involved in the formation of receptor-heat shock protein 90 complexes. *J Biol Chem* 265:20686-20691.

164. Kumar, P., Wu, Q., Chambliss, K.L., Yuhanna, I.S., Mumby, S.M., Mineo, C., Tall, G.G., and Shaul, P.W. 2007. Direct Interactions with G alpha i and G betagamma mediate nongenomic signaling by estrogen receptor alpha. *Mol Endocrinol* 21:1370-1380.

165. Pedram, A., Razandi, M., and Levin, E.R. 2006. Nature of functional estrogen receptors at the plasma membrane. *Mol Endocrinol* 20:1996-2009.

166. Li, L., Haynes, M.P., and Bender, J.R. 2003. Plasma membrane localization and function of the estrogen receptor alpha variant (ER46) in human endothelial cells. *Proc Natl Acad Sci U S A* 100:4807-4812.

167. Doolan, C.M., and Harvey, B.J. 2003. A Galphas protein-coupled membrane receptor, distinct from the classical oestrogen receptor, transduces rapid effects of oestradiol on [Ca2+]i in female rat distal colon. *Mol Cell Endocrinol* 199:87-103.

168. Song, R.X., Barnes, C.J., Zhang, Z., Bao, Y., Kumar, R., and Santen, R.J. 2004. The role of Shc and insulin-like growth factor 1 receptor in mediating the translocation of estrogen receptor alpha to the plasma membrane. *Proc Natl Acad Sci U S A* 101:2076-2081.

169. Chambliss, K.L., Yuhanna, I.S., Mineo, C., Liu, P., German, Z., Sherman, T.S., Mendelsohn, M.E., Anderson, R.G., and Shaul, P.W. 2000. Estrogen receptor alpha and endothelial nitric oxide synthase are organized into a functional signaling module in caveolae. *Circ Res* 87:E44-52.

170. Shaul, P.W., and Anderson, R.G. 1998. Role of plasmalemmal caveolae in signal transduction. *Am J Physiol* 275:L843-851.

171. Martin, M.B., Franke, T.F., Stoica, G.E., Chambon, P., Katzenellenbogen, B.S., Stoica, B.A., McLemore, M.S., Olivo, S.E., and Stoica, A. 2000. A role for Akt in mediating the estrogenic functions of epidermal growth factor and insulin-like growth factor I. *Endocrinology* 141:4503-4511.

172. Ikenoue, T., Inoki, K., Yang, Q., Zhou, X., and Guan, K.L. 2008. Essential function of TORC2 in PKC and Akt turn motif phosphorylation, maturation and signalling. *EMBO J* 27:1919-1931.

173. Chen, D., Pace, P.E., Coombes, R.C., and Ali, S. 1999. Phosphorylation of human estrogen receptor alpha by protein kinase A regulates dimerization. *Mol Cell Biol* 19:1002-1015.

174. Rothberg, K.G., Heuser, J.E., Donzell, W.C., Ying, Y.S., Glenney, J.R., and Anderson, R.G. 1992. Caveolin, a protein component of caveolae membrane coats. *Cell* 68:673-682.

175. Cohen, A.W., Hnasko, R., Schubert, W., and Lisanti, M.P. 2004. Role of caveolae and caveolins in health and disease. *Physiol Rev* 84:1341-1379.

176. Glenney, J.R., Jr., and Soppet, D. 1992. Sequence and expression of caveolin, a protein component of caveolae plasma membrane domains phosphorylated on tyrosine in Rous sarcoma virus-transformed fibroblasts. *Proc Natl Acad Sci U S A* 89:10517-10521.

177. Scherer, P.E., Okamoto, T., Chun, M., Nishimoto, I., Lodish, H.F., and Lisanti, M.P. 1996. Identification, sequence, and expression of caveolin-2 defines a caveolin gene family. *Proc Natl Acad Sci U S A* 93:131-135.

178. Tang, Z., Scherer, P.E., Okamoto, T., Song, K., Chu, C., Kohtz, D.S., Nishimoto, I., Lodish, H.F., and Lisanti, M.P. 1996. Molecular cloning of caveolin-3, a novel member of the caveolin gene family expressed predominantly in muscle. *J Biol Chem* 271:2255-2261.

179. Lisanti, M.P., Scherer, P.E., Vidugiriene, J., Tang, Z., Hermanowski-Vosatka, A., Tu, Y.H., Cook, R.F., and Sargiacomo, M. 1994. Characterization of caveolin-rich membrane domains isolated from an endothelial-rich source: implications for human disease. *J Cell Biol* 126:111-126.

180. Vogel, U., Sandvig, K., and van Deurs, B. 1998. Expression of caveolin-1 and polarized formation of invaginated caveolae in Caco-2 and MDCK II cells. *J Cell Sci* 111 (Pt 6):825-832.

181. Ikezu, T., Ueda, H., Trapp, B.D., Nishiyama, K., Sha, J.F., Volonte, D., Galbiati, F., Byrd, A.L., Bassell, G., Serizawa, H., et al. 1998. Affinity-purification and characterization of caveolins from the brain: differential expression of caveolin-1, -2, and -3 in brain endothelial and astroglial cell types. *Brain Res* 804:177-192.

182. Galbiati, F., Engelman, J.A., Volonte, D., Zhang, X.L., Minetti, C., Li, M., Hou, H., Jr., Kneitz, B., Edelmann, W., and Lisanti, M.P. 2001. Caveolin-3 null mice show a loss of caveolae, changes in the microdomain distribution of the dystrophin-glycoprotein complex, and t-tubule abnormalities. *J Biol Chem* 276:21425-21433.

183. Razani, B., Combs, T.P., Wang, X.B., Frank, P.G., Park, D.S., Russell, R.G., Li, M., Tang, B., Jelicks, L.A., Scherer, P.E., et al. 2002. Caveolin-1-deficient mice are lean, resistant to diet-induced obesity, and show hypertriglyceridemia with adipocyte abnormalities. *J Biol Chem* 277:8635-8647.

184. Razani, B., Wang, X.B., Engelman, J.A., Battista, M., Lagaud, G., Zhang, X.L., Kneitz, B., Hou, H., Jr., Christ, G.J., Edelmann, W., et al. 2002. Caveolin-2-deficient mice show evidence of severe pulmonary dysfunction without disruption of caveolae. *Mol Cell Biol* 22:2329-2344.

185. Razani, B., Woodman, S.E., and Lisanti, M.P. 2002. Caveolae: from cell biology to animal physiology. *Pharmacol Rev* 54:431-467.

186. Kim, H.P., Lee, J.Y., Jeong, J.K., Bae, S.W., Lee, H.K., and Jo, I. 1999. Nongenomic stimulation of nitric oxide release by estrogen is mediated by estrogen receptor alpha localized in caveolae. *Biochem Biophys Res Commun* 263:257-262.

187. Razandi, M., Oh, P., Pedram, A., Schnitzer, J., and Levin, E.R. 2002. ERs associate with and regulate the production of caveolin: implications for signaling and cellular actions. *Mol Endocrinol* 16:100-115.

188. Lu, Q., Pallas, D.C., Surks, H.K., Baur, W.E., Mendelsohn, M.E., and Karas, R.H. 2004. Striatin assembles a membrane signaling complex necessary for rapid, nongenomic activation of endothelial NO synthase by estrogen receptor alpha. *Proc Natl Acad Sci U S A* 101:17126-17131.

189. Castets, F., Rakitina, T., Gaillard, S., Moqrich, A., Mattei, M.G., and Monneron, A. 2000. Zinedin, SG2NA, and striatin are calmodulin-binding, WD repeat proteins principally expressed in the brain. *J Biol Chem* 275:19970-19977.

190. Castets, F., Bartoli, M., Barnier, J.V., Baillat, G., Salin, P., Moqrich, A., Bourgeois, J.P., Denizot, F., Rougon, G., Calothy, G., et al. 1996. A novel calmodulin-binding protein, belonging to the WD-repeat family, is localized in dendrites of a subset of CNS neurons. *J Cell Biol* 134:1051-1062.

191. Edgell, C.J., McDonald, C.C., and Graham, J.B. 1983. Permanent cell line expressing human factor VIII-related antigen established by hybridization. *Proc Natl Acad Sci U S A* 80:3734-3737.

192. Nichols, W.W., Murphy, D.G., Cristofalo, V.J., Toji, L.H., Greene, A.E., and Dwight, S.A. 1977. Characterization of a new human diploid cell strain, IMR-90. *Science* 196:60-63.

193. Kobayashi, M., Inoue, K., Warabi, E., Minami, T., and Kodama, T. 2005. A simple method of isolating mouse aortic endothelial cells. *J Atheroscler Thromb* 12:138-142.

194. Renart, J., Reiser, J., and Stark, G.R. 1979. Transfer of proteins from gels to diazobenzyloxymethyl-paper and detection with antisera: a method for studying antibody specificity and antigen structure. *Proc Natl Acad Sci U S A* 76:3116-3120.

195. Towbin, H., Staehelin, T., and Gordon, J. 1979. Electrophoretic transfer of proteins from polyacrylamide gels to nitrocellulose sheets: procedure and some applications. *Proc Natl Acad Sci U S A* 76:4350-4354.

196. Gomez-Sanchez, C.E., de Rodriguez, A.F., Romero, D.G., Estess, J., Warden, M.P., Gomez-Sanchez, M.T., and Gomez-Sanchez, E.P. 2006. Development of a panel of monoclonal antibodies against the mineralocorticoid receptor. *Endocrinology* 147:1343-1348.

197. Russel, S.a. 2001. *Molecular Cloning: A Laboratory Manual*: Cold Spring Harbor Laboratory Press.

198. Berchtold, M.W. 1989. A simple method for direct cloning and sequencing cDNA by the use of a single specific oligonucleotide and oligo(dT) in a polymerase chain reaction (PCR). *Nucleic Acids Res* 17:453.

199. Noonan, K.E., and Roninson, I.B. 1988. mRNA phenotyping by enzymatic amplification of randomly primed cDNA. *Nucleic Acids Res* 16:10366.

200. Rappolee, D.A., Mark, D., Banda, M.J., and Werb, Z. 1988. Wound macrophages express TGF-alpha and other growth factors in vivo: analysis by mRNA phenotyping. *Science* 241:708-712.

201. Dhanasekaran, S., Doherty, T.M., and Kenneth, J. Comparison of different standards for real-time PCR-based absolute quantification. *J Immunol Methods* 354:34-39.

202. Schefe, J.H., Lehmann, K.E., Buschmann, I.R., Unger, T., and Funke-Kaiser, H. 2006. Quantitative real-time RT-PCR data analysis: current concepts and the novel "gene expression's CT difference" formula. *J Mol Med (Berl)* 84:901-910.

203. Nailis, H., Coenye, T., Van Nieuwerburgh, F., Deforce, D., and Nelis, H.J. 2006. Development and evaluation of different normalization strategies for gene expression studies in Candida albicans biofilms by real-time PCR. *BMC Mol Biol* 7:25.

204. Nolan, T., Hands, R.E., and Bustin, S.A. 2006. Quantification of mRNA using real-time RT-PCR. *Nat Protoc* 1:1559-1582.

205. Hamilton, A.J., and Baulcombe, D.C. 1999. A species of small antisense RNA in posttranscriptional gene silencing in plants. *Science* 286:950-952.

206. Elbashir, S.M., Harborth, J., Lendeckel, W., Yalcin, A., Weber, K., and Tuschl, T. 2001. Duplexes of 21-nucleotide RNAs mediate RNA interference in cultured mammalian cells. *Nature* 411:494-498.

207. Bernstein, E., Caudy, A.A., Hammond, S.M., and Hannon, G.J. 2001. Role for a bidentate ribonuclease in the initiation step of RNA interference. *Nature* 409:363-366.

208. Karas, R.H., Gauer, E.A., Bieber, H.E., Baur, W.E., and Mendelsohn, M.E. 1998. Growth factor activation of the estrogen receptor in vascular cells occurs via a mitogen-activated protein kinase-independent pathway. *J Clin Invest* 101:2851-2861.

209. Carrel, A., and Ebeling, A.H. 1922. Action of Shaken Serum on Homologous Fibroblasts. *J Exp Med* 36:399-403.

210. Carrel, A., and Ebeling, A.H. 1922. Pure Cultures of Large Mononuclear Leucocytes. *J Exp Med* 36:365-377.

211. Carrel, A., and Ebeling, A.H. 1922. Heterogenic Serum, Age, and Multiplication of Fibroblasts. *J Exp Med* 35:17-38.

212. Treadwell, P.E., and Ross, J.D. 1963. Characterization of human cells: variation in growth rate, volume, morphology and growth efficiency in media supplemented with human serum or bovine fetal serum. *Exp Cell Res* 29:356-379.

213. Evans, V.J., Bryant, J.C., Fioramonti, M.C., McQuilkin, W.T., Sanford, K.K., and Earle, W.R. 1956. Studies of nutrient media for tissue cells in vitro. I. A protein-free chemically defined medium for cultivation of strain L cells. *Cancer Res* 16:77-86.

214. van der Valk, J., Brunner, D., De Smet, K., Fex Svenningsen, A., Honegger, P., Knudsen, L.E., Lindl, T., Noraberg, J., Price, A., Scarino, M.L., et al. Optimization of chemically defined cell culture media--replacing fetal bovine serum in mammalian in vitro methods. *Toxicol In Vitro* 24:1053-1063.

215. Lagarde, M., Sicard, B., Guichardant, M., Felisi, O., and Dechavanne, M. 1984. Fatty acid composition in native and cultured human endothelial cells. *In Vitro* 20:33-37.

216. Loomis, R.J., Marshall, L.A., and Johnston, P.V. 1983. Sera fatty acid effects on cultured rat splenocytes. *J Nutr* 113:1292-1298.

217. Stoll, L.L., and Spector, A.A. 1984. Changes in serum influence the fatty acid composition of established cell lines. *In Vitro* 20:732-738.

218. Bas, S., James, R.W., and Gabay, C. Serum lipoproteins attenuate macrophage activation and Toll-Like Receptor stimulation by bacterial lipoproteins. *BMC Immunol* 11:46.

219. Schaefer, H.I., van 't Hooft, F.M., and van der Laarse, A. 1992. Growth characteristics of a permanent human endothelial cell line. *In Vitro Cell Dev Biol* 28A:465-467.

220. Miettinen, M., Lindenmayer, A.E., and Chaubal, A. 1994. Endothelial cell markers CD31, CD34, and BNH9 antibody to H- and Y-antigens--evaluation of their specificity and sensitivity in the diagnosis of vascular tumors and comparison with von Willebrand factor. *Mod Pathol* 7:82-90.

221. Soltesz, P., Bereczki, D., Szodoray, P., Magyar, M.T., Der, H., Csipo, I., Hajas, A., Paragh, G., Szegedi, G., and Bodolay, E. Endothelial cell markers reflecting endothelial cell dysfunction in patients with mixed connective tissue disease. *Arthritis Res Ther* 12:R78.

222. Schmitt-Graff, A., Desmouliere, A., and Gabbiani, G. 1994. Heterogeneity of myofibroblast phenotypic features: an example of fibroblastic cell plasticity. *Virchows Arch* 425:3-24.

223. Guo, C., Martinez-Vasquez, D., Mendez, G.P., Toniolo, M.F., Yao, T.M., Oestreicher, E.M., Kikuchi, T., Lapointe, N., Pojoga, L., Williams, G.H., et al. 2006. Mineralocorticoid receptor antagonist reduces renal injury in rodent models of types 1 and 2 diabetes mellitus. *Endocrinology* 147:5363-5373.

224. Lombes, M., Alfaidy, N., Eugene, E., Lessana, A., Farman, N., and Bonvalet, J.P. 1995. Prerequisite for cardiac aldosterone action. Mineralocorticoid receptor and 11 beta-hydroxysteroid dehydrogenase in the human heart. *Circulation* 92:175-182.

225. Hernandez-Diaz, I., Giraldez, T., Arnau, M.R., Smits, V.A., Jaisser, F., Farman, N., and Alvarez de la Rosa, D. The mineralocorticoid receptor is a constitutive nuclear factor in cardiomyocytes due to hyperactive nuclear localization signals. *Endocrinology* 151:3888-3899.

226. Yoshida, M., Ma, J., Tomita, T., Morikawa, N., Tanaka, N., Masamura, K., Kawai, Y., and Miyamori, I. 2005. Mineralocorticoid receptor is overexpressed in cardiomyocytes of patients with congestive heart failure. *Congest Heart Fail* 11:12-16.

227. Moreno, C.S., Lane, W.S., and Pallas, D.C. 2001. A mammalian homolog of yeast MOB1 is both a member and a putative substrate of striatin family-protein phosphatase 2A complexes. *J Biol Chem* 276:24253-24260.

228. Helms, J.B., and Zurzolo, C. 2004. Lipids as targeting signals: lipid rafts and intracellular trafficking. *Traffic* 5:247-254.

229. D'Alessio, A., Al-Lamki, R.S., Bradley, J.R., and Pober, J.S. 2005. Caveolae participate in tumor necrosis factor receptor 1 signaling and internalization in a human endothelial cell line. *Am J Pathol* 166:1273-1282.

230. Palage, G.E. 1953. Fine Structure of Blood Capilaries. *Journal of Applied Physiology* 24:1424-1436.

231. Yamada, E. 1955. The fine structure of the gall bladder epithelium of the mouse. *J Biophys Biochem Cytol* 1:445-458.

232. Lisanti, M.P., Scherer, P.E., Tang, Z., and Sargiacomo, M. 1994. Caveolae, caveolin and caveolin-rich membrane domains: a signalling hypothesis. *Trends Cell Biol* 4:231-235.

233. Rude, M.K., Duhaney, T.A., Kuster, G.M., Judge, S., Heo, J., Colucci, W.S., Siwik, D.A., and Sam, F. 2005. Aldosterone stimulates matrix metalloproteinases and reactive oxygen species in adult rat ventricular cardiomyocytes. *Hypertension* 46:555-561.

234. Karmazyn, M., Liu, Q., Gan, X.T., Brix, B.J., and Fliegel, L. 2003. Aldosterone increases NHE-1 expression and induces NHE-1-dependent hypertrophy in neonatal rat ventricular myocytes. *Hypertension* 42:1171-1176.

235. Turchin, A., Guo, C.Z., Adler, G.K., Ricchiuti, V., Kohane, I.S., and Williams, G.H. 2006. Effect of acute aldosterone administration on gene expression profile in the heart. *Endocrinology* 147:3183-3189.

236. Brilla, C.G., and Weber, K.T. 1992. Reactive and reparative myocardial fibrosis in arterial hypertension in the rat. *Cardiovasc Res* 26:671-677.

237. Selye, H. 1946. The general adaptation syndrome and the diseases of adaptation. *J Clin Endocrinol Metab* 6:117-230.

238. Theodosiou, A., and Ashworth, A. 2002. MAP kinase phosphatases. *Genome Biol* 3:REVIEWS3009.

239. Andreeva, A.V., and Kutuzov, M.A. 1999. RdgC/PP5-related phosphatases: novel components in signal transduction. *Cell Signal* 11:555-562.

240. Manegold, J.C., Falkenstein, E., Wehling, M., and Christ, M. 1999. Rapid aldosterone effects on tyrosine phosphorylation in vascular smooth muscle cells. *Cell Mol Biol (Noisy-le-grand)* 45:805-813.

241. Rossol-Haseroth, K., Zhou, Q., Braun, S., Boldyreff, B., Falkenstein, E., Wehling, M., and Losel, R.M. 2004. Mineralocorticoid receptor antagonists do not block rapid ERK activation by aldosterone. *Biochem Biophys Res Commun* 318:281-288.

242. Calhoun, D.A., Nishizaka, M.K., Zaman, M.A., Thakkar, R.B., and Weissmann, P. 2002. Hyperaldosteronism among black and white subjects with resistant hypertension. *Hypertension* 40:892-896.

243. Fardella, C.E., Mosso, L., Gomez-Sanchez, C., Cortes, P., Soto, J., Gomez, L., Pinto, M., Huete, A., Oestreicher, E., Foradori, A., et al. 2000. Primary hyperaldosteronism in essential hypertensives: prevalence, biochemical profile, and molecular biology. *J Clin Endocrinol Metab* 85:1863-1867.

244. Lim, P.O., and MacDonald, T.M. 2003. Primary aldosteronism, diagnosed by the aldosterone to renin ratio, is a common cause of hypertension. *Clin Endocrinol (Oxf)* 59:427-430.

245. Loh, K.C., Koay, E.S., Khaw, M.C., Emmanuel, S.C., and Young, W.F., Jr. 2000. Prevalence of primary aldosteronism among Asian hypertensive patients in Singapore. *J Clin Endocrinol Metab* 85:2854-2859.

246. Mosso, L., Carvajal, C., Gonzalez, A., Barraza, A., Avila, F., Montero, J., Huete, A., Gederlini, A., and Fardella, C.E. 2003. Primary aldosteronism and hypertensive disease. *Hypertension* 42:161-165.

247. Stowasser, M., Gordon, R.D., Gunasekera, T.G., Cowley, D.C., Ward, G., Archibald, C., and Smithers, B.M. 2003. High rate of detection of primary aldosteronism, including surgically treatable forms, after 'non-selective' screening of hypertensive patients. *J Hypertens* 21:2149-2157.

248. Young, W.F., Jr. 2003. Minireview: primary aldosteronism--changing concepts in diagnosis and treatment. *Endocrinology* 144:2208-2213.

249. Kumar, V., Abbas, A.K., Fausto, N., Robbins, S.L., and Cotran, R.S.R.p.b.o.d. 2005. *Robbins and Cotran pathologic basis of disease*. Philadelphia, Pa. ; [London]: Elsevier Saunders.

250. Perschel, F.H., Schemer, R., Seiler, L., Reincke, M., Deinum, J., Maser-Gluth, C., Mechelhoff, D., Tauber, R., and Diederich, S. 2004. Rapid screening test for primary hyperaldosteronism: ratio of plasma aldosterone to renin concentration determined by fully automated chemiluminescence immunoassays. *Clin Chem* 50:1650-1655.

251. Rousseau, M.F., Gurne, O., Duprez, D., Van Mieghem, W., Robert, A., Ahn, S., Galanti, L., and Ketelslegers, J.M. 2002. Beneficial neurohormonal profile of spironolactone in severe congestive heart failure: results from the RALES neurohormonal substudy. *J Am Coll Cardiol* 40:1596-1601.

252. Weber, K.T. 2001. Aldosterone in congestive heart failure. *N Engl J Med* 345:1689-1697.

253. Sorrentino, R., Autore, G., Cirino, G., d'Emmanuele de Villa Bianca, R., Calignano, A., Vanasia, M., Alfieri, C., Sorrentino, L., and Pinto, A. 2000. Effect of spironolactone and its metabolites on contractile property of isolated rat aorta rings. *J Cardiovasc Pharmacol* 36:230-235.

254. Chun, T.Y., Bloem, L.J., and Pratt, J.H. 2003. Aldosterone inhibits inducible nitric oxide synthase in neonatal rat cardiomyocytes. *Endocrinology* 144:1712-1717.

255. Pearce, D. 2001. The role of SGK1 in hormone-regulated sodium transport. *Trends Endocrinol Metab* 12:341-347.

256. Wade, J.B., Stanton, B.A., Field, M.J., Kashgarian, M., and Giebisch, G. 1990. Morphological and physiological responses to aldosterone: time course and sodium dependence. *Am J Physiol* 259:F88-94.

257. Shigaev, A., Asher, C., Latter, H., Garty, H., and Reuveny, E. 2000. Regulation of sgk by aldosterone and its effects on the epithelial Na(+) channel. *Am J Physiol Renal Physiol* 278:F613-619.

258. Wagner, C.A., Ott, M., Klingel, K., Beck, S., Melzig, J., Friedrich, B., Wild, K.N., Broer, S., Moschen, I., Albers, A., et al. 2001. Effects of the serine/threonine kinase SGK1 on the epithelial Na(+) channel (ENaC) and CFTR: implications for cystic fibrosis. *Cell Physiol Biochem* 11:209-218.

259. Fejes-Toth, G., and Naray-Fejes-Toth, A. 2007. Early aldosterone-regulated genes in cardiomyocytes: clues to cardiac remodeling? *Endocrinology* 148:1502-1510.

260. Subramanya, A.R., Yang, C.L., McCormick, J.A., and Ellison, D.H. 2006. WNK kinases regulate sodium chloride and potassium transport by the aldosterone-sensitive distal nephron. *Kidney Int* 70:630-634.

261. Peng, J.B., and Warnock, D.G. 2007. WNK4-mediated regulation of renal ion transport proteins. *Am J Physiol Renal Physiol* 293:F961-973.

262. van der Lubbe, N., Lim, C.H., Fenton, R.A., Meima, M.E., Jan Danser, A.H., Zietse, R., and Hoorn, E.J. 2011. Angiotensin II induces phosphorylation of the thiazide-sensitive sodium chloride cotransporter independent of aldosterone. *Kidney Int* 79:66-76.

263. Meneton, P., Jeunemaitre, X., de Wardener, H.E., and MacGregor, G.A. 2005. Links between dietary salt intake, renal salt handling, blood pressure, and cardiovascular diseases. *Physiol Rev* 85:679-715.

264. Pojoga, L.H., Yao, T.M., Sinha, S., Ross, R.L., Lin, J.C., Raffetto, J.D., Adler, G.K., Williams, G.H., and Khalil, R.A. 2008. Effect of dietary sodium on vasoconstriction and eNOS-mediated vascular relaxation in caveolin-1-deficient mice. *Am J Physiol Heart Circ Physiol* 294:H1258-1265.

265. Pojoga, L.H., Romero, J.R., Yao, T.M., Loutraris, P., Ricchiuti, V., Coutinho, P., Guo, C., Lapointe, N., Stone, J.R., Adler, G.K., et al. Caveolin-1 ablation reduces the adverse cardiovascular effects of N-omega-nitro-L-arginine methyl ester and angiotensin II. *Endocrinology* 151:1236-1246.

266. Fang, P.K., Solomon, K.R., Zhuang, L., Qi, M., McKee, M., Freeman, M.R., and Yelick, P.C. 2006. Caveolin-1alpha and -1beta perform nonredundant roles in early vertebrate development. *Am J Pathol* 169:2209-2222.

267. DeWitt, D.L., and Smith, W.L. 1983. Purification of prostacyclin synthase from bovine aorta by immunoaffinity chromatography. Evidence that the enzyme is a hemoprotein. *J Biol Chem* 258:3285-3293.

268. Ullrich, V., Castle, L., and Weber, P. 1981. Spectral evidence for the cytochrome P450 nature of prostacyclin synthetase. *Biochem Pharmacol* 30:2033-2036.

269. Sobrino, A., Mata, M., Laguna-Fernandez, A., Novella, S., Oviedo, P.J., Garcia-Perez, M.A., Tarin, J.J., Cano, A., and Hermenegildo, C. 2009. Estradiol stimulates vasodilatory and metabolic pathways in cultured human endothelial cells. *PLoS One* 4:e8242.

270. Funk, C.D., Funk, L.B., Kennedy, M.E., Pong, A.S., and Fitzgerald, G.A. 1991. Human platelet/erythroleukemia cell prostaglandin G/H synthase: cDNA cloning, expression, and gene chromosomal assignment. *Faseb J* 5:2304-2312.

271. Yokoyama, C., and Tanabe, T. 1989. Cloning of human gene encoding prostaglandin endoperoxide synthase and primary structure of the enzyme. *Biochem Biophys Res Commun* 165:888-894.

272. Gibson, L.L., Hahner, L., Osborne-Lawrence, S., German, Z., Wu, K.K., Chambliss, K.L., and Shaul, P.W. 2005. Molecular basis of estrogen-induced cyclooxygenase type 1 upregulation in endothelial cells. *Circ Res* 96:518-525.

273. Jun, S.S., Chen, Z., Pace, M.C., and Shaul, P.W. 1998. Estrogen upregulates cyclooxygenase-1 gene expression in ovine fetal pulmonary artery endothelium. *J Clin Invest* 102:176-183.

274. Crabbe, J. 1961. Stimulation of active sodium transport by the isolated toad bladder with aldosterone in vitro. *J Clin Invest* 40:2103-2110.

275. Davis, J.O., Carpenter, C.C., Ayers, C.R., Holman, J.E., and Bahn, R.C. 1961. Evidence for secretion of an aldosterone-stimulating hormone by the kidney. *J Clin Invest* 40:684-696.

276. Davis, J.O., Hartroft, P.M., Titus, E.O., Carpenter, C.C., Ayers, C.R., and Spiegel, H.E. 1962. The role of the renin-angiotensin system in the control of aldosterone secretion. *J Clin Invest* 41:378-389.

277. Pearce, P., and Funder, J.W. 1987. High affinity aldosterone binding sites (type I receptors) in rat heart. *Clin Exp Pharmacol Physiol* 14:859-866.

278. Funder, J.W. 2005. The nongenomic actions of aldosterone. *Endocr Rev* 26:313-321.

279. Conn, J.W., and Louis, L.H. 1955. Primary aldosteronism: a new clinical entity. *Trans Assoc Am Physicians* 68:215-231; discussion, 231-213.

280. Virdis, A., Neves, M.F., Amiri, F., Viel, E., Touyz, R.M., and Schiffrin, E.L. 2002. Spironolactone improves angiotensin-induced vascular changes and oxidative stress. *Hypertension* 40:504-510.

281. Zannad, F., Alla, F., Dousset, B., Perez, A., and Pitt, B. 2000. Limitation of excessive extracellular matrix turnover may contribute to survival benefit of spironolactone therapy in patients with congestive heart failure: insights from the randomized aldactone evaluation study (RALES). Rales Investigators. *Circulation* 102:2700-2706.

282. Beato, M., Chavez, S., and Truss, M. 1996. Transcriptional regulation by steroid hormones. *Steroids* 61:240-251.

283. Hendry, L.B. 1988. Stereochemical complementary of DNA and steroid agonists and antagonists. *J Steroid Biochem* 31:493-523.

284. Matthews, L., Berry, A., Ohanian, V., Ohanian, J., Garside, H., and Ray, D. 2008. Caveolin mediates rapid glucocorticoid effects and couples glucocorticoid action to the antiproliferative program. *Mol Endocrinol* 22:1320-1330.

285. Pedram, A., Razandi, M., Sainson, R.C., Kim, J.K., Hughes, C.C., and Levin, E.R. 2007. A conserved mechanism for steroid receptor translocation to the plasma membrane. *J Biol Chem* 282:22278-22288.

286. Razandi, M., Pedram, A., and Levin, E.R. Heat shock protein 27 is required for sex steroid receptor trafficking to and functioning at the plasma membrane. *Mol Cell Biol* 30:3249-3261.

287. Grossmann, C., Husse, B., Mildenberger, S., Schreier, B., Schuman, K., and Gekle, M. Colocalization of mineralocorticoid and EGF receptor at the plasma membrane. *Biochim Biophys Acta* 1803:584-590.

288. Moura, A.M., and Worcel, M. 1984. Direct action of aldosterone on transmembrane 22Na efflux from arterial smooth muscle. Rapid and delayed effects. *Hypertension* 6:425-430.

289. Losel, R., and Wehling, M. 2003. Nongenomic actions of steroid hormones. *Nat Rev Mol Cell Biol* 4:46-56.

290. Gaillard, S., Bartoli, M., Castets, F., and Monneron, A. 2001. Striatin, a calmodulin-dependent scaffolding protein, directly binds caveolin-1. *FEBS Lett* 508:49-52.

291. Moreno, C.S., Park, S., Nelson, K., Ashby, D., Hubalek, F., Lane, W.S., and Pallas, D.C. 2000. WD40 repeat proteins striatin and S/G(2) nuclear autoantigen are members of a novel family of calmodulin-binding proteins that associate with protein phosphatase 2A. *J Biol Chem* 275:5257-5263.

292. Baillat, G., Moqrich, A., Castets, F., Baude, A., Bailly, Y., Benmerah, A., and Monneron, A. 2001. Molecular cloning and characterization of phocein, a protein found from the Golgi complex to dendritic spines. *Mol Biol Cell* 12:663-673.

293. Baillat, G., Gaillard, S., Castets, F., and Monneron, A. 2002. Interactions of phocein with nucleoside-diphosphate kinase, Eps15, and Dynamin I. *J Biol Chem* 277:18961-18966.

294. Schulte, J., Sepp, K.J., Jorquera, R.A., Wu, C., Song, Y., Hong, P., and Littleton, J.T. DMob4/Phocein regulates synapse formation, axonal transport, and microtubule organization. *J Neurosci* 30:5189-5203.

295. Goudreault, M., D'Ambrosio, L.M., Kean, M.J., Mullin, M.J., Larsen, B.G., Sanchez, A., Chaudhry, S., Chen, G.I., Sicheri, F., Nesvizhskii, A.I., et al. 2009. A PP2A phosphatase high density interaction network identifies a novel striatin-interacting phosphatase and kinase complex linked to the cerebral cavernous malformation 3 (CCM3) protein. *Mol Cell Proteomics* 8:157-171.

296. Cornils, H., Kohler, R.S., Hergovich, A., and Hemmings, B.A. Human NDR kinases control G(1)/S cell cycle transition by directly regulating p21 stability. *Mol Cell Biol* 31:1382-1395.

297. Fidalgo, M., Fraile, M., Pires, A., Force, T., Pombo, C., and Zalvide, J. CCM3/PDCD10 stabilizes GCKIII proteins to promote Golgi assembly and cell orientation. *J Cell Sci* 123:1274-1284.

298. Lu, T.J., Lai, W.Y., Huang, C.Y., Hsieh, W.J., Yu, J.S., Hsieh, Y.J., Chang, W.T., Leu, T.H., Chang, W.C., Chuang, W.J., et al. 2006. Inhibition of cell migration by autophosphorylated mammalian sterile 20-like kinase 3 (MST3) involves paxillin and protein-tyrosine phosphatase-PEST. *J Biol Chem* 281:38405-38417.

299. Preisinger, C., Short, B., De Corte, V., Bruyneel, E., Haas, A., Kopajtich, R., Gettemans, J., and Barr, F.A. 2004. YSK1 is activated by the Golgi matrix protein GM130 and plays a role in cell migration through its substrate 14-3-3zeta. *J Cell Biol* 164:1009-1020.

300. Glenney, J.R., Jr. 1989. Tyrosine phosphorylation of a 22-kDa protein is correlated with transformation by Rous sarcoma virus. *J Biol Chem* 264:20163-20166.

301. Glenney, J.R., Jr. 1992. The sequence of human caveolin reveals identity with VIP21, a component of transport vesicles. *FEBS Lett* 314:45-48.

302. Kurzchalia, T.V., Dupree, P., Parton, R.G., Kellner, R., Virta, H., Lehnert, M., and Simons, K. 1992. VIP21, a 21-kD membrane protein is an integral component of trans-Golgi-network-derived transport vesicles. *J Cell Biol* 118:1003-1014.

303. Sargiacomo, M., Scherer, P.E., Tang, Z.L., Casanova, J.E., and Lisanti, M.P. 1994. In vitro phosphorylation of caveolin-rich membrane domains: identification of an associated serine kinase activity as a casein kinase II-like enzyme. *Oncogene* 9:2589-2595.

304. Donato, A.J., Black, A.D., Jablonski, K.L., Gano, L.B., and Seals, D.R. 2008. Aging is associated with greater nuclear NF kappa B, reduced I kappa B alpha, and increased

expression of proinflammatory cytokines in vascular endothelial cells of healthy humans. *Aging Cell* 7:805-812.

305. Stice, J.P., Chen, L., Kim, S.C., Jung, J.S., Tran, A.L., Liu, T.T., and Knowlton, A.A. 17beta-Estradiol, aging, inflammation, and the stress response in the female heart. *Endocrinology* 152:1589-1598.

306. Wu, Q., Chambliss, K., Umetani, M., Mineo, C., and Shaul, P.W. Non-nuclear estrogen receptor signaling in the endothelium. *J Biol Chem* 286:14737-14743.

307. Chambliss, K.L., Wu, Q., Oltmann, S., Konaniah, E.S., Umetani, M., Korach, K.S., Thomas, G.D., Mineo, C., Yuhanna, I.S., Kim, S.H., et al. Non-nuclear estrogen receptor alpha signaling promotes cardiovascular protection but not uterine or breast cancer growth in mice. *J Clin Invest* 120:2319-2330.

308. Moens, S. 2012. Rapid Estrogen Receptor Signaling is Essential for the Protective Effects of Estrogen Against Vascular Injury. *Circulation*.

309. Pitt, B. 2004. Effect of aldosterone blockade in patients with systolic left ventricular dysfunction: implications of the RALES and EPHESUS studies. *Mol Cell Endocrinol* 217:53-58.

310. Blasi, E.R., Rocha, R., Rudolph, A.E., Blomme, E.A., Polly, M.L., and McMahon, E.G. 2003. Aldosterone/salt induces renal inflammation and fibrosis in hypertensive rats. *Kidney Int* 63:1791-1800.

311. Park, J.B., and Schiffrin, E.L. 2001. ET(A) receptor antagonist prevents blood pressure elevation and vascular remodeling in aldosterone-infused rats. *Hypertension* 37:1444-1449.

312. Pu, Q., Neves, M.F., Virdis, A., Touyz, R.M., and Schiffrin, E.L. 2003. Endothelin antagonism on aldosterone-induced oxidative stress and vascular remodeling. *Hypertension* 42:49-55.

313. Rahman, M., Nishiyama, A., Guo, P., Nagai, Y., Zhang, G.X., Fujisawa, Y., Fan, Y.Y., Kimura, S., Hosomi, N., Omori, K., et al. 2006. Effects of adrenomedullin on cardiac oxidative stress and collagen accumulation in aldosterone-dependent malignant hypertensive rats. *J Pharmacol Exp Ther* 318:1323-1329.

314. Sun, Y., Zhang, J., Lu, L., Chen, S.S., Quinn, M.T., and Weber, K.T. 2002. Aldosterone-induced inflammation in the rat heart : role of oxidative stress. *Am J Pathol* 161:1773-1781.

315. Yamamuro, M., Yoshimura, M., Nakayama, M., Abe, K., Shono, M., Suzuki, S., Sakamoto, T., Saito, Y., Nakao, K., Yasue, H., et al. 2006. Direct effects of aldosterone on cardiomyocytes in the presence of normal and elevated extracellular sodium. *Endocrinology* 147:1314-1321.

316. Gekle, M., Mildenberger, S., Freudinger, R., and Grossmann, C. 2007. Altered collagen homeostasis in human aortic smooth muscle cells (HAoSMCs) induced by aldosterone. *Pflugers Arch* 454:403-413.

317. Montezano, A.C., Callera, G.E., Yogi, A., He, Y., Tostes, R.C., He, G., Schiffrin, E.L., and Touyz, R.M. 2008. Aldosterone and angiotensin II synergistically stimulate migration in vascular smooth muscle cells through c-Src-regulated redox-sensitive RhoA pathways. *Arterioscler Thromb Vasc Biol* 28:1511-1518.

318. Rad, A.K., Balment, R.J., and Ashton, N. 2005. Rapid natriuretic action of aldosterone in the rat. *J Appl Physiol* 98:423-428.

319. Wang, H., Shimosawa, T., Matsui, H., Kaneko, T., Ogura, S., Uetake, Y., Takenaka, K., Yatomi, Y., and Fujita, T. 2008. Paradoxical mineralocorticoid receptor activation and left ventricular diastolic dysfunction under high oxidative stress conditions. *J Hypertens* 26:1453-1462.

320. Gekle, M., and Grossmann, C. 2009. Actions of aldosterone in the cardiovascular system: the good, the bad, and the ugly? *Pflugers Arch* 458:231-246.

321. Rossouw, J.E., Anderson, G.L., Prentice, R.L., LaCroix, A.Z., Kooperberg, C., Stefanick, M.L., Jackson, R.D., Beresford, S.A., Howard, B.V., Johnson, K.C., et al. 2002. Risks and benefits of estrogen plus progestin in healthy postmenopausal women: principal results From the Women's Health Initiative randomized controlled trial. *Jama* 288:321-333.

322. Harman, S.M., Naftolin, F., Brinton, E.A., and Judelson, D.R. 2005. Is the estrogen controversy over? Deconstructing the Women's Health Initiative study: a critical evaluation of the evidence. *Ann N Y Acad Sci* 1052:43-56.

323. Tuck, M.L., Williams, G.H., Cain, J.P., Sullivan, J.M., and Dluhy, R.G. 1973. Relation of age, diastolic pressure and known duration of hypertension to presence of low renin essential hypertension. *Am J Cardiol* 32:637-642.

324. Gros, R., Ding, Q., Sklar, L.A., Prossnitz, E.E., Arterburn, J.B., Chorazyczewski, J., and Feldman, R.D. 2011. GPR30 expression is required for the mineralocorticoid receptor-independent rapid vascular effects of aldosterone. *Hypertension* 57:442-451.

Supplements